Elastin-based biomaterials for skin regeneration:

Design, production and evaluation

Roman Krymchenko

RADBOUD UNIVERSITY PRESS

Radboud Dissertation Series

Elastin-based biomaterials for skin regeneration

Design, production and evaluation

Roman Krymchenko

This publication has been made possible by the funding from the European Union's Horizon 2020 research and innovation programme under the Marie Skłodowska-Curie Grant Agreement No. 955722.

Elastin-based biomaterials for skin regeneration:
Design, production and evaluation
Roman Krymchenko

Radboud Dissertation Series
ISSN: 2950-2772 (Online); 2950-2780 (Print)

Published by RADBOUD UNIVERSITY PRESS
Postbus 9100, 6500 HA Nijmegen, The Netherlands
www.radbouduniversitypress.nl

Design: Proefschrift AIO | Guus Gijben
Cover: Proefschrift AIO | Guntra Laivacuma
Printing: DPN Rikken/Pumbo

ISBN: 9789465151465
DOI: 10.54195/9789465151465
Free download at: https://doi.org/10.54195/9789465151465

RADBOUD
UNIVERSITY
PRESS

Elastin-based biomaterials for skin regeneration:

Design, production and evaluation

Proefschrift ter verkrijging van de graad van doctor

aan de Radboud Universiteit Nijmegen

op gezag van de rector magnificus prof. dr. J.M. Sanders,

volgens besluit van het college voor promoties

in het openbaar te verdedigen op

donderdag 23 oktober 2025

om 16.30 uur precies

door

Roman Krymchenko

geboren op 24 april 1995

te Severodonetsk (Oekraïne)

Promotor:
Dr. ir. W.F. Daamen

Copromotoren:
Dr. A.H.M.S.M. van Kuppevelt
Dr. ir. B.K.H.L. Boekema (Vereniging Samenwerkende Brandwondencentra)

Manuscriptcommissie:
Dr. ing. J.J.J.P. van den Beucken
Dr. ir. A.I.P.M. Smits (Technische Universiteit Eindhoven)
Dr. G. Schreibelt

Elastin-based biomaterials for skin regeneration:

Design, production and evaluation

Dissertation to obtain the degree of doctor

from Radboud University Nijmegen

on the authority of the Rector Magnificus prof. dr. J.M. Sanders,

according to the decision of the Doctorate Board

to be defended in public on

Thursday, October 23, 2025

at 4.30 pm

by

Roman Krymchenko

born on April 24, 1995

in Severodonetsk (Ukraine)

PhD supervisor:
Dr. ir. W.F. Daamen

PhD co-supervisors:
Dr. A.H.M.S.M. van Kuppevelt
Dr. ir. B.K.H.L. Boekema(Alliance of Dutch Burn Care)

Manuscript Committee:
Dr. ing. J.J.J.P. van den Beucken
Dr. ir. A.I.P.M. Smits (Eindhoven University of Technology)
Dr. G. Schreibelt

Table of Content

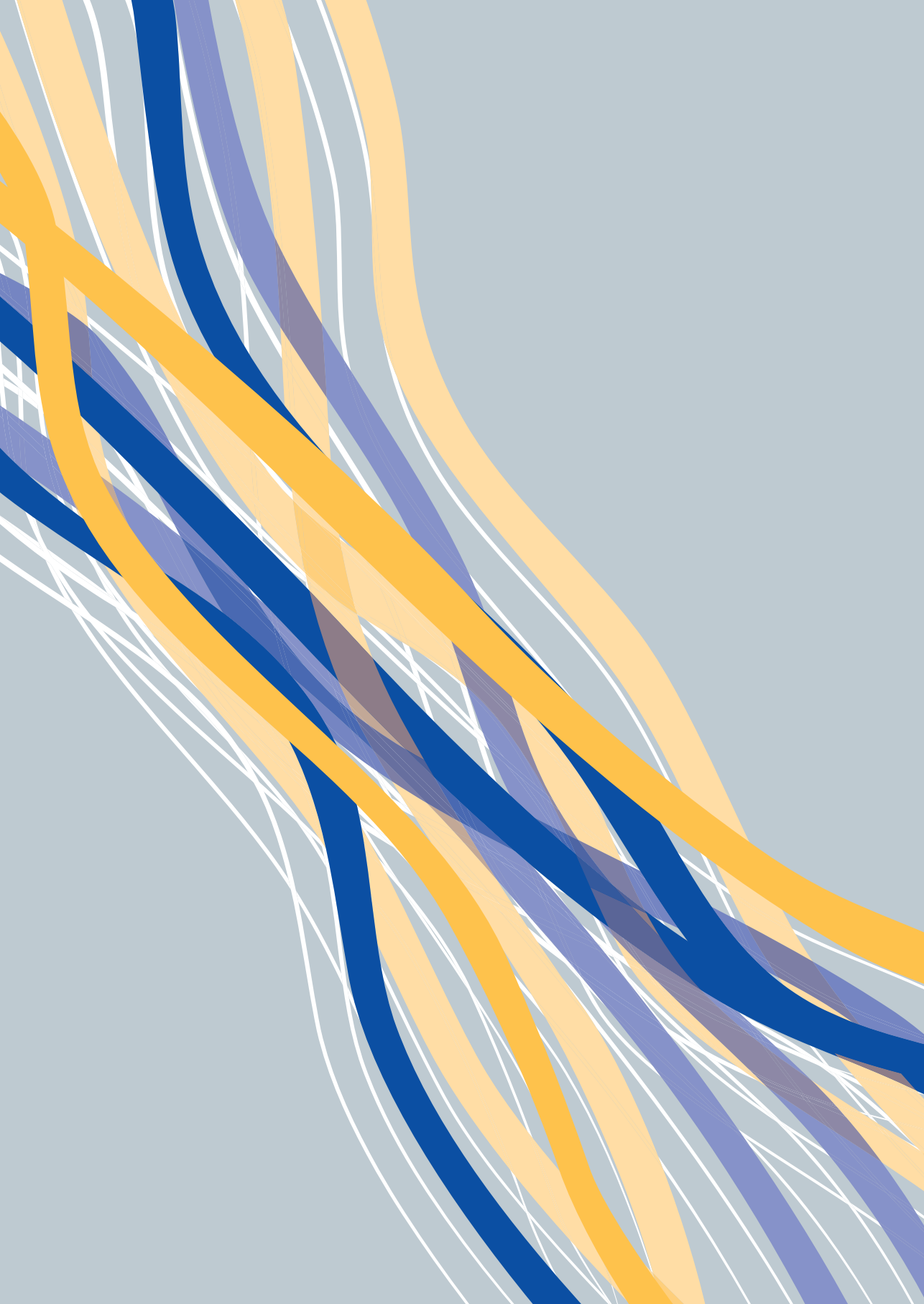

General Introduction

Scope

The skin is the largest human organ and consists of three layers: the epidermis, dermis, and hypodermis. The outer epidermis is primarily composed of keratinocytes and it continuously renews and gives rise to appendages like hair follicles and sweat glands. It also contains immune cells such as Langerhans cells. Beneath the epidermis, the supportive dermis provides structural and biochemical aid through an extracellular matrix (ECM) rich in collagen and elastic fibers, and proteoglycans. Collagen fibers constitute about 70% of the dermal proteins and ensure strength and durability, while elastic fibers maintain flexibility and resilience. Proteoglycans contribute to hydration and viscosity. The ECM undergoes constant remodeling, balanced by matrix metalloproteinases (MMPs) that break down old or damaged components and facilitate renewal. The dermis also contains blood and lymphatic vessels, nerves, and immune cells, which are essential for skin function and homeostasis. The deeper hypodermis or subcutis, sometimes classified as adipose tissue rather than part of the skin, aids in insulation and energy storage.

A wound disrupts the skin's protective barrier, often affecting underlying tissues. While minor injuries heal efficiently, severe or chronic wounds can lead to excessive scarring or fibrosis due to uncontrolled ECM accumulation. Wound healing follows a specific sequence of events and consists of four overlapping phases: hemostasis, inflammation, proliferation, and remodeling. All three skin layers are essential in wound healing. Fibroblasts play a key role in wound healing by producing ECM components, such as collagen and fibronectin, but elastic fiber regeneration is severely limited. Unlike collagen, which accumulates excessively in scars, elastic fibers form slowly and remain short, thin, and disorganized in healed tissue. It results in reduced flexibility of healed regions. This incomplete restoration leads to stiff, non-pliable scars lacking original mechanical properties. Although split-thickness skin grafts remain the gold standard for severe wounds, they do not regenerate lost elastic fibers. Given these limitations, we aim to develop biomaterials that promote proper elastic fiber synthesis and assembly, restoring skin resilience and function after injury.

Outline of the Thesis

Chapter 1 presents a critical perspective on the current state of the field of elastic fiber biology and its integration into tissue engineering strategies. Here, we identify existing knowledge gaps in our understanding of elastin synthesis, assembly, and

functional incorporation into regenerative biomaterials and outline the scientific rationale that forms the basis of the thesis. This introductory chapter provides the essential background needed to contextualize the subsequent research chapters and is structured in the form of a focused literature review. In **Chapter 1**, a range of bioactive compounds that had shown potential in stimulating elastogenesis are evaluated. The potential of these compounds in stimulating elastin production and promoting the assembly of functional elastic fibers in *in vitro* models and, in some cases, *in vivo* studies is described.

Chapter 2 explores the potential of solubilized elastins as bioactive components in skin regeneration, aiming to identify formulations that support extracellular matrix remodeling and modulate immune response – two key factors in successful wound healing. Five types of solubilized elastin are produced through chemical hydrolysis, enzymatic digestion, or a combination of both and their biological effects assessed on primary human dermal fibroblasts and macrophages, as two essential cell types in skin repair. In fibroblasts, we analyze the deposition of extracellular proteins, along with the expression of their respective genes, to assess how different elastins influence matrix synthesis and elastic fiber assembly. Additionally, α-smooth muscle actin expression is measured as a marker of myofibroblast activation and potential fibrosis, which is a common complication in wound healing. In parallel, we investigate how solubilized elastins modulate macrophage polarization from a naive (M0) state toward either a pro-inflammatory (M1-like) or pro-regenerative (M2-like) phenotype. This is done to evaluate their immunomodulatory properties, which are crucial for a proper tissue regeneration.

Chapter 3 describes the development and characterization of two collagen-based scaffolds enriched with elastin hydrolysates identified as the most promising in **Chapter 2**. The aim is to determine whether incorporating these bioactive components into collagen scaffolds could enhance regenerative outcomes across diverse wound healing contexts. For this purpose, the scaffolds are tested on different skin fibroblast types; fetal, eschar-derived, and healthy adult fibroblasts. These cells are chosen for their distinct regenerative capacities and relevance to wound environment. *In vitro* experiments are focused on how these cells deposit extracellular matrix proteins when cultured on the scaffolds, helping to assess scaffold-driven modulation of fibroblast behavior. Additionally, α-smooth muscle actin expression is measured at gene and protein levels as an indicator of myofibroblast activation and potential scar formation. To validate the *in vitro* findings in a more physiologically relevant environment, the scaffolds are further tested in a preclinical rat model. These *in vivo* studies aim to evaluate wound closure

dynamics, tissue architecture, ECM remodeling, contraction, and vascularization. Ultimately, this chapter provides insight into the scaffold's capacity to promote functional and scarless skin regeneration.

Chapter 4 covers the industrial development of collagen-elastin scaffolds, focusing on the translation of lab-scale formulations into clinically relevant, scalable biomaterials. The motivation for this work lies in the need to produce structurally consistent, cost-effective, and biologically active scaffolds suitable for large-scale manufacturing and widespread clinical use. To address this, twelve scaffold formulations are engineered with varying collagen-to-elastin ratios, different lyophilization techniques (room temperature vs. dehydrothermal treatment), and incorporation of chemical crosslinking. Each processing variable is chosen to assess its impact on scaffold architecture, stability, and bioactivity. The resulting materials are thoroughly characterized for their structural, morphological, chemical, mechanical and biological properties. Beyond optimizing scaffold performance, a secondary objective of this chapter is to evaluate the feasibility of large-batch fabrication processes that simulate industrial production workflows. This work bridges the gap between early-stage material design and scalable therapeutic application.

Chapter 5 shifts focus to elastogenesis beyond elastin-derived components to the broader biological regulation of elastogenesis. Given that elastin-derived components alone may not fully restore elastic fiber networks, this chapter explores whether selected bioactive compounds can stimulate elastin and ECM production in primary human dermal fibroblasts. Ten compounds from distinct biochemical categories are chosen based on literature evidence present in **Chapter 1**. The tested agents are retinoic acid (RA), dexamethasone (DXM), minoxidil sulfate (MNX), transforming growth factor beta 1 (TGF-β1), insulin-like growth factor 1 (IGF-1), copper sulfate ($CuSO_4$), dill extract (DE), magnesium ascorbyl phosphate (MAP, a stabilize vitamin C derivative), heparin (HEP), and γ-aminobutyric acid (GABA). A direct comparative analysis is conducted to identify the most promising candidates for promoting elastogenesis and collagenesis while ensuring safety and minimizing cytotoxicity. In addition to ECM-related outcomes, the potential of these compounds to influence scarring is also assessed. This chapter opens new avenues for integrating small-molecule strategies into the design of advanced biomaterials for enhanced dermal regeneration.

Finally, **Chapter 6** combines the key findings from this thesis and their broader implications for biomaterial design and testing, skin tissue engineering, and regenerative medicine.

1

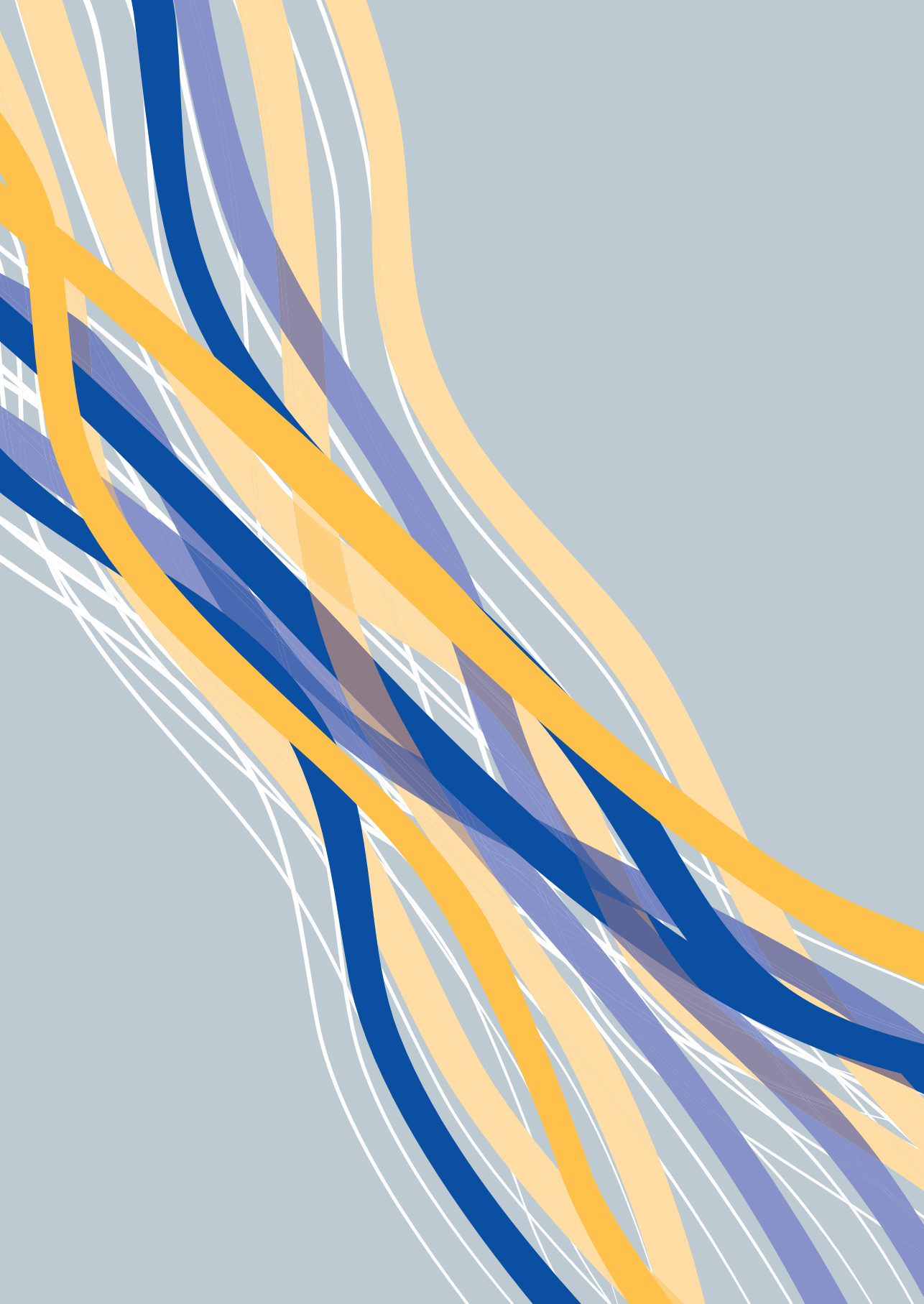

Chapter 1

Elastogenesis in focus: Navigating elastic fibers synthesis for advanced dermal biomaterial formulation

Roman Krymchenko[1], Gizem Coşar Kutluoğlu[1,2], Noor van Hout[3], Dominique Manikowski[2], Claudia Doberenz[2], Toin H. van Kuppevelt[1], Willeke F. Daamen[1]

[1] Department of Medical BioSciences, Research Institute for Medical Innovation, Radboud university medical center, PO Box 9101, 6500 HB Nijmegen, The Netherlands
[2] MedSkin Solutions Dr. Suwelack AG, 48727 Billerbeck, Germany
[3] Department of Dermatology, Radboud university medical center, 6525 GA Nijmegen, The Netherlands

Published in *Advanced Healthcare Materials* (2024, 13, 2400484).
DOI: 10.1002/adhm.202400484

Abstract

Elastin, a fibrous extracellular matrix protein, is the main component of elastic fibers that are involved in tissues' elasticity and resilience, enabling them to undergo reversible extensibility and to endure repetitive mechanical stress. After wounding, it is challenging to regenerate elastic fibers and biomaterials developed thus far have struggled to induce its biosynthesis. This review provides a comprehensive summary of elastic fibers synthesis at the cellular level and its implications for biomaterial formulation, with a particular focus on dermal substitutes. We delve into the intricate process of elastogenesis by cells and investigate potential triggers for elastogenesis encompassing elastin-related compounds, extracellular matrix components, and other molecules for their potential role in inducing elastin formation. Understanding of the elastogenic processes is essential for developing biomaterials that trigger not only the synthesis of the elastin protein, but also the formation of a functional and branched elastic fiber network.

1. Introduction

Elastic fibers provide elasticity and resilience to tissues and enable them to undergo reversible extensibility and endure repetitive mechanical stress. Elastin, a fibrous extracellular matrix (ECM) protein, is the main component of elastic fibers.[1] Major blood vessels, elastic ligaments, lungs and skin represent tissues with a relatively high content of elastin. Unlike other ECM proteins, elastin appeared relatively late in evolution, as it is present in almost all vertebrates, but absent in invertebrates and primitive jawless fishes.[2, 3] Moreover, elastin is one of the most durable proteins in the human body due to its very limited solubility and high metabolic stability. Its degradation rate varies from tissue to tissue. While it is more rapid for skin, it is slow for aorta and lungs with a half-life of 74 years for elastic fibers in lung parenchymal tissue.[4] Although there are no specific half-life values provided for human skin, rat experiments showed a twofold higher turnover compared to lungs.[5] In the course of our lives, degradation is getting more abundant than elastin synthesis, as evidenced by lower expression levels of tropoelastin and increased release of elastin degradation products such as (iso)desmosine.[6-9] Next to degradation rate, the architecture of elastic fiber network in skin differs significantly from that in aorta due to their distinct functional requirements and different content. Elastin comprises less than 5% of the dry weight of the skin,[10] where it is architecturally represented in a loosely organized, mesh-like network interwoven with collagen fibers in the dermis. In contrast, the elastin content in large arteries accounts for more than half of the dry weight,[10] with elastic fibers arranged in densely packed lamellar units with pores.

Elastic fibers are crucial in tissue homeostasis, but cannot be easily replaced when degraded.[11] Vollenweider Roten *et al.* clearly demonstrated the problem using a traditional elastin staining **(Figure 1)**. Non-wounded skin showed a network of elastic fibers in the papillary dermis, but scar tissue either showed thin and separate elastic fibers, thick elastin deposits or even lack of elastic fibers.[12] The protein elastin is not the only element of elastic fibers, as microfibrils are incorporated within and around the fibers. Microfibrillar components include, but are not restricted to, fibrillins, fibulins, latent transforming growth factor β binding proteins (LTBPs), microfibril associated glycoproteins (MAGPs), elastin microfibril interface–located proteins (EMILINs), and proteoglycans (e.g., decorin, biglycan, versican, perlecan).[13-16]

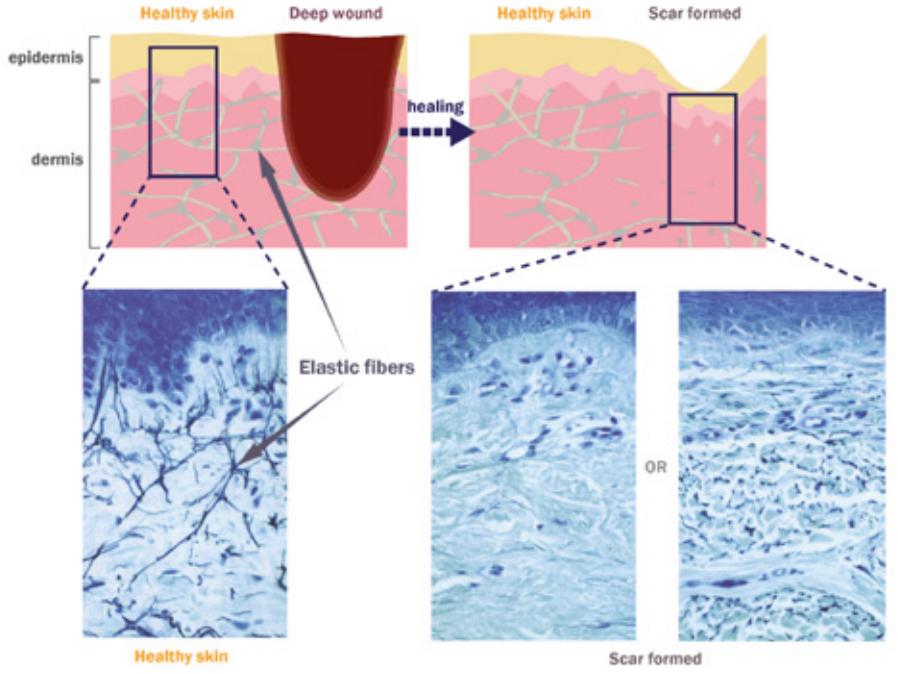

Figure 1. Elastic fiber networks in normal skin and scars. After skin repair, new extracellular matrix is synthesized, but human skin does not restore the network of elastic fibers (in blue/black) in the dermis (left). Instead, Miller's stain shows relatively isolated and thin elastic fibers (middle) or thick deposits that do not look interconnected (right). Miller's stained images were reproduced from Vollenweider Roten *et al.* with permission.[12] Copyright 1996, John Wiley and Sons.

All full-thickness skin wounds share one consequence – they lack the ability to regenerate and to gain the properties and architecture that were present before the injury, as observed from non-restored elasticity, absence of appendages and presence of scar tissue. At present, autologous split-thickness skin grafting remains the primary and one of the most effective choice after severe skin injuries.[17] Split-thickness graft involves transplanting a thin layer of skin, including the epidermis and part of the dermis. In terms of skin appearance after healing and formation of a scar, split-thickness graft showed better outcomes compared to a full-thickness graft, which involves the entire skin thickness.[18] However, coverage with autologous skin can be extremely challenging to perform when a huge part (e.g. more than 80%) of total body surface area is damaged and there is lack of donor site.[19] One option to overcome this can be the application of a dermal substitute with a silicon layer to prevent water loss and protect the wound bed from infection until the donor site regrows.[20] Further benefits of the application of dermal substitutes are that they act as scaffolds for new tissue ingrowth by facilitating

cell attachment, migration and proliferation. Therefore, they need to be porous, non-immunogenic and biodegradable, but they must also not only retain fluids enriched with nutrients crucial for cellular survival but also promote angiogenesis, ensuring the essential delivery of oxygen and nutrients while facilitating the efficient removal of waste products. The majority of dermal biomaterials on the market have collagen as the primary component,[21, 22] although chitosan, silk fibroin and other (bio)polymers may be used as alternative base components.[23] It is important to mention, that reports on currently available products gave varying results in literature. Some were reported to perform superior to skin autografting without any biomaterial applied in terms of clinical results of skin elasticity, diminishing wound contracture and providing better appearance,[24-28] although several competitive biomaterials showed similar outcomes compared to each other.[29-31] While others published that tested dermal biomaterials were not superior to skin grafting.[21, 32] If we specifically focus on the pliability of healed regions and the formation of new elastic fibers with dermal biomaterials, positive flexibility outcomes in clinics were still accompanied by immature, short and thick elastic fibers.[33]

In light of this, we would like to investigate the possibilities to design dermal biomaterials that may overcome the limitations of incomplete restoration of the elastic fibers network after wound healing and are able to fully regain lost resilience and elasticity.[33] Elastogenesis, the formation process of elastic fibers, can be described by three consecutive stages: i) tropoelastin synthesis; ii) coacervation; and iii) deposition and crosslinking. Tropoelastin is synthesized and subsequently secreted by elastogenic cells such as fibroblasts, endothelial cells, and smooth muscle cells (SMCs).[34-36] Upon secretion into the ECM, tropoelastin molecules self-assemble directed by hydrophobic forces, a process called coacervation. Tropoelastin aggregates are deposited onto a preformed microfibrillar network for further initiation of the crosslinking process by lysyl oxidase (LOX) and lysyl oxidase-like (LOXL) enzymes.[37, 38] Elastin itself, its precursor tropoelastin and synthetic analogues are promising candidates for biomaterials. However, some properties of elastin protein, such as its extreme insolubility, have generated challenges to the use of elastic fibers in biomaterials. At the same time, elastin is not merely a structural protein, but it contributes to various cellular activities as do elastin degradation products. That is why it is also important to understand the underlying processes inside the cell, such as the activation of receptors and signaling pathways. Although, in many cases, the corresponding information may be scarce or even uninvestigated. The increased understanding of the significance of elastin for wound healing is leading to a wider exploitation in biomaterials.

Creation of a high-quality, outperforming biomaterial requires a complex, interdisciplinary approach involving various specialists. The primary goal of a new biomaterial is the formation of extensive dermal elastic fiber network, resulting in reversable skin extensibility with a pleasant and healthy-like appearance, and the complete ability to perform any original physical movements. In this way, innovative dermal substitutes should enrich mechanical properties, providing a robust material for cell attachment, proliferation, and differentiation, which are crucial for effective tissue regeneration. We prioritize maximum patient safety; thus biomaterials must be biocompatible and non-toxic, thereby mitigating the risk of severe adverse reactions. For instance, we emphasize on carefully considered use of growth factors to avoid potential side effects, such as tumor cell proliferation. Cost-effective production techniques with utilization of readily available materials may attract both manufacturers and clinicians, since such substitutes can be scaled-up without compromising quality and are accessible to a broader market. In other words, the simplicity and versatility of a novel approach should satisfy the needs of both industry and healthcare sectors, with a clear mode-of-action of the components, bridging the gap between cutting-edge research and practical, real-world applications.

This review provides an overview of elastin synthesis on the cellular level and its potential use for formulation in biomaterials, particularly dermal substitutes, to induce formation of functional elastic fibers rather than merely elastin protein synthesis. We have evaluated various agents and different classes of compounds, including elastin-based substances, ECM-related proteins, growth factors, glycosaminoglycans, hormones, antioxidants, vitamins, metal ions and natural products. These substances demonstrated promising results in the *in vitro,* and some *in vivo,* platforms in increasing elastin production and supporting the formation of functional elastic fibers. These studies provide valuable information for the design of innovative biomaterial formulations to promote elastogenesis and improve clinical outcomes. However, further investigation is necessary to overcome foreseen obstacles, such as the molecular stability of these components, the ability for industrial production, safety tests, reasonable price, etc. The potential applications of these findings are considerable, and they are able to advance the field of tissue engineering and regenerative medicine.

2. Elastic fiber formation

The ELN gene is mainly expressed during the prenatal state and the first years of postnatal life after which its expression is almost completely repressed. Elastic fiber formation comprises the process from tropoelastin mRNA expression to elastic fiber crosslinking **(Figure 2)**. Upon extensive alternative splicing, mature tropoelastin mRNA is transported out of the nucleus and translated on the rough endoplasmic reticulum. After release of the signal peptide, the protein is passed to the Golgi apparatus.[39] In order to prevent aggregation and premature degradation of tropoelastin, the resulting 60-70 kDa polypeptide is chaperoned by the 67 kDa elastin-binding protein (EBP or S-Gal, an enzymatically-inactive splice variant of the lysosomal β-galactosidase with a sustained galactolectin binding site) and transferred to the plasma membrane in acidic intracellular compartments.[40-43] At the cell membrane, EBP associates with the 61 kDa neuraminidase-1 (Neu-1) and the 55 kDa protective protein/cathepsin A (PPCA). All three components together, EBP, PPCA and Neu-1, represent the elastin receptor complex (ERC). PPCA ensures integrity of the two other components and Neu-1 takes the central role in elastogenesis because its subsequent activation promotes the desialylation of microfibrillar proteins.[44-46] Exposure of galactosyl moieties on microfibrillar proteins allows binding of EBP, leading to the release of tropoelastin with subsequent self-aggregation through coacervation, deposition on microfibrils, crosslinking under the influence of lysyl oxidase and EBP recycling into the cell via secretory vesicles.[43, 45] In this process, microfibrils act as a framework that drives and guides elastin deposition. Elastin undergoes several post-translational modifications.[47] These modifications involve but are not limited to processes such as controlled proteolysis (cleavage of the signal peptide when the protein enters the lumen of the rough endoplasmic reticulum[39]), hydroxylation of proline residues in the endoplasmic reticulum,[48] and oxidative deamination of lysine residues outside the cell.[49] These modifications can tune elastin properties. For instance, hydroxyproline incorporation showed increased coacervation temperatures, changed alignment of elastin in a microfibrillar network, assisted crosslinking, stiffer fiber formations, and eventually decreased susceptibility to enzymatic degradation.[48] Experiments with fish skin revealed a higher content of proline and hydroxyproline residues in warm-water species compared to cold-water species.[50]

The protein tropoelastin contains alternating hydrophilic and hydrophobic domains. Hydrophilic domains, containing lysine residues, are responsible for crosslinking, while valine, proline, alanine and glycine in hydrophobic domains

are important for elastin's elasticity.[51] Many crosslinks in elastin are represented by unique amino acids characteristic for elastin e.g., desmosine and isodesmosine **(Figure 3)**. Enzymes in the ECM, lysyl oxidase and lysyl oxidase like 2, catalyze the reaction of oxidative deamination of lysine residues in tropoelastin.[52, 53] The resulting allysine residues can spontaneously form bonds with other allysine or lysine residues through aldol condensation or formation of a Schiff base. These bifunctional products of condensation can attach to other fragments and form tri- (dehydromerodesmosine and neodesmosine), tetra- (desmosine and isodesmosine), or even pentafunctional (pentasine and allodesmosine) crosslinks. Moreover, crosslinks can be classified by the number of participating monomers of tropoelastin (intramolecular or intermolecular) or crosslinking domains (intradomain or interdomain).[49] Condensation can be interrupted at any stage through reduction reactions. For example, dehydrolysinonorleucine and dehydromerodesmosine can be transformed into lysinonorleucine and merodesmosine, respectively. Desmosine and isodesmosine are used as biomarkers due to their unique appearance in elastin.[54-57]

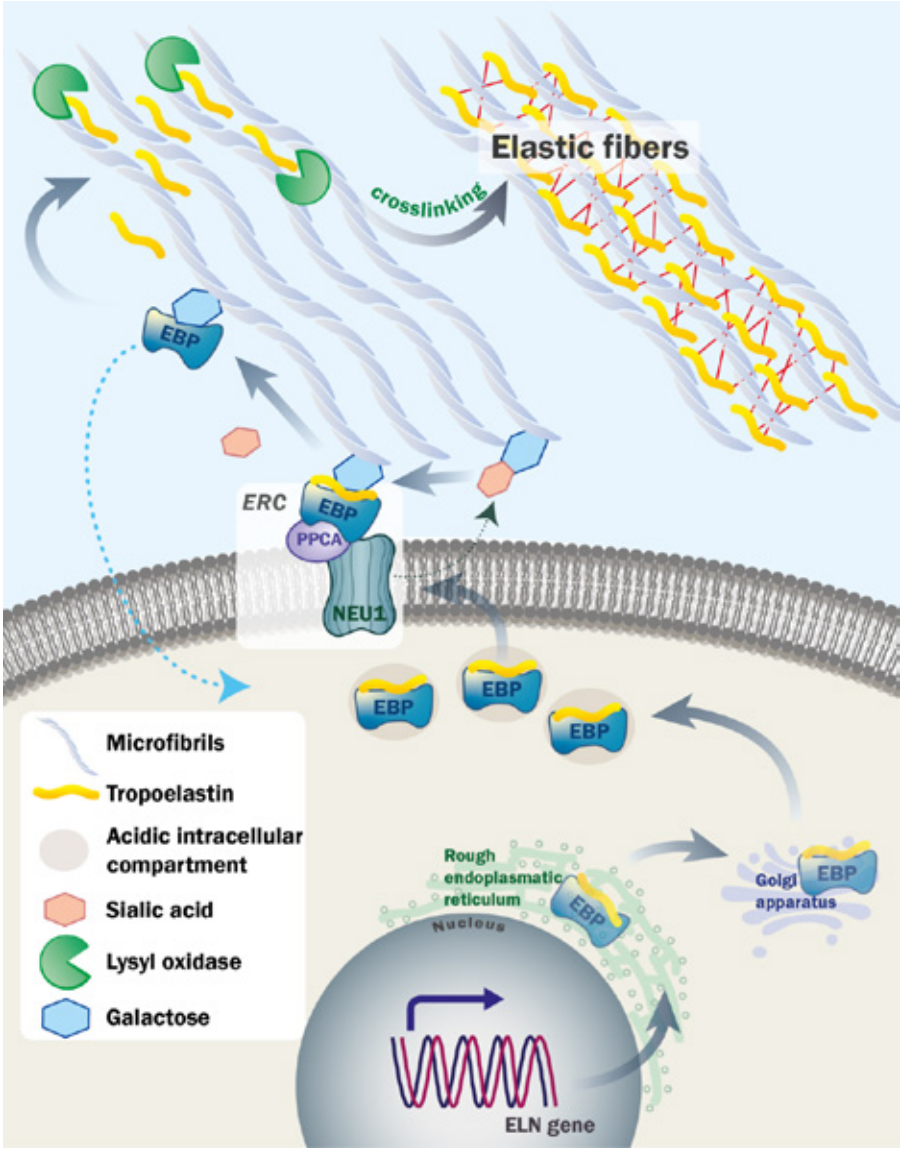

Figure 2. Elastogenesis at the cellular level. Tropoelastin mRNA is transported out of the nucleus, translated on the rough endoplasmic reticulum, and elastin protein is chaperoned by the elastin-binding protein (EBP), passed to the Golgi apparatus, and then transferred to the plasma membrane. EBP associates with transmembrane neuraminidase-1 (Neu-1) and the protective protein/cathepsin A (PPCA) to form the elastin receptor complex (ERC). Neu-1 activation promotes desialylation of microfibrillar proteins, while exposure of galactosyl moieties facilitates the interaction with EBP, followed by the release of tropoelastin. Subsequent self-aggregation of tropoelastin occurs via coacervation. Tropoelastin aggregates that are deposited onto microfibrils are further crosslinked by lysyl oxidase and EBP is recycled back into the cell via secretory vesicles. The figure is based on reports from Pshezhetsky and Hinek,[58] Bennasroune *et al.*,[45] Schmelzer *et al.*,[49] and Tembely *et al*.[42]

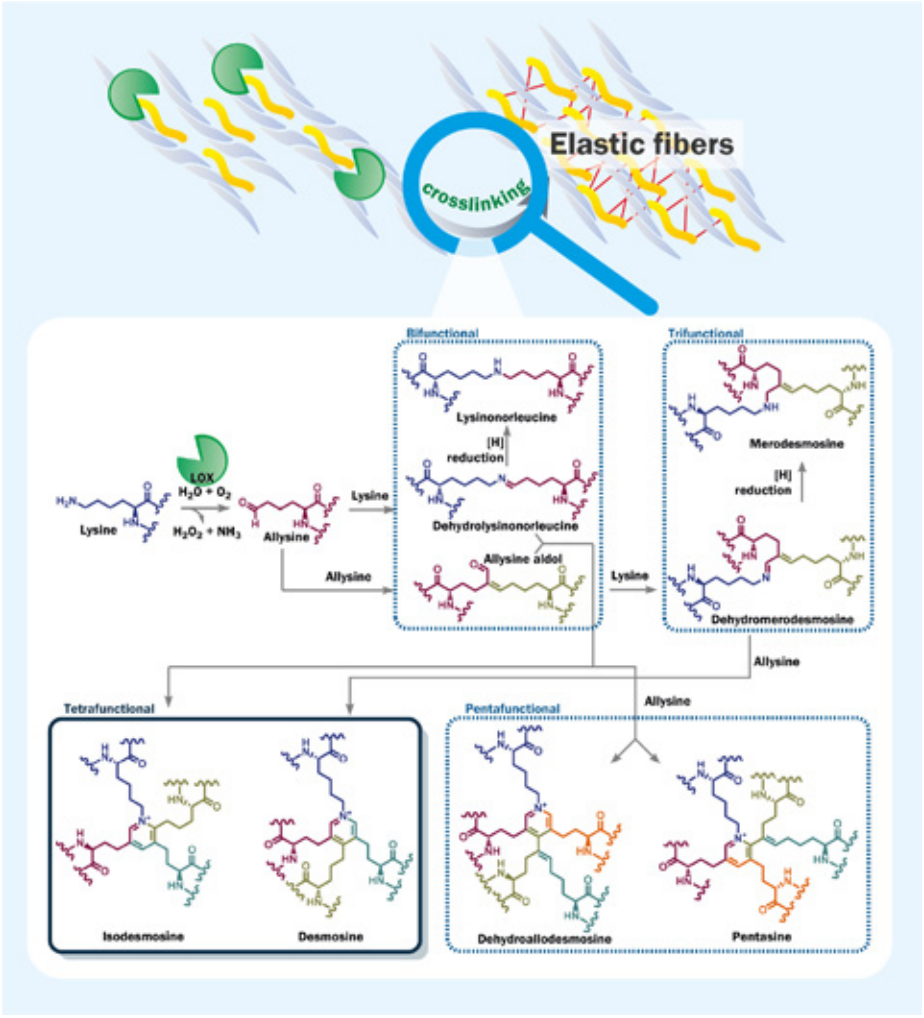

Figure 3. Molecular crosslinks found in elastin. Lysyl oxidase (like) enzymes (LOX) catalyze oxidative deamination of lysine residues. Aldol condensations and formation of Schiff bases are the major reactions for combining the molecular fragments. The formed products can form bifunctional, tri-, tetra-, or pentafunctional crosslinks. Desmosine and isodesmosine can be found only in elastin and are used as biomarkers. Amino acids are depicted in different colors, highlighting their input in the obtained structures.

Some pathological conditions and genetic mutations affect proper elastogenesis, and can be associated with mutations in genes encoding for elastin or elastin-associated proteins.[59, 60] Some diseases are causing abnormalities in dermal elastic fibers and skin characteristics. For instance, cutis laxa, a condition characterized by loose, sagging and wrinkled skin is a genetically diverse condition including mutations in genes coding for elastin, fibulin-4, fibulin-5, lysyl oxidase, latent TGFβ-binding protein 1,

and ATPA7, a protein involved in copper transport.[61, 62] Such skin harbors sparce and fragmented elastic fibers, and lacks elasticity, elastic recoil and resilience. Next to skin, other organs, notably the lung, are affected. Marfan syndrome, a multi-systemic disease caused by mutations in the gene encoding fibrillin-1, is associated with aortic aneurysm/dissection as a life-threatening condition.[63] It is characterized by a tall and thin stature with long extremities including arms, legs and fingers. Degradation and loss of elastic fibers lead to a weakened skin with stretch marks (striae).[64] However, in stiff skin syndrome, also associated with mutations in the gene for fibrillin-1, the skin is thick and hard and excessive skin fibrosis is seen.[65] Although the phenotypes of Marfan syndrome and stiff skin syndrome are quite different, disregulation of TGFβ seems a common denominator, as fibrillin-1 is known for its role in sequestering TGFβ. The deletion 7q11.23 syndrome (Williams-Beuren syndrome) is caused by a hemizygous deletion of 1.5 – 1.8 Mb on chromosome 7q11.23 spanning about 28 genes, including the elastin gene. Soft, lax skin and arterial stenosis are characteristics of the disease.[66, 67] The vocal cord abnormalities (hoarse or low-pitched voice) have been correlated to the elastin deficiency.[68] In the 7q11.23 duplication syndrome, a duplication is seen of a similar DNA segment that is deleted in the Williams-Beuren syndrome, including the elastin gene.[67] It has been suggested that the extra copy of the elastin gene may result in an increase in the amount of tropoelastin giving rise to the aortic dilatation observed in this syndrome. Taken together, pathologies caused by genetic defects in genes coding for proteins that make up the elastic fiber network underscore its relevance not only for endowing structural elasticity to organs, but its role in preserving overall body homeostasis.

While the mechanism of elastic fiber synthesis is well investigated[38, 69-71], many questions remain about what induces or halts this process. A variety of compounds, however, have been implicated as promotors of elastogenesis, as can be appreciated in the next section.

3. Potential inducers of elastic fiber formation

In order to steer repair more towards a regenerative process, functional elastogenesis induced by biomaterials is one of the goals of dermal substitute materials to restore elastic and resilient properties of the healed skin.

To ensure a comprehensive narrative review, we performed our search in PubMed and Google Scholar using corresponding keywords, such as “elastin”, “elastogenesis”,

"elastic fibers", "elastogenic effect", "dermal substitutes", "biomaterials" and "wound healing" for articles published up to 2023 in English. Inclusion criteria involved peer-reviewed studies focused on (dermal) elastogenesis, and the development and application of dermal substitutes. Exclusion criteria included non-peer-reviewed articles, personal websites, irrelevant studies, and those with obvious methodological flaws. Titles and abstracts were screened for relevance, followed by a detailed full-text review and data extraction. Some articles were included based on information (reference list) of retrieved papers. A summarizing table of evidence was included in order to better compare the selected compounds and making a selection of the most promising candidates.

Different elastin derivatives have been investigated as potential ingredients in biomatrices, but their effect on cells was highly dependent on various factors such as the state of elastin (soluble or insoluble), concentration of soluble compounds, amino acid sequence and cell type.[72, 73] For instance, low concentrations of elastin hydrolysate in 2D cell culture (10–100 µg/ml) led to cell proliferation of human lymphocytes, whereas high concentrations induced apoptosis in these cells.[74, 75] The ERC does not only play a role in elastogenesis to deposit elastin onto microfibrils and proper assembly of the fibers,[46] but it can also transduce intracellular signals and modulate bioactive elastin degradation products, so called elastokines.[76, 77] Binding of compounds to the ERC activates internal signaling pathways which can cause cellular responses, like elastogenesis,[34, 78] chemotaxis,[79] proliferation,[80] angiogenesis,[81] and apoptosis.[75] While EBP protected with PPCA can form complexes with elastin peptides and galactosugars (e.g., lactose), Neu-1 is crucial because of its ability to desialylate glycoproteins and glycolipids, and consequently modulate the signal transduction pathways of such compounds. Neu-1 can interact with a variety of additional surface receptors, expanding the biological or pathological impact of elastin-derived or elastin-resembling peptides.[39] Elastin-derived peptides may interact with other proteins than the ERC, e.g. galectin-3.[82] Moreover, other receptors that are known to sense elastin-derived peptides include a lactose-insensitive receptor (or ribosomal protein SA[83]) and cell adhesion transmembrane receptors (e.g. integrins $\alpha_V\beta_3$[84] and $\alpha_V\beta_5$[85]). Hence, depending on the type and concentration of an elastogenic compound, the underlying mechanism may differ, as could the eventual effects.

In the following sections we discuss different strategies to promote elastogenesis, i.e. by applying elastin-based components or by other compounds that trigger elastic fiber production, (extracellular matrix components, hormones, potassium channel openers, natural products, metals, antioxidants, vitamins, etc). **Table 1**

summarizes the elastogenic evidence for most of the compounds discussed, indicating their level of evidence. We here focus on compounds that promote the restoration of a network of elastic fibers resembling those in healthy skin tissues. Where such effects have not been tested in dermal cells, different cell types are exemplified.

3.1. Elastin-based components

Elastin-based components, i.e., insoluble elastic fibers, elastin-derived peptides and tropoelastin protein/mRNA, are particularly interesting as they mimic natural conditions and/or compositions and either contain the natural crosslinks or may be crosslinked later **(Figure 4)**. Depending on their physical properties and stability these components can be used in different ways, such as by incorporation into biomaterials[86-92] or as intradermal injections[93], and can be found naturally in decellularized extracellular matrix.[94] Different species possess particular differences in amino acids composition of elastin proteins, thus porcine, bovine and human elastin are not identical but share a lot of similarities.[95] Using sequences available in the UniProt database and the Basic Local Alignment Search Tool, we have compared the alignment of rat, porcine and bovine elastin proteins with humans and obtained 77%, 82% and 86% amino acid alignments, respectively. When animal-origin elastin is used for biomaterials, possible issues related to this aspect, e.g. immunogenic response and calcification, should be considered during *in vivo* testing of novel biomaterials.[89, 96, 97] Since it is difficult to appreciate the specific effects related to elastin in decellularized biomaterials due to their complex composition with many other extracellular matrix components, they will not be discussed in this review.

3.1.1. Insoluble elastic fibers

Elastic fibers provide the necessary mechanical characteristics of resilience and elasticity that are crucial for the functioning of elastic tissues. Although the approach of using elastic fibers in biomaterials formulation for enhancing elasticity is compelling, there are several complications with this idea. First of all, elastic fibers in healthy tissues form a complex network with other ECM components and it is challenging to replicate such networks.[98] Naturally crosslinked elastin that is present in elastic fibers (~90%[98]) in its intact state is highly insoluble in water and rather inert to both intrinsic and external impacts. When elastic fibers are isolated and purified they differ from intact fibers due to mechanical processing (like pulverization) and chemical treatments.[15]

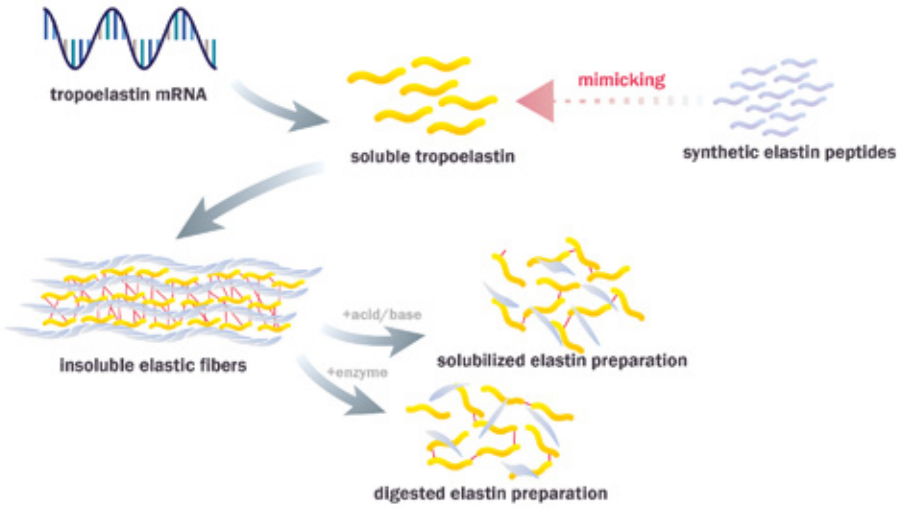

Figure 4. Major elastin-based components and their interconnection. Translation of tropoelastin mRNA leads to the soluble tropoelastin protein, that may be mimicked by (smaller) elastin peptides and polypeptides. Mature insoluble elastic fibers may also be solubilized by chemical agents or digested by enzymes, leading to soluble fragments.

Insoluble elastic fibers as the sole component of biomaterials are not likely to be used as a component of elastogenic biomaterials, which may be due to the above mentioned inertness and high insolubility of the fibers. Nevertheless, insoluble elastin demonstrated its ability to impact physical properties of biomaterials by decreasing the rigidity of collagen scaffolds and enhancing viscoelastic characteristics.[99-101] Biological effects of biomaterials containing isolated insoluble elastin included promotion of a contractile phenotype of SMCs in collagen-elastin and selective proliferation of primary human keratinocytes co-cultured with fibroblasts.[102, 103] In addition, these materials exhibited calcification of soft tissue in a young Sprague-Dawley rat model, highly sensitive to forming calcium deposits.[89] Combining obstacles with utilization of insoluble elastin, researchers focused on solubilized forms of insoluble elastin.

3.1.2. Solubilized elastin

Elastin is repeatedly subjected to a range of enzymatic, chemical and biophysical stimuli during our lifespan that may (partly) solubilize elastin.[11] Generally, there are two approaches to solubilize elastin from its insoluble form in the laboratory: enzymatic digestion and chemical treatment.[104] Like tropoelastin during

elastogenesis, digested and solubilized elastin display lower critical solution temperature behavior that allows it to coacervate from a mixture above a certain temperature and revert to the soluble form when the temperature is lowered under the lower critical temperature.[105] Self-assembly properties are also influenced by amino acid composition, pH and ionic strength.[106] The stimulus-responsive properties make solubilized elastins a promising material in drug delivery systems, medical devices and tissue engineered constructs, including dermal substitutes. Their coacervation profile, however, is also dependent on the solubilization method, where significant prolongation of hydrolysis time can even deprive this ability of solubilized elastin preparations.[105]

Enzymatic digestion

Elastolytic enzymes can be divided into four categories: serine, cysteine (mainly cathepsins), aspartic proteases, and zinc-dependent endopeptidases (matrix metalloproteinases). For each category, data about cleavage specificity for elastin and tropoelastin are available.[104] Elastic fibers that experienced some prior damage are more readily degraded by enzymes.[107] Preparation of solubilized elastin via degradation of naturally occurring elastic fibers is a promising approach for induction of elastogenesis due to its properties to promote elastin-enriched matrix deposition and mimicking processes that are occurring in the human body.[108] For instance, bovine elastin digested with proteinase K resulted in a preparation with molecular weight of ≤10,000 Da and showed enhanced elastogenesis with primary human dermal fibroblasts, skin explants and pre-treated fibroblasts implanted in the dermis of athymic nude mice.[108] The *in vitro* experiments demonstrated induced formation of collagen fibers and elastic fibers along with elevated proliferation of the cells, accompanied with decreased expression of fibronectin and chondroitin sulfate proteoglycans. More elastin deposits were noticed in *ex vivo* experiments as well. Furthermore, abundant elastic fiber network production was seen in mice after injection of fibroblasts stimulated with the elastin digest.[108] Also fish-derived elastin treated with two enzymes -protin AC10 and protease N- resulting in a digest with a molecular weight around 1,000 Da, increased proliferation and elastin production by primary human dermal fibroblasts.[109] Although enzymatic digestion results in specific cleavage at certain amino acid residues in elastin, they are costly (especially for human elastases), may be contaminated with endotoxins and still give a large molecular weight distribution of soluble elastin. In addition, the high affinity of enzyme to elastin makes it difficult to remove the enzyme after solubilization. These drawbacks to produce active ingredients for biomaterial formulation may cause serious issues in further clinical translation and substantially raise costs for production.

Chemical hydrolysis

In contrast to enzymatic digestion, bond cleavages are non-specific when solubilization is performed using oxalic acid that results in α-elastin along with β-elastin or potassium hydroxide that results in κ-elastin.[105] Fractionation after chemical treatment may be performed, for instance by chromatographical methods like size exclusion chromatography. We would like to stress that the terms 'α-elastin' and 'κ-elastin' still refer to mixtures of soluble compounds and not to a single component. Thus, it is important to check the characteristics of such formulations from different publications when comparing biological activities. Note that specificity of chemical hydrolysis is by definition lower than for elastases. The use of large amounts of bases and organic solvents or acids is a drawback of the methodology, as is the extremely wide range of molecular weight for obtained preparations (up to 2,000 kDa). However, these methods come with straightforward removal of the used compounds and obtained molecular weights can be lowered with longer incubation or higher temperature.

Elastin-derived peptides from acidic or alkaline hydrolysis can promote elastogenesis and replenish the elastin content in wounds when incorporated in biomaterials.[89, 110, 111] In a porcine model, the elastin component in scaffolds containing type I collagen α-elastin was responsible for reduced contraction of the wound along with decreased numbers of myofibroblasts and formation of native collagen bundles.[110, 112] Additionally, these scaffolds revealed fewer fibroblasts in the early wound healing phase compared to other tested constructs.[112] Implantation of a scaffold containing a similar combination of elastin-derived peptides produced by oxalic acid hydrolysis and type I collagen in young rats induced neovascularization and synthesis of thin elastic fibers containing fibrillin-1.[89] MatriDerm®, a commercially available dermal substitute composed of types I, III, and V collagen and α-elastin hydrolysate, evidenced improved healing process in terms of function and appearance by minimizing contractures and increasing skin elasticity.[113, 114] κ-elastin fraction with a specified molecular weight of 75 kDa enhanced adhesion and alignment of insoluble elastic fibers to human dermal fibroblasts and may serve as a reagent for oriented elastogenesis.[115] It is noteworthy that KOH-solubilized elastin can ultimately lead to insulin resistance of the cells due to desialylation of the insulin receptor by activated Neu-1 and reduced insulin receptor signaling as seen in mice.[116] In biomaterials, chemical modifications can provide additional properties to solubilized elastin preparations on demand. Conjugation of acrylate groups onto elastin solubilized with oxalic acid resulted in an injectable hydrogel that was photocrosslinked by visible light. This hydrogel accelerated dermal wound healing along with active recruitment

of neutrophils and macrophages, followed by subsequent polarization of macrophages primarily toward the pro-regenerative M2 phenotype. Recruitment of innate immune cells thereby promoted angiogenesis, collagenesis and dermal repair in a murine full-thickness skin defect model.[87]

3.1.3. Synthetic elastin peptides

Soluble elastin compounds can also possess much smaller molecular weights compared to solubilized elastins. Small bioactive elastin peptides from human elastin are generally generated from building blocks of Gx, Px, PGx and GGx (where x = A, G, V, I or L) of the hydrophobic domains, VGVAPG sequence being the most investigated one.[104] The biological activity of the GxxPG sequence was explained by its capacity to take a type VIII β-turn conformation, crucial for binding to EBP.[104] Different xGVxxG sequences, found in elastin, rice bran, and the human IGF-1 binding protein 1, activated elastogenesis in cultures of human primary dermal fibroblasts.[78] Moreover, the presence of such moieties in high molecular weight hydrolysates or the exposure of such sequences in damaged elastic fibers may explain sensing of these compounds by transmembrane receptors to activate different intracellular signaling cascades.

Elastin-like peptides (ELPs) and elastin-like recombinamers (ELRs) resemble hydrophobic sequences of natural tropoelastin and represent a vast category of synthetically made or genetically engineered polymers made up of repeated oligopeptides, generally with a specific pH-temperature-ionic strength coacervation profile.[117] ELPs/ELRs are beyond the scope of this review, however they serve as a promising tool in wound healing.[118] For further familiarization with ELPs/ELRs some publications are recommended.[119-121]

3.1.4. Tropoelastin protein

Another approach to stimulate elastogenesis is to skip the tropoelastin synthesis phase within the cell, and directly introduce the elastin precursor tropoelastin. Initially, tropoelastin used to be obtained from copper-deficient animals[122] (copper is an essential cofactor for crosslinking by lysyl oxidase) or by administration of lysyl oxidase inhibitors[123] as part of the animals' dietary regimen. However, nowadays tropoelastin can be obtained from fetal and neonatal tissues, but recombinant techniques provide the largest yields.[124] Recombinant human tropoelastin has shown to be exploited as a substrate for the production of branched elastic fibers network *in vitro*.[125] Meanwhile in rats, immunostaining of injected human recombinant tropoelastin monomers and host elastin did not show colocalization. However, tropoelastin has been tested crosslinked with hyaluronic acid, an essential

ECM component (see section 3.2.2) that is also involved in wound healing processes among various other characteristics.[126] The crosslinked combination of tropoelastin and hyaluronic acid demonstrated proper incorporation of exogenous tropoelastin in a newly synthesized elastic fiber network in rats.[125] *Ex vivo* experiments with such a crosslinked preparation demonstrated improved moisture content and deposition of acidic glycosaminoglycans compared to untreated controls.[125] Chemical modifications have also been applied to tropoelastin to enable visible light photocrosslinking of biomaterials. Conjugation of methacrylate groups onto recombinant human tropoelastin and gelatin offered a novel antimicrobial sprayable and flexible adhesive for future management of chronic wounds.[127] This approach can also be used for the production of dermal biomaterials.

Despite several examples of promising biomaterials based solely on recombinant tropoelastin for healing of full-thickness skin wounds in pigs and mice,[128, 129] tropoelastin usually serves as an additive to biomaterials.[34, 86, 130] Elastogenic potential was not assessed after application of scaffolds made from tropoelastin alone, however it was studied upon injections of aqueous tropoelastin in a swine burn wound model. When tropoelastin was administered after wound closure, it showed substantially increased elastic fiber synthesis than when supplied earlier after wounding. Newly formed elastic fibers appeared thin, disorganized and fragmented.[93] Hence, it is essential to investigate the long-term outcomes in order to comprehensively assess the impact on triggered elastogenesis. Tropoelastin incorporation into biomaterials can lead to improved dermal wound healing with induced elastogenesis. For instance, stimulated elastogenesis by human vascular smooth muscle cells in culture was achieved in a controllable manner using tropoelastin applied onto the scaffolds fabricated from fibrin, type I collagen, and chondroitin-6-sulfate. It is noteworthy that only a particular drop-loading technique of tropoelastin onto the cells incorporated in the scaffold resulted in lamellar mature elastic fibers.[34] Commercial two-layered Integra® Dermal Regeneration Template (crosslinked collagen with chondroitin-6-sulfate glycosaminoglycan covered with a silicone sheet) can be additionally functionalized with tropoelastin. One approach was to seed patient's fibroblasts on the collagen-glycosaminoglycan layer of Integra®, culturing them in the presence of tropoelastin to prefabricate elastic fibers before implantation.[131] Isolated from donors ranging from neonatal to more than 90 years old, fibroblasts originating from older participants produced fewer and less branched elastic fibers. The other method of functionalization of Integra® with tropoelastin was based on covalent conjugation of tropoelastin during the production stage.[132] Compared to Integra® alone, tropoelastin-Integra® demonstrated early vascularization in mice and pigs with small capillaries

after 2 weeks and considerably more new blood vessels in the deep neodermis. However, no specific report was made on synthesis of elastic fibers.

Moreover, skin substitutes using human type I collagen and recombinant human tropoelastin were produced by electrospinning, a technique that yields fibers/threads using electric forces.[86, 130] Such scaffolds were able to promote re-epithelization and deposition of new elastic fibers as well as a more natural extracellular matrix at the healed site in mice.[130] Full-thickness wounds in diabetic mice treated with an electrospun collagen-tropoelastin skin substitute demonstrated better resemblance of tissue mechanics with intact skin compared to commercial Oasis® Wound Matrix (an acellular ECM derived from porcine small intestinal submucosa).[86] Hence, scaffolds that contain tropoelastin may particularly aid healing of chronic wounds along with a lower chance of wound dehiscence.

3.1.5. Tropoelastin mRNA

Even though it is widely acknowledged that elastin biosynthesis ceases in adult tissues, it was demonstrated that transcription levels of pre-mRNA of tropoelastin in adults are similar to neonatal lung tissue.[133] It was hypothesized that posttranscriptional mechanisms rather than transcriptional changes influence elastin deposition since the change was mainly caused by decreased stability of tropoelastin mRNA.[134-137] Supporting this hypothesis, mRNA stability is also reduced by exogenous factors such as ascorbic acid.[138] It may be a promising approach to find factors that enhance elastogenesis by stabilizing tropoelastin mRNA.

One such example is that synthetically modified tropoelastin-encoding mRNA enhanced the stability by attaching a poly-A tail at the 3' and a cap analogue at the 5' end, thereby increasing elastin synthesis in umbilical vein endothelial cells, fibroblasts, and mesenchymal cells.[6] After intradermal administration of synthetic mRNA by microinjection, elastin protein content in porcine skin increased by about 20%.[6] Although *ex vivo* proof of principle is given, extensive *in vivo* studies are needed to assess whether elastin deposits result in functional elastic fibers.

Despite the use of synthetic mRNAs as a novel therapy for the creation of desired proteins in cells has attracted increasing attention in recent years,[139, 140] limited stability of mRNA is the obstacle that should be taken into consideration. Nonetheless, mRNA vaccination strategies, obviously progressed after the SARS-CoV-2 outbreak, with various delivery systems and the gained knowledge can

be used in the development of tropoelastin mRNA delivery methods.[141] For instance, peptide-mRNA nanoparticles in porous collagen scaffolds have shown efficient mRNA transfection of cells *in vitro* which resulted in local protein production.[142] Thus, this approach may be utilized in dermal biomaterials in order to promote elastogenesis.

3.2. Extracellular matrix components

Extracellular matrix components not only ensure structural integrity but are also required for elastogenesis and have been investigated to understand how they contribute to elastogenesis based on four categories: i) elastic fiber associated components, ii) proteoglycans and glycosaminoglycans, iii) ECM-associated growth factors/cytokines, and iv) collagens. It is noteworthy that growth factors and cytokines are not typically components of the extracellular matrix proper itself, but are generally stored there and are produced by other cells than they are acting on. However they play important roles in the cellular activities that occur within the extracellular matrix.

3.2.1. Elastic fiber associated components

Elastic fiber-associated proteins such as fibulins, fibrillins, fibronectin and latent TGFβ binding protein-4 (LTBP-4), play a role during various elastogenesis stages, instructing and/or facilitating particular processes.[143] Exogenous administration of some of these components have improved elastogenesis, e.g. in cell culture, and they may thus be of interest for incorporation in dermal templates.

Fibrillin-1 is involved in the construction of microfibrils, and plays an important role in wound healing as was shown with a periodontal disease model, where wound healing delayed with decreased fibrillin-1 expression[144] and fibroblasts differentiated into alpha smooth muscle actin (α-SMA)-positive myofibroblasts.[145] In absence of cells, recombinant fibrillin-1 protein improved self-assembly of recombinant elastin-like polypeptide.[146]

Fibronectin is also required for elastic fiber assembly.[147] Fibronectin is an adhesion molecule that contributes to the formation of extracellular matrix during wound healing by providing cell-cell and cell-extracellular matrix signaling via specific binding sites in its structure.[148] Exogenous fibronectin has been shown to play a role in scaffold remodeling by SMCs seeded in collagen gels toward the production of an elastic fiber-containing ECM.[149] Furthermore, it improves biomaterial stability,[150] cell adhesion, migration and proliferation,[151] making it an excellent candidate for use in skin tissue materials. Human dermal fibroblast

adhesion and proliferation are enhanced by fibronectin-functionalized hydrogel in comparison to fibronectin free hydrogel.[152]

Fibulin-5 plays a crucial role in the formation and organization of elastic fibers by interacting with them and acting as a ligand for specific cell surface integrins, namely $\alpha_5\beta_1$, $\alpha_v\beta_3$, and $\alpha_v\beta_5$. This interaction allows fibulin-5 to bind to important structural components such as tropoelastin and fibrillin-1, as well as crosslinking enzymes that aid in the formation and assembly of elastic fibers. Thus, fibulin-5 helps to stabilize and organize elastic fibers in various structures, including the skin, lungs, and blood vessels.[153, 154] In serum-free skin fibroblast cultures, the addition of fibulin-5 protein enhanced the development of elastic fibers, whereas tropoelastin was not organized into elastic fibers in its absence.[155]

Latent TGFβ binding protein-4 (LTBP-4) is another significant protein for elastogenesis and interacts with fibulin-5 in order to cause a proper assembly of elastic fibers.[156] Human dermal fibroblasts were found to assemble microfibrillar components and elastin protein into elastic fibers when the cell culture medium was supplemented with recombinant LTBP-4S protein, a short isoform of LTBP-4.[156] Beneficial effects of recombinant LTBP-4S protein were further exploited using crosslinked collagen scaffolds. (Immuno)histological analysis demonstrated that the presence of LTBP-4S in both 3D cell cultures of dermal fibroblasts on collagen scaffolds and in collagen dermal substitutes implanted between the dermis and cutaneous muscle of mice improved elastogenesis.[157]

As elastic fiber components are needed for proper assembly, alignment and cross-linking of tropoelastin, they are interesting candidates for functional elastogenesis in dermal substitutes.

3.2.2. Proteoglycans and glycosaminoglycans

Proteoglycans consist of a core protein to which one or more glycosaminoglycan chains (GAGs) are bound. They are important structural components of the extracellular matrix, and their ability to modulate elastogenesis is promising in the regulation of elastin synthesis and deposition during wound healing. As polyanions, GAGs bind to positively charged lysine residues in a temperature and concentration dependent manner and may facilitate tropoelastin release from EBP to promote coacervate formation and elastin deposition.[158-160] However, not all GAGs are advantageous for elastogenesis. GAGs containing galactosamines, such as chondroitin sulfate and dermatan sulfate, bind to EBP and disrupt elastic fiber formation.[158, 161] Gene delivery of V3, a versican isoform

that lacks chondroitin sulfate, enhanced elastic fiber assembly and reduced SMC proliferation.[162] Upregulated expression of versican V3 led to enhanced tissue stiffness of engineered skin and vascular grafts, and elevated both tropoelastin expression and insoluble elastin protein deposition.[163, 164] In Hurler disease and Costello syndrome, the opposite is seen as accumulations of chondroitin sulfate and dermatan sulfate proteoglycans are linked to impaired elastogenesis.[163, 165] Chondroitin sulfate containing dermal matrix, Integra®, did not demonstrate the elastic fiber formation when implanted in mice skin wound, unlike other tested dermal matrices without chondroitin sulfate.[166] This dermal matrix also did not show elastic fibers formation after 2 years from application in humans.[167] Disaccharides from marine chondroitin sulfate, however, increased elastin protein synthesis by human dermal fibroblasts.[168]

Hyaluronan or hyaluronic acid (HA), a large non-sulfated GAG, is a key component in skin tissue regeneration and wound healing. This compound is known to possess a high affinity for water and readily attract and retain moisture, provide structural support during early stages wound healing, and can demonstrate molecular weight-dependent functions, such as anti-inflammatory responses, angiogenesis, antioxidative properties, cells migration and proliferation.[169] In addition to abovementioned properties, hyaluronan plays a key role in elastogenesis by promoting tropoelastin self-assembly, lysyl oxidase-mediated crosslinking, and preserving elastic fibers from degradation.[170, 171] A mixture of low and high molecular weight HA resulted in elastin gene expression and elastin protein deposition in a co-culture of human keratinocyte and dermal fibroblast cell lines.[172] Synthesis of collagen and elastin at the mRNA and protein level was improved upon injection with a high molecular weight hyaluronan gel in Phenion®, a commercial full-thickness skin model. The elastogenic effect of hyaluronan gel was higher when combined with sulfate-free chondroitin.[173] HA-based dermal fillers added to dermal fibroblast cultures improved the production of elastin, type I and type III collagen together with TGF-β1 levels in the cultures.[174] Exogenous administration of hyaluronan oligosaccharides (tetra- to octamers) enhanced tropoelastin synthesis and elastin deposition by SMCs nearly threefold. Furthermore, surface-immobilized tetramers improved elastic fiber organization and induced SMCs to generate significantly more elastin-stabilizing desmosine crosslinks.[175, 176] Encapsulation of rat aortic SMCs in a hydrogel containing hyaluronan tetramers doubled their elastin-matrix production in 21 days, which is thought to be related to HA oligomer interaction with cell surface receptors such as CD44.[177] Moreover, intradermal injections of different HA-containing dermal fillers showed elastogenic properties *in vivo* and in a clinical trial with 60 patients.[178-180] There is also a commercially

available Hyalomatrix dermal template, an esterified hyaluronan scaffold covered with a silicon layer.[181] To the best of our knowledge, there is a lack of convincing evidence for significant elastogenic properties *in vivo* with Hyalomatrix,[182] though a thorough assessment with appropriate competitors is recommended.

Heparan sulfate and heparin are both GAGs with a similar chemical structure, but heparin has a higher degree of sulfation. The binding sites for heparan sulfate and heparin in fibrillin-1 play a crucial role in the binding of fibrillin-1 molecules along heparan sulfate chains and the assembly of microfibrils.[183] For instance, heparan sulfate is involved in the assembly and stability of elastin coacervates and has been shown to promote tropoelastin assembly when exogenously provided to human dermal fibroblasts.[184] Heparin mediates the coacervation of positively charged tropoelastin due to its high negative charge density[185] and possesses anti-proteolytic properties that inhibited leukocyte elastase by 85-95%, which may be exploited as a protecting agent for existing elastic fibers.[186] In actively growing SMCs, heparin increased elastin mRNA expression 2-3 fold, but this effect weakened when cells aged.[187] Moreover, a heparin-releasing biomaterial system based on silk enhanced elastic fiber production by SMCs.[188]

HA and heparin may be the most interesting glycosaminoglycans for biomaterials as they can be commercially obtained. Hyalomatrix®, a HA containing collagen template, improved wound healing in burn patients, however, further research is needed to determine its effect on elastogenesis.[189, 190] In addition to these GAGs, the effect of recombinant human versican V3 protein may be investigated, especially taking into account its elastogenic effect when overexpressed in skin fibroblasts.[163, 191]

3.2.3. Growth factors and cytokines

Growth factors are responsible for performing specific functions by binding to receptors on target cells. They are generated by producer cells when required. Their intrinsic drawbacks, instability or quick dispersion from the delivery site, may be avoided by combining them with biomaterials to enable controlled release.[192]

Among these compounds, insulin-like growth factor 1 (IGF-1) and TGF-β1 showed the most positive results in terms of inducing elastin synthesis.[8] The involvement of IGF-1 in elastogenesis is demonstrated by enhanced elastin gene expression and soluble elastin production in rat aortic SMCs with elevated IGF-1 concentrations.[193, 194] Moreover, in cultures of rat aortic SMCs treated with IGF-1, tropoelastin mRNA levels were found to be 3-5 fold higher, peaking 8 h after administration of IGF-1.[195] Next to IGF-1, the IGF-1 receptor has been demonstrated as an important player in

elastogenesis with various compounds, including xGVxxG peptides and glucagon-like peptide-1.[78] The xGVxxG peptide enhanced elastin gene and protein expression and elastic fiber development in human dermal fibroblasts and explants via activating the IGF-1 receptor.[196] Despite glucagon-like peptide-1 being an insulinotropic hormone, it did not alter insulin secretion in cardiac fibroblasts but induced elastin production in the absence of a classic glucagon-like peptide-1 receptor via cross-activation of the IGF-1 receptor.[78] Furthermore, administration of a combination of IGF-1 and fibroblast growth factor-2 (FGF2) elevated the expression of lysyl oxidase *in vivo* and may assist in formation of crosslinked elastin.[197] IGF-1 treatment showed an elastogenic effect on SMCs, but had no elastogenic effect on rat pulmonary fibroblasts, indicating that the control of elastin gene expression may be tissue specific.[194]

TGF-β1 is an important regulator of collagen and fibronectin production in wound healing and a known pro-fibrotic growth factor associated with scar formation. The importance of TGF-β1 signaling in elastin formation is shown by abnormalities in elastic fiber structure induced by cells lacking functional TGF-β1 receptors.[198] TGF-β1 effects in elastogenesis goes two ways; it can increase tropoelastin mRNA levels and elastin formation by modulating tropoelastin promoter activity, but on the other hand diminish tropoelastin mRNA levels and increase elastin degradation.[8, 153, 199-206] *In vitro* systems designed based on biological compounds and biomechanical environments are promising to improve elastin synthesis. For instance, in a bioreactor system TGF-β1 and mechanical stress treatment of primary human vascular SMCs seeded on a scaffold resulted in higher levels of deposited microfibrillar components compared to standard 2D controls.[207] TGF-β1-coated polymeric discs were implanted layer by layer subcutaneously in Wistar rats, and in three weeks, the controlled release of TGF-β1 from the discs enhanced elastin synthesis compared to discs without TGF-β1.[208] Elastin production, however, seems to be age-specific, since TGF-β1 stimulated elastin formation in neonatal rat lung fibroblasts and smooth muscle cells, but not in adult equivalents,[209] even though enhanced elastogenesis is especially needed in adults. In 3D cell culture experiments with vocal fold fibroblasts, TGF-β1 did not show elastogenic potential, but hepatocyte growth factor (HGF) did.[210] As TGF-β1 has progressively been linked with several pathologies (e.g. apoptosis, fibrosis, formation of granulation tissue), it would be controversial to select this molecule as a candidate to induce elastic fibers in biomaterials.[203-205, 211]

Pro-inflammatory cytokines can negatively influence elastin synthesis and promote degradation. For example, TNF-α reduced tropoelastin mRNA levels and stimulated

elastin digestion by increasing the release of elastolytic enzymes such as MMP-2, and MMP-9.[8] In contrast, interleukin (IL)-1β increased elastin gene expression in human dermal fibroblast cultures and in mice skin after subcutaneous injections.[212]

More research is needed on dermal fibroblasts to fully understand the effects of various cytokines on elastogenesis, but especially IGF-1 shows potential in directing of elastogenesis when used in the formulation of biomaterials.

3.2.4 Collagen

Collagen is a structural protein in skin and an important component of biomaterials that serves as a template for cell adhesion, migration, and proliferation to remodel lost ECM in wounds.[213] Type I collagen, a common component of biomaterials, may have elastogenic potential as it has been reported that human type I collagen alpha-2 (COL1A2) peptides increase wound healing efficacy, collagen and elastin synthesis, cell proliferation and migration by simultaneous activation of the TGF-β signaling pathway.[214] When human dermal fibroblasts were cultured in the presence of recombinant human COL1A1-collagen effective domain (CED), it increased cell proliferation and migration, as well as collagen and elastin deposition.[215] Collagen peptides isolated from fish skin alone as well as in combination with soy peptides showed mRNA upregulation of elastin, fibronectin, type I and type II collagen in dermal fibroblasts.[216] Elastin expression was also elevated at both gene and protein levels when type II collagen isolated from sturgeon cartilage was used in human dermal fibroblast culture and a mouse full-thickness lesion.[217] While there are promising indications of elastogenic potential of different collagen peptides, it should be noted that type I collagen alone as a biomaterial is insufficient to fully restore the elastic properties of the skin.

3.3. Hormones

The skin has developed complex mechanisms that include, among others, steroidogenic ability in order to maintain proper homeostasis, meanwhile defending the body from external interventions and biological influences.[218] Hormones and hormonal imbalances have a substantial impact on the morphology and physiology of the skin, as well as on its numerous functions, including wound healing.[219, 220] Skin cells possess the whole biochemical machinery required to produce glucocorticoids, androgens, and estrogens from systemic precursors or, alternatively, through the conversion of cholesterol to biologically active steroids, e.g., estradiol, dihydrotestosterone, cortisol, etc. Circulating hormone levels, for instance growth hormones and sex steroids, gradually decline with age. While topical application of some hormones demonstrated positive effects on wound

healing in animals and humans,[221-223] it is worthy to elucidate their potential utilization in elastogenic dermal biomaterials.

3.3.1. Steroids

Besides being one of the most important female sex hormones and one of the most potent estrogens, 17β-estradiol (E2) may increase synthesis of elastin in the skin, enhance epidermal thickness and repair extracellular matrix.[224-226] *In vivo* experiments showed that injection of estradiol elevated elastin levels in vocal fold injuries in rabbits.[227] Synergy between estradiol and progesterone may help to properly align the extracellular matrix.[228] Since 17β-estradiol possesses sex-dependent effects on elastin synthesis (enhanced for female dermal fibroblasts), these sex distinctions may be abolished with incorporation of cyclic adenosine monophosphate in dermal substitutes.[228] It will be a challenge to retain the effects of estradiol to the biomaterial site of application. As estradiol has a wide variety of effects beyond the skin,[227, 229-233] its systemic effects must be included in experimental designs.[234]

Aldosterone is a mineralocorticoid steroid hormone produced by adrenal glands and responsible for water and electrolyte balance in the body, e.g., regulation of blood pressure and levels of Na^+ and K^+ ions in plasma. Aldosterone demonstrated induction of elastogenesis in human skin and cardiac fibroblasts as well as in skin explants derived from *striae distensae*, independent of mineralocorticoid receptor signaling.[235, 236] Where aldosterone enhances collagen production via the mineralocorticoid receptor, activation of elastogenesis involves the IGF-1 receptor.[235] Using aldosterone in combination with mineralocorticoid receptor inhibitors may selectively induce elastogenesis without induction of collagenesis, which may consequently prevent from the formation of hypertrophic and keloid scars.[236]

Dexamethasone is a synthetic glucocorticoid steroid hormone with a very broad spectrum of clinical applications ranging from asthma and allergies to different cancer types. While this compound possesses suppressive impact on collagenesis and hyaluronic acid synthesis by human dermal fibroblast cell lines,[237, 238] its elastogenic properties are ambiguous. For example, injection of dexamethasone showed no effect on elastin levels in vocal fold injuries in rabbits,[227] but demonstrated elastogenic potency (up to 3 times increase) in cell culture experiments with fibroblasts derived from bovine *ligamentum nuchae*,[239] where especially in older bovine ligament fibroblasts elastin synthesis was induced.[240] In keloid explants, dexamethasone alone did not increase elastin synthesis.[236] Dexamethasone has also been reported to suppress elastin mRNA expression

in normal human fibroblasts.[135, 241] Additional experiments conducted with primary human fibroblasts focusing on protein deposition and architecture are needed to provide conclusive evidence regarding the impact of dexamethasone on dermal elastogenesis.

Compared to dexamethasone, other glucocorticoids, especially cortisol, its medication form hydrocortisone, and methylated derivative, methylprednisolone, demonstrated much lower potency in stimulation of elastin production by fetal bovine fibroblasts.[240] Cortisol inhibited elastin and elastin mRNA production in normal human dermal fibroblasts but not in keloid cells.[241] The elastogenic effects of hydrocortisone may be dependent on age, as in chickens the effect was quite prominent in embryos and 1-day-old organisms, but lost in 1- or 2-weeks-old chickens.[242]

3.3.2. Peptide hormones

Insulin is a peptide hormone and growth factor released by pancreatic beta cells and plays a crucial role in regulating blood glucose levels in the body.[243] It is also able to improve wound healing as was seen when insulin was topically administered *in vivo*, resulting in a decreased healing time, reduced wound contraction, and enhanced angiogenesis and re-epithelization.[221] Its potential may be expanded to trigger elastin synthesis.

In human aortic SMCs, low insulin doses induced an elastogenic effect mediated by the insulin receptor,[244] without promoting deposition of type I collagen and fibronectin. Insulin results in elastic fiber deposition by activating elastin gene expression and enhancing tropoelastin secretion. In human skin fibroblast cultures, supplementation of insulin alone and especially in combination with epidermal growth factor (EGF) promoted synthesis of dermis-like sheets, and production of elastin, type I collagen and fibrillin-1.[245] Interestingly, two fibrillin derived peptide hormones influence insulin levels. These hormones, asprosin and placensin (140 and 133 amino acids residues, respectively), are derived from the C-terminal region of profibrillin 1 and 2 respectively, by furin mediated cleavage.[246-248] Both hormones are glucogenic and act by cAMP-PKA signaling, likely through a G protein coupled receptor. It remains to be investigated what role they play in skin regeneration, but the direct coupling of hormone production and elastic fiber formation is challenging.

3.4. Potassium channel openers

Potassium channels in cell membranes play a crucial role in the regulation of membrane potential and cellular excitability. Potassium channel openers are a class

of drugs that influence the movement of potassium ions across the cell membrane, leading to hyperpolarization and reduced cellular excitability. Some studies suggest that potassium channel openers may have beneficial effects on wound healing, including the skin,[249-251] and it may even lead to elastic fiber formation.[252]

The effect of minoxidil, an ATP-dependent potassium channel opener that causes vasodilation and is applied topically to promote hair growth, has mostly been studied on SMCs.[252] There minoxidil induced tropoelastin mRNA levels and elastin synthesis independently from cell proliferation.[253] *Ad libitum* administration of minoxidil in tap water to adult[254] and aged mice[254, 255] as well as in young[252] and adult rats[256] preserved integrity of existing elastic fibers, improved elastic fiber synthesis, lowered blood pressure and decreased aortic stiffness, with gender-specific differences. Adverse effects included cardiac hypertrophy, an effect that may be avoided when an angiotensin II–receptor antagonist (e.g., irbesartan) is simultaneously administered.[252] Another potassium channel opener, diazoxide, had a three times lower elastogenic effect compared to minoxidil in young rats, but could reduce side effects.[252] Chemical derivatives of diazoxide and cromakalim also enhanced elastogenesis in vascular SMCs at a ten times lower dose than their unmodified counterparts.[257, 258] The potassium channel opener nicorandil demonstrated a very selective increase in aortic elastin protein content when orally administered to young rats.[259]

Regarding dermal elastogenesis, the evidence is limited to minoxidil in cell culture experiments in chicken skin fibroblasts, where medium supplementation stimulated elastin synthesis and overexpression of elastin mRNA.[260] Local application of potassium channel openers may stimulate elastogenesis while avoiding systemic side effects.

3.5. Metals

Metal ions such as copper and iron directly or indirectly affect wound repair, and their effects on elastogenesis are being studied.

3.5.1. Copper

Copper is a necessary element for skin formation and wound healing, as it is involved in the synthesis of elastin by fibroblasts and the crosslinking of collagen and elastin as a cofactor for the lysyl oxidase enzymes.[261, 262]

Several studies used copper sulfate, $CuSO_4$, to administer Cu^{2+}. In rat aortic SMCs, $CuSO_4$ boosted elastin crosslinking, promoted elastin synthesis fourfold and

increased LOX protein production 2.5 times.[263] Copper nanoparticles, used to overcome the mild cytotoxicity of copper ions, with hyaluronan led to mature elastic fiber formation rather than amorphous accumulations.[264] In a human fibroblast cell line, $CuSO_4$ administration showed increased elastin and type I collagen alpha 2 chain gene expression and increased deposition of elastin and type I collagen protein.[265] When combining copper sulfate with a mixture of amino acids (Gly, Pro, Ala, Val, Leu, Lys), these cells demonstrated a synergetic effect of improved elastogenesis.[265] It was also shown that valine and alanine were essential for elastin expression in primary human skin fibroblasts, while proline and glycine were responsible for collagenesis.[266] In a small clinical trial with five volunteers, a commercial product containing Gly, Pro, Ala, Val, Leu, Lys, copper ions and hyaluronic acid showed reduced wrinkles, improved moisture and enhanced elasticity.[267] A combination of low-dose $CuSO_4$ together with heparin was proposed to promote elastogenesis in lungs as inhalation therapy in patients with emphysema.[268]

Other forms of copper also showed elastogenic potential. Copper oxide particles stimulated elastin deposition in dermal fibroblasts along with other ECM components.[269] A Gly-His-Lys-copper complex (GHK-Cu) stimulated collagen and elastin production in primary human dermal fibroblasts even at low concentrations (0.01 nM), increased mRNA expression levels and the ratio of tissue inhibitors of metalloproteinases (TIMPs) to MMPs.[270] In a clinical study with 40 female middle-aged volunteers, topical application of GHK-Cu reduced wrinkle volume and depth.[270]

3.5.2. Iron

Iron has also been implicated in elastogenesis, although its mechanism is not clear. Low dosage of iron supplementation (2-20 μM Fe(III) citrate) to cultured human dermal fibroblasts induced elastogenesis with a 3-fold increase of tropoelastin mRNA and a significant enhancement of elastic fiber formation.[271] Additionally, iron citrate protected elastic fibers in rat vascular SMCs and prevented fragmentation of elastic fibers of calcified aortic rings.[272] Iron(II,III) oxide nanoparticles revealed a concentration-dependent and shape-dependent stimulatory effect on elastin deposition in spheroids of primary rat aortic SMCs.[273] The relationship between iron ions and elastogenesis is complex, and an imbalance in iron homeostasis can have negative effects. For example, excessive iron or iron overload can lead to oxidative stress, which may contribute to the degradation of elastin and other structural proteins.[274] Iron deficiency on the other hand has detrimental impact on the development of elastic fibers.[275]

3.6. Antioxidants & vitamins

Various antioxidants serve as promising candidates for ingredients of biomaterials due to their capacity to eliminate free radicals and protect cells.[276] Natural extracts that possess antioxidant properties due to the presence of complex phytochemicals will be reviewed in the next section.

Retinol, or vitamin A_1, is a fat-soluble vitamin that enhances both elastogenesis and collagenesis in monolayered and 3D cultured human skin fibroblasts.[277] Topical retinol treatment of skin explants increased elastin, fibrillin-1 and type I collagen gene expression together with elastic fiber network formation *ex vivo*. *In vivo* experiments where full-thickness punch biopsies were collected from sun-protected buttock skin of elderly individuals who followed topical retinol application demonstrated that retinol activated ECM deposition (elastin, type I collagen and fibronectin) by fibroblasts with epidermal thickening along with increased endothelial cell proliferation.[278] The vitamin A derivative, all-trans retinoic acid, decreased proliferation of chicken embryonic dermal fibroblasts, but almost doubled elastin protein production.[279] A similar elastogenic effect was observed in neonatal rat lung fibroblasts.[280] In UVA-treated human foreskin fibroblast cell line, retinoic acid-loaded nanoparticles lowered MMP-1 production and enhanced the synthesis of type I collagen and elastin.[281] Retinoic acid nanoencapsulation decreased cytotoxicity in human dermal fibroblasts and reduced skin damage in a nude mouse model after topical administration of nanoparticles compared to free retinoic acid.[208]

Polyphenols are antioxidants with multiple phenol structures in their chemical makeup. They represent a large and diverse group of naturally occurring compounds found in plants. The polyphenols pentagalloyl glucose (PGG) and epigallocatechin gallate (ECGC) promote production, alignment, crosslinking and preservation of elastin by binding to monomeric tropoelastin, improving coacervation and enhancing lysyl oxidase production.[282, 283] Upon short-term UVA exposure, they promote significant elastin (30-45x) and collagen extracellular matrix deposition,[284] without changing intracellular tropoelastin production.[285] Upon addition of another polyphenolic compound, ellagic acid, to human dermal fibroblasts, elastin mRNA synthesis was threefold higher than retinol-supplemented culture. Moreover, elastin deposition improved significantly in the retinol coupled ellagic acid group, demonstrating that combining polyphenols with retinol could be promising to improve elastin synthesis and deposition.[286]

Ascorbic acid or vitamin C has a well-known stimulatory effect on collagen synthesis. However, initially it was believed to have negative impact on elastogenesis as seen in

murine SMCs.[287] Also, a direct correlation between ascorbic acid concentration and incorporation of hydroxyproline in elastin protein was seen in those experiments. *In vivo* study with vitamin C-deficient guinea pigs revealed that lack of ascorbic acid prevented hydroxylation of already existed proline residues in aortic elastin but did not affect synthesis of elastin protein in scurvy.[288, 289] Later it was discovered that ascorbic acid was capable of increasing elastin synthesis by chicken aortic SMCs and in a rat model, as did its stable analogue 2-O-D-glucopyranosyl L-ascorbic acid in rat pulmonary fibroblasts.[290-292] Moreover, sodium L-ascorbate improved production and preservation of elastic fibers by human skin fibroblasts.[293, 294]

Nicotinamide, a form of vitamin B_3, and its derivatives (e.g. 2,6-dihydroxynicotinamide) may also have elastogenic potential as shown in skin fibroblasts[295] and in clinical trials with topical cream application in 50 women.[296] Nicotinamide mixed with polydeoxyribonucleotide and vitamin C was tested by microneedle injections in UVB irradiated mouse skin, where especially the combination of the three components led to prominent elastin synthesis.[297]

Coenzyme Q_{10} is a crucial component of the electron transport chain and a widely used antioxidant in cosmetic formulations. The cofactor exists as an equilibrium between its oxidized (ubiquinone) and reduced (ubiquinol) form. Compared to ubiquinone, ubiquinol was more efficient in reverting the expression of the senescent phenotype of fibroblasts.[298] In human primary foreskin fibroblasts, it induced elastin and type IV collagen gene expression, while suppressing MMP-1 levels.[299] At specific doses, coenzyme Q_{10} promoted elastin mRNA expression in human dermal fibroblasts.[300]

3.7. Natural products

Screening of natural products for induction of elastic fiber production seems to become more popular in recent years. It could be economically advantageous to use available natural products rather than synthetic compounds, especially if their synthesis and purification are laborious and as some natural compounds cannot be synthesized yet because of their steric complexity. Natural extracts represent a complex mixture of components whose properties may not be directly related to those of a single component. It may be difficult to compare studies from different research groups as variations in extraction process likely result in varying final products.

3.7.1. Defined chemicals from natural sources

The beneficial dermal effect of notoginseng or Chinese ginseng is mainly attributed to steroid glycosides, protopanaxadiol and protopanaxatriol, present in extracts.

In vitro experiments with protopanaxadiol and protopanaxatriol resulted in enhanced mRNA expression of elastin, type I collagen and fibrillin-1 in human skin fibroblasts isolated from both young (20-years-old) and old (60-years-old) donors.[301] A crude extract of nanosized ginseng stem increased the cell proliferation and synthesis of ECM proteins (collagen, fibronectin, elastin) of human keratinocyte and skin fibroblast cell lines and accelerated the wound closure in mice by decreasing inflammation.[302]

Gamma-aminobutyric acid, commonly known as GABA, is the primary inhibitory neurotransmitter in the central nervous system. GABA promoted production of elastin intracellularly in human dermal fibroblasts, but no extracellular elastic fibers were observed.[303] In another study, skin elasticity was found to be improved after topical application, but a detailed ECM analysis was not conducted.[304] This compound also triggered type I collagen transcription, diminished MMP-1 expression,[305] and abated atopic dermatitis skin lesions via suppression of IgE and IL-4 production.[306] Additional experiments are required to investigate the exact impact of GABA on the ECM during wound healing and elucidate its potential applications in biomaterials.

Tetrahydrocurcumin is a metabolite of curcumin with stronger antioxidative properties[307] and was able to elevate elastin, collagen and HA content in a human dermal fibroblast cell line.[308] Camphor, a compound found in essential oils of various herbs, induced gene expression of elastin in primary human skin fibroblasts and UV-exposed murine skin.[309] In addition, its safety and anti-aging properties have recently been assessed in reconstructed skin substitutes.[310] Two main compounds from sheep laurel extract, avicularin and epicatechin-(2β→O→7,4β→6)-ent-epicatechin, were identified for their bioactivity to upregulate elastin and type I collagen expression and increasing skin thickness.[310]

Linoleic acid, an essential polyunsaturated omega-6 fatty acid, is a structural component of cell membranes and a key contributor to the lipid barrier of the skin, helping to prevent excessive water loss and maintaining skin hydration.[311] Linoleic acid's analogue 8-[2-(2-pentyl-cyclopropylmethyl)-cyclopropyl]-octanoic acid (DCP-LA) upregulated elastic fiber deposition and fibulin-5 expression in human skin fibroblasts, without changing their mRNA expression.[312]

The phytoestrogen tanshinone IIA is a lipophilic diterpene quinone that possesses anti-inflammatory and antioxidant properties.[313] In human cardiac fibroblasts, tanshinone IIA enhanced elastin production while hindering collagenesis.[314]

Subsequently, it would be worthwhile to investigate the consistency of this effect on dermal fibroblasts as this could aid in preventing hypertrophic scars characterized by excessive collagen deposition.

3.7.2. Extracts

Several herbs have been investigated for their potential for elastogenesis and include low-cost products like dill. A study in mice with dill extract in drinking water showed elastic fiber neosynthesis and protection of existing fibers from degradation in blood vessels together with increased tropoelastin and LOXL-1 mRNA expressions.[315] Also in skin, dill extract protected the elastic network from digestion by elastase in injured mice.[316] In human skin fibroblasts, dill extract induced elastin production together with upregulated gene expression of LOXL-1.[317] Recently, combined use of dill and blackberry extracts enhanced the effects both *in vitro* (human dermal fibroblasts) and *in vivo* (clinical trials with a topical lotion) by inducing elastin and collagen production, inhibiting elastases and forming a functional ECM.[318]

As mentioned in section 3.2.4, soy peptides with collagen peptides induced elastin expression in dermal fibroblasts.[216] In rat cardiac myoblasts, soy bean extract showed elastic fiber stimulation with enhanced elastin promoter activity and suppressed elastase activity, while topical application induced elastic fiber formation in murine and porcine skin.[319]

Some evidence of natural extracts is more incidental and require further investigation. We will give some examples thereof. An aqueous wheat extract increased expression of type I collagen and elastin in a human keratinocyte cell line.[320] Blackcurrant extract promoted protein deposition of elastin and type I and III collagen by a dermal fibroblast cell line and oral intake by ovariectomized rats raised elastin, collagen, and HA levels in skin.[321] An extract of the Orpheus flower upregulated elastin and type VI and XVI collagen mRNA expression in H_2O_2-treated normal human skin fibroblasts and topical application demonstrated better skin elasticity in a small clinical study with 20 middle aged women.[322] Sponge gourd stem sap inhibited MMP-1, MMP-2 and MMP-9 expression,[323] and stimulated elastin and type I procollagen synthesis in human dermal cells in a dose-dependent manner by controlling the epidermal growth factor receptor and proliferator-activated receptor gamma (PPARγ) signaling.[324] Tasmanian pepper berry extract enhanced synthesis of elastin and type I collagen in five human skin explants and induced skin smoothness, restored dermal thickness and reduced scar appearance of stabilized stretch marks upon topical application in 30 women.[325]

New trends include the use of fermented extracts and probiotics. Fermented adlay bran extract added to human primary dermal fibroblasts increased elastin mRNA levels and decreased MMP-12 and MMP-9 gene expression.[326] *Rhodiola rosea* fermented by *Lactobacillus plantarum* shielded fibroblasts from UVA-induced oxidative stress by lowering levels of reactive oxygen species and raising the antioxidant level. Moreover, it diminished MMP activity, and enhanced collagen and elastin production in comparison to non-fermented *Rhodiola rosea*.[327] Upon topical application of a living *Lactobacillus plantarum* Lp90, a probiotic, to Epiderm®, elastin expression was elevated, while other studied ECM components, collagen and hyaluronan, did not change.[328] In conclusion, investigation of elastogenic properties of various natural extracts and fermentation methods can shift the focus to a completely different field – probiotics and microbiome. However, detailed studies on the active ingredients in such an extract would reduce the impact of cultivation, extraction methods and raw materials and allow for more consistent and robust results.

4. Discussion and future outlook

In this review we collected available information about compounds that may be capable of inducing elastogenesis in biomaterial formulations. Our particular focus lied in the realm of skin regeneration after severe excisional and burn injuries as there is ample room for improvement in terms of reducing scar formation, and improving healing pace and skin elasticity.[329] The distinguishment between induction of the elastin protein only, elastic fiber deposition and functional elastogenesis leading to enhanced biomechanical properties is quite challenging. Thus, our findings are consolidated in Table 1, where abovementioned candidates are assessed based on the published evidence for the creation of novel elastogenic biomaterials. A compound receiving three green ticks is considered as a possible elastogenic candidate to perform further investigation (highlighted in bold), while a compound with more than three ticks is deemed a promising elastogenic substance (highlighted with bold green font style). Our primary emphasis was directed towards dermal cells (e.g. skin fibroblasts), although encouraging results for other cells sometimes were also included (e.g. SMCs, cardiac fibroblasts), as these compounds may be worthy to study in a dermal setting as well. To date, there is no universal manual for investigation of functional elastic fibers, which is why we pointed out the major aspects to look at: firstly whether the effect was observed in cell culture, explants and/or living organisms, and secondly on what level the effect was found, i.e., gene expression, protein deposition (with immunoblotting,

mass spectrometry etc.), histological & morphological findings (e.g. histological assays and immunofluorescent detection) and/or biomechanical tests (e.g. elastic modulus, stiffness, tensile strength, strain to failure, etc.). Note that an increased gene expression does not automatically result in an increase of protein expression. At the same time, protein synthesis cannot guarantee the formation of elastic fibers (that have microfibrillar components, see Figure 2). Even if elastic fibers are formed, they should be tested for biomechanical properties, in order to show whether they really improve elasticity and resilience on the tissue level.

When we discuss advanced elastogenic skin biomaterials, we should consider multiple aspects of the supplementary compounds, i.e. their properties for restoration of the complex network of elastic fibers, biocompatibility, integration in the wound, potential sustained or controlled release and ultimate elimination from the implantation site. Additionally, angiogenesis and innervation in tissue-engineered constructs is crucial to ensure clinical translation.[337] The goal is to propose new options for biomaterials that not only provide structural support but also actively contribute to the formation of new elastic fibers and skin regeneration. Advances in nanotechnology allow the creation of smart materials with unique properties that can respond to specific environmental conditions and provide release mechanisms for bioactive compounds.[338] From Table 1, the most encouraging substantiation was for the following type of compounds: recombinant human tropoelastin and digested elastin peptides preparations, hyaluronan, dill extract, derivatives of vitamin A, minoxidil and 17β-estradiol. A direct comparison of these bioactive substances in experimental setups will provide deeper insights to this topic, as will the testing of combinations of compounds. **Tropoelastin**, as the building block for crosslinked elastin primarily obtained through recombinant techniques, can serve both as a biomaterial main component and as an additive. Its main advantage is that it bypasses the elastin secretion by cells. While exogenous tropoelastin can serve as a substrate to produce more elastic fibers, there is the evidence that it (in the form of the crosslinked tropoelastin-derivatized HA matrix) can also be exploited in the formation of new elastic fiber networks in skin tissue in rats.[125] **Enzymatically digested elastin**, generally with a lower molecular weight than tropoelastin, is less likely to be directly incorporated in newly formed elastic fibers but shows proficiency to induce elastogenesis by cells. Enzymatic digestion results in degradation products that can be released in the human body, thus forming peptides that can be sensed by cells, who respond by launching corresponding internal signaling pathways, similar to matrikines or growth factors. Stable pyridinium core structures may play the key role in recognition of elastin-derived compounds by the cells and leading to activation of particular effects. Such

digests can stimulate cell migration, proliferation, and differentiation, promoting skin repair and regeneration of damaged tissues. The complete signaling picture by elastokines is unclear, but the phosphoinositide 3-kinase (PI3K)/protein kinase B (PKB/Akt) pathway can be triggered by soluble elastins.[196, 339, 340] At the same time, this pathway is targeted in cancer treatment as its aberrant activation leads to tumorigenesis, cancer progression, and drug resistance.[341] Processes in cancer biology, like cell proliferation and migration, are also essential for the repair of damaged tissues. However, effects of elastokines could be beneficial for biomaterials if they can be spatiotemporally controlled.[342, 343] **Hyaluronan** is pivotal in wound healing with its affinity to water, structural support, anti-inflammatory responses, angiogenesis and may particularly stimulate elastogenesis, especially considering its effects on promoting elastin gene expression and protein deposition.[178, 179] At the same time, experiments with crosslinking of tropoelastin with hyaluronan resulted not only in induced elastogenesis, but also in a proper incorporation of the applied biomaterial.[125] Despite this compound shows molecular weight- and crosslinking state-dependent properties, it is an important substance to consider in formulation of novel elastogenic biomaterials. While **minoxidil** is primarily known for its vasodilatory effects and use in the treatment of hair loss, its dermal elastogenic potential is of interest. This potassium channel opener showed improved wound healing, as well angiogenesis, when applied topically in rats.[344] Although this compound has been extensively tested for aortic elastogenesis *in vivo*, it is worthwhile to check the dermal elastogenic effect upon topical or local application, which will also prevent its off-target effects, such as weight gain and cardiac hypertrophy.[255] **Dill extract**, derived from a low-cost and easily accessible herb, shows promise in elastic fiber neosynthesis and in protection of existing elastic fibers. Natural extracts constitute complex mixtures of various compounds usually not easily synthesized in the lab and the driving force of this extract remains unknown. It could be a specific component of the extract or multiple components in the mixture. **Vitamin A and its derivatives** demonstrated elastogenic potency, although collagen synthesis was also enhanced. Excessive collagenesis goes hand in hand with scar formation.[345] Thus, vitamin A compounds should be used in combination with collagen-suppressive molecules, such as human cathelicidin peptide LL-37[346] or Lipo-PGE_1 (a lipid-encapsulated preparation of prostaglandin E_1).[347] It is crucial to highlight that application of additional compounds can have other consequences in wound healing (e.g. increased cyclic AMP signaling by prostaglandin E_1[348]) and may increase the complexity of biomaterial production. **17β-estradiol (E2)**, the major female sex hormone and the most potent estrogen found in humans, possesses broad biological activity, including elastogenic potential. Despite some methods

to eliminate its sex-specificity are available,[228] systemic effects should be studied when applied in the dermal biomaterials. Estradiol and hyaluronan were reported to act on elastogenesis through the TGF-β/Smad signaling pathway.[180, 349] Therefore, investigating their combination is recommended, as it may lead to the amplification of each other's effects. At the same time, crosslinking of tropoelastin with hyaluronan resulted not only in induced elastogenesis but also in proper incorporation of the applied biomaterial. Hence, a comprehensive assessment of individual and synergistic effects of candidates could contribute significantly to improving our understanding of their roles in promoting functional elastogenesis, thereby enhancing the development of skin biomaterials for wound healing and tissue regeneration.

We here propose multiple components that may act as stimulators of elastic fiber formation. While some researchers investigated both elastogenic potentials and activated corresponding internal signaling pathways, others have yet to publish information about the possible underlying mechanisms. It was seen that certain compounds can either exert the effect via elastin receptor complex[196], show cross-activation of multiple receptors,[78, 196] possess the mechanism described for particular cell types[254] -not directly applicable for dermal cells- or demonstrate an opposing effect when used together with another elastogenic compound.[116] Undoubtedly, when a compound is reported to trigger production of elastic fibers, a detailed and comprehensive analysis of its effects is needed. Such unveiled cellular mechanisms not only explain the nature of the effect but offers insight into alternative approaches or potentially more efficacious candidates. As a future outlook, it is important that scientists more systematically study the cell biological pathways responsible for elastogenic effects, not only looking at elastin gene expression or elastin protein, but effective elastic fiber formation including its microfibrillar components. When proper mode-of-actions are established, it can be studied whether the elastogenic effect is maintained in a biomaterial formulation and the compound itself is compatible with the production process. Biomaterials offer an effective spatial administration route, where a sustained release of active compound can reduce systemic off-target or toxic effects. The key principle that needs to be adopted in this respect is to keep it as simple as possible, while maintaining the desired effect. At the same time, ensuring patient safety is paramount, necessitating biocompatibility and an appropriate degradation rate, while excluding inflammation, toxicity, and other adverse effects. Aligning to this reasoning, single (pure) biological or chemical compounds are favored over complex mixtures or extracts as batch-to-batch variation may give rise to variations in effects. The whole process of biomaterial production must be reproducible in

order to deliver a new product to the market. In addition, compounds that can act extracellularly are favored over intracellular effector molecules, as these do not need to be taken up by the cell and route to the desired cell organelle.

In summary, it is highly important to continue research on elastogenesis. In the process of identifying novel substances with the potential to augment the synthesis of new elastic fibers, elucidation of either the comprehensive mechanisms, previously undisclosed facets of functional elastic fiber production, and/or the revelation of a novel class of elastogenic compounds may be uncovered. At the same time, biomaterial formulation is a complex topic where we should think about its components, mechanical and physical properties, and state.[350] Even though the construction of elastic fibers *in vivo* must be significantly more challenging than in *in vitro* two-dimensional culture, this review gives ample suggestions for components of dermal substitutes that can be further investigated.

Table 1. Proof of evidence for dermal elastogenic effect of various substances.

	Compound	Cell culture				In vivo			
		Genes expression	Proteins deposition	Histology/ Morphology	Mechanical/ Functional properties	Genes expression	Proteins deposition	Histology/ Morphology	Mechanical/ Functional properties
Elastin-based compounds	Soluble elastin via KOH hydrolysis [115]	✓	✓	✓	✗	✗	✗	✗	✗
	Synthetic elastin-like peptides [78]	✓	✓	✓	✗	✗	✗	✗	✗
	Elastin enzymatic digest with mix of two proteases [109]	✗	✓	✗	✗	✗	✗	✗	✓
	Elastin enzymatic digest with Proteinase K [108]	✓	✓	✓	✗	✗	✗	✓	✗
	Recombinant human tropoelastin [34, 86, 93, 128, 130, 131]	✓*	✓	✓	✓*	✓	✗	✓	✓
	Tropoelastin mRNA [6]	✗	✓	✗	✗	✗	✗	✗	✗

Table 1. Continued

	Compound	Cell culture				In vivo			
		Genes expression	Proteins deposition	Histology/ Morphology	Mechanical/ Functional properties	Genes expression	Proteins deposition	Histology/ Morphology	Mechanical/ Functional properties
Extracellular matrix components	Fibrillin-2 [330]	✓	✓	✓	✗	✗	✗	✓	✗
	LTBP-4 [156, 157]	✓	✓	✓	✗	✗	✗	✓	✗
	Fibulin-5 [153, 331, 332]	✓	✓	✓	✗	✗	✗	✓	✗
	Fibronectin [149]	✗	✓*	✓*	✓*	✗	✗	✗	✗
	Collagen proteins [214-217]	✓	✓	✓	✗	✗	✓	✓	✗
	Versican V3 [162-164, 191]	✓	✓	✓	✓	✗	✓*	✓*	✗
	Hyaluronan [171, 173, 175-177, 263, 267, 333, 334]	✓	✓*	✓*	✗	✓	✓	✓	✓
	Heparan sulfate [184]	✓	✓	✓	✗	✗	✗	✗	✗
	Heparin [187, 188]	✓*	✓*	✓*	✗	✗	✗	✗	✗
	IGF-1 [194, 195, 197, 335]	✓	✓	✓	✗	✗	✗	✓	✗
	TGF-β1 [153, 199-202, 209, 317]	✓	✓*	✓	✗	✗	✗	✗	✗

Table 1. Continued

	Compound	Cell culture				In vivo			
		Genes expression	Proteins deposition	Histology/ Morphology	Mechanical/ Functional properties	Genes expression	Proteins deposition	Histology/ Morphology	Mechanical/ Functional properties
Hormones	**Insulin** [244, 245]	✓*	✓*	✓	✗	✗	✗	✗	✗
	Aldosterone [235, 236]	✓	✓	✓	✗	✗	✗	✗	✗
	Dexamethasone [227, 239, 240, 317, 336]	✓	✓*	✓**	✗	✗	✓*	✓*	✗
	17β-estradiol [224-230, 232, 233]	✓*	✓*	✓*	✗	✓	✓	✓	✗
	Tanshinone IIA [314]	✓*	✓*	✓*	✗	✗	✗	✗	✗
	Cortisol [240-242]	✓*	✓*	✗	✗	✗	✓*	✗	✗
Potassium channel openers	**Minoxidil** [252-256, 260]	✓	✓	✗	✗	✓*	✓*	✓*	✓*
	Diazoxide [252, 257, 258]	✓*	✓*	✗	✗	✗	✓*	✓*	✗
	Pinacidil [252]	✓*	✗	✗	✗	✗	✗	✗	✗
	Nicorandil [259]	✗	✗	✗	✗	✗	✓*	✓*	✗
	Cromakalim analogues [258]	✗	✓*	✗	✗	✗	✗	✗	✗

Table 1. Continued

	Compound	Cell culture				In vivo			
		Genes expression	Proteins deposition	Histology/ Morphology	Mechanical/ Functional properties	Genes expression	Proteins deposition	Histology/ Morphology	Mechanical/ Functional properties
Metal ions	**Ferric ammonium citrate** [271]	✓	✓	✓	×	×	×	×	×
	Copper oxide [269]	×	✓	×	×	×	×	×	×
	Copper sulfate [263-265, 267]	✓	✓*	✓*	×	×	×	×	?
Vitamins	**Vitamin A and its derivatives** [277-280, 285, 317]	✓	✓	✓	×	×	✓	✓	×
	Pentagalloyl glucose with/without epigallocatechin gallate [282, 284, 285]	✓*	✓	✓*	×	×	×	×	×
	Sodium L-ascorbate [293]	✓	✓	✓	×	×	×	×	×
	Nicotinamide and its derivatives [295, 296]	×	✓	×	×	×	×	×	✓
	Coenzyme Q_{10} [298, 299]	✓	×	×	×	×	×	×	×

Table 1. Continued

	Compound	Cell culture				In vivo			
		Genes expression	Proteins deposition	Histology/ Morphology	Mechanical/ Functional properties	Genes expression	Proteins deposition	Histology/ Morphology	Mechanical/ Functional properties
Natural products	**Dill extract** [315, 317, 318]	✓	✓	✓	✗	✓*	✗	✓	✓
	GABA [303, 304]	✓	✗	✓	✗	✗	✗	✗	✓
	Linoleic acid [312]	✓	✓	✓	✗	✗	✗	✗	✗
	Tanshinone IIA [314]	✓*	✓*	✓*	✗	✗	✗	✗	✗
	Sponge gourd stem sap [323, 324]	✗	✓	✗	✗	✗	✗	✗	✗

✗ – no experiments performed

✓ – results are not convincing or additional evidence is needed

? – ambiguous results

✓ – results are excellent/promising/convincing

✓ – results are excellent/promising/convincing for *ex vivo* (for cell culture) or in humans (for *in vivo*)

* – experiments are performed on non-dermal cells, or non-skin effect

** – experiments are performed on a disease model

[possible elastogenic candidates to investigate further are **highlighted in bold**, while compounds that are considered as promising elastogenic substances are **highlighted with bold green font style**]

References

1. Bichakjian, C.K. and T.M. Johnson, *CHAPTER 1 - Anatomy of the skin*, in *Local Flaps in Facial Reconstruction (Second Edition)*, S.R. Baker, Editor. 2007, Mosby: Edinburgh. p. 3-13.
2. Sage, H. and W.R. Gray, *Studies on the evolution of elastin—I. Phylogenetic distribution.* Comparative Biochemistry and Physiology Part B: Comparative Biochemistry, 1979. **64**(4): p. 313-327.
3. Sage, H., *Structure-function Relationships in the Evolution of Elastin.* Journal of Investigative Dermatology, 1982. **79**(1, Supplement): p. 146-153.
4. Shapiro, S.D., et al., *Marked longevity of human lung parenchymal elastic fibers deduced from prevalence of D-aspartate and nuclear weapons-related radiocarbon.* J Clin Invest, 1991. **87**(5): p. 1828-34.
5. Pierce, J.A., H. Resnick, and P.H. Henry, *Collagen and elastin metabolism in the lungs, skin, and bones of adult rats.* J Lab Clin Med, 1967. **69**(3): p. 485-93.
6. Lescan, M., et al., *De Novo Synthesis of Elastin by Exogenous Delivery of Synthetic Modified mRNA into Skin and Elastin-Deficient Cells.* Molecular Therapy - Nucleic Acids, 2018. **11**: p. 475-484.
7. Singh, M., et al., *Structural studies of elastic fibre and microfibrillar proteins.* Matrix biology plus, 2021. **12**: p. 100078-100078.
8. Sproul, E.P. and W.S. Argraves, *A cytokine axis regulates elastin formation and degradation.* Matrix Biol, 2013. **32**(2): p. 86-94.
9. Ayala, P., et al., *Elastin degradation products in acute lung injury induced by gastric contents aspiration.* Respir Res, 2018. **19**(1): p. 165.
10. Rosenbloom, J., W.R. Abrams, and R. Mecham, *Extracellular matrix 4: The elastic fiber.* The FASEB Journal, 1993. **7**(13): p. 1208-1218.
11. Daamen, W.F., et al., *Elastin as a biomaterial for tissue engineering.* Biomaterials, 2007. **28**(30): p. 4378-98.
12. Roten, S.V., S. Bhat, and J. Bhawan, *Elastic fibers in scar tissue.* Journal of Cutaneous Pathology, 1996. **23**(1): p. 37-42.
13. Godwin, A.R.F., et al., *The role of fibrillin and microfibril binding proteins in elastin and elastic fibre assembly.* Matrix Biology, 2019. **84**: p. 17-30.
14. Kielty, C.M., M.J. Sherratt, and C.A. Shuttleworth, *Elastic fibres.* J Cell Sci, 2002. **115**(Pt 14): p. 2817-28.
15. Daamen, W.F., et al., *Isolation of intact elastin fibers devoid of microfibrils.* Tissue Eng, 2005. **11**(7-8): p. 1168-76.
16. Ono, R.N., et al., *Latent Transforming Growth Factor β-binding Proteins and Fibulins Compete for Fibrillin-1 and Exhibit Exquisite Specificities in Binding Sites*.* Journal of Biological Chemistry, 2009. **284**(25): p. 16872-16881.
17. Lee, S.K., Y.S. An, and W.S. Choy, *Management of Hardware-Exposed Soft Tissue Defects Using Dermal Substitutes and Negative Pressure Wound Therapy.* Annals of Plastic Surgery, 2023. **90**(3).
18. Alsaif, A., et al., *Full thickness skin graft versus split thickness skin graft in paediatric patients with hand burns: Systematic review and meta-analysis.* Burns, 2023. **49**(5): p. 1017-1027.
19. Guo, F., et al., *Management of burns of over 80% of total body surface area: A comparative study.* Burns, 2009. **35**(2): p. 210-214.
20. Chang, D.K., et al., *The Basics of Integra Dermal Regeneration Template and its Expanding Clinical Applications.* Semin Plast Surg, 2019. **33**(03): p. 185-189.

21. Cottone, G., et al., *Comparison of Efficacy among Three Dermal Substitutes in the Management of Critical Lower-Limb Wounds: The Largest Biases-Reduced Single-Center Retrospective Cohort Study in Literature.* Medicina, 2021. **57**(12): p. 1367.
22. Shahrokhi, S., A. Arno, and M.G. Jeschke, *The use of dermal substitutes in burn surgery: Acute phase.* Wound Repair and Regeneration, 2014. **22**(1): p. 14-22.
23. Ulrich, M.M.W., M. Vlig, and B.K.H.L. Boekema, *9 - Biomaterials for dermal substitutes*, in *Wound Healing Biomaterials*, M.S. Ågren, Editor. 2016, Woodhead Publishing. p. 227-252.
24. Haslik, W., et al., *Management of full-thickness skin defects in the hand and wrist region: first long-term experiences with the dermal matrix Matriderm®.* Journal of Plastic, Reconstructive & Aesthetic Surgery, 2010. **63**(2): p. 360-364.
25. Ryssel, H., et al., *The use of MatriDerm® in early excision and simultaneous autologous skin grafting in burns—A pilot study.* Burns, 2008. **34**(1): p. 93-97.
26. Murray, R.C., et al., *Reconstruction of the radial forearm free flap donor site using integra artificial dermis.* Microsurgery, 2011. **31**(2): p. 104-108.
27. Pirayesh, A., et al., *Clinical Evaluation of Glyaderm, a Dermal Substitute Based on Glycerinized Donor Skin*, in *Skin Grafts*, S. Marcia, Editor. 2011, IntechOpen: Rijeka. p. Ch. 20.
28. Pirayesh, A., et al., *Comparison of Glyaderm with different dermal substitute matrices in a porcine wound model.* JPRAS Open, 2022. **34**: p. 257-267.
29. Schneider, J., et al., *Matriderm® versus Integra®: A comparative experimental study.* Burns, 2009. **35**(1): p. 51-57.
30. Böttcher-Haberzeth, S., et al., *Matriderm® 1 mm versus Integra® Single Layer 1.3 mm for one-step closure of full thickness skin defects: a comparative experimental study in rats.* Pediatric Surgery International, 2012. **28**(2): p. 171-177.
31. Philandrianos, C., et al., *Comparison of five dermal substitutes in full-thickness skin wound healing in a porcine model.* Burns, 2012. **38**(6): p. 820-829.
32. Almeida, I.R., et al., *Evaluation of Clinical and Biomechanical Features of Scars Resulting from the Treatment of Burn Contractures Comparing Acellular Dermal Matrices: A Randomized Clinical Trial.* Annals of Surgery, 2023. **277**(2).
33. Dickson, K., et al., *A Histological and Clinical Study of MatriDerm® Use in Burn Reconstruction.* Journal of Burn Care & Research, 2023. **44**(5): p. 1100-1109.
34. Almeida-González, F.R., et al., *A step closer to elastogenesis on demand; Inducing mature elastic fibre deposition in a natural biomaterial scaffold.* Materials Science and Engineering: C, 2021. **120**: p. 111788.
35. Mecham, R.P., et al., *Increased cyclic GMP levels lead to a stimulation of elastin production in ligament fibroblasts that is reversed by cyclic AMP.* Journal of Biological Chemistry, 1985. **260**(6): p. 3255-3258.
36. Cantor, J.O., et al., *Elastin synthesis by endothelial cells*, in *Biology of Endothelial Cells*, E.A. Jaffe, Editor. 1984, Springer US: Boston, MA. p. 189-193.
37. Wise, S.G., et al., *Tropoelastin: A versatile, bioactive assembly module.* Acta Biomaterialia, 2014. **10**(4): p. 1532-1541.
38. Ozsvar, J., et al., *Tropoelastin and Elastin Assembly.* Frontiers in Bioengineering and Biotechnology, 2021. **9**.

39. Scandolera, A., et al., *The Elastin Receptor Complex: A Unique Matricellular Receptor with High Anti-tumoral Potential.* Frontiers in Pharmacology, 2016. **7**.
40. Wang, Y., E.C. Song, and M.B. Resnick, *Elastin in the Tumor Microenvironment*, in *Tumor Microenvironment*, A. Birbrair, Editor. 2020, Springer Nature. p. 1-16.
41. Hucthagowder, V., et al., *Loss-of-function mutations in ATP6V0A2 impair vesicular trafficking, tropoelastin secretion and cell survival.* Human Molecular Genetics, 2009. **18**(12): p. 2149-2165.
42. Tembely, D., et al., *The Elastin Receptor Complex: An Emerging Therapeutic Target Against Age-Related Vascular Diseases.* Frontiers in Endocrinology, 2022. **13**.
43. Hinek, A., F.W. Keeley, and J. Callahans, *Recycling of the 67-kDa Elastin Binding Protein in Arterial Myocytes Is Imperative for Secretion of Tropoelastin.* Experimental Cell Research, 1995. **220**(2): p. 312-324.
44. Malvagia, S., et al., *New mutations in the PPBG gene lead to loss of PPCA protein which affects the level of the β-galactosidase/neuraminidase complex and the EBP-receptor.* Molecular Genetics and Metabolism, 2004. **82**(1): p. 48-55.
45. Bennasroune, A., et al., *Elastic fibers and elastin receptor complex: Neuraminidase-1 takes the center stage.* Matrix Biol, 2019. **84**: p. 57-67.
46. Hinek, A., et al., *Lysosomal Sialidase (Neuraminidase-1) Is Targeted to the Cell Surface in a Multiprotein Complex That Facilitates Elastic Fiber Assembly*.* Journal of Biological Chemistry, 2006. **281**(6): p. 3698-3710.
47. Rucker, R.B. and M.A. Dubick, *Elastin metabolism and chemistry: potential roles in lung development and structure.* Environmental Health Perspectives, 1984. **55**: p. 179-191.
48. Schmelzer, C.E.H., et al., *Prolyl hydroxylation in elastin is not random.* Biochimica et Biophysica Acta (BBA) - General Subjects, 2016. **1860**(10): p. 2169-2177.
49. Schmelzer, C.E.H., T. Hedtke, and A. Heinz, *Unique molecular networks: Formation and role of elastin cross-links.* IUBMB Life, 2020. **72**(5): p. 842-854.
50. Akita, M., et al., *Correlation of proline, hydroxyproline and serine content, denaturation temperature and circular dichroism analysis of type I collagen with the physiological temperature of marine teleosts.* Food Chemistry, 2020. **329**: p. 126775.
51. Li, B. and V. Daggett, *Molecular basis for the extensibility of elastin.* Journal of Muscle Research & Cell Motility, 2002. **23**(5): p. 561-573.
52. Schmelzer, C.E.H., et al., *Lysyl oxidase-like 2 (LOXL2)-mediated cross-linking of tropoelastin.* Faseb j, 2019. **33**(4): p. 5468-5481.
53. Vallet, S.D. and S. Ricard-Blum, *Lysyl oxidases: from enzyme activity to extracellular matrix cross-links.* Essays Biochem, 2019. **63**(3): p. 349-364.
54. Iskandar, Z., et al., *Exaggerated elastin turnover in young individuals with Marfan syndrome: new insights from the AIMS trial.* European Heart Journal Open, 2023. **3**(5).
55. Shek, N., et al., *Accelerated elastin degradation by age-disease interaction: a common feature in age-related diseases.* npj Aging, 2024. **10**(1): p. 15.
56. Iskandar, Z., et al., *5 Exaggerated elastin turnover in childhood and adolescence in marfan syndrome - correlation with age - new insights from the aims trial.* Heart, 2021. **107**(Suppl 1): p. A4-A5.
57. Huang, J.T.-J., et al., *Clinical validity of plasma and urinary desmosine as biomarkers for chronic obstructive pulmonary disease.* Thorax, 2012. **67**(6): p. 502-508.
58. Pshezhetsky, A.V. and A. Hinek, *Serine Carboxypeptidases in Regulation of Vasoconstriction and Elastogenesis.* Trends in Cardiovascular Medicine, 2009. **19**(1): p. 11-17.
59. Heinz, A., *Elastic fibers during aging and disease.* Ageing Research Reviews, 2021. **66**: p. 101255.

60. Amberger, J.S., et al., *OMIM.org: Online Mendelian Inheritance in Man (OMIM®), an online catalog of human genes and genetic disorders.* Nucleic Acids Research, 2014. **43**(D1): p. D789-D798.
61. Mohamed, M., et al., *Cutis Laxa*, in *Progress in Heritable Soft Connective Tissue Diseases*, J. Halper, Editor. 2014, Springer Netherlands: Dordrecht. p. 161-184.
62. Berk, D.R., et al., *Cutis laxa: A review.* Journal of the American Academy of Dermatology, 2012. **66**(5): p. 842.e1-842.e17.
63. Judge, D.P. and H.C. Dietz, *Marfan's syndrome.* The Lancet, 2005. **366**(9501): p. 1965-1976.
64. Tahirović, E., *Striae in an Adolescent with Marfan Syndrome.* The Journal of Pediatrics, 2022. **245**: p. 244-245.
65. Liu, T., et al., *The Stiff Skin Syndrome: Case Series, Differential Diagnosis of the Stiff Skin Phenotype, and Review of the Literature.* Archives of Dermatology, 2008. **144**(10): p. 1351-1359.
66. Kozel, B.A., et al., *Williams syndrome.* Nature Reviews Disease Primers, 2021. **7**(1): p. 42.
67. Osborne, L.R. and C.B. Mervis, *7q11.23 deletion and duplication.* Current Opinion in Genetics & Development, 2021. **68**: p. 41-48.
68. Vaux, K.K., et al., *Vocal cord abnormalities in Williams syndrome: A further manifestation of elastin deficiency.* American Journal of Medical Genetics Part A, 2003. **119A**(3): p. 302-304.
69. Wagenseil, J.E. and R.P. Mecham, *New insights into elastic fiber assembly.* Birth Defects Research Part C: Embryo Today: Reviews, 2007. **81**(4): p. 229-240.
70. Kozel, B.A. and R.P. Mecham, *Elastic fiber ultrastructure and assembly.* Matrix Biology, 2019. **84**: p. 31-40.
71. Wang, K., X. Meng, and Z. Guo, *Elastin Structure, Synthesis, Regulatory Mechanism and Relationship With Cardiovascular Diseases.* Frontiers in Cell and Developmental Biology, 2021. **9**.
72. Chatron-Colliet, A., et al., *The elastin peptide (VGVAPG)3 induces the 3D reorganisation of PML-NBs and SC35 speckles architecture, and accelerates proliferation of fibroblasts and melanoma cells.* Histochem Cell Biol, 2015. **143**(3): p. 245-58.
73. Kamoun, A., et al., *Growth stimulation of human skin fibroblasts by elastin-derived peptides.* Cell Adhes Commun, 1995. **3**(4): p. 273-81.
74. Péterszegi, G., S. Texier, and L. Robert, *Cell death by overload of the elastin-laminin receptor on human activated lymphocytes: protection by lactose and melibiose.* Eur J Clin Invest, 1999. **29**(2): p. 166-72.
75. Péterszegi, G. and L. Robert, *Cell death induced in lymphocytes expressing the elastin-laminin receptor by excess agonists: Necrosis and apoptosis.* Biomedicine & Pharmacotherapy, 1998. **52**(9): p. 369-377.
76. Duca, L., et al., *The Elastin Receptor Complex Transduces Signals through the Catalytic Activity of Its Neu-1 Subunit*.* Journal of Biological Chemistry, 2007. **282**(17): p. 12484-12491.
77. Scandolera, A., et al., *Uncoupling of Elastin Complex Receptor during In Vitro Aging Is Related to Modifications in Its Intrinsic Sialidase Activity and the Subsequent Lactosylceramide Production.* PLoS One, 2015. **10**(6): p. e0129994.
78. Qa'aty, N., et al., *The Antidiabetic Hormone Glucagon-Like Peptide-1 Induces Formation of New Elastic Fibers in Human Cardiac Fibroblasts After Cross-Activation of IGF-IR.* Endocrinology, 2015. **156**(1): p. 90-102.
79. Grosso, L.E. and M. Scott, *PGAIPG, a Repeated Hexapeptide of Bovine and Human Tropoelastin, Is Chemotactic for Neutrophils and Lewis Lung Carcinoma Cells.* Archives of Biochemistry and Biophysics, 1993. **305**(2): p. 401-404.

80. Mochizuki, S., B. Brassart, and A. Hinek, *Signaling Pathways Transduced through the Elastin Receptor Facilitate Proliferation of Arterial Smooth Muscle Cells**. Journal of Biological Chemistry, 2002. **277**(47): p. 44854-44863.
81. Robinet, A., et al., *Elastin-derived peptides enhance angiogenesis by promoting endothelial cell migration and tubulogenesis through upregulation of MT1-MMP.* Journal of Cell Science, 2005. **118**(Pt 2): p. 343-56.
82. Ochieng, J., et al., *Galectin-3 regulates the adhesive interaction between breast carcinoma cells and elastin.* J Cell Biochem, 1999. **75**(3): p. 505-14.
83. Bretaudeau, C., et al., *AG-9, an Elastin-Derived Peptide, Increases In Vitro Oral Tongue Carcinoma Cell Invasion, through an Increase in MMP-2 Secretion and MT1-MMP Expression, in a RPSA-Dependent Manner.* Biomolecules, 2021. **11**(1): p. 39.
84. Rodgers, U.R. and A.S. Weiss, *Integrin αvβ3 binds a unique non-RGD site near the C-terminus of human tropoelastin.* Biochimie, 2004. **86**(3): p. 173-178.
85. Lee, P., et al., *A novel cell adhesion region in tropoelastin mediates attachment to integrin αVβ5*. The Journal of biological chemistry, 2014. **289**(3): p. 1467-1477.
86. Kellar, R.S., et al., *Improved Wound Closure Rates and Mechanical Properties Resembling Native Skin in Murine Diabetic Wounds Treated with a Tropoelastin and Collagen Wound Healing Device.* J Diabetes Clin Res, 2020. **2**(3): p. 86-99.
87. Tian, D.-M., et al., *In-situ formed elastin-based hydrogels enhance wound healing via promoting innate immune cells recruitment and angiogenesis.* Materials Today Bio, 2022. **15**: p. 100300.
88. Jiménez Vázquez, J. and E. San Martín Martínez, *Collagen and elastin scaffold by electrospinning for skin tissue engineering applications.* Journal of Materials Research, 2019. **34**(16): p. 2819-2827.
89. Daamen, W.F., et al., *A biomaterial composed of collagen and solubilized elastin enhances angiogenesis and elastic fiber formation without calcification.* Tissue Engineering Part A, 2008. **14**(3): p. 349-60.
90. Wang, X., M.S. Ali, and C.M.R. Lacerda, *A Three-Dimensional Collagen-Elastin Scaffold for Heart Valve Tissue Engineering.* Bioengineering, 2018. **5**(3): p. 69.
91. Rodriguez-Cabello, J.C., et al., *Fibrous Scaffolds From Elastin-Based Materials.* Frontiers in Bioengineering and Biotechnology, 2021. **9**.
92. Nivison-Smith, L. and A.S. Weiss, *Elastin Based Constructs*, in *Regenerative Medicine and Tissue Engineering*, E. Daniel, Editor. 2011, IntechOpen: Rijeka. p. Ch. 15.
93. Xie, H., et al., *Treatment of Burn and Surgical Wounds With Recombinant Human Tropoelastin Produces New Elastin Fibers in Scars.* J Burn Care Res, 2017. **38**(5): p. e859-e867.
94. Kim, H.-S., et al., *Effect of Decellularized Extracellular Matrix Bioscaffolds Derived from Fibroblasts on Skin Wound Healing and Remodeling.* Frontiers in Bioengineering and Biotechnology, 2022. **10**.
95. Gerber, G.E. and R.A. Anwar, *Comparative studies of the cross-linked regions of elastin from bovine ligamentum nuchae and bovine, porcine and human aorta.* Biochemical Journal, 1975. **149**(3): p. 685-695.
96. Hinds, M.T., et al., *Biocompatibility of a xenogenic elastin-based biomaterial in a murine implantation model: The role of aluminum chloride pretreatment.* Journal of Biomedical Materials Research Part A, 2004. **69A**(1): p. 55-64.
97. *Absence of Immune Responses with Xenogeneic Collagen and Elastin*. Tissue Engineering Part A, 2013. **19**(13-14): p. 1592-1600.
98. Schmelzer, C.E.H. and L. Duca, *Elastic fibers: formation, function, and fate during aging and disease.* The FEBS Journal, 2022. **289**(13): p. 3704-3730.

99. Daamen, W.F., et al., *Preparation and evaluation of molecularly-defined collagen–elastin–glycosaminoglycan scaffolds for tissue engineering.* Biomaterials, 2003. **24**(22): p. 4001-4009.
100. Buttafoco, L., et al., *First steps towards tissue engineering of small-diameter blood vessels: Preparation of flat scaffolds of collagen and elastin by means of freeze drying.* Journal of Biomedical Materials Research Part B: Applied Biomaterials, 2006. **77B**(2): p. 357-368.
101. Chong, C., et al., *Skin wound repair: Results of a pre-clinical study to evaluate electropsun collagen-elastin-PCL scaffolds as dermal substitutes.* Burns, 2019. **45**(7): p. 1639-1648.
102. Ryan, A.J. and F.J. O'Brien, *Insoluble elastin reduces collagen scaffold stiffness, improves viscoelastic properties, and induces a contractile phenotype in smooth muscle cells.* Biomaterials, 2015. **73**: p. 296-307.
103. Lammers, G., et al., *A molecularly defined array based on native fibrillar collagen for the assessment of skin tissue engineering biomaterials.* Biomaterials, 2009. **30**(31): p. 6213-6220.
104. Heinz, A., *Elastases and elastokines: elastin degradation and its significance in health and disease.* Crit Rev Biochem Mol Biol, 2020. **55**(3): p. 252-273.
105. Jacob, M.P. and W. Hornebeck, *Isolation and characterization of insoluble and kappa elastins.* Robert, L , M Moczar And E Moczar (Ed) Frontiers Of Matrix Biology, Vol, 1985. **10 Methods Of Connec**(Ed): p. Basel, Switzerland; New York, N Y , Usa Illus 92-129.
106. Navon, Y. and R. Bitton, *Elastin-Like Peptides (ELPs) – Building Blocks for Stimuli-Responsive Self-Assembled Materials.* Israel Journal of Chemistry, 2016. **56**(8): p. 581-589.
107. Le Page, A., et al., *The role of elastin-derived peptides in human physiology and diseases.* Matrix Biol, 2019. **84**: p. 81-96.
108. Hinek, A., et al., *Proteolytic digest derived from bovine Ligamentum Nuchae stimulates deposition of new elastin-enriched matrix in cultures and transplants of human dermal fibroblasts.* Journal of Dermatological Science, 2005. **39**(3): p. 155-166.
109. Shiratsuchi, E., M. Nakaba, and M. Yamada, *Elastin hydrolysate derived from fish enhances proliferation of human skin fibroblasts and elastin synthesis in human skin fibroblasts and improves the skin conditions.* Journal of the Science of Food and Agriculture, 2016. **96**(5): p. 1672-1677.
110. Lamme, E.N., et al., *Extracellular matrix characterization during healing of full-thickness wounds treated with a collagen/elastin dermal substitute shows improved skin regeneration in pigs.* Journal of Histochemistry and Cytochemistry, 1996. **44**(11): p. 1311-22.
111. Petersen, W., et al., *The use of collagen-based matrices in the treatment of full-thickness wounds.* Burns, 2016. **42**(6): p. 1257-1264.
112. de Vries, H.J., et al., *Dermal regeneration in native non-cross-linked collagen sponges with different extracellular matrix molecules.* Wound Repair Regen, 1994. **2**(1): p. 37-47.
113. Gi-Yeun, H., S. Dong-Kook, and L. Jong-Wook, *Contracture of skin graft in human burns: Effect of artificial dermis.* Burns, 2014. **40**(8): p. 1497-1503.
114. Lempert, M., et al., *Long-term experience with a collagen-elastin scaffold in combination with split-thickness skin grafts for the treatment of full-thickness soft tissue defects: improvements in outcome-a retrospective cohort study and case report.* Langenbecks Arch Surg, 2022. **407**(1): p. 327-335.
115. Groult, V., et al., *Mechanisms of interaction between human skin fibroblasts and elastin: Differences between elastin fibres and derived peptides.* Cell Biochemistry and Function, 1991. **9**(3): p. 171-182.
116. Blaise, S., et al., *Elastin-Derived Peptides Are New Regulators of Insulin Resistance Development in Mice.* Diabetes, 2013. **62**(11): p. 3807.
117. Yeboah, A., et al., *Elastin-like polypeptides: A strategic fusion partner for biologics.* Biotechnology and Bioengineering, 2016. **113**(8): p. 1617-1627.

118. Rodríguez-Cabello, J.C., et al., *Bioactive scaffolds based on elastin-like materials for wound healing.* Advanced Drug Delivery Reviews, 2018. **129**: p. 118-133.
119. Varanko, A.K., J.C. Su, and A. Chilkoti, *Elastin-Like Polypeptides for Biomedical Applications.* Annual Review of Biomedical Engineering, 2020. **22**(1): p. 343-369.
120. Bandiera, A., *Elastin-like polypeptides: the power of design for smart cell encapsulation.* Expert Opinion on Drug Delivery, 2017. **14**(1): p. 37-48.
121. van Strien, J., et al., *Elastin-like polypeptide-based micelles as a promising platform in nanomedicine.* Journal of Controlled Release, 2023. **353**: p. 713-726.
122. Sandberg, L.B. and T.B. Wolt, *[37] Production and isolation of soluble elastin from copper-deficient swine*, in *Methods in Enzymology*. 1982, Academic Press. p. 657-665.
123. Rich, C.B. and J.A. Foster, *[38] Isolation of soluble elastin-lathyrism*, in *Methods in Enzymology*. 1982, Academic Press. p. 665-673.
124. Wen, Q., S.M. Mithieux, and A.S. Weiss, *Elastin Biomaterials in Dermal Repair.* Trends in Biotechnology, 2020. **38**(3): p. 280-291.
125. Mitzmacher, M.G., et al., *Novel Recombinant Tropoelastin Implants Restore Skin Extracellular Matrix.* Journal of drugs in dermatology : JDD, 2020. **19**(12): p. 1166-1172.
126. Garantziotis, S. and R.C. Savani, *Hyaluronan biology: A complex balancing act of structure, function, location and context.* Matrix Biology, 2019. **78-79**: p. 1-10.
127. Annabi, N., et al., *Engineering a sprayable and elastic hydrogel adhesive with antimicrobial properties for wound healing.* Biomaterials, 2017. **139**: p. 229-243.
128. Mithieux, S.M., et al., *Tropoelastin Implants That Accelerate Wound Repair.* Advanced Healthcare Materials, 2018. **7**(10): p. 1701206.
129. *Electrospun Tropoelastin for Delivery of Therapeutic Adipose-Derived Stem Cells to Full-Thickness Dermal Wounds.* Advances in Wound Care, 2014. **3**(5): p. 367-375.
130. Diller, R.B. and R.S. Kellar, *An acellular tissue engineered biomimetic wound healing device created using collagen and tropoelastin accelerates wound healing.* Journal of Tissue Viability, 2022. **31**(3): p. 485-490.
131. Mithieux, S.M. and A.S. Weiss, *Design of an elastin-layered dermal regeneration template.* Acta Biomater, 2017. **52**: p. 33-40.
132. Wang, Y., et al., *Tropoelastin incorporation into a dermal regeneration template promotes wound angiogenesis.* Adv Healthc Mater, 2015. **4**(4): p. 577-84.
133. Swee, M.H., W.C. Parks, and R.A. Pierce, *Developmental regulation of elastin production. Expression of tropoelastin pre-mRNA persists after down-regulation of steady-state mRNA levels.* J Biol Chem, 1995. **270**(25): p. 14899-906.
134. Parks, W.C., *Posttranscriptional Regulation of Lung Elastin Production.* American Journal of Respiratory Cell and Molecular Biology, 1997. **17**(1): p. 1-2.
135. Kähäri, V.M., *Dexamethasone suppresses elastin gene expression in human skin fibroblasts in culture.* Biochem Biophys Res Commun, 1994. **201**(3): p. 1189-96.
136. McGowan, S.E., et al., *Serine proteinase inhibitors influence the stability of tropoelastin mRNA in neonatal rat lung fibroblast cultures.* American Journal of Physiology-Lung Cellular and Molecular Physiology, 1996. **270**(3): p. L376-L385.
137. Johnson, D.J., et al., *Decreased Elastin Synthesis in Normal Development and in Long-term Aortic Organ and Cell Cultures Is Related to Rapid and Selective Destabilization of mRNA for Elastin.* Circulation Research, 1995. **77**(6): p. 1107-1113.

138. Davidson, J.M., et al., *Ascorbate Differentially Regulates Elastin and Collagen Biosynthesis in Vascular Smooth Muscle Cells and Skin Fibroblasts by Pretranslational Mechanisms*.* Journal of Biological Chemistry, 1997. **272**(1): p. 345-352.
139. Steinle, H., et al., *Concise Review: Application of In Vitro Transcribed Messenger RNA for Cellular Engineering and Reprogramming: Progress and Challenges.* Stem Cells, 2017. **35**(1): p. 68-79.
140. Stadler, C.R., et al., *Elimination of large tumors in mice by mRNA-encoded bispecific antibodies.* Nat Med, 2017. **23**(7): p. 815-817.
141. Wang, Y., et al., *mRNA vaccine: a potential therapeutic strategy.* Molecular Cancer, 2021. **20**(1): p. 33.
142. Oude Egberink, R., et al., *Biomaterial-Mediated Protein Expression Induced by Peptide-mRNA Nanoparticles Embedded in Lyophilized Collagen Scaffolds.* Pharmaceutics, 2022. **14**(8): p. 1619.
143. Zhang, X., et al., *Elastic Fibre Proteins in Elastogenesis and Wound Healing.* International Journal of Molecular Sciences, 2022. **23**(8): p. 4087.
144. Handa, K., et al., *Fibrillin-1 insufficiency alters periodontal wound healing failure in a mouse model of Marfan syndrome.* Archives of Oral Biology, 2018. **90**: p. 53-60.
145. Yoshiba, N., et al., *Correlation between Fibrillin-1 Degradation and mRNA Downregulation and Myofibroblast Differentiation in Cultured Human Dental Pulp Tissue.* Journal of Histochemistry & Cytochemistry, 2015. **63**(6): p. 438-448.
146. Cirulis, J.T., et al., *Fibrillins, Fibulins, and Matrix-Associated Glycoprotein Modulate the Kinetics and Morphology of in Vitro Self-Assembly of a Recombinant Elastin-like Polypeptide.* Biochemistry, 2008. **47**(47): p. 12601-12613.
147. Hinderer, S., et al., *In vitroelastogenesis: instructing human vascular smooth muscle cells to generate an elastic fiber-containing extracellular matrix scaffold.* Biomedical Materials, 2015. **10**(3): p. 034102.
148. Lenselink, E.A., *Role of fibronectin in normal wound healing.* Int Wound J, 2015. **12**(3): p. 313-6.
149. Pezzoli, D., et al., *Fibronectin promotes elastin deposition, elasticity and mechanical strength in cellularised collagen-based scaffolds.* Biomaterials, 2018. **180**: p. 130-142.
150. Nakahara, Y., M. Matsusaki, and M. Akashi, *Fabrication and enzymatic degradation of fibronectin-based ultrathin films.* J Biomater Sci Polym Ed, 2007. **18**(12): p. 1565-73.
151. Ravi, S., et al., *Incorporation of fibronectin to enhance cytocompatibility in multilayer elastin-like protein scaffolds for tissue engineering.* J Biomed Mater Res A, 2013. **101**(7): p. 1915-25.
152. Walia, R., et al., *Hydrogel–Solid Hybrid Materials for Biomedical Applications Enabled by Surface-Embedded Radicals.* Advanced Functional Materials, 2020. **30**(38): p. 2004599.
153. Katsuta, Y., et al., *Fibulin-5 accelerates elastic fibre assembly in human skin fibroblasts.* Exp Dermatol, 2008. **17**(10): p. 837-42.
154. Yanagisawa, H., M.K. Schluterman, and R.A. Brekken, *Fibulin-5, an integrin-binding matricellular protein: its function in development and disease.* Journal of Cell Communication and Signaling, 2009. **3**(3): p. 337-347.
155. Hirai, M., et al., *Fibulin-5/DANCE has an elastogenic organizer activity that is abrogated by proteolytic cleavage in vivo.* J Cell Biol, 2007. **176**(7): p. 1061-71.
156. Noda, K., et al., *Latent TGF-β binding protein 4 promotes elastic fiber assembly by interacting with fibulin-5.* Proceedings of the National Academy of Sciences, 2013. **110**(8): p. 2852-2857.
157. Aya, R., et al., *Regeneration of elastic fibers by three-dimensional culture on a collagen scaffold and the addition of latent TGF-β binding protein 4 to improve elastic matrix deposition.* Biomaterials, 2015. **72**: p. 29-37.

158. McGowan, S.E., R. Liu, and C.S. Harvey, *Effects of heparin and other glycosaminoglycans on elastin production by cultured neonatal rat lung fibroblasts.* Arch Biochem Biophys, 1993. **302**(2): p. 322-31.

159. Fornieri, C., et al., *Lysyl oxidase activity and elastin/glycosaminoglycan interactions in growing chick and rat aortas.* J Cell Biol, 1987. **105**(3): p. 1463-9.

160. Wu, W.J., B. Vrhovski, and A.S. Weiss, *Glycosaminoglycans mediate the coacervation of human tropoelastin through dominant charge interactions involving lysine side chains.* J Biol Chem, 1999. **274**(31): p. 21719-24.

161. Hinek, A., et al., *Impaired elastin fiber assembly related to reduced 67-kD elastin-binding protein in fetal lamb ductus arteriosus and in cultured aortic smooth muscle cells treated with chondroitin sulfate.* J Clin Invest, 1991. **88**(6): p. 2083-94.

162. Merrilees, M.J., et al., *Retrovirally Mediated Overexpression of Versican V3 by Arterial Smooth Muscle Cells Induces Tropoelastin Synthesis and Elastic Fiber Formation In Vitro and In Neointima After Vascular Injury.* Circulation Research, 2002. **90**(4): p. 481-487.

163. Merrilees, M.J., et al., *Use of versican variant V3 and versican antisense expression to engineer cultured human skin containing increased content of insoluble elastin.* Journal of Tissue Engineering and Regenerative Medicine, 2017. **11**(1): p. 295-305.

164. Keire, P.A., et al., *Expression of Versican Isoform V3 in the Absence of Ascorbate Improves Elastogenesis in Engineered Vascular Constructs.* Tissue Engineering Part A, 2009. **16**(2): p. 501-512.

165. Hinek, A. and S.E. Wilson, *Impaired Elastogenesis in Hurler Disease: Dermatan Sulfate Accumulation Linked to Deficiency in Elastin-Binding Protein and Elastic Fiber Assembly.* The American Journal of Pathology, 2000. **156**(3): p. 925-938.

166. Truong, A.T., et al., *Comparison of dermal substitutes in wound healing utilizing a nude mouse model.* J Burns Wounds, 2005. **4**: p. e4.

167. Moiemen, N.S., et al., *Reconstructive Surgery with Integra Dermal Regeneration Template: Histologic Study, Clinical Evaluation, and Current Practice.* Plastic and Reconstructive Surgery, 2006. **117**(7S): p. 160S-174S.

168. Augustyniak, A. and H. McMahon, *Effect of Marine-Derived Saccharides on Human Skin Fibroblasts and Dermal Papilla Cells.* Mar Drugs, 2023. **21**(6).

169. Dovedytis, M., Z.J. Liu, and S. Bartlett, *Hyaluronic acid and its biomedical applications: A review.* Engineered Regeneration, 2020. **1**: p. 102-113.

170. Graça, M.F.P., et al., *Hyaluronic acid-Based wound dressings: A review.* Carbohydr Polym, 2020. **241**: p. 116364.

171. Sylvester, A., et al., *Nanoparticles for localized delivery of hyaluronan oligomers towards regenerative repair of elastic matrix.* Acta Biomater, 2013. **9**(12): p. 9292-302.

172. D'Agostino, A., et al., *In Vitro Evaluation of Novel Hybrid Cooperative Complexes in a Wound Healing Model: A Step Toward Improved Bioreparation.* Int J Mol Sci, 2019. **20**(19).

173. D'Agostino, A., et al., *Potential of Biofermentative Unsulfated Chondroitin and Hyaluronic Acid in Dermal Repair.* Int J Mol Sci, 2022. **23**(3).

174. Varì, S., P. Minoretti, and E. Emanuele, *Human dermal fibroblast response to hyaluronic acid-based injectable dermal fillers: an in vitro study.* Postepy Dermatol Alergol, 2022. **39**(6): p. 1088-1092.

175. Joddar, B. and A. Ramamurthi, *Elastogenic effects of exogenous hyaluronan oligosaccharides on vascular smooth muscle cells.* Biomaterials, 2006. **27**(33): p. 5698-707.

176. Joddar, B., S. Ibrahim, and A. Ramamurthi, *Impact of delivery mode of hyaluronan oligomers on elastogenic responses of adult vascular smooth muscle cells.* Biomaterials, 2007. **28**(27): p. 3918-27.

177. Ibrahim, S., et al., *Characterization of glycidyl methacrylate - crosslinked hyaluronan hydrogel scaffolds incorporating elastogenic hyaluronan oligomers.* Acta Biomater, 2011. **7**(2): p. 653-65.

178. Iannitti, T., et al., *Experimental and Clinical Efficacy of Two Hyaluronic Acid-based Compounds of Different Cross-Linkage and Composition in the Rejuvenation of the Skin.* Pharmaceutical Research, 2016. **33**(12): p. 2879-2890.

179. Paliwal, S., et al., *Skin Extracellular Matrix Stimulation following Injection of a Hyaluronic Acid–Based Dermal Filler in a Rat Model.* Plastic and Reconstructive Surgery, 2014. **134**(6): p. 1224-1233.

180. Fan, Y., et al., *Hyaluronic acid-cross-linked filler stimulates collagen type 1 and elastic fiber synthesis in skin through the TGF-β/Smad signaling pathway in a nude mouse model.* Journal of Plastic, Reconstructive & Aesthetic Surgery, 2019. **72**(8): p. 1355-1362.

181. *Hyalomatrix: A Temporary Epidermal Barrier, Hyaluronan Delivery, and Neodermis Induction System for Keratinocyte Stem Cell Therapy.* Tissue Engineering, 2007. **13**(11): p. 2733-2741.

182. Erratico, S., et al., *Effective high-throughput isolation of enriched platelets and circulating pro-angiogenic cells to accelerate skin-wound healing.* Cellular and Molecular Life Sciences, 2022. **79**(5): p. 259.

183. Tiedemann, K., et al., *Interactions of fibrillin-1 with heparin/heparan sulfate, implications for microfibrillar assembly.* J Biol Chem, 2001. **276**(38): p. 36035-42.

184. Annovi, G., et al., *Heparan sulfate affects elastin deposition in fibroblasts cultured from donors of different ages.* Rejuvenation Res, 2012. **15**(1): p. 22-31.

185. Howard, V., M.M. Suzanne, and S.W. Anthony, *Elastin architecture.* Matrix Biology, 2019. **84**: p. 4-16.

186. Walsh, R.L., et al., *Heparin and heparan sulphate are inhibitors of human leucocyte elastase.* Clin Sci (Lond), 1991. **81**(3): p. 341-6.

187. Wachi, H., Y. Seyama, and S. Tajima, *Modulation of Elastin Expression by Heparin Is Dependent on the Growth Condition of Vascular Smooth Muscle Cells: Up-Regulation of Elastin Expression by Heparin in the Proliferating Cells Is Mediated by the Inhibition of Protein Kinase C Activity.* The Journal of Biochemistry, 1995. **118**(3): p. 582-586.

188. Saitow, C., D.L. Kaplan, and J.J. Castellot, *Heparin stimulates elastogenesis: Application to silk-based vascular grafts.* Matrix Biology, 2011. **30**(5): p. 346-355.

189. Gravante, G., et al., *The use of Hyalomatrix PA in the treatment of deep partial-thickness burns.* J Burn Care Res, 2007. **28**(2): p. 269-74.

190. Simman, R., et al., *Use of Hyaluronic Acid-Based Biological Bilaminar Matrix in Wound Bed Preparation: A Case Series.* Eplasty, 2018. **18**: p. e10.

191. Hinek, A., et al., *Retrovirally mediated overexpression of versican v3 reverses impaired elastogenesis and heightened proliferation exhibited by fibroblasts from Costello syndrome and Hurler disease patients.* Am J Pathol, 2004. **164**(1): p. 119-31.

192. Ren, X., et al., *Growth Factor Engineering Strategies for Regenerative Medicine Applications.* Frontiers in Bioengineering and Biotechnology, 2020. **7**.

193. Foster, J.A., et al., *Effect of age and IGF-I administration on elastin gene expression in rat aorta.* J Gerontol, 1990. **45**(4): p. B113-8.

194. Rich, C.B., et al., *IGF-I regulation of elastogenesis: comparison of aortic and lung cells.* American Journal of Physiology-Lung Cellular and Molecular Physiology, 1992. **263**(2): p. L276-L282.

195. Wolfe, B.L., et al., *Insulin-like growth factor-I regulates transcription of the elastin gene.* Journal of Biological Chemistry, 1993. **268**(17): p. 12418-12426.

196. Qa'aty, N., et al., *Synthetic ligands of the elastin receptor induce elastogenesis in human dermal fibroblasts via activation of their IGF-1 receptors.* Journal of Dermatological Science, 2015. **80**(3): p. 175-185.

197. Trackman, P.C., et al., *Inflammation-associated lysyl oxidase protein expression in vivo, and modulation by FGF-2 plus IGF-1.* Histochemistry and Cell Biology, 1998. **110**(1): p. 9-14.

198. Chen, P.Y., L. Qin, and M. Simons, *TGFβ signaling pathways in human health and disease.* Front Mol Biosci, 2023. **10**: p. 1113061.

199. Liu, J.-m. and J.M. Davidson, *The elastogenic effect of recombinant transforming growth factor-beta on porcine aortic smooth muscle cells.* Biochemical and Biophysical Research Communications, 1988. **154**(3): p. 895-901.

200. McGowan, S.E. and R. McNamer, *Transforming growth factor-beta increases elastin production by neonatal rat lung fibroblasts.* Am J Respir Cell Mol Biol, 1990. **3**(4): p. 369-76.

201. Kähäri, V.M., et al., *Transforming growth factor-beta up-regulates elastin gene expression in human skin fibroblasts. Evidence for post-transcriptional modulation.* Lab Invest, 1992. **66**(5): p. 580-8.

202. Zhang, M.C., et al., *Transforming growth factor-beta reverses a posttranscriptional defect in elastin synthesis in a cutis laxa skin fibroblast strain.* J Clin Invest, 1995. **95**(3): p. 986-94.

203. Neptune, E.R., et al., *Dysregulation of TGF-beta activation contributes to pathogenesis in Marfan syndrome.* Nat Genet, 2003. **33**(3): p. 407-11.

204. Holm, T.M., et al., *Noncanonical TGFβ signaling contributes to aortic aneurysm progression in Marfan syndrome mice.* Science, 2011. **332**(6027): p. 358-61.

205. Yao, Z., et al., *A Marfan syndrome gene expression phenotype in cultured skin fibroblasts.* BMC Genomics, 2007. **8**: p. 319.

206. Davidson, J.M., O. Zoia, and J.-M. Liu, *Modulation of transforming growth factor-beta 1 stimulated elastin and collagen production and proliferation in porcine vascular smooth muscle cells and skin fibroblasts by basic fibroblast growth factor, transforming growth factor-α, and insulin-like growth factor-I.* Journal of Cellular Physiology, 1993. **155**(1): p. 149-156.

207. Hinderer, S., et al., *In vitro elastogenesis: instructing human vascular smooth muscle cells to generate an elastic fiber-containing extracellular matrix scaffold.* Biomed Mater, 2015. **10**(3): p. 034102.

208. Damanik, F.F.R., et al., *Long-Term Controlled Growth Factor Release Using Layer-by-Layer Assembly for the Development of In Vivo Tissue-Engineered Blood Vessels.* ACS Appl Mater Interfaces, 2022. **14**(25): p. 28591-28603.

209. McGowan, S.E., *Influences of endogenous and exogenous TGF-beta on elastin in rat lung fibroblasts and aortic smooth muscle cells.* Am J Physiol, 1992. **263**(2 Pt 1): p. L257-63.

210. *Effects of Growth Factors on Extracellular Matrix Production by Vocal Fold Fibroblasts in 3-Dimensional Culture.* Tissue Engineering, 2006. **12**(12): p. 3365-3374.

211. Rifkin, D.B., W.J. Rifkin, and L. Zilberberg, *LTBPs in biology and medicine: LTBP diseases.* Matrix Biol, 2018. **71-72**: p. 90-99.

212. Mauviel, A., et al., *Human recombinant interleukin-1 beta up-regulates elastin gene expression in dermal fibroblasts. Evidence for transcriptional regulation in vitro and in vivo.* J Biol Chem, 1993. **268**(9): p. 6520-4.

213. Mathew-Steiner, S.S., S. Roy, and C.K. Sen, *Collagen in Wound Healing.* Bioengineering (Basel), 2021. **8**(5).

214. Hwang, S.J., et al., *Human collagen alpha-2 type I stimulates collagen synthesis, wound healing, and elastin production in normal human dermal fibroblasts (HDFs).* BMB reports, 2020. **53**(10): p. 539-544.

215. Hwang, S.J., et al., *Effects of human collagen α-1 type I-derived proteins on collagen synthesis and elastin production in human dermal fibroblasts.* BMB Reports, 2021. **54**(6): p. 329-334.

216. Zhang, S.Y., et al., *Collagen and soy peptides attenuate contractile loss from UVA damage and enhance the antioxidant capacity of dermal fibroblasts.* Journal of Cosmetic Dermatology, 2021. **20**(7): p. 2277-2286.

217. Lai, C.-S., et al., *Type II Collagen from Cartilage of Acipenser baerii Promotes Wound Healing in Human Dermal Fibroblasts and in Mouse Skin.* Marine Drugs, 2020. **18**(10): p. 511.

218. Slominski, A., et al., *Steroidogenesis in the skin: Implications for local immune functions.* The Journal of Steroid Biochemistry and Molecular Biology, 2013. **137**: p. 107-123.

219. Makrantonaki, E. and C.C. Zouboulis, *Dermatoendokrinologie.* Der Hautarzt, 2010. **61**(6): p. 505-510.

220. Gilliver, S.C., J.J. Ashworth, and G.S. Ashcroft, *The hormonal regulation of cutaneous wound healing.* Clinics in Dermatology, 2007. **25**(1): p. 56-62.

221. Oryan, A. and E. Alemzadeh, *Effects of insulin on wound healing: A review of animal and human evidences.* Life Sciences, 2017. **174**: p. 59-67.

222. Demling, R.H., *The role of anabolic hormones for wound healing in catabolic states.* J Burns Wounds, 2005. **4**: p. e2.

223. Brincat, M.P., *Oestrogens and the skin.* Journal of Cosmetic Dermatology, 2004. **3**(1): p. 41-49.

224. Son, E.D., et al., *Topical application of 17beta-estradiol increases extracellular matrix protein synthesis by stimulating tgf-Beta signaling in aged human skin in vivo.* J Invest Dermatol, 2005. **124**(6): p. 1149-61.

225. Zong, W., et al., *Estradiol plays a role in regulating the expression of lysyl oxidase family genes in mouse urogenital tissues and human Ishikawa cells.* J Zhejiang Univ Sci B, 2015. **16**(10): p. 857-64.

226. Punnonen, R., P. Vaajalahti, and K. Teisala, *Local oestriol treatment improves the structure of elastic fibers in the skin of postmenopausal women.* Ann Chir Gynaecol Suppl, 1987. **202**: p. 39-41.

227. Yildiz, M., et al., *Effects of Intracordal Estradiol and Dexamethasone Injection on Wound Healing in Vocal Fold Injuries.* J Voice, 2019. **33**(5): p. 759-766.

228. Moset Zupan, A., C. Nietupski, and S.C. Schutte, *Cyclic Adenosine Monophosphate Eliminates Sex Differences in Estradiol-Induced Elastin Production from Engineered Dermal Substitutes.* International Journal of Molecular Sciences, 2021. **22**(12): p. 6358.

229. Natoli, A.K., et al., *Sex steroids modulate human aortic smooth muscle cell matrix protein deposition and matrix metalloproteinase expression.* Hypertension, 2005. **46**(5): p. 1129-34.

230. Mangır, N., et al., *Oestradiol-releasing Biodegradable Mesh Stimulates Collagen Production and Angiogenesis: An Approach to Improving Biomaterial Integration in Pelvic Floor Repair.* Eur Urol Focus, 2019. **5**(2): p. 280-289.

231. Baron, Y.M., R. Galea, and M. Brincat, *Carotid artery wall changes in estrogen-treated and -untreated postmenopausal women.* Obstet Gynecol, 1998. **91**(6): p. 982-6.

232. Tyagi, T., et al., *Local oestrogen therapy modulates extracellular matrix and immune response in the vaginal tissue of post-menopausal women with severe pelvic organ prolapse.* J Cell Mol Med, 2019. **23**(4): p. 2907-2919.

233. Kim, J.M., et al., *Effect of sex hormones on extracellular matrix of lamina propria in rat vocal fold.* Laryngoscope, 2020. **130**(3): p. 732-740.

234. Rzepecki, A.K., et al., *Estrogen-deficient skin: The role of topical therapy.* International Journal of Women's Dermatology, 2019. **5**(2): p. 85-90.

235. Bunda, S., et al., *Aldosterone stimulates elastogenesis in cardiac fibroblasts via mineralocorticoid receptor-independent action involving the consecutive activation of Galpha13, c-Src, the insulin-like growth factor-I receptor, and phosphatidylinositol 3-kinase/Akt.* J Biol Chem, 2009. **284**(24): p. 16633-16647.

236. Mitts, T.F., et al., *Aldosterone and Mineralocorticoid Receptor Antagonists Modulate Elastin and Collagen Deposition in Human Skin.* Journal of Investigative Dermatology, 2010. **130**(10): p. 2396-2406.
237. Choi, D., et al. *β-Ionone Attenuates Dexamethasone-Induced Suppression of Collagen and Hyaluronic Acid Synthesis in Human Dermal Fibroblasts*. Biomolecules, 2021. **11**, DOI: https://doi.org/10.3390/biom11050619.
238. Oikarinen, A., E. Vuorio, and T. Vuorio, *Comparison of the effects of dexamethasone and 13-cis-retinoic acid on connective tissue biosynthesis in human skin fibroblasts.* Archives of Dermatological Research, 1989. **281**(4): p. 273-278.
239. Mecham, R.P., et al., *Elastin synthesis by ligamentum nuchae fibroblasts: effects of culture conditions and extracellular matrix on elastin production.* Journal of Cell Biology, 1981. **90**(2): p. 332-338.
240. Mecham, R.P., et al., *Glucocorticoids stimulate elastin production in differentiated bovine ligament fibroblasts but do not induce elastin synthesis in undifferentiated cells.* Journal of Biological Chemistry, 1984. **259**(20): p. 12414-12418.
241. Russell, S.B., et al., *Glucocorticoid regulation of elastin synthesis in human fibroblasts: down-regulation in fibroblasts from normal dermis but not from keloids.* J Invest Dermatol, 1995. **104**(2): p. 241-5.
242. Keeley, F.W. and D.J. Johnson, *Age Differences in the Effect of Hydrocortisone on the Synthesis of Insoluble Elastin in Aortic Tissue of Growing Chicks.* Connective Tissue Research, 1987. **16**(3): p. 259-268.
243. Wilcox, G., *Insulin and insulin resistance.* The Clinical biochemist. Reviews, 2005. **26**(2): p. 19-39.
244. Shi, J., et al., *Insulin Induces Production of New Elastin in Cultures of Human Aortic Smooth Muscle Cells.* The American Journal of Pathology, 2012. **180**(2): p. 715-726.
245. Lee, D.-Y., J.-M. Yang, and K.-H. Park, *A dermal equivalent developed from fibroblast culture alone: Effect of EGF and insulin.* Wound Repair and Regeneration, 2007. **15**(6): p. 936-939.
246. Romere, C., et al., *Asprosin, a Fasting-Induced Glucogenic Protein Hormone.* Cell, 2016. **165**(3): p. 566-579.
247. Yu, Y., et al., *Placensin is a glucogenic hormone secreted by human placenta.* EMBO reports, 2020. **21**(6): p. e49530.
248. Basu, B., M. Jain, and A.R. Chopra, *Caudamins, a new subclass of protein hormones.* Trends in Endocrinology & Metabolism, 2021. **32**(12): p. 1007-1014.
249. Mai, K., et al., *Maintaining and Restoring Gradients of Ions in the Epidermis: The Role of Ion and Water Channels in Acute Cutaneous Wound Healing.* Advances in Wound Care, 2023.
250. Zhang, W., et al., *Potassium channels as potential drug targets for limb wound repair and regeneration.* Precision Clinical Medicine, 2020. **3**(1): p. 22-33.
251. Zhang, W. and M. Bei, *Kcnh2 and Kcnj8 interactively regulate skin wound healing and regeneration.* Wound Repair and Regeneration, 2015. **23**(6): p. 797-806.
252. Slove, S., et al., *Potassium Channel Openers Increase Aortic Elastic Fiber Formation and Reverse the Genetically Determined Elastin Deficit in the BN Rat.* Hypertension, 2013. **62**(4): p. 794-801.
253. Hayashi, A., et al., *Minoxidil stimulates elastin expression in aortic smooth muscle cells.* Arch Biochem Biophys, 1994. **315**(1): p. 137-41.
254. Fhayli, W., et al., *Chronic administration of minoxidil protects elastic fibers and stimulates their neosynthesis with improvement of the aorta mechanics in mice.* Cellular Signalling, 2019. **62**: p. 109333.
255. Coquand-Gandit, M., et al., *Chronic Treatment with Minoxidil Induces Elastic Fiber Neosynthesis and Functional Improvement in the Aorta of Aged Mice.* Rejuvenation Research, 2017. **20**(3): p. 218-230.

256. Tsoporis, J., et al., *Arterial Vasodilation and Vascular Connective Tissue Changes in Spontaneously Hypertensive Rats.* Journal of Cardiovascular Pharmacology, 1998. **31**(6).

257. Bouider, N., et al., *Design and synthesis of new potassium channel activators derived from the ring opening of diazoxide: Study of their vasodilatory effect, stimulation of elastin synthesis and inhibitory effect on insulin release.* Bioorganic & Medicinal Chemistry, 2015. **23**(8): p. 1735-1746.

258. Bouhedja, M., et al., *Design, synthesis and biological evaluation of novel ring-opened cromakalim analogues with relaxant effects on vascular and respiratory smooth muscles and as stimulators of elastin synthesis.* European Journal of Medicinal Chemistry, 2018. **144**: p. 774-796.

259. Raveaud, S., et al., *Effects of chronic treatment with a low dose of nicorandil on the function of the rat aorta during ageing.* Clinical and Experimental Pharmacology and Physiology, 2009. **36**(10): p. 988-994.

260. Tajima, S., et al., *Stimulation of elastin expression by minoxidil in chick skin fibroblasts.* Archives of Dermatological Research, 1995. **287**(5): p. 494-497.

261. Borkow, G., *Using Copper to Improve the Well-Being of the Skin.* Current chemical biology, 2014. **8**(2): p. 89-102.

262. Harris, E.D., et al., *Copper and the Synthesis of Elastin and Collagen*, in *Ciba Foundation Symposium 79 - Biological Roles of Copper*. 1980. p. 163-182.

263. Kothapalli, C.R. and A. Ramamurthi, *Biomimetic regeneration of elastin matrices using hyaluronan and copper ion cues.* Tissue engineering. Part A, 2009. **15**(1): p. 103-113.

264. Kothapalli, C.R. and A. Ramamurthi, *Copper nanoparticle cues for biomimetic cellular assembly of crosslinked elastin fibers.* Acta Biomaterialia, 2009. **5**(2): p. 541-553.

265. Chung, K.W., S.H. Song, and M.-s. Kim, *Synergistic effect of copper and amino acid mixtures on the production of extracellular matrix proteins in skin fibroblasts.* Molecular Biology Reports, 2021. **48**(4): p. 3277-3284.

266. De Servi, B., et al., *Amino acid and hyaluronic acid mixtures differentially regulate extra cellular matrix genes in cultured human fibroblasts.* J Biol Regul Homeost Agents, 2018. **32**(3): p. 517-527.

267. Kim, M.-S., et al., *Evaluation of the Efficacy of an Elastin-Inducing Composition Containing Amino Acids, Copper, and Hyaluronic Acid: Results of an Open Single-Center Clinical Trial Study.* Cosmetics, 2022. **9**(3): p. 51.

268. Janssen, R., et al., *Copper-Heparin Inhalation Therapy To Repair Emphysema: A Scientific Rationale.* International journal of chronic obstructive pulmonary disease, 2019. **14**: p. 2587-2602.

269. Philips, N., et al., *Beneficial Regulation of Fibrillar Collagens, Heat Shock Protein-47, Elastin Fiber Components, Transforming Growth Factor-β1, Vascular Endothelial Growth Factor and Oxidative Stress Effects by Copper in Dermal Fibroblasts.* Connective Tissue Research, 2012. **53**(5): p. 373-378.

270. Badenhorst, T., et al., *Effects of GHK-Cu on MMP and TIMP Expression, Collagen and Elastin Production, and Facial Wrinkle Parameters.* Journal of Aging Science, 2016. **4**: p. 1-7.

271. Bunda, S., N. Kaviani, and A. Hinek, *Fluctuations of intracellular iron modulate elastin production.* J Biol Chem, 2005. **280**(3): p. 2341-51.

272. Ciceri, P., et al., *High-phosphate induced vascular calcification is reduced by iron citrate through inhibition of extracellular matrix osteo-chondrogenic shift in VSMCs.* International Journal of Cardiology, 2019. **297**: p. 94-103.

273. Casco, M., et al. *Iron Oxide Nanoparticles Stimulates Extra-Cellular Matrix Production in Cellular Spheroids*. Bioengineering, 2017. **4**, DOI: 10.3390/bioengineering4010004.

274. Bunda, S., N. Kaviani, and A. Hinek, *Fluctuations of Intracellular Iron Modulate Elastin Production*.* Journal of Biological Chemistry, 2005. **280**(3): p. 2341-2351.

275. Hill, C.H., et al., *Dietary Iron Deficiency Compromises Normal Development of Elastic Fibers in the Aorta and Lungs of Chicks1,2,3.* The Journal of Nutrition, 2007. **137**(8): p. 1895-1900.

276. Kattappagari, K., et al., *Role of antioxidants in facilitating the body functions: A review.* Journal of Orofacial Sciences, 2015. **7**(2): p. 71-75.

277. Rossetti, D., et al., *A novel anti-ageing mechanism for retinol: induction of dermal elastin synthesis and elastin fibre formation.* International Journal of Cosmetic Science, 2011. **33**(1): p. 62-69.

278. Shao, Y., et al., *Molecular basis of retinol anti-ageing properties in naturally aged human skin in vivo.* International Journal of Cosmetic Science, 2017. **39**(1): p. 56-65.

279. Tajima, S., A. Hayashi, and T. Suzuki, *Elastin expression is up-regulated by retinoic acid but not by retinol in chick embryonic skin fibroblasts.* Journal of Dermatological Science, 1997. **15**(3): p. 166-172.

280. Liu, B., C.S. Harvey, and S.E. McGowan, *Retinoic acid increases elastin in neonatal rat lung fibroblast cultures.* American Journal of Physiology-Lung Cellular and Molecular Physiology, 1993. **265**(5): p. L430-L437.

281. Lee, W.-R., et al., *Laser-assisted nanoparticle delivery to promote skin absorption and penetration depth of retinoic acid with the aim for treating photoaging.* International Journal of Pharmaceutics, 2022. **627**: p. 122162.

282. Sinha, A., N. Nosoudi, and N. Vyavahare, *Elasto-regenerative properties of polyphenols.* Biochemical and Biophysical Research Communications, 2014. **444**(2): p. 205-211.

283. Crandall, C.L., et al., *Pentagalloyl Glucose (PGG) Prevents and Restores Mechanical Changes Caused by Elastic Fiber Fragmentation in the Mouse Ascending Aorta.* Ann Biomed Eng, 2023. **51**(4): p. 806-819.

284. Chowdhury, A., et al., *Polyphenol treatments increase elastin and collagen deposition by human dermal fibroblasts; Implications to improve skin health.* Journal of Dermatological Science, 2021. **102**(2): p. 94-100.

285. Sanaei, K., et al., *Effect of all-trans retinoic acid and pentagalloyl glucose on smooth muscle cell elastogenesis.* Biomed Mater Eng, 2021. **32**(3): p. 145-157.

286. Duckworth, C., et al., *Effect of ellagic acid and retinoic acid on collagen and elastin production by human dermal fibroblasts.* Biomed Mater Eng, 2023. **34**(5): p. 473-480.

287. de Clerck, Y.A. and P.A. Jones, *The effect of ascorbic acid on the nature and production of collagen and elastin by rat smooth-muscle cells.* Biochemical Journal, 1980. **186**(1): p. 217-225.

288. Barnes, M.J., et al., *Studies in vivo on the biosynthesis of collagen and elastin in ascorbic acid-deficient guinea pigs. Evidence for the formation and degradation of a partially hydroxylated collagen.* Biochemical Journal, 1970. **119**(3): p. 575-585.

289. Barnes, M.J., B.J. Constable, and E. Kodicek, *Studies in vivo on the biosynthesis of collagen and elastin in ascorbic acid-deficient guinea pigs.* Biochemical Journal, 1969. **113**(2): p. 387-397.

290. Derricks, K.E., et al., *Ascorbate enhances elastin synthesis in 3D tissue-engineered pulmonary fibroblasts constructs.* Tissue and Cell, 2013. **45**(4): p. 253-260.

291. Tanaka, A., et al., *Controlled release of ascorbic acid from gelatin hydrogel attenuates abdominal aortic aneurysm formation in rat experimental abdominal aortic aneurysm model.* Journal of Vascular Surgery, 2014. **60**(3): p. 749-758.

292. S. Tajima, H.W., A. Hayashi, *Accumulation of Tropoelastin by a Short-term Ascorbic Acid Treatment in the Culture Medium of Aortic Smooth Muscle Cells in vitro.* The Keio Journal of Medicine, 1995. **44**(4): p. 140-145.

293. Hinek, A., et al., *Sodium l-ascorbate enhances elastic fibers deposition by fibroblasts from normal and pathologic human skin.* Journal of Dermatological Science, 2014. **75**(3): p. 173-182.

294. Widgerow, A.D., et al., *Antioxidants with proven efficacy and elastin-conserving vitamin C-A new approach to free radical defense.* J Cosmet Dermatol, 2023.

295. Philips, N., J. Chalensouk-Khaosaat, and S. Gonzalez, *Simulation of the Elastin and Fibrillin in Non-Irradiated or UVA Radiated Fibroblasts, and Direct Inhibition of Elastase or Matrix Metalloptoteinases Activity by Nicotinamide or Its Derivatives.* J Cosmet Sci, 2018. **69**(1): p. 47-56.

296. Bissett, D.L., J.E. Oblong, and C.A. Berge, *Niacinamide: A B Vitamin that Improves Aging Facial Skin Appearance.* Dermatologic Surgery, 2005. **31**(s1): p. 860-866.

297. Kim, H.M., et al., *A Mixture of Topical Forms of Polydeoxyribonucleotide, Vitamin C, and Niacinamide Attenuated Skin Pigmentation and Increased Skin Elasticity by Modulating Nuclear Factor Erythroid 2-like 2.* Molecules, 2022. **27**(4).

298. Marcheggiani, F., et al., *Anti-ageing effects of ubiquinone and ubiquinol in a senescence model of human dermal fibroblasts.* Free Radical Biology and Medicine, 2021. **165**: p. 282-288.

299. Zhang, M., et al., *Coenzyme Q10 enhances dermal elastin expression, inhibits IL-1α production and melanin synthesis in vitro.* International Journal of Cosmetic Science, 2012. **34**(3): p. 273-279.

300. Mine, Y., T. Takahashi, and T. Okamoto, *Stimulatory effects of collagen production induced by coenzyme Q(10) in cultured skin fibroblasts.* J Clin Biochem Nutr, 2022. **71**(1): p. 29-33.

301. Lee, S., et al., *Solid-State Fermentation With Aspergillus cristatus Enhances the Protopanaxadiol- and Protopanaxatriol-Associated Skin Anti-aging Activity of Panax notoginseng.* Frontiers in Microbiology, 2021. **12**.

302. Yang, S., et al., *Ginseng-derived nanoparticles induce skin cell proliferation and promote wound healing.* J Ginseng Res, 2023. **47**(1): p. 133-143.

303. Uehara, E., et al., *GABA promotes elastin synthesis and elastin fiber formation in normal human dermal fibroblasts (HDFs).* Bioscience, Biotechnology, and Biochemistry, 2017. **81**(6): p. 1198-1205.

304. Gaizono, H. and E. Uehara, *Effect of oral intake of γ-aminobutyric acid to improve skin condition.* Journal of Japan Society for Food Science and Engineering, 2016. **63**(7): p. 306-311.

305. Uehara, E., et al., *Effects of GABA on the expression of type I collagen gene in normal human dermal fibroblasts.* Bioscience, Biotechnology, and Biochemistry, 2017. **81**(2): p. 376-379.

306. Hokazono, H., T. Omori, and K. Ono, *Effects of Single and Combined Administration of Fermented Barley Extract and γ-Aminobutyric Acid on the Development of Atopic Dermatitis in NC/Nga Mice.* Bioscience, Biotechnology, and Biochemistry, 2010. **74**(1): p. 135-139.

307. Lai, C.-S., et al., *Tetrahydrocurcumin is more effective than curcumin in preventing azoxymethane-induced colon carcinogenesis.* Molecular Nutrition & Food Research, 2011. **55**(12): p. 1819-1828.

308. Trivedi, M.K., et al., *Protective effects of tetrahydrocurcumin (THC) on fibroblast and melanoma cell lines in vitro: it's implication for wound healing.* Journal of Food Science and Technology, 2017. **54**(5): p. 1137-1145.

309. Tran, T.A., et al., *Camphor Induces Proliferative and Anti-senescence Activities in Human Primary Dermal Fibroblasts and Inhibits UV-Induced Wrinkle Formation in Mouse Skin.* Phytotherapy Research, 2015. **29**(12): p. 1917-1925.

310. Grenier, A., et al., *Antioxidant, Anti-Inflammatory, and Anti-Aging Potential of a Kalmia angustifolia Extract and Identification of Some Major Compounds.* Antioxidants, 2021. **10**(9): p. 1373.

311. Simard, M., et al., *α-Linolenic acid and linoleic acid modulate the lipidome and the skin barrier of a tissue-engineered skin model.* Acta Biomaterialia, 2022. **140**: p. 261-274.

312. Nishizaki, T., *PKCε Increases Extracellular Elastin and Fibulin-5/DANCE in Dermal Fibroblasts.* Cellular Physiology and Biochemistry, 2018. **46**(1): p. 291-302.

313. Rhiu, S., et al., *Effect of Tanshinone IIA in an In Vitro Model of Graves' Orbitopathy.* Investigative Ophthalmology & Visual Science, 2014. **55**(9): p. 5900-5910.

314. Mao, S., et al., *Phytoestrogen, tanshinone IIA diminishes collagen deposition and stimulates new elastogenesis in cultures of human cardiac fibroblasts.* Exp Cell Res, 2014. **323**(1): p. 189-197.
315. Fhayli, W., et al., *Dill Extract Induces Elastic Fiber Neosynthesis and Functional Improvement in the Ascending Aorta of Aged Mice with Reversal of Age-Dependent Cardiac Hypertrophy and Involvement of Lysyl Oxidase-Like-1.* Biomolecules, 2020. **10**(2): p. 173.
316. Aimond, G., et al., *Dill extract preserves dermal elastic fibers network and functionality. Implication of elafin.* Skin Pharmacol Physiol, 2023.
317. Cenizo, V., et al., *LOXL as a target to increase the elastin content in adult skin: a dill extract induces the LOXL gene expression.* Experimental Dermatology, 2006. **15**(8): p. 574-581.
318. Meza, D., et al., *A blackberry–dill extract combination synergistically increases skin elasticity.* International Journal of Cosmetic Science, 2020. **42**(5): p. 444-451.
319. Zhao, R., et al., *Extracts from Glycine max (soybean) induce elastin synthesis and inhibit elastase activity.* Experimental Dermatology, 2009. **18**(10): p. 883-886.
320. D'Agostino, A., et al., *Molecular Mechanisms at the Basis of Pharmaceutical Grade Triticum vulgare Extract Efficacy in Prompting Keratinocytes Healing.* Molecules, 2020. **25**(3): p. 431.
321. Nanashima, N., et al., *Blackcurrant Anthocyanins Increase the Levels of Collagen, Elastin, and Hyaluronic Acid in Human Skin Fibroblasts and Ovariectomized Rats.* Nutrients, 2018. **10**(4): p. 495.
322. Dell'Acqua, G. and K. Schweikert, *Skin benefits of a myconoside-rich extract from resurrection plant Haberlea rhodopensis.* International Journal of Cosmetic Science, 2012. **34**(2): p. 132-139.
323. Lee, J., et al., *Evaluating the effect of Luffa cylindrica stem sap on dermal fibroblasts; An invitro study.* Biochemical and Biophysical Research Communications, 2021. **580**: p. 41-47.
324. Lee, J., et al., *An in vitro evaluation of luffa cylindrica stem sap in preadipocytes and dermal fibroblasts.* Biochem Biophys Res Commun, 2022. **599**: p. 100-105.
325. Gaillard, E., et al., *Tasmannia lanceolata leaf extract alleviates stretch mark appearance in a randomized, placebo-controlled clinical trial in women and stimulates extracellular matrix synthesis in ex vivo human skin explants.* Journal of Cosmetic Dermatology, 2021. **20**(6): p. 1923-1932.
326. Nguyen, H.T., et al., *Enhanced anti-wrinkle activity of adlay bran fermented with Lactobacillus brevis MJM60390.* J Cosmet Dermatol, 2022. **21**(11): p. 6351-6362.
327. Fu, H., et al., *Anti-Photoaging Effect of Rhodiola rosea Fermented by Lactobacillus plantarum on UVA-Damaged Fibroblasts.* Nutrients, 2022. **14**(11).
328. Gruber, J.V. and R. Holtz, *Living, quiescent Lactobacillus plantarum Lp90 probiotic, delivered topically to full thickness tissues in vitro via a just-add-water cream delivery system, stimulates the expression of elastin protein.* J Cosmet Dermatol, 2023. **22**(10): p. 2852-2860.
329. Wang, Y., et al., *Burn injury: Challenges and advances in burn wound healing, infection, pain and scarring.* Advanced Drug Delivery Reviews, 2018. **123**: p. 3-17.
330. Boizot, J., et al., *FBN2 Silencing Recapitulates Hypoxic Conditions and Induces Elastic Fiber Impairment in Human Dermal Fibroblasts.* International Journal of Molecular Sciences, 2022. **23**(3): p. 1824.
331. Papke, C.L. and H. Yanagisawa, *Fibulin-4 and fibulin-5 in elastogenesis and beyond: Insights from mouse and human studies.* Matrix Biol, 2014. **37**: p. 142-9.
332. Nakamura, T., et al., *Fibulin-5/DANCE is essential for elastogenesis in vivo.* Nature, 2002. **415**(6868): p. 171-175.
333. Joddar, B. and A. Ramamurthi, *Fragment size- and dose-specific effects of hyaluronan on matrix synthesis by vascular smooth muscle cells.* Biomaterials, 2006. **27**(15): p. 2994-3004.

334. Kothapalli, C.R., C.E. Gacchina, and A. Ramamurthi, *Utility of Hyaluronan Oligomers and Transforming Growth Factor-Beta1 Factors for Elastic Matrix Regeneration by Aneurysmal Rat Aortic Smooth Muscle Cells.* Tissue Engineering Part A, 2009. **15**(11): p. 3247-3260.

335. Sen, S., et al., *Retinoblastoma Protein Modulates the Inverse Relationship between Cellular Proliferation and Elastogenesis*.* Journal of Biological Chemistry, 2011. **286**(42): p. 36580-36591.

336. Barnett, C.P., et al., *Dexamethasone normalizes aberrant elastic fiber production and collagen 1 secretion by Loeys-Dietz syndrome fibroblasts: a possible treatment?* European journal of human genetics : EJHG, 2011. **19**(6): p. 624-633.

337. Ibáñez-Fonseca, A., et al., *Trends in the design and use of elastin-like recombinamers as biomaterials.* Matrix Biol, 2019. **84**: p. 111-126.

338. Zhao, Y., et al., *Advanced bioactive nanomaterials for biomedical applications.* Exploration, 2021. **1**(3): p. 20210089.

339. Duca, L., et al., *Elastin Peptides Activate Extracellular Signal-Regulated Kinase 1/2 via a Ras-Independent Mechanism Requiring Both p110γ/Raf-1 and Protein Kinase A/B-Raf Signaling in Human Skin Fibroblasts.* Molecular Pharmacology, 2005. **67**(4): p. 1315-1324.

340. Duca, L., et al., *The elastin peptides-mediated induction of pro-collagenase-1 production by human fibroblasts involves activation of MEK/ERK pathway via PKA- and PI3K-dependent signaling.* FEBS Letters, 2002. **524**(1): p. 193-198.

341. Mayer, I.A. and C.L. Arteaga, *The PI3K/AKT Pathway as a Target for Cancer Treatment.* Annual Review of Medicine, 2016. **67**(1): p. 11-28.

342. Oliva, N. and B.D. Almquist, *Spatiotemporal delivery of bioactive molecules for wound healing using stimuli-responsive biomaterials.* Advanced Drug Delivery Reviews, 2020. **161-162**: p. 22-41.

343. Gansevoort, M., et al., *Initial Steps towards Spatiotemporal Signaling through Biomaterials Using Click-to-Release Chemistry.* Pharmaceutics, 2022. **14**(10): p. 1991.

344. Khazaeli, P., et al., *Effects of minoxidil gel on burn wound healing in rats.* Iran J Pharm Res, 2014. **13**(1): p. 243-51.

345. Mathew-Steiner, S.S., S. Roy, and C.K. Sen *Collagen in Wound Healing*. Bioengineering, 2021. **8**, DOI: 10.3390/bioengineering8050063.

346. Park, H.J., et al., *Collagen Synthesis Is Suppressed in Dermal Fibroblasts by the Human Antimicrobial Peptide LL-37.* Journal of Investigative Dermatology, 2009. **129**(4): p. 843-850.

347. Yang, Y., et al., *Lipo-PGE1 suppresses collagen production in human dermal fibroblasts via the ERK/Ets-1 signaling pathway.* PLOS ONE, 2017. **12**(6): p. e0179614.

348. Rich, T.C., et al., *Cellular mechanisms underlying prostaglandin-induced transient cAMP signals near the plasma membrane of HEK-293 cells.* American Journal of Physiology-Cell Physiology, 2007. **292**(1): p. C319-C331.

349. Lin, G., et al., *Estrogen Attenuates TGF-β1 Induced Elastogenesis in Rat Urethral Smooth Muscle Cells by Inhibiting Smad Response Elements.* Journal of Urology, 2015. **193**(6): p. 2131-2137.

350. Sharma, S., et al., *Collagen-based formulations for wound healing: A literature review.* Life Sciences, 2022. **290**: p. 120096.

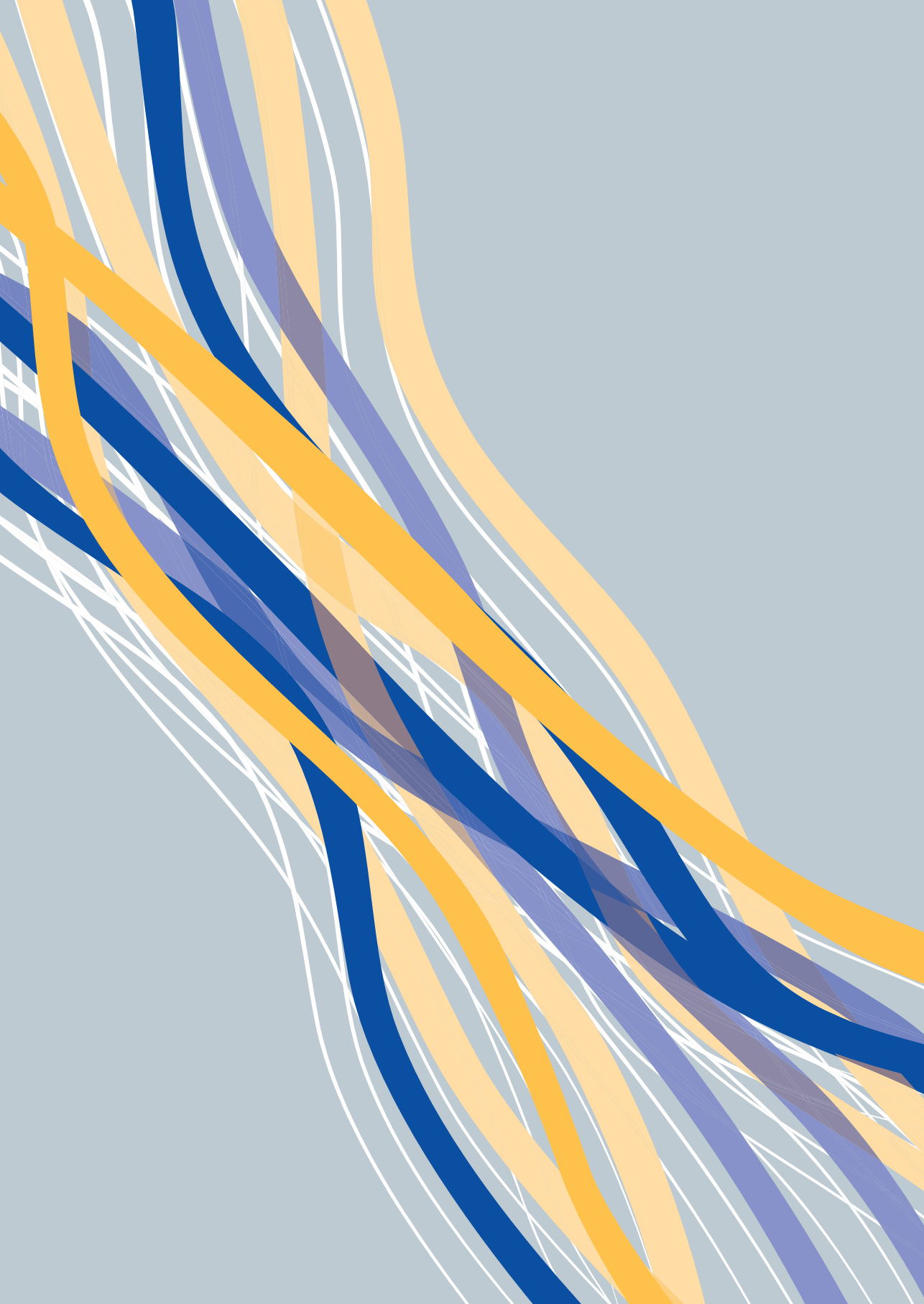

Chapter 2

Preparation, fractionation, and characterization of solubilized elastin and comparison of cellular response on fibroblasts and macrophages

Roman Krymchenko[1], Maren Pfirrmann[1], Sjoerd van der Leeuw[1], Nancy Avila-Martinez[1], Elly M. M. Versteeg[1], Rob T. C. Meuwese[1], Marcel Vlig[2], Martijn Verdoes[1,3], Bouke K. H. L. Boekema[2,4,5,6], Toin H. van Kuppevelt[1], Willeke F. Daamen[1]

[1]Radboud university medical center, Research Institute for Medical Innovation, Department of Medical BioSciences, Nijmegen, The Netherlands

[2]Alliance of Dutch Burn Care, Burn Research Lab, Beverwijk, The Netherlands

[3]Leiden University Medical Center, Department of Immunology, Leiden, The Netherlands

[4]Amsterdam University Medical Center (AUMC), Amsterdam, The Netherlands

[5]Tissue Function and Regeneration, Amsterdam Movement Sciences Research Institute, Amsterdam, The Netherlands

[6]Department of Plastic, Reconstructive and Hand Surgery, AUMC, location VUmc, Amsterdam, The Netherlands

Published in *International Journal of Biological Macromolecules* (2025, 315, 144548).

DOI: 10.1016/j.ijbiomac.2025.144548

Abstract

Elastin and elastin-derived compounds are promising biomaterials due to their biological activity, unique natural crosslinks, and ability to mimic native tissue properties. Solubilized elastin peptides retain the bioactivity of elastin and are more suitable for wound care applications than the insoluble form. Chemically solubilized elastins have shown advantageous effects in skin regeneration in humans. Here, five solubilized elastins were prepared via chemical (stepwise and continuously hydrolyzed with oxalic acid - OxA-st-ELN and OxA-ELN, or with potassium hydroxide - KOH-ELN), enzymatic (Enz-ELN), or combined (Combi-ELN) methods. OxA-st-ELN had the largest molecular weights (MWs) fragments, while Enz-ELN and Combi-ELN yielded the smallest. The effects of elastin preparations were evaluated on primary human cells – dermal fibroblasts and macrophages. In fibroblast assays, Enz-ELN induced elastin, collagen, and fibrillin-2 protein deposition, while other preparations exhibited levels comparable to the control. α-smooth muscle actin (SMA) expression remained low across all conditions. Continuous oxalic acid hydrolysis simplified the traditional stepwise approach while maintaining bioactivity. Macrophage studies showed chemical hydrolysates preserved the M0-like subtype, while Enz-ELN promoted a pro-inflammatory M1-like phenotype, and Combi-ELN had mixed effects. OxA-ELN and KOH-ELN appeared to be the most promising options for developing biomaterial dermal scaffolds that support tissue regeneration *in vivo*.

Graphical abstract

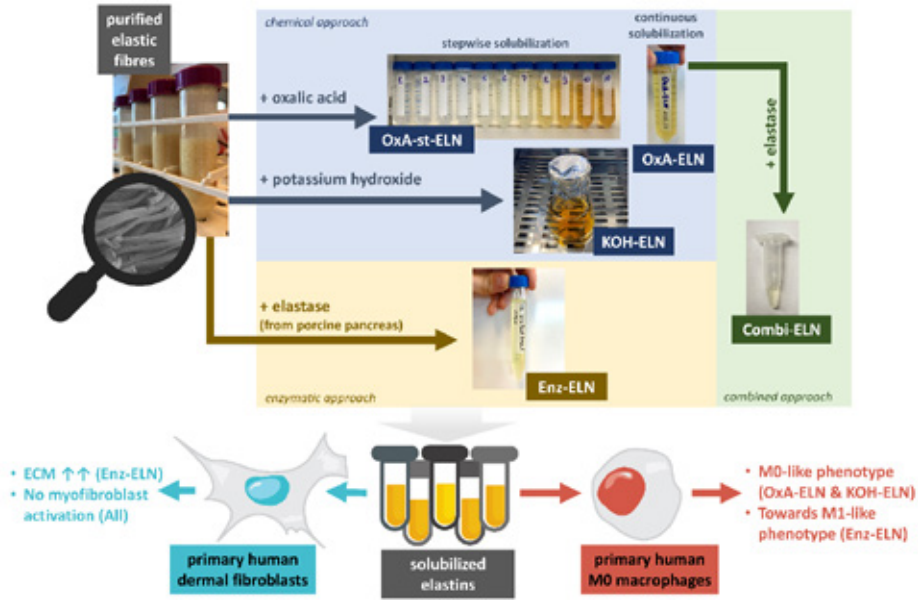

1. Introduction

The combination of collagen and elastic fibers affords strength and flexibility to the skin [1]. When skin is injured, dermal fibroblasts are key players in healing processes by transforming into myofibroblasts, which are specialized for contraction and remodeling of the extracellular matrix (ECM) [2]. After healing, myofibroblasts undergo apoptosis, but in pathological cases, excessive activity can lead to fibrosis and scarring [3]. While collagen fibers undergo partial remodeling, the intricate elastic fiber network, once damaged, cannot be fully restored [4]. Although elastin production increases after injury, it is usually insufficient, and its disordered deposition results in scar formation and contractions [5].

Elastin protein is an essential component of elastic fibers, with the microfibrillar network integrated both within and surrounding these fibers [6]. Elastin-derived compounds are reported to have various biological activity [5, 7, 8]. These compounds are particularly appealing as biomaterials because they mimic natural conditions/compositions and possess unique crosslinks (e.g., desmosine and isodesmosine). Compared to the insoluble and relatively inert mature elastin protein, solubilized elastins hold more promise for wound care applications [9-12].

In experimental settings, insoluble elastin can typically be solubilized through two main approaches: enzymatic digestion or chemical hydrolysis. The enzymatic approach can replicate physiological mechanisms present in the human body with specific cleavage sites [13]. Digested elastin can have beneficial bioactivity in wound management, e.g., by stimulation of cell adhesion and proliferation, chemotaxis, promotion of angiogenesis, and elevated elastin expression [14-19]. Unlike enzymatic digestion, solubilization with chemicals leads to non-specific bond cleavages. Stepwise oxalic acid hydrolysis and alkaline KOH treatment in aqueous ethanol are the most used approaches [20-23]. Chemically solubilized elastins have also shown beneficial effects in wound healing and are known to be incorporated into dermal scaffolds [10-12, 16, 24, 25], such as MatriDerm, that enhance skin elasticity and reduces contractures [26-28].

When testing new compounds on skin wound healing, an *in vitro* model using human dermal fibroblasts is the most optimal choice to start with. Ascorbic acid and its derivatives are known to stimulate ECM production by fibroblasts [29]. The yield of deposited ECM can be further enhanced by applying macromolecular crowders (MMCs), increasing the effective concentration and thermodynamic activity of other molecules in the system [30]. In addition to fibroblasts, macrophages are also pivotal in skin wound healing, influencing all stages, from inflammation to

remodeling [31]. The pro-inflammatory M1 macrophages are the predominant subtype present in the early stages of wound healing [32]. Later, anti-inflammatory M2 macrophages take over, promoting tissue repair [33]. The functional plasticity of macrophages allows them to adapt to the wound microenvironment, regulate fibroblasts, keratinocytes and endothelial cells, and support vascularization [34].

In the present study, we aim to assess the differences among distinct solubilized elastins, with a particular focus on their preparation methods, physicochemical characterization, and biological effects on human primary skin fibroblasts and macrophages. Such comparisons should improve the understanding of how variations in solubilization techniques influence the composition of obtained structures and functional properties. We specifically select potent chemical hydrolysates, focusing on the most studied methods – solubilizations with oxalic acid and potassium hydroxide, assess the altered mechanism of oxalic acid hydrolysis through continuous solubilization, and examine a novel enzymatic digestion approach with elastase from porcine pancreas. Furthermore, we investigate the impact of these different preparations on cellular behavior, including cell viability, gene, and protein expression in fibroblasts, as well as polarization of macrophages. This comprehensive analysis is expected to provide valuable insights into the suitability of specific solubilized elastins for applications in the development of bioactive materials and regenerative medicine.

2. Materials and methods

Unless otherwise specified, chemicals, enzymes, and cell culture supplements were purchased from Sigma-Aldrich/Merck, while cell culture media and antibiotics were obtained from Gibco.

2.1. Purification and analysis of insoluble elastic fibers

Insoluble elastin was purified from pulverized equine *ligamentum nuchae* using a protocol developed by our research group [35]. This involved sequential treatments with aqueous sodium chloride, chloroform/methanol, acetone, diethyl ether, cyanogen bromide in anhydrous formic acid, demineralized water, β-mercaptoethanol in aqueous urea, and trypsin digestion. The final product was washed with aqueous sodium chloride and demineralized water.

For SDS-PAGE, the purified elastin was incubated at 100°C for 5 min in reducing buffer (5% [v/v] β-mercaptoethanol) and analyzed on a 10% (w/v) polyacrylamide

gel. Notably, with this approach, only soluble compounds (contaminants and elastin degradation products) permeate the gel, while fibrillar elastin remains unaffected and insoluble. Proteins were visualized with a 0.1% (w/v) silver nitrate solution. A MW marker, PageRuler Plus Prestained Protein Ladder (10–250 kDa; Thermo Scientific, Waltham, MA, USA), was included.

For histological analysis, elastic fibers were embedded in 1.5% (w/v) agarose, fixed in 2% (v/v) glutaraldehyde in 0.1 M phosphate buffer (pH 7.4), post-fixed with 1% (w/v) osmium tetroxide, dehydrated in an ascending series of ethanol, and embedded in Epon 812. Sections (1 µm) were stained with 1% toluidine blue in 1% sodium borate and examined using a light microscope. Lyophilized elastin samples were prepared for scanning electron microscopy (SEM) by attaching fibers to carbon tape, sputtering with gold in a Polaron E5100 SEM coating system (Quorum Technologies, Newhaven, UK), and imaging with a Zeiss Sigma 300 SEM at 3 kV.

2.2. Preparation of solubilized elastin peptides

Detailed abbreviations of elastin preparations used are listed in Table 1.

Table 1. List of abbreviations of solubilized elastin preparations.

Abbreviation	Definition
OxA-st-ELN	Hydrolyzed elastin preparation by stepwise treatment with oxalic acid
OxA-ELN	Hydrolyzed elastin preparation by continuous treatment with oxalic acid
KOH-ELN	Hydrolyzed elastin preparation by treatment with potassium hydroxide
Enz-ELN	Digested elastin preparation by treatment with elastase from porcine pancreas
Combi-ELN	Digested elastin preparation by additional treatment of OxA-ELN preparation with elastase

2.2.1. Hydrolyzed elastin preparation by stepwise treatment with oxalic acid (OxA-st-ELN)

The goal of stepwise solubilization is to achieve mild hydrolysis with the retention of larger MW fragments. Complete solubilization of elastic fibers was achieved with 10-12 consecutive incubations with 0.25 M oxalic acid at 95 °C for 1 h, followed by centrifugations and collection of supernatants. For this method, 4.0 g purified elastin fibers were incubated in 40 mL 0.25 M oxalic acid at 95 °C for 1 h followed by collection of the supernatant with centrifuging at 500 x g for 5 min at 4 °C. The pellet was resuspended in the same volume of 0.25 M oxalic acid and incubated again for 1 h at 95 °C. These steps were repeated until the pellet was completely dissolved (9-11 times) to collect 10-12 supernatant fractions in total. The absorbance of supernatants was assessed at 280 nm (protein indication) and 420

nm (yellow color). For OxA-st-ELN, fractions 7-11 were combined and concentrated using 10 kDa filter tubes (Amicon Ultra-15 Centrifugal Filter Device) at 4,500 x g for 30 min. Then, the solution was neutralized with 10 mM phosphate buffer (pH 7.4). The neutralized solution was dialyzed against demineralized water using the same filter tubes. After the successful removal of ions, the final preparation was filtered with 0.45 µm filters (Whatman FP 30/0.45 CA-S, Cytiva, Marlborough, MA, USA) and stored at -20°C.

2.2.2. Hydrolyzed elastin preparation by continuous treatment with oxalic acid (OxA-ELN)

For faster hydrolyzation, acidic solubilization was performed without hourly renewal of oxalic acid. 15.3 g of dry elastin was suspended in 50 mL 0.25 M oxalic acid at 95°C and incubated for 9 h, resulting in complete solubilization, and centrifuged at 500 x g for 5 min to remove impurities. Next, the solubilized elastin was neutralized with 1 M sodium acetate until pH ~6 and dialyzed against 10 L demineralized water in 3,500 MWCO dialysis tubes five times. The final preparation was filtered through 0.20 µm filters (Acrodisc 25 mm Supor STRL, Pall Corporation, Port Washington, NY, USA) and stored at -20°C.

2.2.3. Hydrolyzed elastin preparation by treatment with potassium hydroxide (KOH-ELN)

4.0 g of purified elastin fibers were incubated in 100 mL 1 M KOH in 80% aqueous ethanol for 7 h at 37 °C with periodical shaking until all fibers were solubilized. The solution was then centrifuged at 15,000 x g for 20 min at 4 °C to remove impurities, and the supernatant was neutralized with $HClO_4$. The obtained precipitate of $KClO_4$ was removed by centrifuging at 15,000 × g for 20 min at 4 °C. The collected supernatant was dialyzed against 10 L demineralized water in 3,500 MWCO dialysis tubes in five steps. The final preparation was filtered with 0.20 µm filters and stored at -20°C.

2.2.4. Digested elastin preparation by treatment with elastase (Enz-ELN)

1.04 g of purified elastin fibers were suspended in 6 mL of 3.7 mM NH_4HCO_3 (pH 8.05) containing 350 µL of type I elastase from porcine pancreas (E-1250), corresponding to 9.6 Sigma units of enzyme. The mixture was gently shaken for five days. Afterward, the mixture was incubated with 1 g of insoluble elastic fibers for 30 min to remove elastase via affinity absorption, then centrifuged at 3,000 × g for 5 min at room temperature. The affinity absorption step was performed four more times with unused insoluble elastic fibers. The supernatant was filtered through a 0.20 µm filter and stored at -20°C.

2.2.5. Digested elastin preparation by additional treatment of OxA-ELN preparation with elastase (Combi-ELN)

In a combined approach, OxA-ELN was further digested with elastase. A total of 250 mg of lyophilized OxA-ELN was dissolved in 5 mL of 3.7 mM NH_4HCO_3 (pH 8.05) with 300 µL of elastase, corresponding to 1.5 mg enzyme. Samples were collected at six time points (6, 24, 48, 72, 96, and 168 h), filtered using 10 kDa Amicon tubes (5,000 × g, 40 min, 4 °C), and the retentate (with molecules >10 kDa) reconstituted to 5 mL with NH_4HCO_3 for further incubation. Filtrates were then processed with 2 kDa Vivaspin filter tubes (Satrorius Stedim Biotech, Goettingen, Germany; 3,000 × g, 30 min, 4 °C), and the retentate containing 2-10 kDa elastin fragments was dialyzed with demineralized water using the same filter tubes. The final preparation was filtered with 0.20 µm filters and stored at -20°C.

2.2.6. Analysis of solubilized elastin peptides

For glycine-SDS-PAGE, solubilized elastin was incubated in a reducing buffer at 100 °C for 5 min and analyzed on 10% polyacrylamide or 4-15% gradient gels. A MW marker, PageRuler™ Plus Prestained Protein Ladder, was included. Tricine-SDS-PAGE was used for low MW samples (1-100 kDa), and the gels contained an additional intermediate layer. A low MW marker, Spectra Multicolor Low Range Protein Ladder, was included in tricine-SDS-PAGE. Proteins were visualized with Coomassie brilliant blue or silver staining. Elastin protein concentrations were determined using Lowry assay with BSA and KOH-ELN as references. Primary amine groups were quantified via 2,4,6-trinitrobenzene sulfonic acid (TNBS) assay. Calibration was performed with glycine solutions (0-80 µg/mL) in 4% $NaHCO_3$, and absorbance was measured at 420 nm on a SpectraMax iD3 plate reader (Molecular Devices, CA, USA).

Size-exclusion chromatography was conducted using HiPrep 26/60 Sephacryl S-100 HR and S-400 HR columns (Cytiva) on an ÄKTA FPLC explorer system (Amersham Biosciences, Amersham, UK). The columns were washed with demineralized water before measurements. All liquids were filtered with 0.2 µm cellulose nitrate filters (Whatman, Dassel, Germany) before use. Approximately 1 mL of saturated protein solution (≥ 50 mg) was loaded on the column in 50 mM phosphate buffer (pH 7.6), and absorbance was measured at 280 nm. The following protein standard mix (69385) was used for column calibration: thyroglobulin bovine (~670 kDa), γ-globulins from bovine blood (~150 kDa), albumin chicken egg grade VI (~44.3 kDa), ribonuclease A type I-A from bovine pancreas (~13.7 kDa), p-aminobenzoic acid (137 Da).

Endotoxin levels were measured by ToxinSensor™ Chromogenic LAL endotoxin assay kit (Genscript, Piscataway, USA) according to the manufacturer's instructions.

Calibration was performed using a serial dilution of the kit's endotoxin standard (0.1-0.01 EU/mL), and absorbances were measured at 545 nm on a SpectraMax iD3 plate reader.

2.3. Human fibroblasts

2.3.1. Cell culture with primary human dermal fibroblasts

Before the start of experiments with ECM production, normal adult primary human dermal fibroblasts (3 donors) were propagated in Dulbecco's modified Eagle medium (DMEM) containing 5 U/mL penicillin and 5 µg/mL streptomycin, 1% GlutaMAX™ and 10% fetal bovine serum (FBS) at 37°C in 5% CO_2. All cells were assessed negative for mycoplasma. At the start of the experiment, cells were starved for 24 h in a medium with 0.5% FBS. Experiments for ECM production were conducted in a medium with 10% FBS, whereas 1% FBS was used for cell viability assay, both supplemented with 100 µM sodium ascorbate as a stimulator for ECM production and 21.5 mg/mL PVP40 as a macromolecular crowder. The prepared media were filtered through a 0.2 µm filter. For evaluating the effect of different soluble elastin preparations, 50 µg/mL concentrations were applied. A condition without elastin served as a control, and 5 ng/mL TGF-β1 (Peprotech, London, UK) served as a positive control for myofibroblast differentiation. Medium and compounds were refreshed every 48 h. At the end of the cell culture, wells were washed with PBS (phosphate-buffered saline) twice and proceeded for further analysis.

2.3.2. alamarBlue™ cell viability assay

To assess the effect of solubilized elastin preparations (50 and 150 µg/mL) on the viability of primary human dermal fibroblasts (n = 3 donors), cells were seeded at low density (9,000 cells per well) in 48-well plates. Cell viability was evaluated on day 0 (before stimulation) and on days 1 and 3 (after stimulation). 10% solution of alamarBlue Cell Viability Reagent (Invitrogen, Carlsbad, CA, USA) was added to the culture medium and incubated for 4 h at 37°C in 5% CO_2. Fluorescence intensity was measured using a SpectraMax iD3 plate reader, with excitation at 540 nm and emission at 590 nm. Condition without solubilized elastin preparations served as a control.

2.3.3. RNA isolation, cDNA synthesis, and gene expression analysis by real-time qPCR

Samples for qPCR analysis were collected on days 2, 4, and 7, with the media being exchanged 24 h before RNA harvest. Cellular RNA was isolated using Trizol reagent, followed by chloroform treatment, centrifugation (12,000 × g, 4°C, 15 min), and dilution with 70% aqueous ethanol. Subsequent steps were performed using the

RNeasy Mini Kit (74106, Qiagen, Hilden, Germany) according to the manufacturer's protocol. RNA quality and quantity were assessed using the NanoDrop ND-1000 spectrophotometer (NanoDrop Technologies, Wilmington, DE, USA) by measuring absorbance ratios at 230, 260, and 280 nm. Isolated RNA samples were reverse-transcribed into first-strand cDNA using the iScript cDNA synthesis kit (Bio-Rad Laboratories Inc., Hercules, CA, USA) following the manufacturer's instructions.

Expression levels of sixteen genes related to ECM production were analyzed – *ACTA2, TGFB1, COL1A1, COL3A1, ELN, FN1, FBN1, FBN2, FBLN4, FBLN5, LOX, MAGP2, MMP12* and *TIMP1* (Table S1), with *YWHAZ* and *GAPDH* as reference genes. RT-qPCR primers were designed based on human gene sequences.

PCR amplifications were performed in duplicate using SYBR Green I Master Mix (Bio-Rad Laboratories Inc.) under the following conditions: 3 min at 95°C; 40 cycles of 15 s at 95°C and 30 s at 60°C (with plate reading), followed by 1 min at 95°C and 1.5 min at 65°C. Amplifications were carried out on a CFX Connect Real-Time PCR Detection System (Bio-Rad Laboratories Inc.). Data were processed using CFX Maestro™ Software (Bio-Rad Laboratories Inc.) and visualized using GraphPad Prism version 10.4.1. Relative gene expression levels were calculated using the ΔΔCT method.

2.3.4. SDS-PAGE and Western blot analysis

Cells were mixed with 200 of reducing sample buffer, and the suspension was collected. The samples were heated at 95 °C for 5 min, and 10 µL was separated on a 10% polyacrylamide gel via SDS-PAGE. A MW marker, PageRuler™ Plus Prestained Protein Ladder, was included. Electrophoresis was run at 130 V for 60 min.

Following SDS-PAGE, proteins were transferred to nitrocellulose membranes for Western blotting and immunostaining. Membranes were blocked overnight at 4 °C with 2% bovine serum albumin (BSA) in PBST (PBS with 0.1% Tween-20) to prevent non-specific binding. Primary antibody – monoclonal mouse anti-alpha smooth muscle actin (clone 1A4, A-2547), polyclonal rabbit anti-type I collagen (ab34710, Abcam, USA), rabbit anti-fibrillin-2 (gift from Dieter P. Reinhardt), or monoclonal rabbit anti-GAPDH antibody (Cell Signaling, USA, 2118) – was diluted (1:1,000) in blocking buffer and incubated with the membranes for 1 h at room temperature (RT). After washing with PBST, membranes were incubated with secondary antibody –goat polyclonal anti-mouse IgG (H+L) conjugated to IRDye 800CW (LI-COR Biotechnology, Lincoln, NE, USA, 926-32210), anti-rabbit IgG (H+L) conjugated to IRDye 800CW (LI-COR Biotechnology, 926-32211) or anti-rabbit IgG (H+L) conjugated to IRDye 680CW (LI-COR Biotechnology, 926-68071)– at a 1:20,000

dilution for 1 h at RT. GAPDH was used as an internal loading control. Signals were detected using the LI-COR® Odyssey® CLx Infrared Imaging System and analyzed with Image Studio™ Software 5.0. Values of signals of interest were normalized by dividing the target protein signal by the internal loading control to exclude discrepancies due to variations in sample loading or protein transfer. Values were subsequently normalized to the experimental control.

2.3.5. Immunofluorescence staining

Type I collagen deposition was visualized by immunofluorescence staining on cells fixed with 4% paraformaldehyde in PBS for 10 min. For intracellular detection of α-smooth muscle actin (α-SMA), cells were permeabilized with 0.5% Triton X-100 in PBS for 10 min. The cells were blocked in PBS containing 2% BSA for 1 h at RT before incubation with primary antibody (rabbit anti-type I collagen, 1:500 dilution, mouse anti-α-SMA, 1:2,000 dilution, or mouse anti-elastin (E-4013), 1:500 dilution) for 1 h at RT. After washing, cells were incubated with secondary antibody (goat anti-mouse IgG (H+L) Alexa Fluor 488 (Invitrogen, Waltham, MA, USA; A-11001), goat anti-rabbit IgG (H+L) Alexa Fluor 594 (A-11012), or goat anti-mouse IgG (H+L) Alexa Fluor 594 (A-11032) or Alexa Fluor 488 phalloidin (A-12379) for 1 h at RT. Nuclei were stained with DAPI (1 µg/mL), and all washes were performed with PBST. Finally, cells were mounted using Mowiol and imaged with a Zeiss Axio Imager A2 microscope (Zeiss Group, Oberkochen, Germany) using Zen 2 (Blue Edition) software.

2.3.6. Picrosirius red staining

Collagen protein deposition was assessed using Picrosirius Red staining. Cells were first fixed with Kahle fixative (3.7% formaldehyde, 2% glacial acetic acid in 28% aqueous ethanol) for 10 min. After a single PBS wash, samples were stained with a solution of 50 mg Direct Red 80 dissolved in 4 mL of saturated aqueous picric acid for 3 h. Excess stain was removed with repeated washes until the rinse water ran clear. Brightfield imaging was performed using a Zeiss Axio Imager A2 microscope with Zen 2 software. For quantification, stained proteins were eluted with a destaining solution (0.1 M NaOH in 50% aqueous methanol) for 10 min with continuous shaking. The eluted dye was collected in duplicate, and optical density was measured at 540 nm using a SpectraMax iD3 plate reader.

2.3.7. Fastin elastin assay

The Fastin Elastin Kit (Biocolor, Carrickfergus, UK) was used to measure elastin content in cell culture experiments, following the manufacturer's protocol. α-elastin standards (12.5, 25, and 50 µg) were prepared to quantify elastin levels in the samples. Elastin samples were collected by adding 500 µL of 0.25 M oxalic acid to

the cells, followed by manual scraping of the wells. To solubilize elastin, the samples were treated with oxalic acid at 95°C for 3 h and the obtained solutions were centrifuged at 13,000 × g for 10 min at 23°C. Aliquots of the supernatant (200 µL) were used to quantify elastin content according to the manufacturer's instructions.

2.4. Human macrophages

Primary human monocytes were isolated from peripheral blood mononuclear cells of healthy donors (4 donors) by magnetic-activated cellular sorting using a monocyte-specific monoclonal antibody ($CD14^+$) coupled to magnetic beads (Miltenyi Biotec, 130-050-201). Informed consent was given in accordance with the Declaration of Helsinki and Dutch national and Sanquin internal ethic boards (Blood Bank Sanquin, Nijmegen, Netherlands). Monocytes were differentiated to macrophages during 6 days with 50 ng/mL M-CSF (macrophage colony-stimulating factor; Miltenyi Biotec) in RPMI 1640 medium with 10% fetal calf serum (Biowest), 1% ultraglutamine (Lonza), and 1% antibiotic-antimycotic (1.5 million cells/well, 37°C in 5% CO_2). On day 6, 50 µg/mL of elastin preparations were applied to evaluate the effect of different soluble elastin preparations on macrophages and incubated for 2 days. The untreated cells were used as M0 phenotype control. Macrophages were also stimulated with human 20 ng/mL IFN-γ (interferon gamma; Gibco) and 100 ng/mL LPS (lipopolysaccharides; Invitrogen) for 48 h to induce an M1-like phenotype or stimulated with human 20 ng/mL IL-4 and 20 ng/mL IL-13 (interleukin 4 and interleukin 13; Gibco) for 48 h to induce an M2-like phenotype. The cells were harvested via mechanical detachment by gentle scraping. eFluor 780 (ThermoFisher, 65-0865-14) was used as a viability dye. Flow cytometry (BD FACSVerse, BD Biosciences) was performed to assess CD80, PDL1, HLA-DR, CD163, CD206, CD11b, MerTK markers (antibodies from BD Biosciences and BioLegend). Data were analyzed using FlowJo v10 software (BD Biosciences). The gating strategy was based on M1- and M2-like controls (see Figure S1).

2.5. Statistical analysis

Statistical testing was performed in GraphPad Prism version 10.4.1. Relative measurements, normalized to the control condition without soluble elastin, were compared using a one-sample t-test. Comparisons between groups were calculated with one-way ANOVA, followed by Tukey's multiple comparisons test (comparisons between any soluble elastin and TGF-β1 were not displayed). A p-value of <0.05 (95% confidence interval) was considered statistically significant. For the flow cytometry analysis of macrophages, the Compact Letter Display method was used as an alternative approach for visualizing multiple pairwise comparisons in graphical representations, reducing the need for numerous brackets with asterisks

on the graph. In this method, each group was assigned a combination of letters, ensuring that every group received at least one letter (while potentially sharing multiple letters with others). This letter assignment allows for straightforward comparisons: if two groups share at least one letter, it indicates that the p-value for their pairwise comparison is not below the significance threshold ($\alpha < 0.05$), suggesting no statistically significant difference between them. Conversely, groups with entirely different letters indicate the presence of a significant difference.

3. Results

3.1. Purified insoluble elastin obtained from ligamentum nuchae

Our purification procedure of elastin fibers enabled the gradual elimination of impurities and other ECM components (e.g., collagen, microfibrils), resulting in elastin of high purity and preserved structure (Figure S2). The entire purification process was completed within 10 days, and four independent batches of purified elastin fibers were obtained. The purity of the insoluble elastin preparations was assessed using SDS-PAGE followed by silver staining to visualize impurities (Figure 1A). The SDS-PAGE analysis confirmed the removal of the contaminants typically found in the initial *ligamentum nuchae* tissue. A faint protein band was consistently observed at approximately 24 kDa in all batches of purified insoluble elastin and most likely corresponded to trypsin. Histological analysis of elastic fibers was performed using ultrathin sections stained with toluidine blue (Figure 1B). These sections showed no residual contamination from the starting *ligamentum nuchae* tissue. The structural integrity of the fibers was preserved during the purification process. Scanning electron microscopy (SEM) further characterized the morphology of the purified elastin (Figure 1C). SEM images additionally proved that the elastin fibers retained a fibrous structure, though partial disintegration of the fibers was noted.

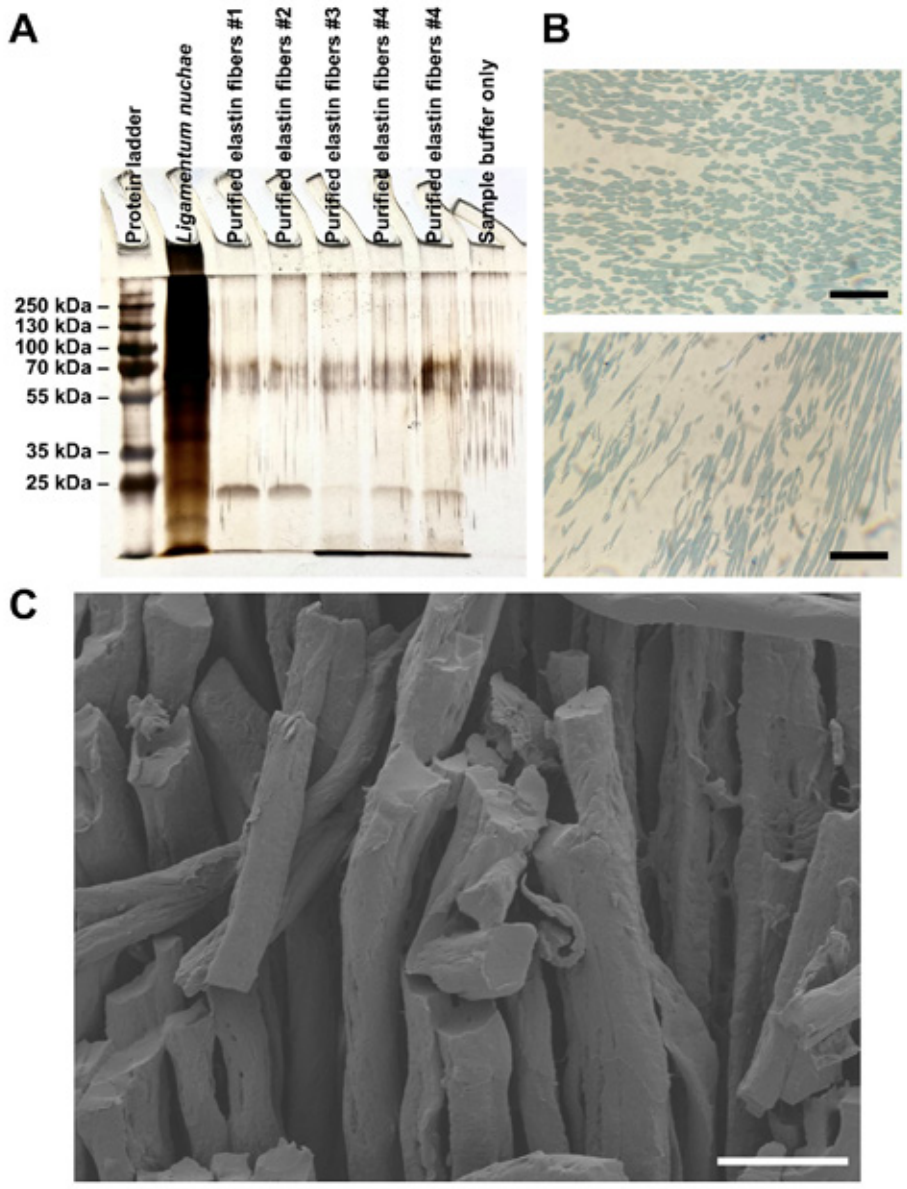

Figure 1. Analysis of purified elastin fibers. A) Silver-stained SDS-PAGE with insoluble elastin (1 µg of pulverized ligament and 2 µg of purified fibers on gel) from four different batches to visualize impurities and degradation products as elastin fibers are too large to enter this gel. The ~60-70 kDa band is an artifact also present in sample buffer, and the ~24 kDa band is likely due to residual trypsin from the purification. B) Light microscopy pictures showed even staining of 1 µm sections of elastic fibers treated with toluidine blue, cross-section (top) and longitudinal section (bottom). Scale bar is 50 µm. C) SEM image of isolated elastin fibers showed fibrous structures. Scale bar is 10 µm.

3.2. Different approaches to solubilize elastin

Two primary approaches for solubilization of elastin fibers were utilized: chemical hydrolysis and enzymatic digestion. Oxalic acid was selected for acidic hydrolysis (OxA-ELN and OxA-st-ELN) and potassium hydroxide for alkaline hydrolysis (KOH-ELN). Oxalic acid was applied in two ways: conventional stepwise solubilization (OxA-st-ELN) and, alternatively, continuous hydrolysis (OxA-ELN). Elastase from porcine pancreas was used to digest insoluble elastin (Enz-ELN). To combine the chemical hydrolysis approaches with enzymatic digestion, OxA-ELN preparation was further digested with elastase from porcine pancreas (Combi-ELN). Hence, five different solubilized elastin preparations were obtained.

Twelve consecutive incubations with 0.25 M oxalic acid at 95 °C for 1 h followed by centrifugations resulted in complete solubilization of elastin fibers (Figure 2A). Lowry protein measurements correlated with optical density (OD) at 420 nm of the supernatant fractions. The majority of soluble proteins (38%) was in supernatant 10, while the combined supernatants 3, 4, 5, and 12 comprised oy 2% of the total protein amount. Alternative acidic solubilization where oxalic acid was not renewed after each 1 h incubation step also resulted in complete solubilization after 9 h. Potassium hydroxide treatment dissolved the fibers the fastest, i.e., in 7 h, while enzymatic digestion required at least 5 days.

The MWs of all soluble elastin preparations were examined by SDS-PAGE with Coomassie brilliant blue and silver staining (Figure 2B). Chemical preparations formed smears extending from the stacking gel to the front and contained proteins with a broad range of MWs. For oxalic acid hydrolysates, these ranges shifted to larger sizes with higher supernatant numbers. Assessment of MW ranges for OxA-st-ELN showed differences among the fractions, although no definite conclusion about MW for a particular fraction could be made (Figure S3A). Notably, SDS-PAGE patterns revealed that OxA-st-ELN, OxA-ELN, and KOH-ELN were rather similar, whereas Enz-ELN and Combi-ELN indicated distinctively lower MWs. To remove elastase from the Enz-ELN, additional insoluble elastin fibers were added, incubated in the mixture, and removed by centrifugation five consecutive times. SDS-PAGE revealed that the majority of elastase, which was used for obtaining Enz-ELN, was absorbed onto these elastin fibers (Figure S3B). Nevertheless, slight traces of elastase were detected with a sensitive silver staining. For Combi-ELN, selective filtration tubes were used to collect distinct MWs (2-10 kDa) while excluding elastase (26 kDa) but was unsuccessful, as shown by silver stained SDS-PAGE (Figure 2B, Figure S3B).

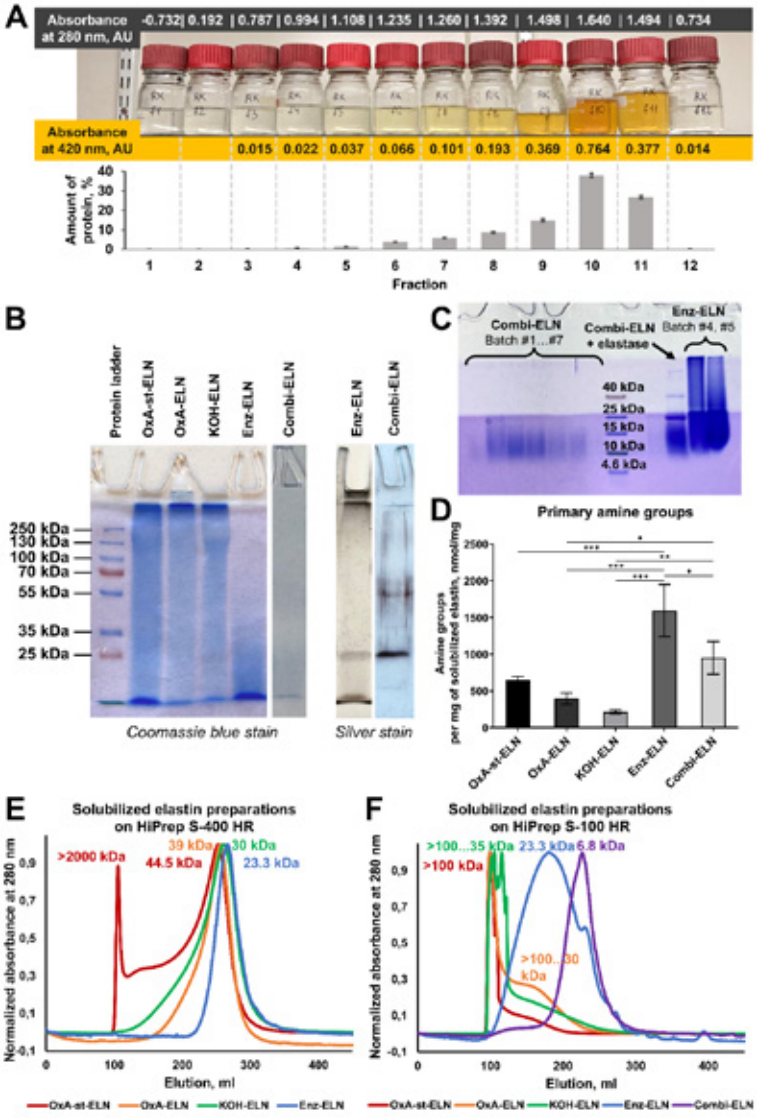

Figure 2. Analysis of four different solubilized elastin preparations. A) Stepwise solubilized elastin with oxalic acid hydrolysis (OxA-st-ELN), showing a macroscopic image of collected supernatants and 280 and 420 nm absorbances and distribution of protein content over the different supernatants from OxA-st-ELN as determined by Lowry protein assay. B) Coomassie brilliant blue (left) and silver (right) stained glycine SDS-PAGE gels of solubilized elastins. Enz-ELN and Combi-ELN showed the presence of elastase (26 kDa). C) Coomassie brilliant blue stained trycine SDS-PAGE gels of different batches of Enz-ELN, Combi-ELN, and a mixture of Combi-ELN with elastase before filter tube centrifugations. D) Primary amine group quantification via TNBS assay. E-F) Elution curves for representative samples of four different types of solubilized elastins on HiPrep S-400 HR with 20 – 8,000 kDa range for globular proteins (E) and on HiPrep S-100 HR with 1 – 100 kDa range (F). Error bars represent standard deviation. * $p<0.05$, ** $p<0.01$, *** $p<0.001$.

Tricine SDS-PAGE gels were used to analyze different batches of Enz-ELN, Combi-ELN, and a mixture of Combi-ELN with elastase prior to filter tube centrifugation (Figure 2C). Combi-ELN displayed a narrow MW range, although the observed range was higher than the expected 2–10 kDa. Enz-ELN exhibited a broad smear, indicating a wider MW distribution.

A biochemical assay for the number of amine groups showed the largest values for Enz-ELN (~1600 nmol amine groups per mg protein), whereas values for Combi-ELN (950 nmol/mg), OxA-st-ELN (650 nmol/mg), OxA-ELN (400 nmol/mg) and KOH-ELN (200 nmol/mg) were significantly lower (Figure 2D).

MW distributions were evaluated by using two size exclusion columns: one for large molecules (20-8000 kDa; Figure 2E and Figure S3C) and one for smaller compounds (with 1-100 kDa range; Figure 2F and Figure S3C). Combi-ELN demonstrated the lowest range of MWs, with a peak at 6.8 kDa. Peak values for Enz-ELN were at 23.3 kDa, similar on both columns. The remnants of elastase were not detected on gel filtration curves. For acidic hydrolysis, stepwise solubilization yielded some large proteins (>2,000 kDa) detected in the latest supernatant fractions (Figure S3D) but mostly proteins around 44 kDa. Continuous solubilization resulted in smaller proteins peaking at 39 kDa, with no prominent fraction of large molecules. KOH-ELN had intermediate sizes, with a peak at 30 kDa. To assess the effectiveness of gel filtration in selective isolation of specific MWs, ten KOH-ELN chromatographical fractions were concentrated and analyzed using SDS-PAGE and the Lowry protein assay (Figure S3E). Protein concentrations calculated from the chromatograms correlated well with the values obtained from the Lowry protein assay.

Given the potential impact of endotoxins on *in vitro* and *in vivo* experiments, endotoxin levels were assessed using a chromogenic assay. All chemical hydrolysates tested negative for endotoxin contamination (<0.01 EU/mL). In contrast, Enz-ELN exhibited 0.22 ± 0.01 EU/mL and Combi-ELN 1.16 ± 0.07 EU/mL. The source of contamination was found in the applied elastase with 12 EU/mL.

3.3. Biological effects of soluble elastins on human primary cells

3.3.1. Dermal fibroblasts

Cell viability of primary dermal fibroblasts was assessed under serum-deprived conditions (1% FBS), with measurements taken at cell seeding (day 0) and on days 1 and 3. Results showed that elastin preparations at 50 µg/mL and 150 µg/mL did not statistically impact cell viability or cause cytotoxicity (Figure 3A).

100 µM sodium ascorbate, together with 10% FBS, was selected as a stimulant for ECM production and 21.5 mg/mL PVP40 as MMC to simulate a 3D microenvironment for the main experiments. A concentration of 50 µg/mL of soluble elastin was evaluated, and 5 ng/mL TGF-β1 served as a positive control to induce myofibroblast activation.

Expression of genes related to scar formation and elastic fiber synthesis was analyzed using RT-qPCR on days 2, 4, and 7 (Figure 3B). Results showed that OxA-ELN significantly downregulated *COL3A1* and *ELN,* while Enz-ELN upregulated *FN1, FBN2, TIMP1*, and drastically increased *MMP12* expression. In general, OxA-st-ELN showed similar profiles to OxA-ELN. Chemical hydrolysates and Combi-ELN demonstrated comparable patterns, whereas Enz-ELN exhibited the most distinct profile.

The addition of TGF-β1 notably elevated the expression of genes associated with wound healing and scar formation, such as *ACTA2, COL1A1, and COL3A1*. The effect of TGF-β1 increased over time. Additionally, the addition of TGF-β1 signifcantly upregulated some elastogenesis-related genes, e.g. *ELN*, *FN1, FBN1, LOX,* and *MAGP2*. A marked downregulation of *MMP12* was also observed.

Protein expression of α-SMA was evaluated through Western blotting and immunofluorescence staining. Immunostaining demonstrated the absence of α-SMA across all tested conditions, while it was abundantly present in the TGF-β1 condition (Figure 4A). Western blotting strengthened these findings, with a clear α-SMA positive band in the TGF-β1 condition (Figure 4B). To summarize, all these findings indicated that soluble elastin preparations did not induce myofibroblast differentiation.

Collagen protein levels were assessed using Western Blot and Picrosirius Red staining and quantification. No significant differences were observed by Western blotting among the elastin preparations (Figure 3C). Combi-ELN and Enz-ELN slightly elevated type I collagen deposition, with 1.1 and 1.4 times relative protein expression, respectively. Expression of another ECM component, fibrillin-2, appeared to be 1.5 times increased with Enz-ELN and OxA-ELN (Figure 3C). TGF-β1 seemed to increase deposition of collagen and fibrillin-2 the most. Moreover, Picrosirius Red staining that visualizes collagen proteins was employed. By day 18, noticeable differences in staining intensity were visually observed between experimental conditions and the TGF-β1 control (Figure 3D). Quantitative analysis of Picrosirius Red staining on day 7 showed that soluble elastin preparations did not affect collagen deposition, while TGF-β1 had the strongest effect (Figure 3E). On day 18,

TGF-β1 revealed a 1.6-fold increase in collagen protein deposition compared to the untreated control, with Enz-ELN exhibiting the second largest effect at 1.2-fold. Enz-ELN showed a significant increase in collagen proteins compared to other preparations, except for OxA-st-ELN. Other solubilized elastins resulted in collagen levels comparable to the control.

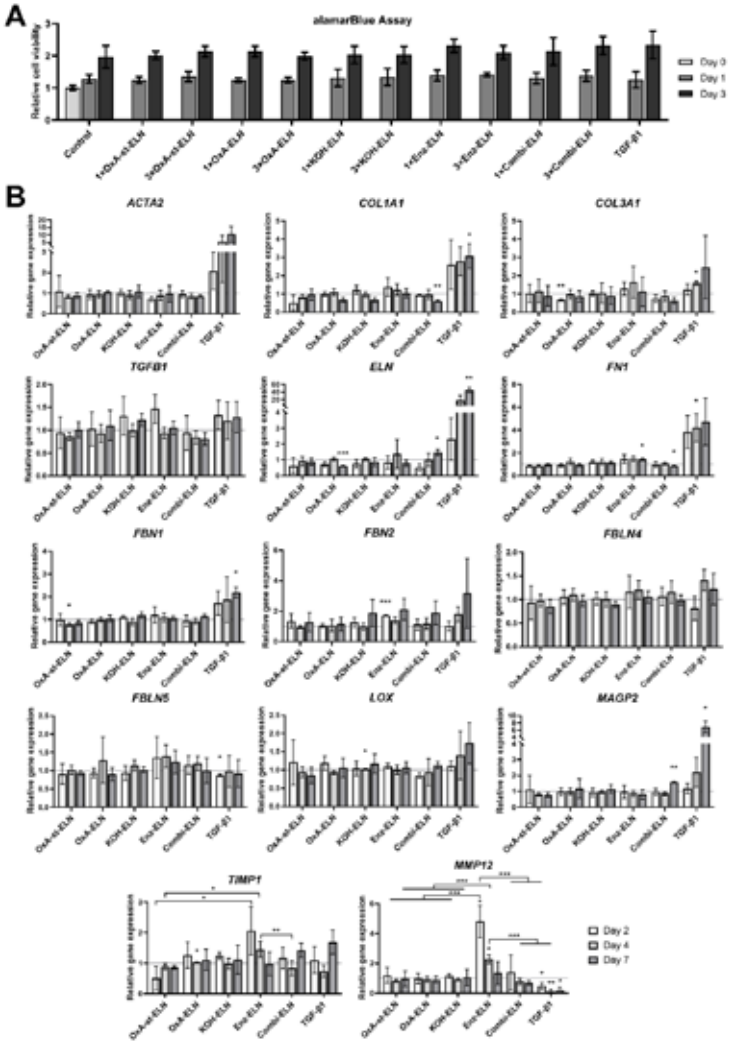

Figure 3. Biological effects of solubilized elastin preparation on primary human dermal fibroblasts (3 donors). A) Cell viability assessed by alamarBlue assay for solubilized elastins at two concentrations (50 µg/mL and 150 µg/mL). Values were normalized to control on day 0. B) Relative mRNA expression levels of target genes tested on primary human dermal fibroblasts at day 2, 4, and 7 and calculated using the $2^{-\Delta\Delta CT}$ method. Results are represented as the fold change of the target gene in the analyzed sample to the control sample (without solubilized elastin at the same day) and normalized to the expression of the housekeeping genes *YWHAZ* and *GAPDH*. Data are expressed as the mean ± standard

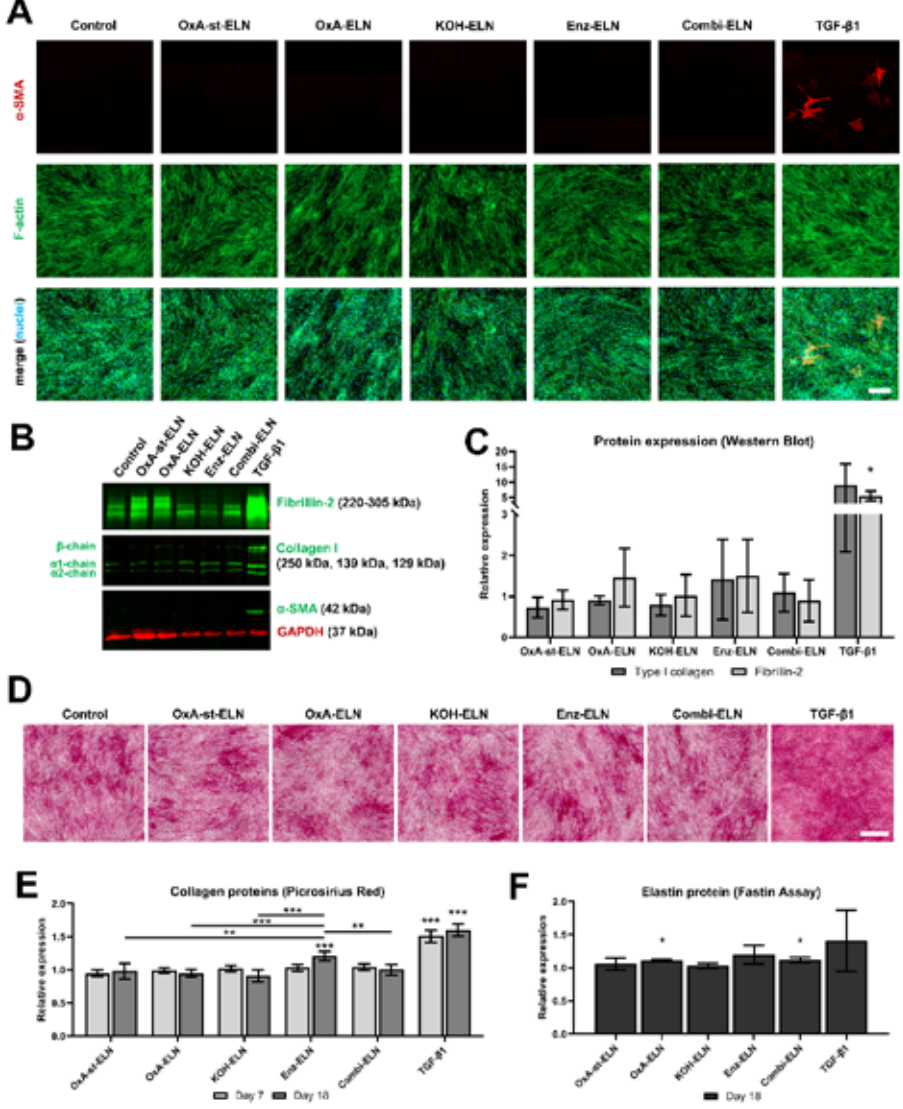

Figure 4. Biological effects of solubilized elastin preparation on primary human dermal fibroblasts (3 donors). A) Immunofluorescent analysis of α-SMA (red) and filamentous actin (green) at day 7. Cell nuclei were stained with DAPI (blue). Scale bar is 200 µm. B) Representative Western blot staining for fibrillin-2, type I collagen, and α-SMA from one donor at day 18. GAPDH was used as an internal control (red). C) Quantitative analysis of normalized Western blot results from three donors revealed no significant overexpression for any tested conditions. D) Representative images of cells stained with Picrosirius Red for detection of collagen proteins. Scale bar is 500 µm. E) Quantitative relative collagen protein expressions measured with Picrosirius Red staining. Values were normalized to control. F) Quantitative analysis of relative elastin protein expression using a Fastin Elastin Assay revealed no statistical significance. Error bars represent standard deviation; * $p<0.05$, ** $p<0.01$, *** $p<0.001$.

No statistically significant differences in elastin protein deposition were observed across any of the tested preparations. Elastin protein expression was highest under TGF-β1 stimulation, followed by Enz-ELN, Combi-ELN, and OxA-ELN (Figure 3F). Elastin levels for OxA-st-ELN and KOH-ELN were comparable to the untreated control.

These fibroblast experiments demonstrated an absence of fibrotic response to soluble elastins, and Enz-ELN outperformed other preparations in terms of ECM synthesis.

3.3.2. Macrophages

Macrophage polarization plays a key role in tissue repair, including skin regeneration [36]. The response of human primary macrophages to soluble elastins was analyzed by measuring cell-surface marker expression by flow cytometry (Figure 5 and Figure S4). To evaluate the macrophage polarization state, we assessed typical M1 and M2 markers as the extreme ends of the polarization spectrum and included M0, M1-, and M2-like controls alongside the test conditions. In addition, elastase only was included as a control because of its endotoxin contamination. OxA-st-ELN was not included because of its similarity to OxA-ELN.

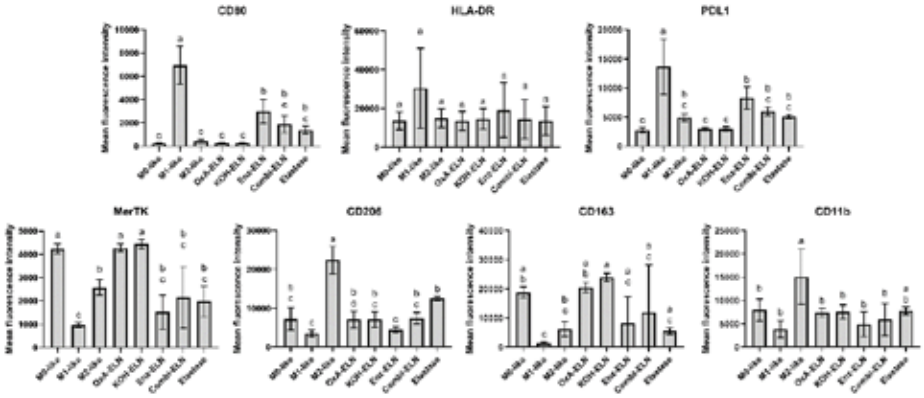

Figure 5. Effect of solubilized elastin preparations on macrophage cell-surface marker expressions (4 donors). Cells were incubated in elastin preparations for 48 h and analyzed by flow cytometry. Data are expressed as the mean value of mean fluorescence intensity ± standard deviation. Compact Letter Display (using lowercase letters a–e) was used to present multiple pairwise comparisons. Each group was assigned one or more letters, and shared letters indicate no significant difference ($p \geq 0.05$) between groups. Groups with different letters are significantly different ($p < 0.05$).

Chemical hydrolysates of elastin had no impact on the expression of markers CD80, CD163, CD206, CD11b, PDL1, HLA-DR, and MerTK, indicating that the macrophages maintained the M0-like subtype. Combi-ELN and, especially, Enz-ELN showed higher expression of CD80 and PDL1 and lower expression of CD163 and MerTK, compared to M0-like, indicating a more pro-inflammatory M1-like macrophage phenotype. The M1-like stimulation induced by Enz-ELN differed from that of the elastase control, while Enz-ELN and the diluted elastase control possessed comparable levels of endotoxin, 0.22 and 0.24 EU/mL, respectively, and Combi-

ELN 1.16 EU/mL. Endotoxin levels alone, therefore, cannot explain the different responses in macrophages, suggesting a specific effect of Enz-ELN.

4. Discussion

Acidic stepwise hydrolyzed and organo-alkaline hydrolyzed elastins (reported as α-elastin and κ-elastin) are the most extensively studied solubilized elastin preparations [20, 21, 37]. After conventional stepwise oxalic acid solubilization, we noticed that the last supernatant fractions showed very large proteins (with MW >2,000 kDa) that seemed to obstruct the membrane during filtration. These observations were in line with previously published information that the first supernatant fractions are usually rich in hydrophilic amino acids, while the last supernatants mimic the characteristics of insoluble elastin [21, 38]. Our oxalic acid hydrolysates differ from traditional α-elastin in two key aspects. First, the MW of α-elastin is reported to range from 60 to 84 kDa [39, 40], while our protein mixtures exhibit a much broader range. Second, we did not perform coacervation to remove low MW fragments. Instead, we used MW filters and dialysis to remove low MW compounds and impurities. Regarding the methods using oxalic acid, the benefits of continuous over stepwise oxalic acid hydrolysis were reducing experimental time, simplifying the protocol, and decreasing the average MW, although also diminishing amounts of primary amine groups. The unexpectedly lower number of primary amine groups may be due to deamination or the formation of new peptide bonds with exposed carboxyl groups, as continuous oxalic acid hydrolysis imposes harsher hydrolytic conditions compared to the stepwise approach. Nevertheless, substantial differences on primary human dermal fibroblasts were not seen between the two approaches. Hence, we suggest that continuous solubilization of elastic fibers with oxalic acid can substitute the stepwise process. The key distinction between KOH-ELN and κ-elastin is that κ-elastin consists of a single fraction (usually 75 kDa [16, 25, 41, 42]), whereas KOH-ELN includes all hydroxylated components.

Retaining specific amino acid sequences within solubilized preparations is critical, as these sequences are essential for biological activity and likely facilitate interaction with transmembrane receptors, triggering intracellular signaling cascades [43]. The soluble state of elastin should also facilitate its use in biomaterials at later stages due to its improved processability and enhanced bioavailability. Among elastin bioactive sequences, the hydrophobic VGVAPG motif is the most studied [17, 44-46]. The ability to take type VIII β-turn conformations by some sequences, such as xGVxxG and GxxPG [47], may explain their properties in the activation of elastogenesis in primary human dermal fibroblasts. We suggest that the exceptional stability of heterocyclic

elastin crosslinks, desmosine and isodesmosine, could also play a crucial role in the biological recognition of these peptides. With regards to particular effects in wound management, α-elastin showed potential in biomaterial applications by increasing elastin expression and improving dermal healing [10, 12, 48]. κ-elastin has been shown to enhance mesenchymal cell adhesion to elastic fibers, trigger biosynthesis of adhesive proteins, and mediate strong cell-elastin interactions [49]. Alkaline hydrolysates have also found applications in cosmetics due to their UV-protective properties and ability to improve skin elasticity [50, 51]. Digested elastin preparations were reported to result in enhanced elastogenesis in skin explants and in mice [18]. Those studies showed increased cell proliferation and induced formation of collagen and elastic fibers.

Characterization of solubilized elastin preparations is challenging due to the complex mixture of fragments and the specificity of elastin peptides themselves [52]. SDS-PAGE was limited in its ability to indicate MW ranges, partly due to the extremely high MWs of some preparations, which prevented migration through the gel. Size exclusion chromatography proved to be more effective for determining MW ranges of solubilized elastins and for separating specific MWs.

In contrast to chemical hydrolysates, enzymatic digestion of elastin targets specific amino acid residues [13]. Notably, such enzymatic preparations generally have relatively low MWs, ranging from 1 to 10 kDa [18, 19]. Our Enz-ELN had a higher MW peak, and it demonstrated the most distinguishable effects on both fibroblasts and macrophages compared to other solubilized elastins assessed. Nevertheless, the method of enzymatic digestion also had some important limitations. Enzymes, particularly human elastases, are expensive, may be contaminated with endotoxins, and can significantly complicate later translation. Moreover, the high affinity of enzymes for elastin moieties makes them difficult to remove after solubilization because they bind to both insoluble and soluble elastin. A microcolumn with immobilized elastase offers an alternative solution, avoiding the need for enzyme removal and accelerating digestion due to improved enzyme-substrate interactions, greater surface-to-volume ratio, and reduced spatial constraints [53-55].

Our solubilized elastin preparations promoted matrix remodeling without driving cells toward a fibrotic phenotype, ultimately ensuring better functional tissue regeneration. We hypothesize that solubilized elastin may be sensed by cells to initiate elastogenic processes and serve as a building block for the synthesis of new elastic fibers. Enz-ELN showed trends to upregulate a set of microfibril-related genes without an increasing *ELN* gene expression. At the same time, Enz-ELN appeared to trigger the largest deposition of collagen, fibrillin-2, and elastin proteins compared

to other solubilized elastins. Interestingly, thought-provoking results were obtained regarding the effects of Enz-ELN on macrophages. Although macrophages exist on a continuum of activation states rather than in discrete categories [56], and macrophage colony-stimulating factor was reported to pre-differentiate macrophages towards an M2-like phenotype [57], Enz-ELN demonstrated possible potency in stimulating an M1-like phenotype. M1-like polarization of macrophages is known to be crucial during the early stages of wound healing but is also linked to the upregulation of pro-inflammatory cytokines, proteases, and reactive oxygen species [58, 59]. However, M1 macrophages are capable of decreasing the number of myofibroblasts in cell culture experiments [60]. Our research on enzymatic preparations is currently limited by the presence of endotoxins. It is important to note that most endotoxins refer to the lipid A part of lipopolysaccharides, making both terms often interchangeable as they describe biologically active molecules derived from the outer membrane of bacteria that interact with the immune system, primarily through the TLR4 receptor on macrophages [61, 62]. Hence, investigating the immune response to endotoxin-free Enz-ELN *in vitro* and *in vivo* would provide additional valuable insights. OxA-ELN and KOH-ELN that retained the M0-like phenotype may be more advantageous for wound healing, as they preserve macrophage plasticity and adaptability. This enables macrophages to respond dynamically to the evolving demands of the wound environment throughout the healing process. Additionally, they can generate both pro-inflammatory and anti-inflammatory mediators as required, contributing to a well-regulated inflammatory response [33].

This study has several limitations. The elastin preparations were evaluated exclusively *in vitro*, which does not fully replicate the complex three-dimensional tissue environment, mechanical forces, multiple cell types and their dynamic interactions involved in wound healing *in vivo*. Additionally, the analysis was limited to two primary cell types, and the inclusion of other relevant cells, such as keratinocytes and endothelial cells, would provide a more comprehensive assessment. The short-term assays may not accurately predict the long-term cellular responses or material stability required for successful tissue regeneration. One of the main challenges we encountered during cell culture experiments was assessing elastic fiber synthesis. For future studies on solubilized elastin preparations, we suggest conducting additional chemical and biological tests to better understand the compositional differences between the obtained preparations, for example, amino acid analysis, mass spectrometry, Fourier-transform infrared spectroscopy, circular dichroism spectroscopy, cell adhesion and proliferation assays, and, most importantly, Western Blot for elastogenic markers (e.g., tropoelastin, fibrillin-1, fibulin-5, lysyl oxidase). In terms of *in vitro* testing, we strongly recommend using

endotoxin-free components, and enzymes that are preferably of human origin. Furthermore, we aim to evaluate fibrotic conditions to better assess the potential of solubilized elastins in promoting scarless regeneration. Further research should aim to assess the regenerative performance of selected elastin preparations in advanced 3D skin models and *in vivo* wound healing models, capturing the full cellular interplay during tissue repair.

5. Conclusions

Five types of solubilized elastin were prepared and characterized, revealing distinct physicochemical and biological profiles. OxA-st-ELN demonstrated the largest MWs, while Enz-ELN and Combi-ELN produced the smallest. Evaluating the effects on human primary dermal fibroblasts showed that none of the elastin preparations induced myofibroblast activation, a desirable aspect for minimizing fibrotic risk in tissue engineering applications. Enz-ELN appeared to further stimulate ECM deposition, potentially triggering a fibrotic response. This study is among the first to systematically compare different solubilized elastin preparations, evaluating not only their effects on fibroblasts but also their impact on immune cell responses. Macrophage studies indicated that chemical hydrolysates maintained an M0 phenotype, whereas Enz-ELN promoted pro-inflammatory M1-like polarization, likely due to endotoxin contamination. Among the tested elastin preparations, OxA-ELN and KOH-ELN emerged as the most promising candidates for incorporation into dermal scaffolds, promoting tissue regeneration while minimizing adverse immune reactions. Our findings advance current knowledge by highlighting the distinct characteristics of various solubilized elastins, identifying those with favorable properties for skin substitute development and wound healing applications, and providing a rational basis for selecting elastin types in future bioengineered materials.

References

1. Freinkel, R.K. and D. Woodley, *The biology of the skin*. 2001, New York: Parthenon Pub. Group. 432 p.
2. Darby, I.A. and T.D. Hewitson, *Fibroblast Differentiation in Wound Healing and Fibrosis.* International Review of Cytology, 2007. **257**: p. 143-179.
3. Antar, S.A., et al., *Fibrosis: Types, Effects, Markers, Mechanisms for Disease Progression, and Its Relation with Oxidative Stress, Immunity, and Inflammation.* International Journal of Molecular Sciences, 2023. **24**(4): p. 4004.
4. Gardeazabal, L. and A. Izeta, *Elastin and collagen fibres in cutaneous wound healing.* Experimental Dermatology, 2024. **33**(3): p. e15052.
5. Almine, J.F., S.G. Wise, and A.S. Weiss, *Elastin signaling in wound repair.* Birth Defects Research Part C: Embryo Today: Reviews, 2012. **96**(3): p. 248-57.
6. Schmelzer, C.E.H. and L. Duca, *Elastic fibers: formation, function, and fate during aging and disease.* The FEBS Journal, 2022. **289**(13): p. 3704-3730.
7. Robinet, A., et al., *Elastin-derived peptides enhance angiogenesis by promoting endothelial cell migration and tubulogenesis through upregulation of MT1-MMP.* Journal of Cell Science, 2005. **118**(Pt 2): p. 343-56.
8. Brassart, B., et al., *Conformational dependence of collagenase (matrix metalloproteinase-1) up-regulation by elastin peptides in cultured fibroblasts.* Journal of Biological Chemistry, 2001. **276**(7): p. 5222-7.
9. Wen, Q., S.M. Mithieux, and A.S. Weiss, *Elastin Biomaterials in Dermal Repair.* Trends in Biotechnology, 2020. **38**(3): p. 280-291.
10. de Vries, H.J.C., et al., *Dermal regeneration in native non-cross-linked collagen sponges with different extracellular matrix molecules.* Wound Repair and Regeneration, 1994. **2**(1): p. 37-47.
11. Lamme, E.N., et al., *Extracellular matrix characterization during healing of full-thickness wounds treated with a collagen/elastin dermal substitute shows improved skin regeneration in pigs.* Journal of Histochemistry and Cytochemistry, 1996. **44**(11): p. 1311-22.
12. Daamen, W.F., et al., *A biomaterial composed of collagen and solubilized elastin enhances angiogenesis and elastic fiber formation without calcification.* Tissue Engineering Part A, 2008. **14**(3): p. 349-60.
13. Heinz, A., *Elastases and elastokines: elastin degradation and its significance in health and disease.* Crit Rev Biochem Mol Biol, 2020. **55**(3): p. 252-273.
14. Senior, R.M., et al., *Val-Gly-Val-Ala-Pro-Gly, a repeating peptide in elastin, is chemotactic for fibroblasts and monocytes.* Journal of Cell Biology, 1984. **99**(3): p. 870-874.
15. MORELLI, M.A.C., et al., *Structure-activity relationships for some elastin-derived peptide chemoattractants.* The Journal of Peptide Research, 1997. **49**(6): p. 492-499.
16. Kamoun, A., et al., *Growth Stimulation of Human Skin Fibroblasts by Elastin-Derived Peptides.* Cell Adhesion and Communication, 1995. **3**(4): p. 273-281.
17. Tajima, S., et al., *Modulation by elastin peptide VGVAPG of cell proliferation and elastin expression in human skin fibroblasts.* Archives of Dermatological Research, 1997. **289**(8): p. 489-492.
18. Hinek, A., et al., *Proteolytic digest derived from bovine Ligamentum Nuchae stimulates deposition of new elastin-enriched matrix in cultures and transplants of human dermal fibroblasts.* Journal of Dermatological Science, 2005. **39**(3): p. 155-166.

19. Shiratsuchi, E., M. Nakaba, and M. Yamada, *Elastin hydrolysate derived from fish enhances proliferation of human skin fibroblasts and elastin synthesis in human skin fibroblasts and improves the skin conditions.* Journal of the Science of Food and Agriculture, 2016. **96**(5): p. 1672-1677.
20. Adair, G.S., H.F. Davis, and S.M. Partridge, *A Soluble Protein derived from Elastin.* Nature, 1951. **167**(4250): p. 605-605.
21. Partridge, S.M. and H.F. Davis, *The chemistry of connective tissues. 3. Composition of the soluble proteins derived from elastin.* Biochemical Journal, 1955. **61**(1): p. 21-30.
22. Kornfeld-Poullain, N. and L. Robert, *[Effect of various organic solvents on the alkaline degradation of elastin].* Bull Soc Chim Biol (Paris), 1968. **50**(4): p. 759-71.
23. Moczar, M., E. Moczar, and L. Robert, *Peptides Obtained From Elastin by Hydrolysis with Aqueous Ethanolic Potassium Hydroxide.* Connective Tissue Research, 1979. **6**(4): p. 207-213.
24. Petersen, W., et al., *The use of collagen-based matrices in the treatment of full-thickness wounds.* Burns, 2016. **42**(6): p. 1257-1264.
25. Groult, V., et al., *Mechanisms of interaction between human skin fibroblasts and elastin: Differences between elastin fibres and derived peptides.* Cell Biochemistry and Function, 1991. **9**(3): p. 171-182.
26. Gi-Yeun, H., S. Dong-Kook, and L. Jong-Wook, *Contracture of skin graft in human burns: Effect of artificial dermis.* Burns, 2014. **40**(8): p. 1497-1503.
27. Lempert, M., et al., *Long-term experience with a collagen-elastin scaffold in combination with split-thickness skin grafts for the treatment of full-thickness soft tissue defects: improvements in outcome-a retrospective cohort study and case report.* Langenbecks Arch Surg, 2022. **407**(1): p. 327-335.
28. Haslik, W., et al., *First experiences with the collagen-elastin matrix Matriderm® as a dermal substitute in severe burn injuries of the hand.* Burns, 2007. **33**(3): p. 364-368.
29. Boyera, N., I. Galey, and B.A. Bernard, *Effect of vitamin C and its derivatives on collagen synthesis and cross-linking by normal human fibroblasts.* International Journal of Cosmetic Science, 1998. **20**(3): p. 151-158.
30. Assunção, M., et al., *Cell-Derived Extracellular Matrix for Tissue Engineering and Regenerative Medicine.* Frontiers in Bioengineering and Biotechnology, 2020. **8**.
31. Delavary, B.M., et al., *Macrophages in skin injury and repair.* Immunobiology, 2011. **216**(7): p. 753-762.
32. Kuninaka, Y., et al., *Macrophage polarity and wound age determination.* Scientific Reports, 2022. **12**(1): p. 20327.
33. Hassanshahi, A., et al., *Macrophage-Mediated Inflammation in Skin Wound Healing.* Cells, 2022. **11**(19): p. 2953.
34. Stout, R.D. and J. Suttles, *Functional plasticity of macrophages: reversible adaptation to changing microenvironments.* Journal of Leukocyte Biology, 2004. **76**(3): p. 509-513.
35. Daamen, W.F., et al., *Isolation of intact elastin fibers devoid of microfibrils.* Tissue Eng, 2005. **11**(7-8): p. 1168-76.
36. Chen, C., et al., *Epigenetic regulation of macrophage polarization in wound healing.* Burns & Trauma, 2023. **11**.
37. Jacob, M.P. and W. Hornebeck. *Isolation and characterization of insoluble and kappa elastins*. 1985.
38. Halabi, C.M. and R.P. Mecham, *Chapter 12 - Elastin purification and solubilization*, in *Methods in Cell Biology*, R.P. Mecham, Editor. 2018, Academic Press. p. 207-222.

39. Kamisato, S., et al., *Involvement of Intracellular Cyclic GMP and Cyclic GMP-Dependent Protein Kinase in α-Elastin-Induced Macrophage Chemotaxis.* The Journal of Biochemistry, 1997. **121**(5): p. 862-867.
40. Partridge, S.M., H.F. Davis, and G.S. Adair, *The chemistry of connective tissues. 2. Soluble proteins derived from partial hydrolysis of elastin*.* Biochemical Journal, 1955. **61**(1): p. 11-21.
41. Donet, M., et al., *Elastin peptides regulate HT-1080 fibrosarcoma cell migration and invasion through an Hsp90-dependent mechanism.* British Journal of Cancer, 2014. **111**(1): p. 139-148.
42. Toupance, S., et al., *Elastin-derived peptides increase invasive capacities of lung cancer cells by post-transcriptional regulation of MMP-2 and uPA.* Clinical & Experimental Metastasis, 2012. **29**(5): p. 511-522.
43. Qa'aty, N., et al., *Synthetic ligands of the elastin receptor induce elastogenesis in human dermal fibroblasts via activation of their IGF-1 receptors.* Journal of Dermatological Science, 2015. **80**(3): p. 175-185.
44. Szychowski, K.A., T. Pomianek, and J. Gmiński, *Elastin-Derived Peptide VGVAPG Affects Production and Secretion of Testosterone in Mouse Astrocyte In Vitro.* Neurochemical Research, 2020. **45**(2): p. 385-394.
45. Szychowski, K.A. and J. Gmiński, *Specific role of N-methyl-D-aspartate (NMDA) receptor in elastin-derived VGVAPG peptide-dependent calcium homeostasis in mouse cortical astrocytes in vitro.* Scientific Reports, 2019. **9**(1): p. 20165.
46. Pocza, P., et al., *Locally generated VGVAPG and VAPG elastin-derived peptides amplify melanoma invasion via the galectin-3 receptor.* International Journal of Cancer, 2008. **122**(9): p. 1972-1980.
47. Floquet, N., et al., *Structural characterization of VGVAPG, an elastin-derived peptide.* Peptide Science, 2004. **76**(3): p. 266-280.
48. Leach, J.B., et al., *Crosslinked α-elastin biomaterials: towards a processable elastin mimetic scaffold.* Acta Biomaterialia, 2005. **1**(2): p. 155-164.
49. Hornebeck, W., J.M. Tixier, and L. Robert, *Inducible adhesion of mesenchymal cells to elastic fibers: elastonectin.* Proceedings of the National Academy of Sciences, 1986. **83**(15): p. 5517-5520.
50. Robert, L., *The Saga of κ-Elastin or the Promotion of Elastin Degradation Products from "Garbage" to Receptor Agonists and Pharmacologically Active Principles.* Connective Tissue Research, 2010. **51**(1): p. 8-13.
51. Ménasche, M., et al., *Pharmacological studies on elastin peptides (kappa-elastin). Blood clearance, percutaneous penetration and tissue distribution.* Pathol Biol (Paris), 1981. **29**(9): p. 548-54.
52. Maccioni, F.J. and K.E. Moon, *Characterisation of human lung elastin-derived peptides.* Clinical Biochemistry, 1993. **26**(2): p. 85-91.
53. Slysz, G.W. and D.C. Schriemer, *On-column digestion of proteins in aqueous-organic solvents.* Rapid Communications in Mass Spectrometry, 2003. **17**(10): p. 1044-1050.
54. Yuan, F.-F., et al., *Efficient and rapid digestion of proteins with a dual-enzyme microreactor featuring 3-D pores formed by dopamine/polyethyleneimine/acrylamide-coated KIT-6 molecular sieve.* Scientific Reports, 2024. **14**(1): p. 15667.
55. Nagy, C., R. Szabo, and A. Gaspar, *Microfluidic Immobilized Enzymatic Reactors for Proteomic Analyses—Recent Developments and Trends (2017–2021).* Micromachines, 2022. **13**(2): p. 311.
56. Geiß, C., et al., *Multistability in Macrophage Activation Pathways and Metabolic Implications.* Cells, 2022. **11**(3): p. 404.
57. Mia, S., et al., *An optimized Protocol for Human M2 Macrophages using M-CSF and IL-4/IL-10/TGF-β Yields a Dominant Immunosuppressive Phenotype.* Scandinavian Journal of Immunology, 2014. **79**(5): p. 305-314.

58. Sharifiaghdam, M., et al., *Macrophages as a therapeutic target to promote diabetic wound healing.* Molecular Therapy, 2022. **30**(9): p. 2891-2908.

59. Das, A., et al., *Monocyte and Macrophage Plasticity in Tissue Repair and Regeneration*. The American Journal of Pathology, 2015. **185**(10): p. 2596-2606.

60. Venter, C., K.H. Myburgh, and C.U. Niesler, *Co-culture of pro-inflammatory macrophages and myofibroblasts: Evaluating morphological phenotypes and screening the effects of signaling pathway inhibitors.* Physiological Reports, 2021. **9**(2): p. e14704.

61. Raetz, C.R.H. and C. Whitfield, *Lipopolysaccharide Endotoxins.* Annual Review of Biochemistry, 2002. **71**(Volume 71, 2002): p. 635-700.

62. Wang, X. and P.J. Quinn, *Endotoxins: Lipopolysaccharides of Gram-Negative Bacteria*, in *Endotoxins: Structure, Function and Recognition*, X. Wang and P.J. Quinn, Editors. 2010, Springer Netherlands: Dordrecht. p. 3-25.

Supporting Information

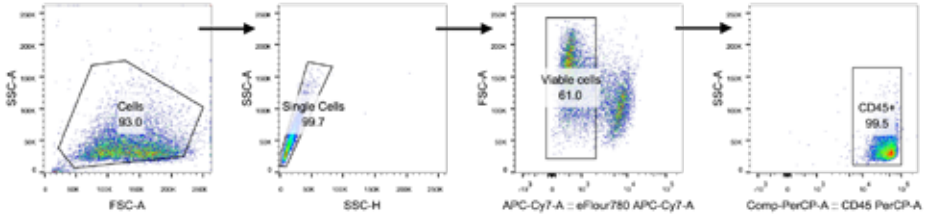

Figure S1. Gating strategy for the analysis of macrophages. Cells were first identified based on forward scatter (FSC-A) and side scatter (SSC-A) properties to exclude debris. Next, single cells were selected using SSC-A vs. SSC-H to eliminate doublets. Viable cells were gated using a viability dye (APC-Cy7-A). Macrophages were identified by CD45 expression. The mean fluorescence intensity of selected markers was extracted for further analysis.

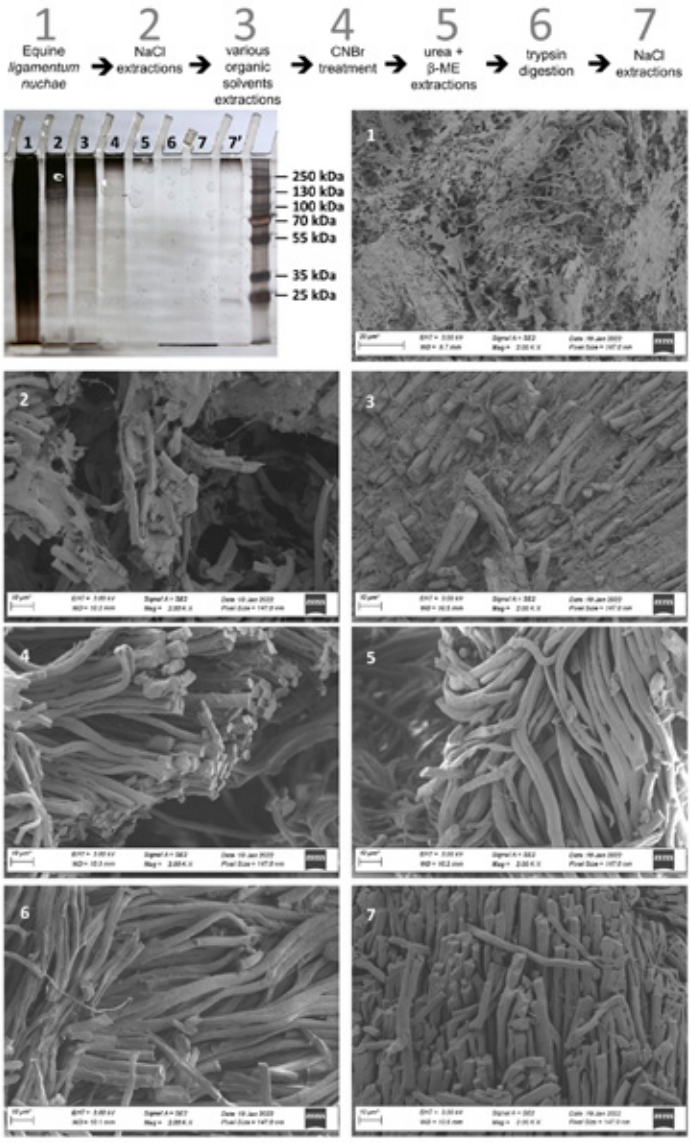

Figure S2. Stepwise analysis of elastic fiber isolation and purification. The protocol includes the following steps: 1) initial *equine ligamentum nuchae*, 2) aqueous sodium chloride washing, 3) organic solvents extractions, 4) cyanogen bromide treatment in anhydrous formic acid, 5) β-mercaptoethanol and urea treatments, 6) trypsin digestion, 7) final aqueous sodium chloride washing steps. In the top left corner, SDS-PAGE gel stained with silver illustrates the gradual elimination of impurities throughout the protocol, as seen through lanes 1 until 7. Lanes 7 and 7′ represent two different batches. Notably, a distinct band at ~24 kDa was evident only in lane 7′, but the band was also visible upon extended staining in lanes 6 and 7. SEM images demonstrated the progressive emergence of fiber structures during the protocol, starting with the untreated equine *ligamentum nuchae*, which exhibited no visible fiber-like structures. Careful examination of elastin fibers showed partial loss of their intact rod form.

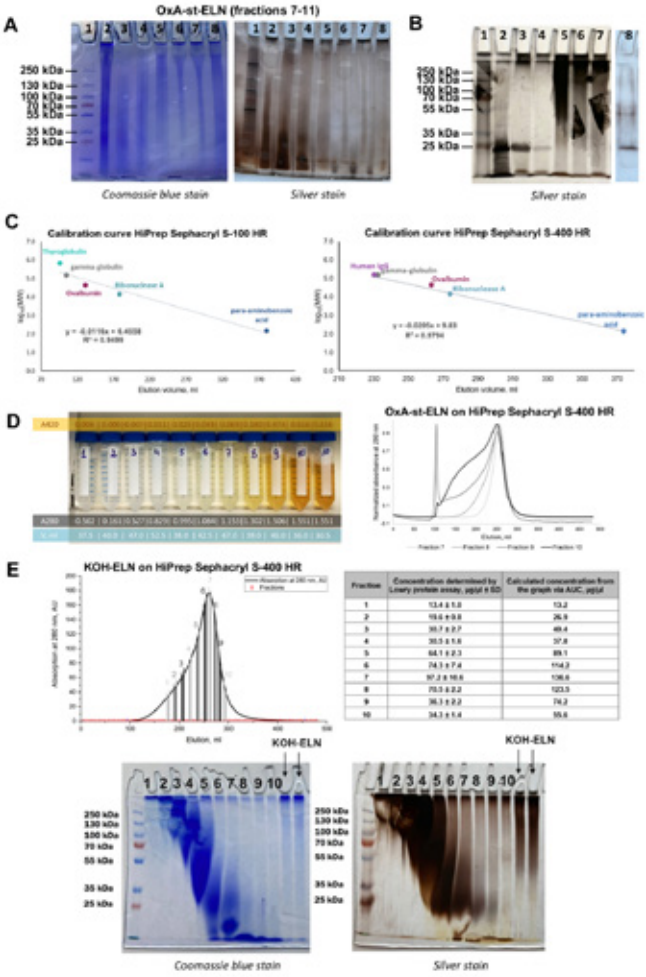

Figure S3. Analysis of solubilized elastin preparations. A) Coomassie brilliant blue and silver stained SDS-PAGE 4-15% gradient gels with OxA-st-ELN (supernatant fractions 7-11). The protein ladder was loaded in lane 1, combined fractions of OxA-st-ELN in lane 2, fraction 7 in lane 3, fraction 8 in lane 4, fraction 9 in lane 5, fraction 10 in lanes 6 and 7, fraction 11 in lane 8. B) Silver stained SDS-PAGE 10% gels with protein ladder (1), elastase (2), Enz-ELN before incubation with insoluble elastic fibers to remove elastase (3), Enz-ELN after incubation with insoluble elastic fibers to remove elastase (4), KOH-ELN (5), OxA-ELN (6), OxA-st-ELN (7), and Combi-ELN (8). C) Calibration curve based on selected compounds for HiPrep Sephacryl S-100 HR (left) and S-400 HR (right) column with the linear trendline equation for elution volume and decimal logarithm for molecular weight. D) One of OxA-st-ELN batches resulted in 10 supernatant fractions (left). Corresponding absorbances at 280 and 420 nm and collected volume are provided. Gel-filtration of supernatant fractions 7-10 (right) revealed that a high molecular weight peak was especially present in the latest fractions (9 and 10). E) Elution curves for KOH-ELN on HiPrep Sephacryl S-400 HR column and highlighted ten selected chromatographical fractions for further analysis (top left). CBB and silver-stained SDS-PAGE (10% gels) for the ten KOH-ELN gel filtration fractions and original KOH-ELN (bottom). Table (top right) showed a correlation among protein concentrations in the isolated fractions using two approaches: Lowry protein assay and computational analysis.

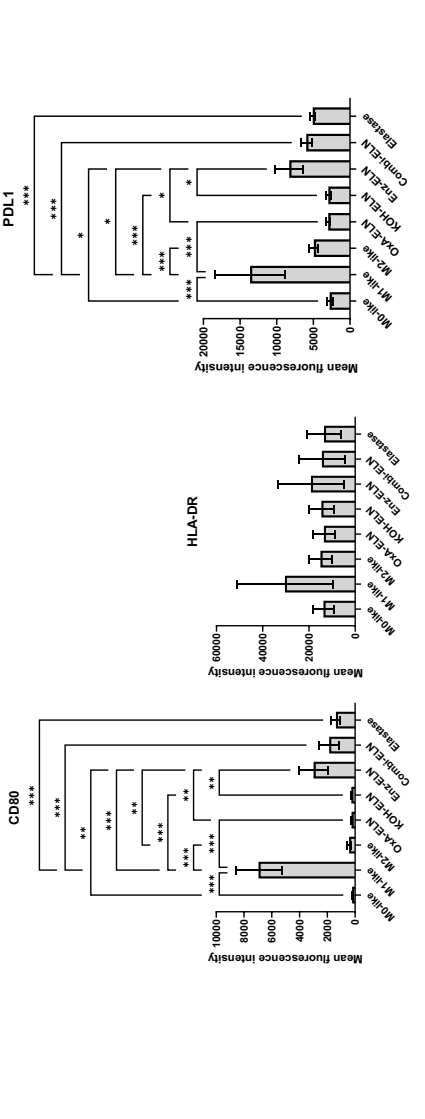

Figure S4. Effect of solubilized elastin preparations on macrophage cell-surface marker expressions (4 donors). Cells were incubated in elastin preparations for 48 h and analyzed by flow cytometry. Data are expressed as the mean value of mean fluorescence intensity ± standard deviation. * p<0.05, ** p<0.01, *** p<0.001.

Table S1. RT-qPCR primer sequences.

Gene	Description	Forward sequence 5'3'	Reverse sequence 5'3'
ACTA2	smooth muscle actin alpha 2	CCGACCGAATGCAGAAGGA	ACAGAGTATTTGCGCTCCGAA
TGFB1	transforming growth factor beta 1	CGCGTGCTAATGGTGGAAA	TGTGTGTACTCTGCTTGAACTTGTCA
COL1A1	alpha-1 type I collagen	GAGAGCATGACCGATGGATT	CGCTGTTCTTGCAGTGGTAG
COL3A1	alpha-1 type III collagen	GATGGTTGCACGAAACACAC	GATCAGGACCACCAATGTCA
ELN	elastin	GGTTGTGTCACCAGAAGCAGCT	CCGTAAGTAGGAATGCCTCCAAC
FN1	fibronectin-1	GAAGCCGAGGTTTTAACTGC	ACCCACTCGGTAAGTGTTCC
FBN1	fibrillin-1	ATGGAAGGAGCTGCAAAGATC	GCCGCCAATGGTGGTAACA
FBN2	fibrillin-2	TGGGCGGCCATTTTACAAAG	AACGGCATTTGAAGCTTCCG
FBLN4	fibulin-4	ATTTGGACTTGGCTGGCTTG	AGGCAGAGTTAGGAATGGAACC
FBLN5	fibulin-5	TATTGATGAATGCCGAACCA	ACCTGAGTAGGGGGTCGAGT
LOX	lysyl oxidase	TGCCAGTGGATTGATATTAC	TACGGTGAAATTGTGCAGCC
MAGP2	microfibril-associated glycoprotein 2	GGGTCAATAGTCAACGAGGAGAC	GCCAAGTCATCTGTGGAAGGTG
TIMP1	metallopeptidase inhibitor 1	GGAGAGTGTCTGCGGATACTTC	GCAGGTAGTGATGTGCAAGAGTC
MMP12	matrix metallopeptidase 12	GATGCTGTCACTACCGTGGGAA	CAATGCCAGATGGCAAGGTTGG
YWHAZ	zeta polypeptide tyrosine 3-monooxygenase/tryptophan 5-monooxygenase activation protein	CATCTTGGAGGGTCGTCTCA	ACTTTGCTCTCTGCTTGTGAA
GAPDH	glyceraldehyde 3-phosphate dehydrogenase	TGGGTGTGAACCATGAGAAG	TGGGTGTGAACCATGAGAAG

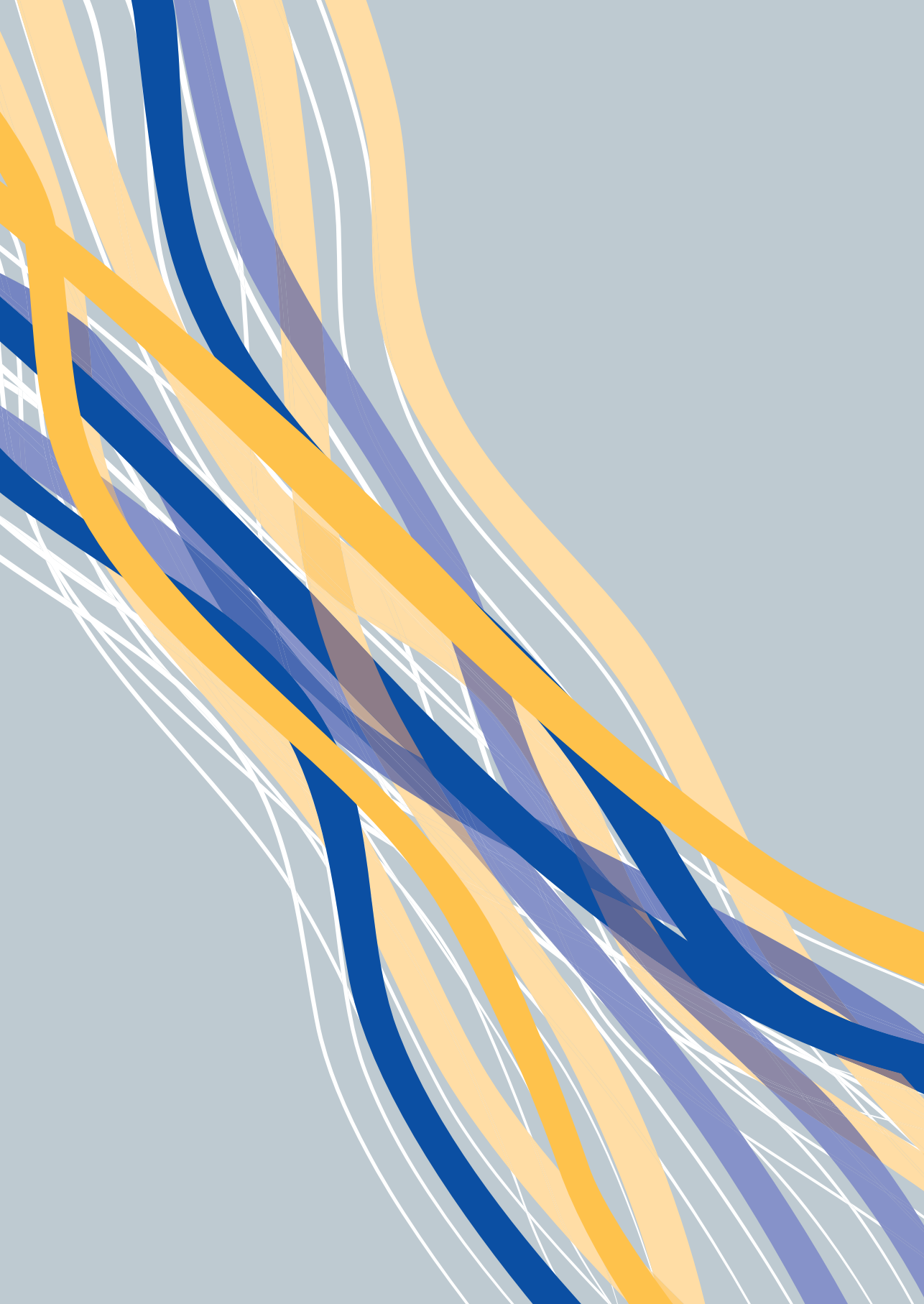

Chapter 3

Collagen-elastin dermal scaffolds enhance tissue regeneration and reduce scarring in preclinical models

Roman Krymchenko[1], Nancy Avila-Martinez[1], Merel Gansevoort[1], Gert-Jan Bakker[1], Madalena L.N.P. Gomes[2,3,4,5], Marcel Vlig[2], Elly M. M. Versteeg[1], Bouke K. H. L. Boekema[2,4,5,6], Toin H. van Kuppevelt[1], Willeke F. Daamen[1]

[1] Radboud university medical center, Research Institute for Medical Innovation, Department of Medical BioSciences, Nijmegen, The Netherlands

[2] Alliance of Dutch Burn Care, Burn Research Lab, Beverwijk, The Netherlands

[3] Department of Pathology, Amsterdam University Medical Center (AUMC), Amsterdam, The Netherlands

[4] Tissue Function and Regeneration, Amsterdam Movement Sciences Research Institute, Amsterdam, The Netherlands

[5] Department of Plastic, Reconstructive and Hand Surgery, AUMC, location VUmc, Amsterdam, The Netherlands

Published in Materials Today Bio (2025, 102239).
DOI: 10.1016/j.mtbio.2025.102239

Abstract

Severe scarring is an inevitable consequence of large full-thickness skin wounds, often leading to long-term complications that affect patients' well-being and necessitate extended medical interventions. While autologous split-thickness skin grafts remain the clinical standard for wound treatment, they frequently result in contractures, excessive scarring, and the need for additional corrective procedures. To address these challenges, bioengineered skin substitutes capable of promoting efficient healing while reducing complications are highly desirable. Elastin, an essential component of the extracellular matrix, plays a crucial role in restoring tissue elasticity and regulating scar formation during wound healing. This study explores the impact of two distinct elastin-derived components, produced through acidic and basic hydrolysis, on wound repair. We developed and characterized collagen-based scaffolds enriched with these elastin hydrolysates and assessed their influence on different types of human skin fibroblasts, including fetal, eschar-derived, and healthy adult dermis-derived fibroblasts. Furthermore, we evaluated their therapeutic potential in a preclinical rat model. Our findings indicated that fetal fibroblasts exhibited the most pronounced extracellular matrix deposition and cellular infiltration within the scaffolds, followed by eschar fibroblasts and, lastly, healthy adult cells. The incorporation of elastin into collagen scaffolds led to a reduction in α-SMA protein expression, a biomarker of fibrosis, compared to collagen-only scaffolds. Notably, collagen scaffolds supplemented with elastin hydrolysate from basic hydrolysis demonstrated the most promising outcomes for scarless healing, characterized by minimal wound contraction, enhanced extracellular matrix formation, and increased neovascularization.

Graphical abstract

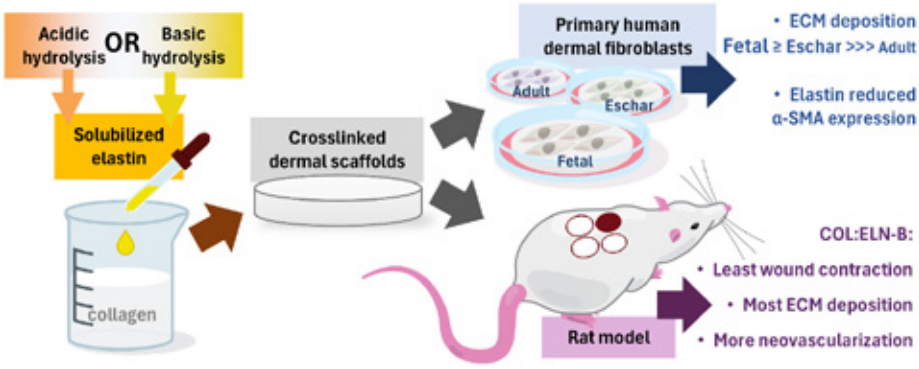

1. Introduction

Skin wounds compromise the body's primary barrier and can vary from minor abrasions to deep tissue damage caused by explosions, trauma, surgeries, burns, or ischemia. Healing occurs in four overlapping stages: hemostasis, inflammation, proliferation, and remodeling [1]. While minor wounds generally heal easily, severe deep wounds take longer to heal due to the destruction of essential stem cell populations on the basement membrane and lack of skin appendages [2]. In contrast to scarless healing observed in fetal skin [3], full-thickness skin wounds do not regenerate fully in adults, leading to severe scarring that impacts patients' quality of life and often requires prolonged treatment [4].

Although dry necrotic tissue (eschar) may temporarily cover a wound, it can impede healing and mask underlying processes, posing additional risks [5]. Therefore, removal of the eschar tissue is a critical step, as it allows for the assessment of the wound bed and enables the formation of a well-vascularized dermis, which is an essential prerequisite for successful re-epithelialization and wound closure [6]. The standard of care method, autologous split-thickness skin grafts, involves harvesting healthy skin (primarily the epidermis and a small part of the dermis) and applying it to the injured area. However, this procedure still leads to significant scarring, contractures, and complications, which often require follow-up treatments such as scar revision surgery [7]. Therefore, appropriate bioengineered dermal scaffolds are necessary to minimize the complications while supporting and accelerating healing [8, 9].

Animal-derived collagen is a versatile and effective biomaterial in a range of applications, especially in wound healing [10]. Collagen, the main component of dermis, provides a suitable environment for fibroblasts, promoting tissue regeneration and accelerating the healing process [11]. Collagen porous scaffolds effectively absorb wound exudate, maintain a moist environment, and reduce the risk of infection and mechanical damage [12]. Their porous structure facilitates nutrient and cell transport, enhancing cell adhesion, proliferation, and migration. When applied to severe wounds, these biomaterials serve as frameworks for new tissue formation, aiding soft tissue repair and improving recovery outcomes.

In contrast to collagen, another key extracellular matrix (ECM) protein, elastin, is often neglected despite its vital role in maintaining skin elasticity and resilience [13]. In adults, elastic fibers regenerate slowly after injury and are significantly reduced in scar tissue [14]. Soluble elastins have been reported to show various beneficial effects crucial for wound healing, including the stimulation of cell adhesion and

proliferation, induced angiogenesis, and boosted elastin expression [15-21]. Based on this, different porous type I collagen scaffolds supplemented with solubilized elastin have been developed [22-29]. Some studies have reported the mechanical characterization of these collagen-elastin scaffolds [29] and the effects of crosslinking [25, 30]. More importantly, the supplementation of elastin in such scaffolds has demonstrated a higher potential for skin regeneration compared to collagen-only analogues [22, 23, 25, 26]. However, despite these promising observations and the established bioactivity of soluble elastin, a comprehensive understanding of its precise role in the complex cascade of wound healing and regeneration remains limited. This is partly attributed to the inherent complexity of the wound microenvironment, also to the limited investigation into how different chemical solubilization methods affect the molecular properties and biological activity of soluble elastin, and thereby its therapeutic potential. A complete elucidation of the mechanisms within the complex regenerative cascade is, however, beyond the scope of this study.

In this study, we investigate and directly compare the effects of two types of chemically solubilized elastins, obtained through acidic or alkaline hydrolysis, on wound healing. We created and characterized novel collagen-elastin scaffolds and evaluated their effects on various types of fibroblasts, including normal adult, eschar, and fetal fibroblasts. Additionally, we examined the regenerative and scarring outcomes of these scaffolds in a rat model, providing the first side-by-side comparison.

2. Materials and methods

Unless otherwise specified, chemicals, enzymes, and cell culture supplements were purchased from Sigma-Aldrich/Merck, while cell culture media and antibiotics were obtained from Gibco. Elastin fibers were isolated from equine *ligamentum nuchae* and purified using a protocol established in our laboratory [31].

2.1. Preparation and characterization of solubilized elastin peptides

2.1.1. Solubilized elastin by acidic hydrolysis (ELN-A)

4.1 g of dry elastin fibers were dispersed in 90 mL of 0.25 M oxalic acid and maintained at 95°C for 9 hours, ensuring complete solubilization. Following incubation, the solution underwent centrifugation at 500 × g for 5 min to eliminate residual contaminants. The resulting elastin solution was then adjusted to

approximately pH 6 using 1 M sodium acetate and subjected to dialysis against 9 L of demineralized water five times using 3,500 MWCO dialysis membranes (44310.02, MEMBRA-CEL, Serva). The solution was passed through 0.20 µm filters (Acrodisc 25 mm Supor STRL, Pall Corporation) before being stored at -20°C.

2.1.2. Solubilized elastin by basic hydrolysis (ELN-B)

3.6 g of purified elastin fibers were treated with 90 mL of 1 M KOH in an 80% aqueous ethanol solution at 37°C for 8 h under intermittent agitation until complete dissolution was achieved. The resulting solution was centrifuged at 15,000 × g for 20 min at 4°C to remove insoluble matter. The supernatant was neutralized using perchloric acid ($HClO_4$), leading to the precipitation of potassium perchlorate ($KClO_4$), which was subsequently eliminated by a second centrifugation step under identical conditions. The clarified supernatant underwent a dialysis process against 9 L of demineralized water five times using 3,500 MWCO membranes. The final purified hydrolysate was filtered through 0.20 µm membranes and preserved at -20°C.

2.1.3. Characterization of solubilized elastins

Solubilized elastins were characterized as previously described [32]. The molecular weights were assessed using glycine-SDS-PAGE and size-exclusion chromatography. For SDS-PAGE analysis, solubilized elastin was heated in a reducing buffer at 100°C for 5 min before being resolved on 10% polyacrylamide gels. Protein bands were visualized using Coomassie Brilliant Blue staining SDS-PAGE. Size-exclusion chromatography was carried out using HiPrep 26/60 Sephacryl S-100 HR and S-400 HR columns (Cytiva) on an ÄKTA FPLC explorer system (Amersham Biosciences). Quantification of primary amine groups was performed via the 2,4,6-trinitrobenzene sulfonic acid (TNBS) assay as described by Buttafoco *et al.* [33] Absence of endotoxin contamination was confirmed using the ToxinSensor™ Chromogenic LAL endotoxin assay kit (Genscript) following the manufacturer's protocol.

2.2. Type I collagen scaffolds with solubilized elastins

2.2.1. Preparation of the scaffolds

Porous non-crosslinked collagen scaffolds (COL) were fabricated by dispersing 0.8% (w/v) bovine tendon-derived collagen fibrils into 0.25 M acetic acid and allowing them to swell overnight at 4°C under continuous stirring. To incorporate solubilized elastins into the scaffolds (COL:ELN-A and COL:ELN-B), two collagen-to-elastin ratios – 97:3 and 95:5, resembling human skin – were tested. This involved dissolving either 0.024% or 0.040% (w/v) of ELN-A or ELN-B in 0.25 M acetic acid, followed by the addition of type I collagen fibrils at 0.776% or 0.760% in 0.25 M acetic acid, respectively. The resulting suspension was mixed thoroughly, swollen overnight at

4°C, homogenized, poured into molds (4 mL per 960 mm^2, 6-well plate), and freeze-dried using a Lyoph-pride 03 system (ilShin Biobase Europe).

Chemical crosslinking was carried out for 3 h using a solution containing 33 mM 1-ethyl-3-(3-dimethylaminopropyl)carbodiimide (EDC) and 6 mM N-hydroxysuccinimide (NHS) in a 50 mM 2-morpholinoethanesulfonic acid (MES) buffer with 40% ethanol at pH 5.0. Then, scaffolds were washed sequentially with 0.1 M Na_2HPO_4, 1 M NaCl, and 2 M NaCl, followed by demineralized water rinses until the conductivity dropped below 200 µS (VWR, HCO 304). The final scaffolds were lyophilized and cut into ⌀12 mm discs for *in vitro* and *in vivo* studies.

2.2.2. Characterization of the scaffolds

The scaffold morphology was examined via scanning electron microscopy (SEM). Dry samples were fixed onto metallic stubs with double-sided carbon tape, sputter-coated with gold for 60 s using a Polaron E5100 SEM coating system (Quorum Technologies), and imaged with a Zeiss Sigma 300 Field Emission Scanning Electron Microscope at 3 kV accelerating voltage.

For elastin visualization, scaffolds were embedded in Tissue-Tek O.C.T. compound (Sakura Finetek Europe), rapidly frozen on dry ice, and stored at -80°C before sectioning. Thin sections (7 µm) were prepared using a Microm HM 550 VP cryostat (Thermo Scientific) at -20°C and left to air dry overnight at room temperature. To block non-specific binding, samples were incubated with 0.5% bovine serum albumin (BSA) in phosphate-buffered saline (pH 7.4) for 30 min. Elastin peptides were stained using a monoclonal elastin antibody (1:200, ab9519, Abcam) for 1 h, and incubated with biotinylated goat anti-mouse IgG (1:200, Vector Laboratories, BA-9200-1.5) for 1 h at room temperature in 0.5% BSA-PBS. The VECTASTAIN Elite ABC Kit (Vector Laboratories) was applied according to the manufacturer's instructions. Elastin was detected in red using the ImmPACT AEC (3-amino-9-ethylcarbazole) HRP substrate kit (Vector Laboratories) and mounted with VectaMount AQ aqueous mounting medium (Vector Laboratories). A combination of Verhoeff's Elastic and Masson's Trichrome (VEMT) staining was performed to visualize collagen in blue and elastin in dark blue or black [34]. Imaging was conducted using a whole-slide scanner (3DHISTECH, Budapest, Hungary) with CaseViewer 2.4 software.

The crosslinking efficiency was assessed by quantifying the reduction in primary amine groups using the TNBS assay. For differential scanning calorimetry (DSC) analysis, approximately 1 mg of each sample was sealed in Tzero pans (TA Instruments) with hermetic lids and heated from 1°C to 220°C at a rate of 5°C/min

using a TA Q1000 DSC system (TA Instruments) equipped with an RCS40 cooler and Universal Analysis software. The onset temperature (T_{onset}) was recorded to determine the denaturation temperature (T_d) of collagen.

2.3. *In vitro* experiments with primary human fibroblasts

2.3.1. Experimental design

Human dermal fibroblasts were obtained from three distinct origins: healthy adult skin, burn wound tissue (eschar), and fetal skin, following established protocols [35, 36]. Cells were isolated from three different donors per tissue type, nine donors in total. Adult fibroblasts were obtained from skin samples of patients undergoing elective surgery at the Department of Plastic and Reconstructive Surgery, Red Cross Hospital (Beverwijk, NL). Eschar samples were collected from burn patients undergoing debridement between post-burn days 13 and 19 at the Red Cross Hospital. Fetal fibroblasts were derived from fetal skin obtained following pregnancy termination between gestational weeks 16 and 22, with written informed consent from the donors at the Center for Contraception, Abortion, and Sexuality (CASA, Leiden and The Hague, NL). Use of anonymized residual tissue was approved via the informed opt-out protocol, following national ethical guidelines (https://www.coreon.org/, accessed on 23 November 2020) and institutional privacy regulations.

Fibroblasts were maintained in fibroblast culture medium consisting of DMEM supplemented with 10% fetal bovine serum (FBS), 5 U/mL penicillin and 5 µg/mL streptomycin, and 1% GlutaMAX. Cultures were incubated at 37°C in a 5% CO_2 atmosphere. For scaffold seeding, 100,000 fibroblasts (passages 3–4) were seeded on pre-wetted scaffold in triplicate per donor, using 24-well suspension culture plates (Cellstar). Media changes were performed on days 3, 7, and 11. On day 14, samples were collected and preserved for analysis by one of three methods: (1) fixed in Kryofix solution (50% ethanol, 3% PEG300) for histology, , (2) frozen at -80°C in cryotubes for SDS-PAGE and Western blotting, or (3) stored in TRIzol™ reagent (Invitrogen) at -80°C for RNA extraction.

2.3.2. Evaluation of cellular response and phenotype

Samples in Kryofix were embedded in paraffin, sectioned at 5 µm, and stained with hematoxylin and eosin (H&E). Processed sections were imaged using CaseViewer 2.4 software.

Protein expression was assessed via Western blotting, separated on 10% SDS-PAGE gels. The primary antibody against α-smooth muscle actin (α-SMA) was applied at

a 1:2,000 dilution (clone 1A4, A-2547), alongside anti-GAPDH at a 1:1,000 dilution (clone 14C10, ID218, Cell Signaling Technology). Secondary antibodies included goat polyclonal anti-mouse IgG (IRDye 800CW, 1:10,000, LI-COR Biotechnology, Lincoln) and goat anti-rabbit polyclonal IgG (IRDye 680CW, 1:15,000, LI-COR Biotechnology). Blots were analyzed using the Odyssey CLx imaging system (LI-COR).

RNA was extracted from TRIzol-preserved samples. Briefly, scaffolds were disrupted using a pipette tip, incubated at room temperature for 20 min, and centrifuged at 12,000 × g at 4°C. The supernatant was collected, and RNA was purified using the RNeasy Mini Kit (74106, Qiagen, Hilden, DE) with an RNase-free DNase set (79254, Qiagen). RNA yield and purity were assessed using a NanoDrop spectrophotometer (Thermo Scientific). Gene expression was quantified via reverse transcription-quantitative PCR (RT-qPCR), following the method described by Oostendorp *et al.* [37]. Target genes included ACTA2, ELN, COL1A1, with GAPDH and YWHAZ as reference genes (Table S1). Relative gene expression to COL scaffolds with adult fibroblasts (ΔΔCq) was calculated using CFX Maestro™ software (Bio-Rad), normalizing target gene expression to the reference genes.

2.4. *In vivo* evaluation of scaffolds

2.4.1. Animal ethics and study approval

All surgical procedures were performed at the Radboudumc Animal Research Facility (Nijmegen, NL) after the Dutch Central Committee on Animal Research and the local Ethical Committee on Animal Research of the Radboud University approved the study under project license AVD10300202317189 and protocol 2023-0016-003, respectively.

2.4.2. Animal model setup and scaffold implantation protocol

Five male Wistar subtype Crl:WI(WU) rats (3 months old, 250-400 g) were housed in groups of two or three per cage to avoid solitary housing. Upon arrival, the rats were labelled using ear punches and acclimated for 1-2 weeks before surgery through handling and training (Figure S1). Rats were provided standard pellet food and water *ad libitum*.

On the day of surgery, anesthesia was used with 1.5-2.5% isoflurane, analgesia was administered via carprofen subcutaneous injections (0.1 mL/100 g), and eye cream (Opthosan) was applied to prevent dryness. The dorsal area was prepared by trimming the fur with clippers and removing residual hair with depilatory cream (Veet), followed by disinfection with a povidone-iodine solution (Betadine, Kuinre,

The Netherlands). Four full-thickness wounds (12 mm diameter) were created on the back of each rat using a biopsy punch (220701, SMI AG) and curved scissors. Untreated wounds (without any biomaterial) and wounds treated with COL served as internal controls, while COL:ELN-A (95:5) and COL:ELN-B (95:5) scaffolds were applied to the remaining two wound sites. Wounds on the back were labelled A-D for blinding, and the four treatments were allocated in a randomized order. Sterile wetted scaffolds were placed into the wounds and sutured using eight resorbable sutures (100L6P, Monocryl™ 4-0, Ethicon). The wounds were then covered with paraffin gauze (Jelonet, 7403, Smith & Nephew PLC), silicone dressing (Mepilex Border Flex Lite, 581277, Mölnlycke), elastic bandages (10009403914, PetFlex or elastic fixation bandage from Kruidvat), and adhesive plaster (250, Leukoplast®). Postoperative analgesia was administered via carprofen injections (0.1 mL/100 g) for three consecutive days. Wound dressings were replaced 1-3 times per week (when needed). Rats received booster food (V1185; ssniff Spezialdiäten) and sunflower seeds for 2-3 weeks after the operation.

Digital photographs were taken at multiple timepoints over a 7-week period to monitor wound healing. On day 56, the rats were euthanized using CO_2 inhalation, and final digital photos of the wounds were taken. Wound sites were excised and bisected. One half was fixed in 4% paraformaldehyde (PFA) in phosphate buffer pH 7.4 (PB) overnight at 4 °C and transferred to 1% PFA in PB for storage prior to further analysis. The other half was embedded in TissueTek, frozen in liquid nitrogen and stored at -80 °C.

2.4.3. Macroscopic and microscopic evaluation of wound healing

The final wound contraction was evaluated through the analysis of digital images captured immediately post-surgery (day 0) and at the last assessment point (day 56). Quantification of the wound area was performed using ImageJ software, with calibration of the measurement scale based on the ruler included within each image. The formula used to calculate the wound contraction was as follows:

$$Wound\ contraction\ (\%) = \frac{S_0 - S_{56}}{S_0} \cdot 100\%$$

where

S_0 = Initial wound area at day 0;

S_{56} = Wound area at day 56.

For histological analysis, PFA-fixed samples were embedded in paraffin, processed, and cut into 5 µm sections. Sections were stained with H&E, followed by digital scanning with a whole-slide scanner and accompanying CaseViewer 2.4 software.

H&E staining was used to measure the epidermal thickness in both wounded and unwounded skin, as an average for five regions per rat. The wound area was identified by the presence of short, loosely organized collagen fibers.

Elastin was labelled with rabbit anti-elastin antibody (AB2039, Chemicon, 1:100), followed by incubation with a biotinylated donkey anti-rabbit IgG (Jackson ImmunoResearch, 711-067-003, 1:200). The VECTASTAIN Elite ABC kit and ImmPACT AEC HRP substrate kit were used according to the manufacturer's instructions. Visualization of α-SMA was performed similarly, using a mouse monoclonal anti-α-SMA antibody (A2547, 1:200) and a biotinylated goat anti-mouse IgG (Vector Laboratories, BA-9200, 1:200). The stained sections were semi-quantitatively evaluated by two independent researchers (RK, NA) for signs of elastin deposition, angiogenesis, fibrotic healing, and foreign body reaction to the remaining scaffold material. Scores ranged from 0 (absent) to 2 (clearly present) with substantial agreement coefficients (weighed Cohen's Kappa ≥ 0.75).

An upright TrimScope II multiphoton microscope (LaVision BioTec, a Miltenyi Biotec company, Bielefeld, Germany) equipped with a 16 x 0.8 NA water immersion objective (CFI75 LWD 16X W, Nikon, Japan) was used to generate Second Harmonic Generation (SHG) and two-photon autofluorescence images from fixed rat-skin 5 µm tissue slices. A tunable Ti:Sa laser (Chameleon Ultra II, Coherent, CA, USA) tuned to 840 nm was used to excite the samples, with an average power of 14 mW under the objective. The microscope was equipped with a 6-channel non-descanned epi-detection port close to the objective. Emission was split with a 560lp followed by a 506lp dichroic mirror, and subsequently bandpass filtered with 417/60 (SHG) and 525/50 (autofluorescence). Emissions were detected with GaAs PMT detectors (H7422A-40, Hamamatsu, Hamamatsu city, Japan). Samples were imaged in bi-directional scanning mode, with a 624 µm scanfield, a 0.58 µm pixel size, and a pixel dwell time of 1.05 µs. Z-stacks were performed with a 3 µm step size. H&E stained sections combined with SHG images were used to semi-quantitatively assess newly formed collagen.

2.4 Statistical analysis

Statistical analyses were conducted using GraphPad Prism version 10.4.1. Relative measurements, normalized to the control condition, were evaluated using a one-sample t-test. Group comparisons were performed with Brown-Forsythe and Welch ANOVA, followed by Dunnett's T3 multiple comparisons test. Differences in gene expression levels between scaffold types and fibroblast types were tested using two-way ANOVA, followed by Tukey's multiple comparisons test. Statistical significance was defined as a p-value <0.05, corresponding to a 95% confidence

interval. To assess the level of agreement between the evaluators for semi-quantitative analysis, a weighted Cohen's Kappa was calculated using R version 4.2.2, with values ≥ 0.75 indicating substantial agreement. The weighting accounted for the severity of disagreement, meaning that a score difference between 0 and 2 reflects a greater discrepancy than between 1 and 2.

3. Results

3.1. Characterization of collagen-elastin scaffolds

As previously reported [32], different chemical solubilization methods for insoluble elastin resulted in distinct molecular weights and primary amine groups. Briefly, the peak molecular mass of ELN-A was approximately 39 kDa, and ELN-B was around 30 kDa, while quantification of primary amine groups resulted in values of 395 ± 77 nmol per mg for ELN-A and 214 ± 28 nmol per mg for ELN-B.

The collagen-elastin scaffolds were fabricated as white, soft, and porous biomaterials. Scanning electron microscopy confirmed that the covalent binding of soluble elastins with EDC/NHS did not alter the structural organization of the collagen matrix, as all scaffolds exhibited similar pore morphology (Figure 1A). Immunohistochemical staining visualized elastin in brown, and VEMT staining highlighted collagen in blue and elastin in dark-blue/black. Both stainings demonstrated a successful incorporation of solubilized elastins and their uniform distribution throughout the scaffold (Figure 1B-C).

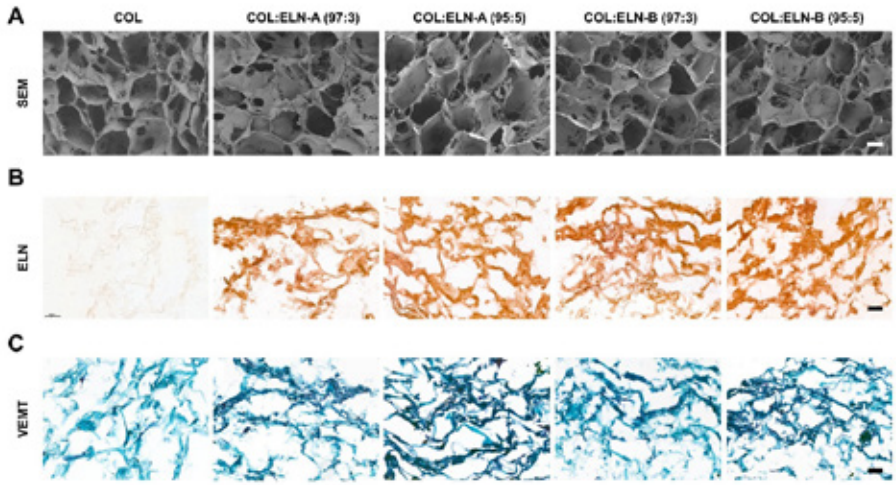

Figure 1. Microscopic imaging of collagen and collagen-elastin scaffolds. A) Scanning electron microscope (SEM) images of cross-sections of the scaffolds. B) Elastin(ELN)-stained sections of the scaffolds, highlighting elastin in brown. C) Verhoeff Elastic Masson Trichrome (VEMT) staining of the scaffolds, highlighting collagen in blue and elastin in dark-blue/black. Scale bars are 50 µm. COL = type I collagen scaffold, COL:ELN-A = type I collagen scaffold supplemented with ELN-A, COL:ELN-B = type I collagen scaffold supplemented with ELN-B.

Table 1 summarizes the biochemical characterization of scaffolds before and after chemical crosslinking. In the non-crosslinked state, collagen-only scaffolds contained the highest concentration of primary amine groups. Following crosslinking, all scaffold types showed amine content of 123 ± 4 nmol per mg of scaffold, resulting in comparable crosslinking efficiencies of 49 ± 2%. Chemical crosslinking facilitated the covalent attachment of soluble elastin to insoluble type I collagen as well as enhanced scaffold stability. This was reflected in a significant increase in denaturation temperature (Td), with collagen and collagen-elastin scaffolds exhibiting respective increases of 19.3 ± 1.2 °C and 20.9 ± 0.5 °C. Furthermore, denaturation enthalpy analysis indicated that COL:ELN-B scaffolds maintained the highest protein structural integrity, regardless of crosslinking. In contrast, COL:ELN-A scaffolds showed reduced enthalpy values after crosslinking, possibly indicating differences in their secondary and tertiary structures compared to COL:ELN-B scaffolds.

Table 1. Characteristics of collagen and collagen-elastin scaffolds.

Scaffold	Amine group content (nmol/mg scaffold)		Denaturation temperature Td (°C)		Denaturation enthalpy ΔH_D (J/g)	
Crosslinked with EDC/NHS	-	+	-	+	-	+
COL	267 ± 51	126 ± 6*	54.7 ± 1.2	74.0 ± 0.2*	1.5 ± 0.3	1.9 ± 0.3
COL:ELN-A (97:3)	238 ± 34	122 ± 12*	52.0 ± 0.4	73.2 ± 0.5*	2.0 ± 0.1	1.6 ± 0.2
COL:ELN-A (95:5)	247 ± 38	126 ± 7*	52.5 ± 0.8	72.5 ± 0.0*	2.4 ± 0.2	1.9 ± 0.2
COL:ELN-B (97:3)	245 ± 30	119 ± 9*	52.7 ± 0.3	73.9 ± 0.1*	2.0 ± 0.2	2.3 ± 0.1
COL:ELN-B (95:5)	263 ± 33	124 ± 9*	52.7 ± 0.8	72.9 ± 0.1*	2.2 ± 0.1	2.5 ± 0.1

N=3, mean ± SD. * Compared to non-crosslinked counterpart, $p < 0.001$.

3.2. *In vitro* assessment of collagen-elastin scaffolds

To determine whether biomaterial composition influences the regenerative or fibrotic response, fibroblasts from different sources were used. We selected skin fibroblasts derived from adult, eschar, and fetal tissues.

H&E staining showed that more fetal fibroblasts were present on the scaffolds after two weeks of culture (Figure 2A), followed by adult and eschar cells, which correlated with the amount of isolated RNA (Table S2). Fetal and adult cells showed slightly higher migration in both scaffold types than eschar cells, which mostly remained on the surface (Figure 2A). In terms of contractile capacity, the scaffold size remained consistent at 1.1–1.2 cm^2 (Figure S2, Table S3).

After 14 days of culture, the expression of type I collagen (*COL1A1*) and elastin (*ELN*) genes was assessed by RT-qPCR analysis (Figure 2B-C and Figure S3A-B). Across three fibroblast types, the group of adult cells exhibited the lowest expression levels, whereas the group of eschar fibroblasts demonstrated significantly higher expression, likely reflecting an active ECM production state (Figure S4). The group of fetal fibroblasts exhibited the highest gene expression for *COL1A1* and *ELN*. In fetal fibroblasts, COL:ELN-B (95:5) scaffolds resulted in higher *COL1A1* gene expression compared to COL and COL:ELN-A (97:3) (Figure 2B). Significantly elevated gene expression was observed on the same scaffolds with adult compared to fetal fibroblasts (Figure S3A-B).

To evaluate myofibroblast presence, α-SMA expression was analyzed at gene (*ACTA2*; Figure 2D) and protein level (Figure 2E and Figure S4D, S5). For all five scaffolds, adult fibroblasts demonstrated significantly lower *ACTA2* expression compared to eschar and fetal cells (Figure S3C). α-SMA expression assessed through

Western blot showed the same trend, with higher expression in fetal ($p<0.001$) and eschar ($p=0.064$) fibroblasts compared to adult cells (Figure S4D). For adult and eschar cells, α-SMA protein expression was reduced in COL:ELN-A (97:3 and 95:5) and COL:ELN-B (97:3), compared to collagen only. Additionally, COL:ELN-B (95:5) decreased α-SMA expression in eschar cells.

3.3. Analysis of wound healing with collagen-elastin scaffolds in vivo

Three types of biomaterials were tested in excisional wounds in a rat model: COL, COL:ELN-A (95:5) and COL:ELN-B (95:5), with an untreated wound as a control. The four wounds exhibited distinct healing trajectories following a similar morphological progression. The wound consistently decreased in size over time, transitioning from a circular shape to an oval form, and ultimately resolving into a linear scar (Figure 3A-B). Among the groups, untreated wounds displayed the fastest closure, reaching near-complete closure by day 14, with approximately 99% wound contraction at the end of the observation period.

The extent of macroscopic wound contraction followed the trend: untreated wound > COL > COL:ELN-A > COL:ELN-B (Figure 3A-D). Although the differences in contraction between scaffolds were not statistically significant, a significant reduction in wound contraction was observed when comparing untreated wounds to those treated with scaffolds supplemented with elastin hydrolysates (Figure 3D). Results from *in vitro* experiments demonstrating reduced α-SMA expression in healthy and wounded (eschar) adult skin fibroblasts cultured on elastin-containing scaffolds suggest that the decreased wound contraction observed with collagen-elastin scaffolds may be attributed, at least in part, to suppressed myofibroblast activation. Among the scaffolds, COL:ELN-B (95:5) demonstrated the most pronounced reduction in visual contraction *in vivo*.

The wounded area can be seen with H&E staining, characterized by thinner and smaller collagen fibrils (Figure 3C and Figure S7). All the wounds exhibited a concave wound geometry under histological examination (grey dotted lines in Figure 3C). Notably, skin sections were obtained from the central perpendicular plane of the wounds, despite the middle region not always representing the widest part of the wound. Wound contraction was additionally quantitatively assessed by measuring the width of the newly formed upper dermis and the minimum wound width (Figure 3C-D). All biomaterials demonstrated higher width values of newly formed ECM regions, while COL:ELN-B (95:5) biomaterials resulted in the largest width values and were significantly different compared to the untreated wounds (Figure 3D).

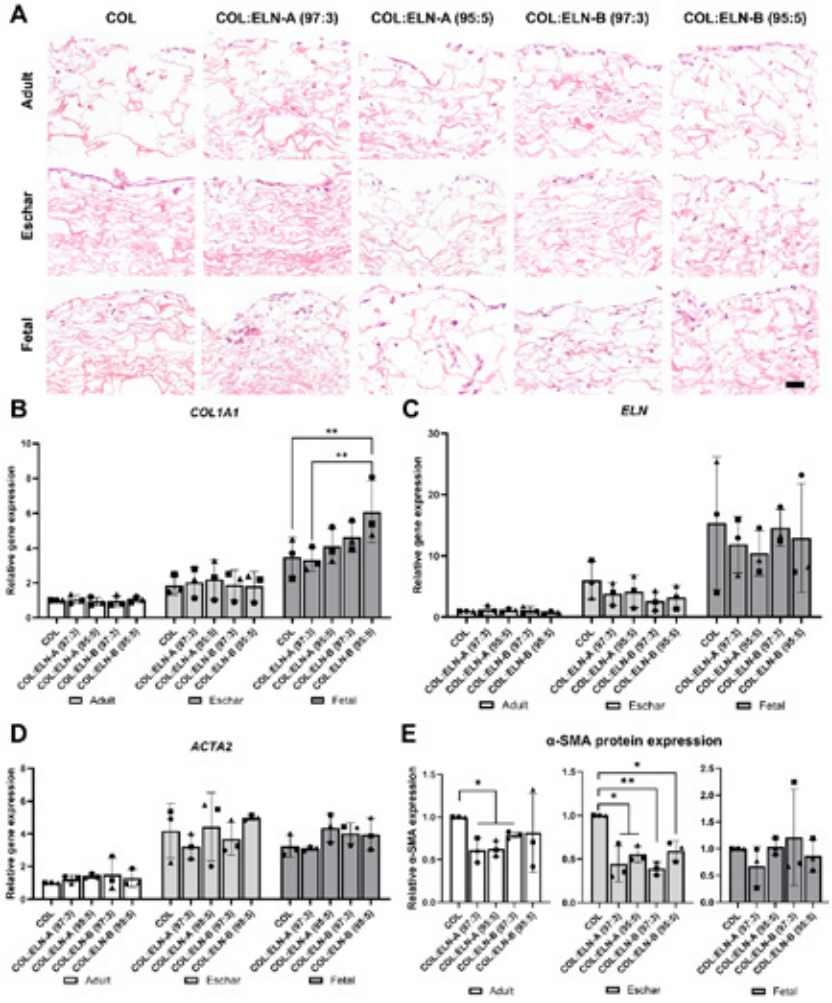

Figure 2. Results from cell culture experiments of primary human dermal fibroblasts (adult, eschar, and fetal) in the presence of scaffolds (day 14, n=3). A) Cellular localization within scaffolds analyzed through H&E staining. Scale bar is 50 µm. B-D) Comparative gene expression levels of *COL1A1*, *ELN*, and *ACTA2* across three fibroblast types, normalized to the mean expression of adult fibroblasts cultured on COL scaffolds. Differences in gene expression levels between scaffold types and fibroblast types were tested using two-way ANOVA, followed by Tukey's multiple comparisons test ($\alpha = 0.05$). Only statistically significant differences between scaffolds within the same fibroblast type are shown, while full pairwise comparisons are provided in Figure S3. E) Relative expression of α-SMA based on intensities of the bands on Western blot, normalized to COL scaffolds for the same type of fibroblasts. Individual donors are represented by different symbols as ● donor 1/4/7, ■ donor 2/5/8, and ▲ donor 3/6/9. Error bars represent standard deviation; * $p<0.05$, ** $p<0.01$, *** $p<0.001$. COL = type I collagen scaffold, COL:ELN-A = type I collagen scaffold supplemented with ELN-A, COL:ELN-B = type I collagen scaffold supplemented with ELN-B, COL1A1 = alpha-1 type I collagen, ELN = elastin, ACTA2 = smooth muscle actin alpha 2, α-SMA = α-smooth muscle actin.

Throughout the study, wounds treated with COL scaffolds generally closed more rapidly, while those treated with COL:ELN-B (95:5) scaffolds exhibited the slowest healing, with closure times extending up to 35 days. Additionally, wounds located in the upper body regions of the rats were less affected by movement-related distortion compared to those in the lower regions, highlighting the impact of anatomical location on healing outcomes. To minimize positional bias, treatment conditions were randomly assigned to different wound locations across animals, ensuring that no rat received the same allocation pattern.

H&E staining also showed other aspects of wound healing, including re-epithelialization, cellular infiltration, and the amount of scaffold remnants. Measurement of epidermal thickness revealed that the COL:ELN-B (95:5) scaffold showed a significant increase in relative epidermal thickness compared to adjacent healthy skin (Figure 3E-F and Figure S6). Untreated wounds, COL and COL:ELN-A scaffolds resulted in comparable epidermal thickness values.

All experimental groups showed increased cellular infiltration in the wounded areas compared to healthy skin, likely due to a transient inflammatory response and ongoing tissue remodelling. α-SMA staining highlighted the formation of new blood vessels and showed weaker overall intensity compared to healthy skin (Figure 4A-B). α-SMA-positive staining around capillaries was interpreted as a marker of vascular maturation, reflecting the presence of pericytes surrounding endothelial cells, which contributed to vessel stabilization and functional integrity. Neovascularization was observed across all treatment groups within the wounded regions (Table 2). When scaffold remnants persisted within the dermis, they were distinctly visible through both α-SMA and H&E staining, and induced a foreign body reaction (Figure 4B). Notably, a strong localized α-SMA positive signal in fibroblasts, coupled with high cellular infiltration and scaffold fragments surrounded by giant cells, suggested active scaffold degradation and local remodelling around the degrading material. The most frequent and apparent presence of COL:ELN-B (95:5) remnants coincided with the longest healing time for this treatment group.

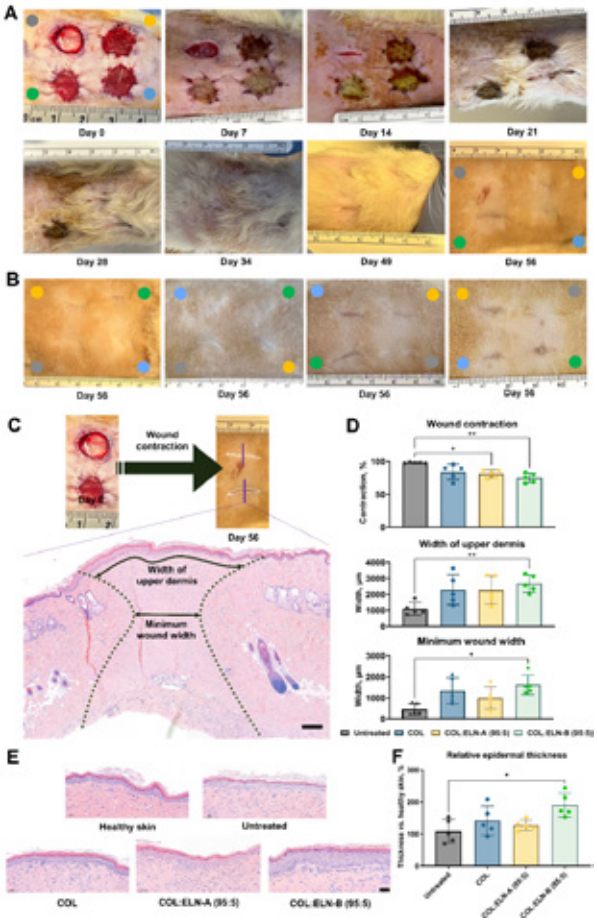

Figure 3. *In vivo* assessment of the scaffolds in a rat model (n=5). A) Representative digital images of the healing process of the wounds throughout the experiment. ● – untreated wound, ● – type I collagen scaffold (COL), ● – type I collagen scaffold supplemented with ELN-A (COL:ELN-A (95:5)), ● – type I collagen scaffold supplemented with ELN-B (COL:ELN-B (95:5)). B) Healed skin regions in the other four rats at day 56. Scale bars in centimetres. C) Representative H&E stained skin sections on day 56 with wound area highlighted with grey dotted lines, and arrows showing how the newly formed upper dermis and minimum wound width were measured. Scale bar is 200 µm. D) Calculated macroscopic wound contraction (top), width of the newly formed upper dermis (middle), and minimum wound width (bottom). E) Representative H&E stained sections showing epidermal thickness of healthy skin and four experimental groups. F) Epidermal thickness within four treatment groups, expressed relative to adjacent healthy skin (%). Scale bar is 50 µm. Error bars represent standard deviation; * $p<0.05$, ** $p<0.01$.

Table 2. Comparable analysis of rat skin tissue sections at day 56 after wounding.

	Untreated	COL	COL:ELN-A (95:5)	COL:ELN-B (95:5)
Scaffold remnants	N/A	0.6 ± 0.8	0.7 ± 0.7	1.1 ± 0.5
Neovascularization	0.6 ± 0.5	1.4 ± 0.8	1.2 ± 0.7	1.5 ± 0.4
Collagen	0.5 ± 0.2	1.2 ± 0.6	1.0 ± 0.4	1.3 ± 0.2**
Elastin	0.2 ± 0.4	1.1 ± 0.2*	1.4 ± 0.4*	1.4 ± 0.5*

The presence of a localized area of strong α-SMA positive staining in response to the presence of residual scaffold fragments and neovascularization was scored from 0 (absence) to 2 (clear detection). Similarly, collagen and elastin deposition were assessed through H&E/SHG and elastin staining, respectively, and scored on the same 0 (absence) to 2 (most detection) scale. n=5, mean ± SD. N/A = not applicable. * compared to untreated wound, $p < 0.05$; ** $p < 0.01$.

Collagen fibers were also visualized using second harmonic generation (SHG) (Figure 4A). In wounded areas, SHG detected weaker collagen signals and revealed finer thickness of newly formed collagen fibrils (Figure S7). Semi-quantitative assessment revealed a significant increase in collagen deposition in wounds treated with the COL:ELN-B scaffold compared to untreated wounds. Elastin immunostaining showed the strongest positive signal in healthy skin, while all scaffold-treated groups (including collagen-only scaffolds) exhibited weaker but consistent signals, likely due to the formation of new elastic fibers. Among the scaffold-treated groups, the COL:ELN-B (95:5) scaffold was associated with the least wound contraction and appeared to support more extensive deposition of collagen and elastic fibers, although deposition patterns were generally similar across all scaffolds and these differences were not statistically significant. In contrast, untreated wounds revealed the minimum collagen deposition and almost no presence of elastin. Two-photon excited autofluorescence imaging did not visualize elastic fibers but highlighted integrated scaffolds into the rat's dermis (Figure S8).

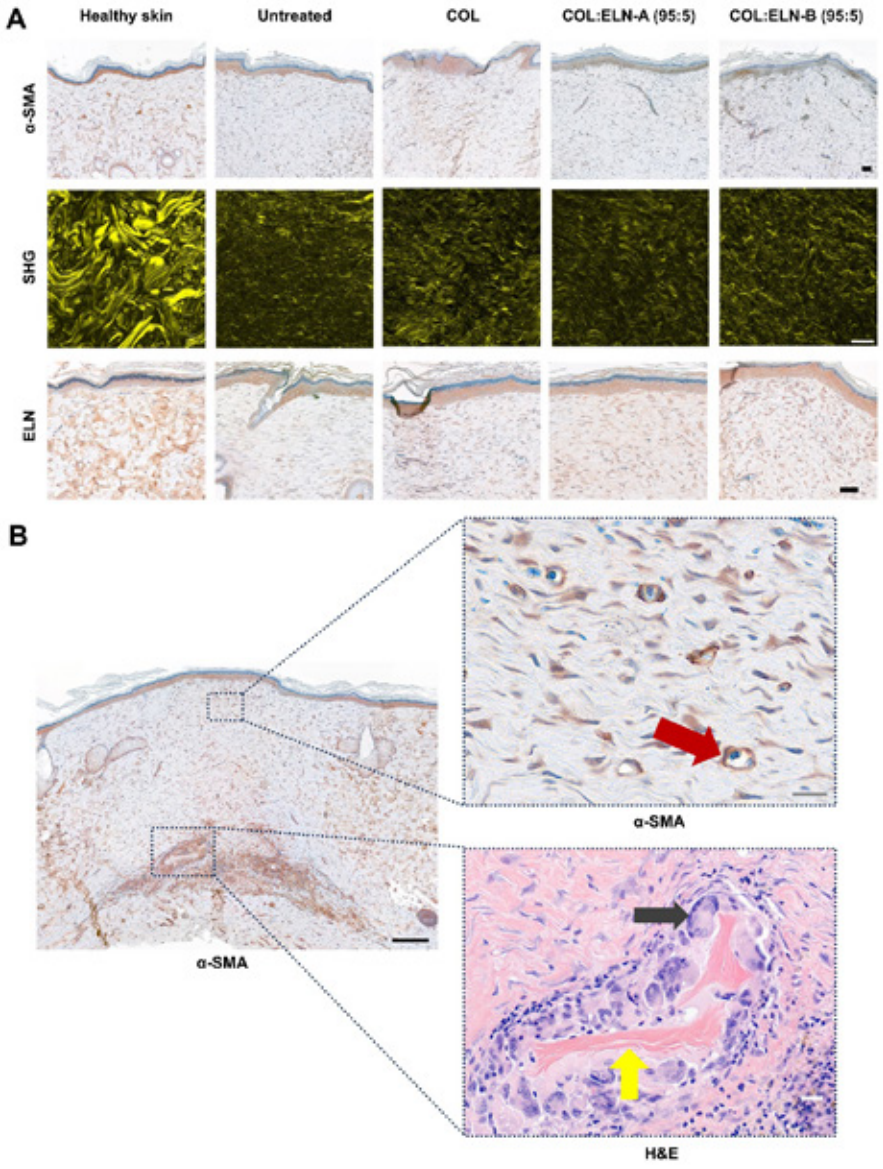

Figure 4. Microscopic examination of healthy and healed rat skin at day 56. A) Representative sections stained for α-SMA, in brown. Collagen fibers visualized with SHG using multiphoton microscopy. Sections stained for elastin, in brown. Scale bars are 50 µm. B) Section stained for α-SMA, presenting an area with strong positive staining, co-localizing with residual scaffold fragments (yellow arrow), surrounded by foreign body giant cells (grey arrow) (magnified area, H&E). α-SMA staining also highlights neovascularization (magnified area, red arrow). Black scale bar is 200 µm, grey and white scale bars are 20 µm. COL = type I collagen scaffold, COL:ELN-A = type I collagen scaffold supplemented with ELN-A, COL:ELN-B = type I collagen scaffold supplemented with ELN-B, α-SMA = α-smooth muscle actin, SHG = second harmonic generation, ELN = elastin, H&E = hematoxylin and eosin.

4. Discussion

Elastin and elastin-based compounds have been extensively studied for their beneficial biological effects in wound healing, appearing in various forms such as insoluble elastic fibers [38], soluble tropoelastin (protein [39] or mRNA [40]), solubilized elastin peptides [22], and synthetic elastin peptides [41]. However, when considering their application in dermal biomaterial development, the primary candidates are elastic fibers (insoluble or solubilized) and recombinant tropoelastin protein. Among these, insoluble elastin derived from animal sources is the least favorable due to challenges such as calcification, poor solubility, and biological inertness [22, 38]. While recombinant tropoelastin offers a promising alternative, its application in dermal biomaterials is complicated by limited stability, high production costs, and significant challenges in large-scale manufacturing [39, 42, 43]. Given these aspects, we opted for solubilized elastins, which offer distinct advantages over the aforementioned compounds and their limitations.

Solubilized elastin peptides can be categorized based on their preparation method: chemical hydrolysis (using acids or bases) or enzymatic digestion. Different enzymatically digested elastins have demonstrated potential in promoting ECM synthesis and dermal regeneration [19, 20]. Although these findings originate from single publications by individual research groups, they provide important insights and a strong foundation for continued investigation. Alternatively, chemically hydrolyzed elastins have been more extensively studied, with demonstrated effects in cell cultures, animal models, and biomaterial formulations [24]. Among acidic hydrolysis methods, oxalic acid is the most commonly used because of its ability to generate solubilized elastin that closely mimics its native, insoluble counterpart [44, 45]. Such a preparation was able to enhance elastin expression and improve dermal healing when incorporated into biomaterials [22, 46, 47]. Alkaline hydrolysis of elastin is typically performed with potassium hydroxide in an ethanol medium, which provides hydroxide ions for nucleophilic cleavage and may lead to β-elimination and deamination reactions (as indicated by an almost twofold reduction in primary amine groups in ELN-B compared to ELN-A). Such solubilized elastins obtained via alkaline hydrolysis have not been widely used in biomaterial formulations but have been reported to enhance mesenchymal cell adhesion to elastic fibers, stimulate the biosynthesis of adhesive proteins, and strengthen cell-elastin interactions [48]. Additionally, they have found applications in cosmetics due to their UV-protective properties and ability to improve skin elasticity [49, 50].

We selected solubilized elastins derived from oxalic acid and potassium hydroxide treatments for further investigation and direct comparison in collagen-based scaffolds. To achieve covalent binding of soluble elastin to insoluble collagen fibers, we used EDC/NHS crosslinking [22]. A previous study has reported similar concentrations of primary amine groups in soluble elastin and collagen (approximately 300 nmol/mg [22]), while our materials showed slight variations: type I collagen contained 270 nmol/mg, ELN-A – 400 nmol/mg, and ELN-B – 200 nmol/mg. After crosslinking, the remaining available primary amine groups were approximately 125 nmol/mg across all formulations, similar to earlier findings of around 180 nmol/mg [22] and resulting in ~50% crosslinking. These discrepancies may be attributed to differences in methods for preparation of soluble elastin (stepwise oxalic acid hydrolysis vs. continuous oxalic acid and alkaline hydrolysis) and scaffold compositions (97:3, 9:1, 1:1 vs. 97:3, 95:5). Although mechanical testing was not performed on our biomaterials, previous studies have shown that collagen-elastin scaffolds crosslinked with genipin or EDC/NHS showed increased elasticity with the addition of elastin [29, 51]. Elastin has also been reported to delay scaffold degradation [29]. In our pilot experiments with soluble elastin, we observed that a higher elastin content accelerated degradation of crosslinked scaffolds in the presence of collagenase, but delayed degradation in non-crosslinked ones (data not shown). Unlike prior study utilizing a 1:1 collagen-elastin ratio for *in vivo* experiments [22], we investigated formulations with 95:5 collagen-elastin ratios, which more closely resemble the elastin content in human skin [9].

Studies on the *in vitro* evaluation of collagen-solubilized elastin scaffolds are limited [29, 30, 51]. We observed that cell distribution, with higher densities closer to the seeded side, aligned with previously reported data [30, 52]. In this study, we explored the potential for scarless healing by analyzing key genes (*COL1A1*, *ACTA2*, *ELN*) and α-SMA protein expression, as well as examining the responses of three distinct skin fibroblast sources, adult, eschar, and fetal cells, in collagen-elastin scaffolds. While these fibroblast types share some similarities, they exhibit unique behaviors in culture, reflecting their respective roles in wound healing and tissue development. Adult fibroblasts cultured on COL:ELN-A scaffolds showed lower α-SMA protein levels, indicating a potentially reduced fibrotic response. Notably, fetal fibroblasts demonstrated features typical of myofibroblasts and generated an environment resembling fibrosis [53], yet contributed to healing without contracture or scar formation [3]. Fetal fibroblasts exhibited higher α-SMA expression compared to adult fibroblasts in cell culture experiments, consistent with previous findings from monolayer cultures [54]. Furthermore, the upregulation of α-SMA at both the gene and protein level for eschar fibroblasts

aligned with recent literature [55]. Nevertheless, cellular responses under fibrotic conditions induced by TGF-β may follow different patterns. For example, studies on collagen gels have shown that fetal fibroblasts exhibit reduced contractile capacity, characterized by lower cell proliferation and decreased expression of α-SMA and integrins [54]. Due to the stiffness of our crosslinked scaffolds and their resistance to cell-mediated contraction, along with the absence of TGF-β stimulation, scaffold size remained stable throughout the *in vitro* experiments. Our findings highlight that different fibroblast sources exhibit distinct biological behaviors, suggesting that each cell type may offer specific advantages depending on the wound context (e.g., incisional vs. burn injuries) or therapeutic application (e.g., in pediatric vs. adult patients).

Collagen-elastin scaffolds represent a valuable alternative to many current wound healing strategies by combining biomimicry with practical application [24]. Unlike synthetic polymers, which often lack the intrinsic biological resemblance [56], these scaffolds simulate the structural and functional properties of the dermis by providing the tensile strength of collagen together with the elasticity provided by elastin. Compared to cell-based therapies, which have issues with viability, retention, risk of tumor formation, and precise delivery within the wound environment [57, 58], collagen-elastin scaffolds serve as supportive, biocompatible matrices that support proliferation and differentiation of host cells. While advanced tissue engineering techniques such as complex skin grafts, 3D bioprinting, aim to closely replicate full skin architecture [59-61], they are often constrained by high costs, technical complexity, and scalability challenges. In contrast, collagen-elastin scaffolds provide a more accessible, cost-effective platform that supports robust tissue regeneration without the need for complex structural design or cellular manipulation, making them also highly attractive for clinical translation.

In animal models, research on biomaterials composed of type I collagen and solubilized elastin has been primarily focused on oxalic acid hydrolysates [22, 23, 26, 47, 62]. When these hydrolysates were incorporated into non-crosslinked collagen scaffolds and applied to full-thickness wounds in Yorkshire pigs, the biomaterials degraded more slowly compared to collagen-only scaffolds [47]. Additionally, more newly formed ECM was observed within the biomaterial's pores, although there was a lower number of infiltrating fibroblasts and myofibroblasts [23, 47]. Most importantly, collagen-elastin matrices significantly reduced wound contraction in pigs and provided the best esthetic outcomes [47]. In Sprague Dawley rats, subcutaneous implantation of EDC/NHS crosslinked collagen-elastin scaffolds showed that oxalic acid hydrolysates of elastin promoted

angiogenesis, as indicated by type IV collagen staining [22]. These scaffolds also supported the formation of elastic fibers, with notable deposits of elastin and fibrillin-1, as well as a more evident collagen network composed of type I and type III collagen [22]. Full-thickness wound healing in Wistar rats with a double-layered skin substitute containing solubilized elastin was also found to promote significant angiogenesis while reducing myofibroblast presence during the early stages of healing [26]. By the end of the 112-day experiment, the tested skin substitute facilitated the formation of new elastic fibers and structures resembling skin appendages [26]. Despite these promising effects, the exact impact of solubilized elastin was not determined because of the scaffold's complex composition (type I collagen, heparin, solubilized elastin, dermatan sulfate, fibroblast growth factors 2 and 7, and vascular endothelial growth factor). Among the tested conditions in our experiments, COL:ELN-B scaffolds exhibited a prolonged wound healing response but the least wound contraction by day 56 post-surgery, although the differences were not statistically significant from other tested scaffolds. Additionally, we observed increased collagen and elastin deposition in collagen-elastin scaffolds, along with enhanced angiogenesis. These findings not only support the hypothesis that collagen-elastin scaffolds have beneficial effects on wound healing but also highlight the promising potential of the incorporation of the potassium hydroxide hydrolysate. While other methods for producing materials for wound healing may require high costs and laborious techniques (e.g., 3D bioprinting, stereolithography, selective laser sintering, and fused deposition modeling), Multiphoton microscopy offers a non-invasive approach for examining ECM structures in unstained tissue sections [63]. In this study, collagen was visualized through SHG, while elastic fibers were expected to be detected via TPEAF [64, 65]. This technique eliminates the need for tissue excision, embedding, fixation, or staining, and can be applied to live animals [66, 67], potentially reducing the number required for experiments. Although dermal elastic fibers were not clearly observed under the chosen TPEAF settings, we did detect autofluorescent signals in the scaffold-treated groups, which are likely associated with parts of biomaterials integrated into the rat skin.

Research on solubilized elastins involves several important considerations. Firstly, it is crucial to determine whether the entire hydrolysate or a specific fraction is used, as their differing molecular characteristics can influence the observed effects. Secondly, studies assessing elastogenic effects should clearly differentiate between elastin upregulation at the gene level and actual protein production. The formation of a well-organized elastic fiber network should be demonstrated, rather than the presence of isolated elastin deposits [68]. Furthermore, fluorescent tagging of solubilized elastins combined with antibody detection of rat's elastic fibers may be

used to distinguish whether soluble elastin was incorporated into new elastic fibers or merely triggered elastogenesis without incorporation [69]. Thirdly, when testing biomaterials in animal models, selecting the appropriate species is essential. Despite their higher costs and relative complexity, larger animals such as pigs are preferred due to their closer resemblance to human skin [70, 71]. Exploring alternative, milder crosslinking agents (e.g., genipin, transglutaminase, epigallocatechin gallate, tannic acid [72, 73]) may promote faster scaffold resorption within wounded skin regions, potentially enhancing tissue regeneration and reducing the risk of an unwanted foreign body response [25]. In this context, evaluating the mechanical stability and biodegradation of these scaffolds, particularly at later timepoints, is crucial for understanding how long they persist in the tissue and how they influence cellular behavior and remodeling dynamics. Additionally, any comparisons to previously published animal studies are complicated by substantial variations in biomaterial composition, preparation methods, and species used.

5. Conclusions

Two differently prepared solubilized elastins were successfully integrated into collagen-based biomaterials and compared side-by-side. Among the three types of skin fibroblasts tested, fetal cells exhibited the highest expression of extracellular matrix-related genes and cellular infiltration within the scaffolds, followed by eschar-derived cells and healthy adult dermal fibroblasts. Compared to collagen-only scaffolds, adult and eschar fibroblasts cultured on collagen-elastin scaffolds demonstrated lower expression of α-SMA, a fibrotic marker, suggesting that the presence of elastin may suppress myofibroblast activation for these types of fibroblasts. In a rat full-thickness skin model, α-SMA staining did not suggest fibrotic responses but did indicate neovascularization and an ongoing degradation and clearance of scaffold remnants by the host tissue. *In vivo*, collagen scaffolds supplemented with elastin hydrolysate obtained by basic hydrolysis showed promising features associated with scarless healing, as evidenced by the lowest wound contraction, the most extensive newly formed ECM, and the highest degree of neovascularization.

References

1. Strodtbeck, F., *Physiology of wound healing.* Newborn and Infant Nursing Reviews, 2001. **1**(1): p. 43-52.
2. Alonso, L. and E. Fuchs, *Stem cells of the skin epithelium.* Proceedings of the National Academy of Sciences, 2003. **100**(suppl_1): p. 11830-11835.
3. Buchanan, E.P., M.T. Longaker, and H.P. Lorenz, *Chapter 6 Fetal Skin Wound Healing*, in *Advances in Clinical Chemistry*. 2009, Elsevier. p. 137-161.
4. Rivera, A.E. and J.M. Spencer, *Clinical aspects of full-thickness wound healing.* Clinics in Dermatology, 2007. **25**(1): p. 39-48.
5. Svensjö, T., et al., *Accelerated Healing of Full-Thickness Skin Wounds in a Wet Environment.* Plastic and Reconstructive Surgery, 2000. **106**(3): p. 602-612.
6. Rittié, L., *Cellular mechanisms of skin repair in humans and other mammals.* Journal of Cell Communication and Signaling, 2016. **10**(2): p. 103-120.
7. Boyce, S.T., et al., *Randomized, Paired-Site Comparison of Autologous Engineered Skin Substitutes and Split-Thickness Skin Graft for Closure of Extensive, Full-Thickness Burns.* Journal of Burn Care & Research, 2017. **38**(2): p. 61-70.
8. Tavakoli, S. and A.S. Klar, *Bioengineered Skin Substitutes: Advances and Future Trends.* Applied Sciences, 2021. **11**(4): p. 1493.
9. Sheikholeslam, M., et al., *Biomaterials for Skin Substitutes.* Advanced Healthcare Materials, 2018. **7**(5): p. 1700897.
10. Rezvani Ghomi, E., et al., *Collagen-based biomaterials for biomedical applications.* Journal of Biomedical Materials Research Part B: Applied Biomaterials, 2021. **109**(12): p. 1986-1999.
11. Mathew-Steiner, S.S., S. Roy, and C.K. Sen, *Collagen in Wound Healing.* Bioengineering, 2021. **8**(5): p. 63.
12. Ferrario, C., et al., *From Food Waste to Innovative Biomaterial: Sea Urchin-Derived Collagen for Applications in Skin Regenerative Medicine.* Marine Drugs, 2020. **18**(8): p. 414.
13. Schmelzer, C.E.H. and L. Duca, *Elastic fibers: formation, function, and fate during aging and disease.* The FEBS Journal, 2022. **289**(13): p. 3704-3730.
14. Cohen, B.E., et al., *The Role of Elastic Fibers in Scar Formation and Treatment*. Dermatologic Surgery, 2017. **43**: p. S19-S24.
15. Senior, R.M., et al., *Val-Gly-Val-Ala-Pro-Gly, a repeating peptide in elastin, is chemotactic for fibroblasts and monocytes.* Journal of Cell Biology, 1984. **99**(3): p. 870-874.
16. MORELLI, M.A.C., et al., *Structure-activity relationships for some elastin-derived peptide chemoattractants.* The Journal of Peptide Research, 1997. **49**(6): p. 492-499.
17. Kamoun, A., et al., *Growth Stimulation of Human Skin Fibroblasts by Elastin-Derived Peptides.* Cell Adhesion and Communication, 1995. **3**(4): p. 273-281.
18. Tajima, S., et al., *Modulation by elastin peptide VGVAPG of cell proliferation and elastin expression in human skin fibroblasts.* Archives of Dermatological Research, 1997. **289**(8): p. 489-492.
19. Hinek, A., et al., *Proteolytic digest derived from bovine Ligamentum Nuchae stimulates deposition of new elastin-enriched matrix in cultures and transplants of human dermal fibroblasts.* Journal of Dermatological Science, 2005. **39**(3): p. 155-166.
20. Shiratsuchi, E., M. Nakaba, and M. Yamada, *Elastin hydrolysate derived from fish enhances proliferation of human skin fibroblasts and elastin synthesis in human skin fibroblasts and improves the skin conditions.* Journal of the Science of Food and Agriculture, 2016. **96**(5): p. 1672-1677.

21. Groult, V., et al., *Mechanisms of interaction between human skin fibroblasts and elastin: Differences between elastin fibres and derived peptides.* Cell Biochemistry and Function, 1991. **9**(3): p. 171-182.
22. Daamen, W.F., et al., *A biomaterial composed of collagen and solubilized elastin enhances angiogenesis and elastic fiber formation without calcification.* Tissue Engineering Part A, 2008. **14**(3): p. 349-60.
23. Lamme, E.N., et al., *Extracellular matrix characterization during healing of full-thickness wounds treated with a collagen/elastin dermal substitute shows improved skin regeneration in pigs.* Journal of Histochemistry and Cytochemistry, 1996. **44**(11): p. 1311-22.
24. Daamen, W.F., et al., *Elastin as a biomaterial for tissue engineering.* Biomaterials, 2007. **28**(30): p. 4378-98.
25. Boekema, B., et al., *Effect of pore size and cross-linking of a novel collagen-elastin dermal substitute on wound healing.* Journal of Materials Science: Materials in Medicine, 2014. **25**: p. 423-433.
26. Nillesen, S.T.M., et al., *Design and in vivo evaluation of a molecularly defined acellular skin construct: Reduction of early contraction and increase in early blood vessel formation.* Acta Biomaterialia, 2011. **7**(3): p. 1063-1071.
27. Jiménez Vázquez, J. and E. San Martín Martínez, *Collagen and elastin scaffold by electrospinning for skin tissue engineering applications.* Journal of Materials Research, 2019. **34**(16): p. 2819-2827.
28. Sawadkar, P., et al., *Three dimensional porous scaffolds derived from collagen, elastin and fibrin proteins orchestrate adipose tissue regeneration.* Journal of Tissue Engineering, 2021. **12**: p. 20417314211019238.
29. Kamaruzaman, N., et al., *Functionalised Hybrid Collagen-Elastin for Acellular Cutaneous Substitute Applications.* Polymers, 2023. **15**(8): p. 1929.
30. Maitz, J., et al., *The effects of cross-linking a collagen-elastin dermal template on scaffold bio-stability and degradation.* J Tissue Eng Regen Med, 2020. **14**(9): p. 1189-1200.
31. Daamen, W.F., et al., *Isolation of intact elastin fibers devoid of microfibrils.* Tissue Eng, 2005. **11**(7-8): p. 1168-76.
32. Krymchenko, R., et al., *Preparation, fractionation, and characterization of solubilized elastin and comparison of cellular response on fibroblasts and macrophages.* International Journal of Biological Macromolecules, 2025. **315**: p. 144548.
33. Buttafoco, L., et al., *First steps towards tissue engineering of small-diameter blood vessels: Preparation of flat scaffolds of collagen and elastin by means of freeze drying.* Journal of Biomedical Materials Research Part B-Applied Biomaterials, 2006. **77B**(2): p. 357-368.
34. O'Connor, W.N. and S. and Valle, *A Combination Verhoeffs Elastic and Masson's Trichrome Stain for Routine Histology.* Stain Technology, 1982. **57**(4): p. 207-210.
35. van den Bogaerdt, A.J., et al., *The suitability of cells from different tissues for use in tissue-engineered skin substitutes.* Arch Dermatol Res, 2002. **294**(3): p. 135-42.
36. Akershoek, J.J., et al., *Cell therapy for full-thickness wounds: are fetal dermal cells a potential source?* Cell and Tissue Research, 2016. **364**(1): p. 83-94.
37. Oostendorp, C., et al., *Sustained Postnatal Skin Regeneration Upon Prenatal Application of Functionalized Collagen Scaffolds.* Tissue Engineering Part A, 2021. **27**(1-2): p. 10-25.
38. Daamen, W.F., et al., *Tissue response of defined collagen–elastin scaffolds in young and adult rats with special attention to calcification.* Biomaterials, 2005. **26**(1): p. 81-92.

39. Mitzmacher, M.G., et al., *Novel Recombinant Tropoelastin Implants Restore Skin Extracellular Matrix.* Journal of drugs in dermatology : JDD, 2020. **19**(12): p. 1166-1172.
40. Lescan, M., et al., *De Novo Synthesis of Elastin by Exogenous Delivery of Synthetic Modified mRNA into Skin and Elastin-Deficient Cells.* Molecular Therapy - Nucleic Acids, 2018. **11**: p. 475-484.
41. Qa'aty, N., et al., *The Antidiabetic Hormone Glucagon-Like Peptide-1 Induces Formation of New Elastic Fibers in Human Cardiac Fibroblasts After Cross-Activation of IGF-IR.* Endocrinology, 2015. **156**(1): p. 90-102.
42. Mithieux, S.M., et al., *Tropoelastin Implants That Accelerate Wound Repair.* Advanced Healthcare Materials, 2018. **7**(10): p. 1701206.
43. Xie, H., et al., *Treatment of Burn and Surgical Wounds With Recombinant Human Tropoelastin Produces New Elastin Fibers in Scars.* J Burn Care Res, 2017. **38**(5): p. e859-e867.
44. Halabi, C.M. and R.P. Mecham, *Chapter 12 - Elastin purification and solubilization*, in *Methods in Cell Biology*, R.P. Mecham, Editor. 2018, Academic Press. p. 207-222.
45. Partridge, S.M. and H.F. Davis, *The chemistry of connective tissues. 3. Composition of the soluble proteins derived from elastin.* Biochemical Journal, 1955. **61**(1): p. 21-30.
46. Leach, J.B., et al., *Crosslinked α-elastin biomaterials: towards a processable elastin mimetic scaffold.* Acta Biomaterialia, 2005. **1**(2): p. 155-164.
47. de Vries, H.J.C., et al., *Dermal regeneration in native non-cross-linked collagen sponges with different extracellular matrix molecules.* Wound Repair and Regeneration, 1994. **2**(1): p. 37-47.
48. Hornebeck, W., J.M. Tixier, and L. Robert, *Inducible adhesion of mesenchymal cells to elastic fibers: elastonectin.* Proceedings of the National Academy of Sciences, 1986. **83**(15): p. 5517-5520.
49. Robert, L., *The Saga of κ-Elastin or the Promotion of Elastin Degradation Products from "Garbage" to Receptor Agonists and Pharmacologically Active Principles.* Connective Tissue Research, 2010. **51**(1): p. 8-13.
50. Ménasche, M., et al., *Pharmacological studies on elastin peptides (kappa-elastin). Blood clearance, percutaneous penetration and tissue distribution.* Pathol Biol (Paris), 1981. **29**(9): p. 548-54.
51. Daamen, W.F., et al., *Preparation and evaluation of molecularly-defined collagen–elastin–glycosaminoglycan scaffolds for tissue engineering.* Biomaterials, 2003. **24**(22): p. 4001-4009.
52. Masci, V.L., et al., *Ultrastructural investigation on fibroblast interaction with collagen scaffold.* Journal of Biomedical Materials Research Part A, 2016. **104**(1): p. 272-282.
53. Walraven, M., et al., *In vitro cultured fetal fibroblasts have myofibroblast-associated characteristics and produce a fibrotic-like environment upon stimulation with TGF-β1: Is there a thin line between fetal scarless healing and fibrosis?* Archives of Dermatological Research, 2017. **309**(2): p. 111-121.
54. Moulin, V., et al., *Fetal and adult human skin fibroblasts display intrinsic differences in contractile capacity.* Journal of Cellular Physiology, 2001. **188**(2): p. 211-222.
55. Kutluoğlu, G.C., et al., *Comparison of dermal and eschar fibroblasts in full skin equivalents.* Wound Repair and Regeneration, 2025. **33**(1): p. e70001.
56. Das, P., et al., *Polymeric biomaterials-based tissue engineering for wound healing: a systemic review.* Burns & Trauma, 2023. **11**.
57. Wu, X., et al., *Chronic wounds: pathological characteristics and their stem cell-based therapies.* Engineered Regeneration, 2023. **4**(1): p. 81-94.
58. Huelsboemer, L., et al., *Cellular therapeutics and immunotherapies in wound healing – on the pulse of time?* Military Medical Research, 2024. **11**(1): p. 23.
59. Zhang, M., et al., *Advances in 3D skin bioprinting for wound healing and disease modeling.* Regenerative Biomaterials, 2022. **10**.

60. Mahajan, N., S. Soker, and S.V. Murphy, *Regenerative Medicine Approaches for Skin Wound Healing: from Allografts to Engineered Skin Substitutes.* Current Transplantation Reports, 2024. **11**(4): p. 207-221.
61. Negut, I., G. Dorcioman, and V. Grumezescu *Scaffolds for Wound Healing Applications*. Polymers, 2020. **12**, DOI: 10.3390/polym12092010.
62. Daamen, W.F., et al., *Depots of solubilised elastin promote the formation of blood vessels and elastic fibres in rat.* Journal of Controlled Release, 2006. **116**(2): p. e84-e85.
63. Schenke-Layland, K., *Non-invasive multiphoton imaging of extracellular matrix structures.* Journal of Biophotonics, 2008. **1**(6): p. 451-462.
64. Gade, P.S., A.M. Robertson, and C.-Y. Chuang, *Multiphoton Imaging of Collagen, Elastin, and Calcification in Intact Soft-Tissue Samples.* Current Protocols in Cytometry, 2019. **87**(1): p. e51.
65. König, K., et al., *Multiphoton autofluorescence imaging of intratissue elastic fibers.* Biomaterials, 2005. **26**(5): p. 495-500.
66. Thorling, C.A., et al., *Multiphoton microscopy and fluorescence lifetime imaging provide a novel method in studying drug distribution and metabolism in the rat liver in vivo.* Journal of biomedical optics, 2011. **16**(8): p. 086013-086013.
67. Jones, J.D., et al., *In vivo multiphoton microscopy detects longitudinal metabolic changes associated with delayed skin wound healing.* Communications Biology, 2018. **1**(1): p. 198.
68. Krymchenko, R., et al., *Elastogenesis in Focus: Navigating Elastic Fibers Synthesis for Advanced Dermal Biomaterial Formulation.* Advanced Healthcare Materials, 2024. **13**(27): p. 2400484.
69. Halm, M., et al., *Visualizing tropoelastin in a long-term human elastic fibre cell culture model.* Scientific Reports, 2016. **6**(1): p. 20378.
70. Sullivan, T.P., et al., *THE PIG AS A MODEL FOR HUMAN WOUND HEALING.* Wound Repair and Regeneration, 2001. **9**(2): p. 66-76.
71. Meyerholz, D.K., et al., *Swine models in translational research and medicine.* Veterinary Pathology, 2024. **61**(4): p. 512-523.
72. Nair, M., et al., *Tunable bioactivity and mechanics of collagen-based tissue engineering constructs: A comparison of EDC-NHS, genipin and TG2 crosslinkers.* Biomaterials, 2020. **254**: p. 120109.
73. Sapuła, P., K. Bialik-Wąs, and K. Malarz, *Are Natural Compounds a Promising Alternative to Synthetic Cross-Linking Agents in the Preparation of Hydrogels?* Pharmaceutics, 2023. **15**(1): p. 253.

Supporting Information

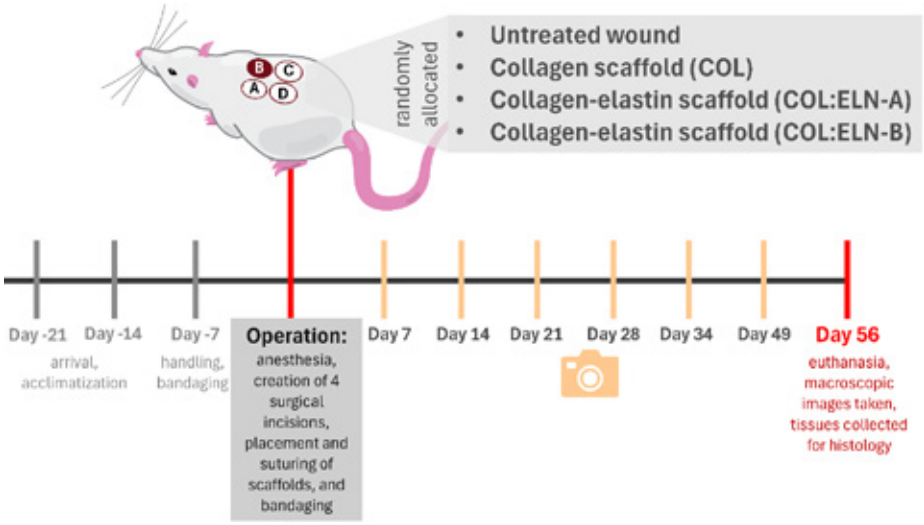

Figure S1. Two to three weeks prior to surgery, the rats were delivered to the animal facility and acclimatized. One week after arrival, handling and training were initiated to prepare the animals for the procedures. On the day of surgery, the animals were anesthetized, and four full-thickness wounds were created on the dorsal region (A, B, C, D). Three different scaffolds (COL, COL:ELN-A and COL:ELN-B) were sutured into the wounds in a randomized order. Untreated wounds (without any biomaterial) and wounds treated with COL served as internal controls. The wounds were then covered with dressings and bandages, which were replaced when needed (1-3 times per week). Digital photographs of the wounds were taken at multiple timepoints over a 7-week period to monitor wound healing progression. On day 56, the animals were euthanized, final digital photographs were taken, and skin tissue samples were collected for further analysis.

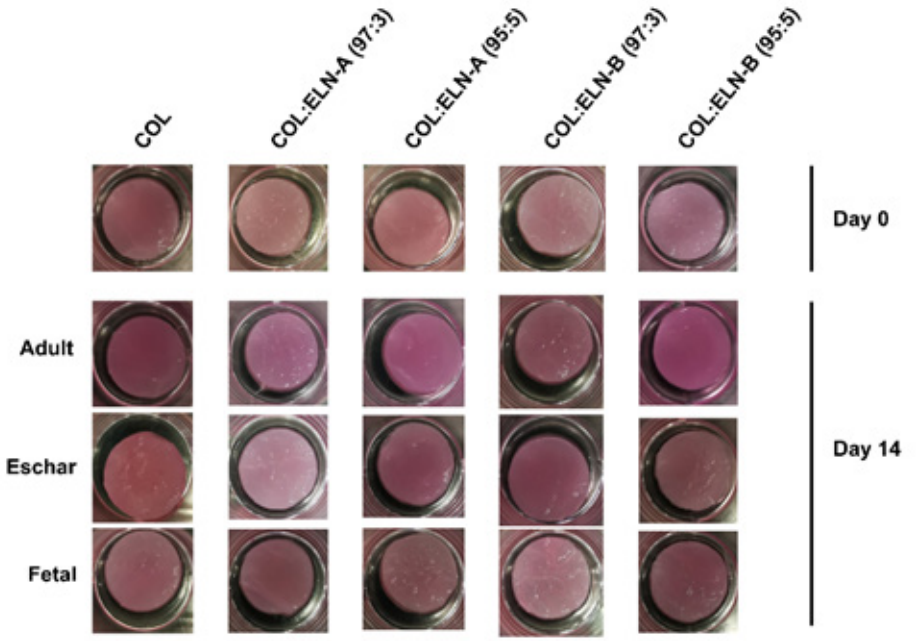

Figure S2. Visual appearance of the scaffolds remained the same before seeding the fibroblasts (day 0) and at the end of the cell culture experiment (day 14). COL = type I collagen scaffold, COL:ELN-A = type I collagen scaffold supplemented with ELN-A, COL:ELN-B = type I collagen scaffold supplemented with ELN-B.

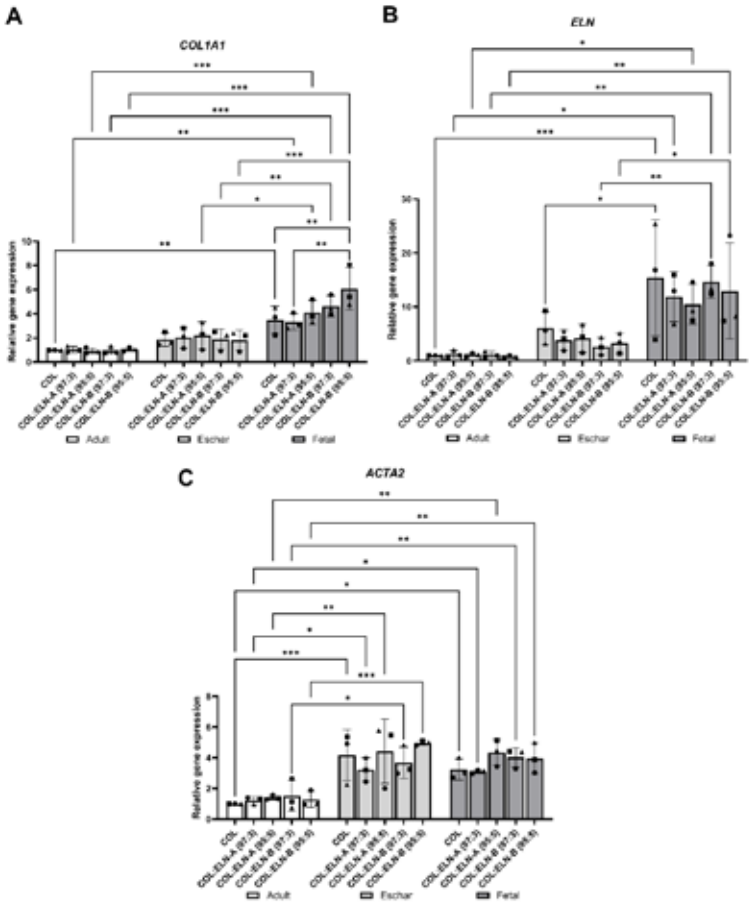

Figure S3. Comparative gene expression levels of A) *COL1A1*, B) *ELN*, and C) *ACTA2* across three fibroblast types, normalized to the mean expression of adult fibroblasts cultured on COL scaffolds (day 14, n=3). Individual donors are represented by different symbols as ● donor 1/4/7, ■ donor 2/5/8, and ▲ donor 3/6/9. Differences in gene expression levels between scaffold types and fibroblast types were tested using two-way ANOVA, followed by Tukey's multiple comparisons test (α = 0.05). Error bars represent standard deviation; * p<0.05, ** p<0.01, *** p<0.001. COL = type I collagen scaffold, COL:ELN-A = type I collagen scaffold supplemented with ELN-A, COL:ELN-B = type I collagen scaffold supplemented with ELN-B, COL1A1 = alpha-1 type I collagen, ELN = elastin, ACTA2 = smooth muscle actin alpha 2.

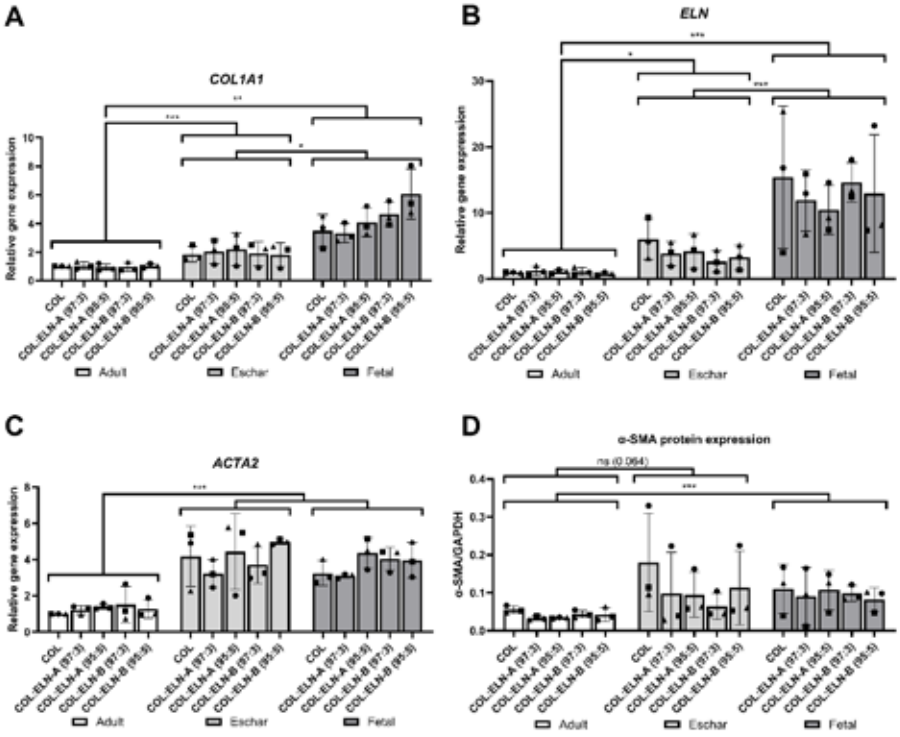

Figure S4. Comparative gene expression levels of A) *COL1A1*, B) *ELN*, and C) *ACTA2* across three fibroblast types, normalized to the mean expression of adult fibroblasts cultured on COL scaffolds (day 14, n=3). D) Quantified expression of the α-SMA/GAPDH ratio based on intensities of the bands on Western blot (day 14, n=3). Individual donors are represented by different symbols as ● donor 1/4/7, ■ donor 2/5/8, and ▲ donor 3/6/9. Differences in gene expression levels between fibroblast groups were tested using Brown-Forsythe and Welch ANOVA, followed by Dunnett's T3 multiple comparisons test (α = 0.05). Error bars represent standard deviation; * $p<0.05$, ** $p<0.01$, *** $p<0.001$. COL = type I collagen scaffold, COL:ELN-A = type I collagen scaffold supplemented with ELN-A, COL:ELN-B = type I collagen scaffold supplemented with ELN-B, COL1A1 = alpha-1 type I collagen, ELN = elastin, ACTA2 = smooth muscle actin alpha 2, α-SMA = α-smooth muscle actin.

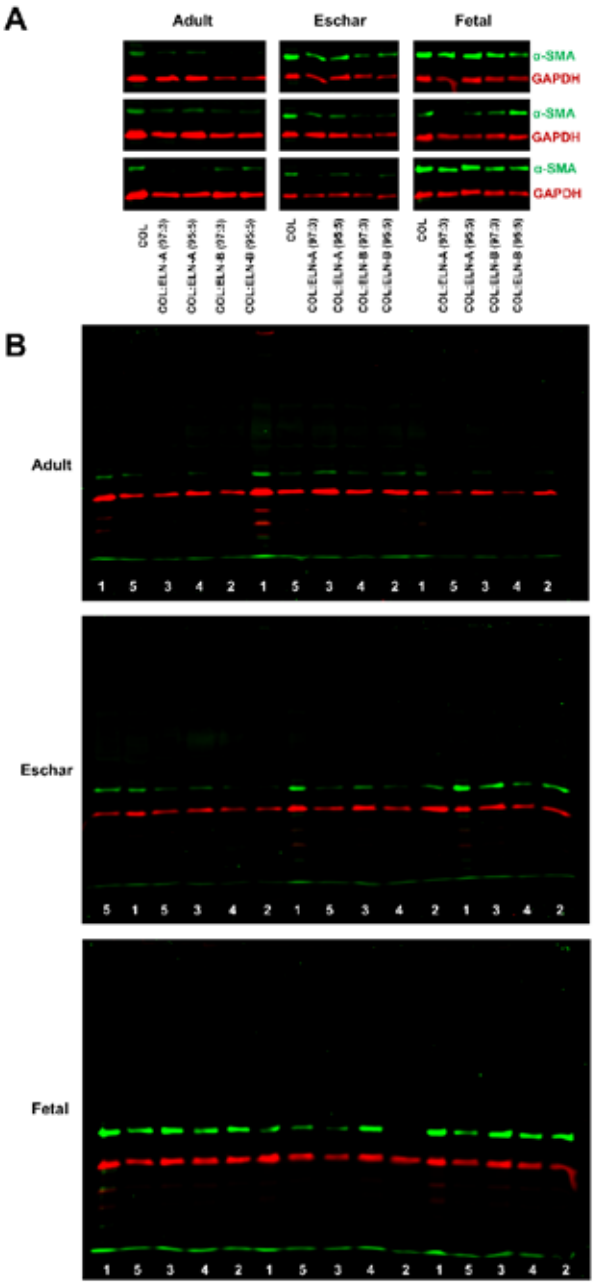

Figure S5. A) Cropped and B) uncropped Western blots stained for α-SMA (green, 42 kDa) at day 14. GAPDH expression was used as an internal control (red, 37 kDa). COL = type I collagen scaffold (**1**), COL:ELN-A = type I collagen scaffold supplemented with ELN-A (97:3 – **2**; 95:5 – **3**), COL:ELN-B = type I collagen scaffold supplemented with ELN-B (97:3 – **4**, 95:5 – **5**).

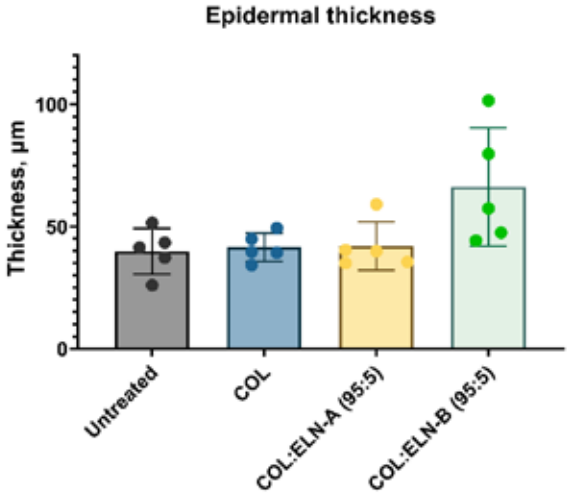

Figure S6. Epidermal thickness within four treatment groups. Error bars represent standard deviation.

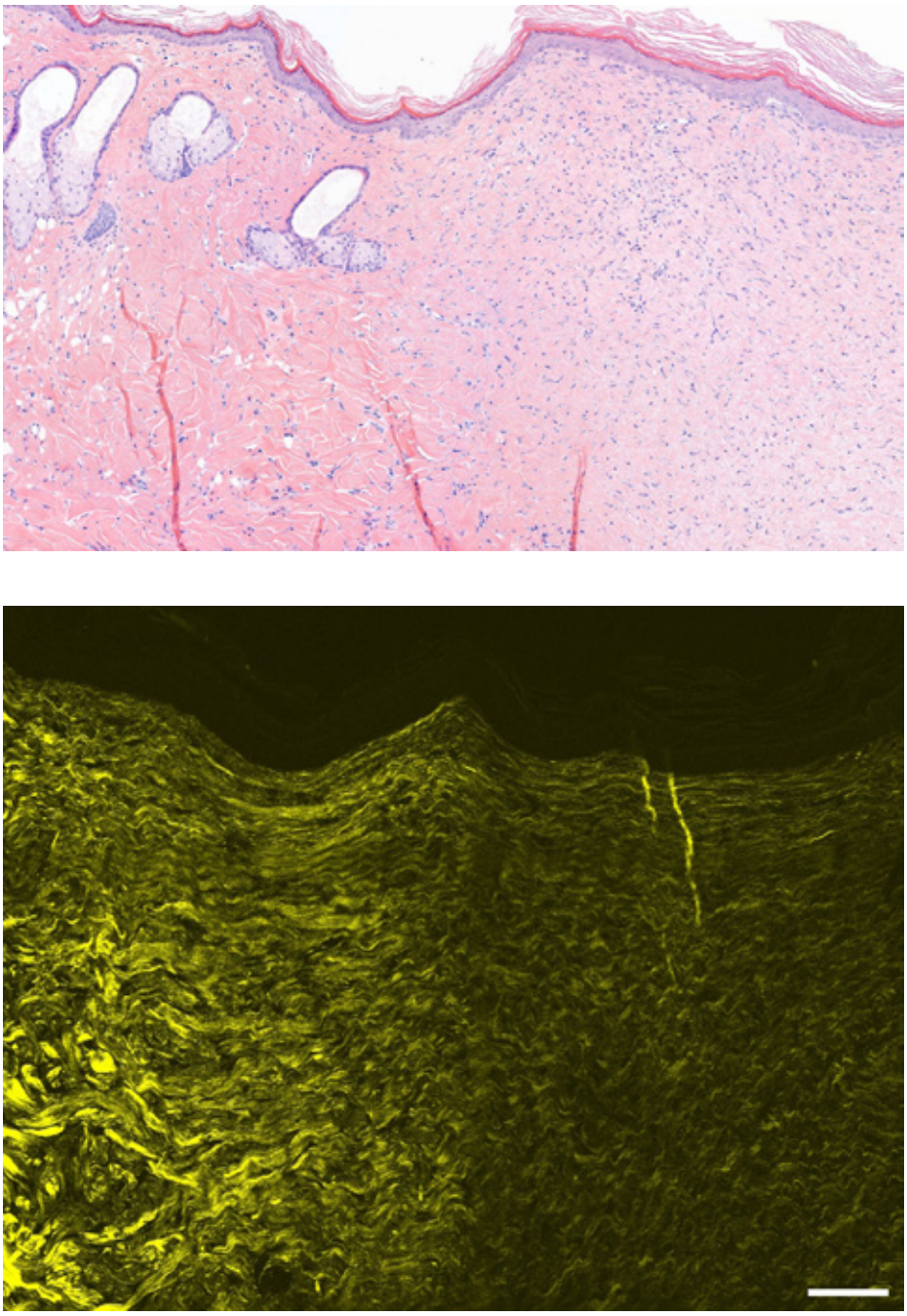

Figure S7. Representative H&E (top) and SHG (bottom) images of thick and long collagen fibers in the healthy skin region (white arrow) and thinner and shorter collagen fibers in the wound bed (grey arrow). Scale bars are 100 μm. H&E = hematoxylin and eosin, SHG = second harmonic generation.

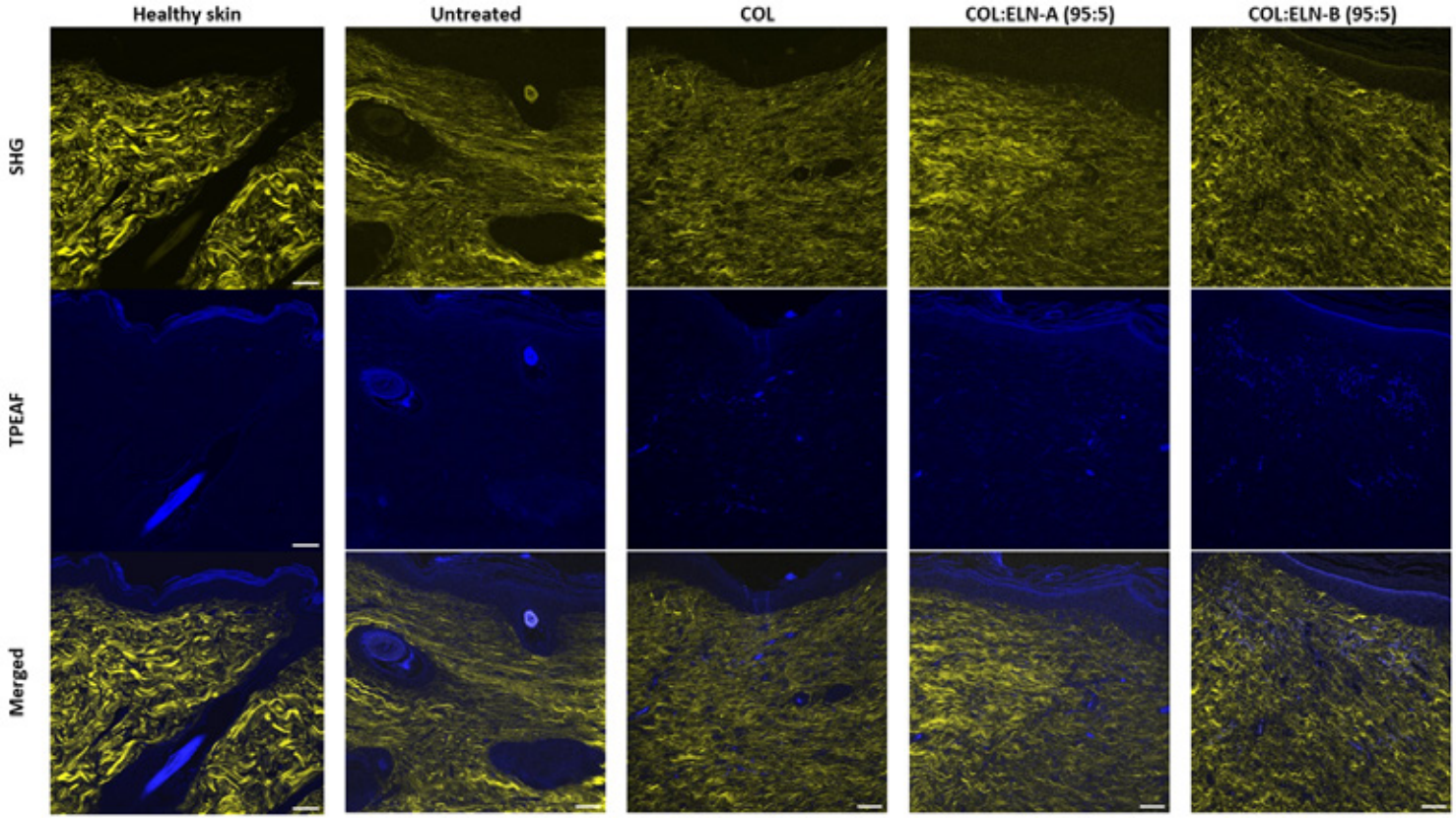

Figure S8. Multiphoton microscopy images, showing collagen fibers with second harmonic generation (SHG) in yellow and two-photon excited autofluorescence (TFEAF) in blue. Scale bar is 50 µm. COL = type I collagen scaffold, COL:ELN-A = type I collagen scaffold supplemented with ELN-A, COL:ELN-B = type I collagen scaffold supplemented with ELN-B.

Table S1. RT-qPCR primer sequences.

Gene	Description	Forward sequence 5'3'	Reverse sequence 5'3'
ACTA2	smooth muscle actin alpha 2	CCGACCGAATGCAGAAGGA	ACAGAGTATTTGCGCTCCGAA
COL1A1	alpha-1 type I collagen	GAGAGCATGACCGATGGATT	CGCTGTTCTTGCAGTGGTAG
ELN	elastin	GGTTGTGTCACCAGAAGCAGCT	CCGTAAGTAGGAATGCCTCCAAC
YWHAZ	zeta polypeptide tyrosine 3-monooxygenase/tryptophan 5-monooxygenase activation protein	CATCTTGGAGGGTCGTCTCA	ACTTTGCTCTCTGCTTGTGAA
GAPDH	glyceraldehyde 3-phosphate dehydrogenase	TGGGTGTGAACCATGAGAAG	TGGGTGTGAACCATGAGAAG

Table S2. Total RNA ng/µl in fibroblasts seeded on scaffolds after 14 days of culturing.

Fibroblasts	COL	COL:ELN-A (97:3)	COL:ELN-A (95:5)	COL:ELN-B (97:3)	COL:ELN-B (95:5)
Adult	110.5 ± 16.5	94.1 ± 33.2	70.3 ± 27.0	87.7 ± 34.0	107.9 ± 35.5
Eschar	85.1 ± 25.1	123.2 ± 61.2	106.0 ± 40.2	142.5 ± 49.2	136.3 ± 52.3
Fetal	210.3 ± 48.0	250.2 ± 54.8	236.1 ± 37.5	219.7 ± 44.4	247.3 ± 48.7

N=3, mean ± SD.

Table S3. The scaffold size (in cm^2) was measured from digital photos of the scaffolds using ImageJ/Fiji.

Fibroblasts	Timepoint	COL	COL:ELN-A (97:3)	COL:ELN-A (95:5)	COL:ELN-B (97:3)	COL:ELN-B (95:5)
Adult	**Day 0**	1.16 ± 0.03	1.14 ± 0.03	1.14 ± 0.05	1.10 ± 0.04	1.20 ± 0.06
	Day 3	1.18 ± 0.02	1.12 ± 0.00	1.15 ± 0.02	1.14 ± 0.03	1.21 ± 0.04
	Day 7	1.16 ± 0.04	1.17 ± 0.02	1.17 ± 0.03	1.15 ± 0.04	1.21 ± 0.05
	Day 11	1.20 ± 0.04	1.14 ± 0.02	1.19 ± 0.04	1.14 ± 0.03	1.24 ± 0.06
	Day 14	1.16 ± 0.03	1.13 ± 0.01	1.14 ± 0.03	1.13 ± 0.03	1.19 ± 0.05
Eschar	**Day 0**	1.15 ± 0.10	1.16 ± 0.08	1.16 ± 0.09	1.17 ± 0.07	1.17 ± 0.06
	Day 3	1.20 ± 0.05	1.18 ± 0.05	1.22 ± 0.01	1.16 ± 0.00	1.18 ± 0.03
	Day 7	1.22 ± 0.03	1.18 ± 0.05	1.16 ± 0.06	1.17 ± 0.05	1.19 ± 0.06
	Day 11	1.17 ± 0.02	1.18 ± 0.01	1.14 ± 0.02	1.16 ± 0.03	1.18 ± 0.04
	Day 14	1.16 ± 0.02	1.16 ± 0.05	1.18 ± 0.02	1.15 ± 0.01	1.17 ± 0.05
Fetal	**Day 0**	1.18 ± 0.03	1.18 ± 0.02	1.23 ± 0.06	1.18 ± 0.03	1.20 ± 0.03
	Day 3	1.17 ± 0.04	1.19 ± 0.03	1.22 ± 0.06	1.16 ± 0.01	1.16 ± 0.01
	Day 7	1.14 ± 0.01	1.18 ± 0.04	1.17 ± 0.01	1.14 ± 0.03	1.20 ± 0.06
	Day 11	1.17 ± 0.01	1.17 ± 0.03	1.19 ± 0.03	1.16 ± 0.02	1.20 ± 0.04
	Day 14	1.19 ± 0.04	1.19 ± 0.05	1.17 ± 0.02	1.15 ± 0.03	1.19 ± 0.07

N=3, mean ± SD.

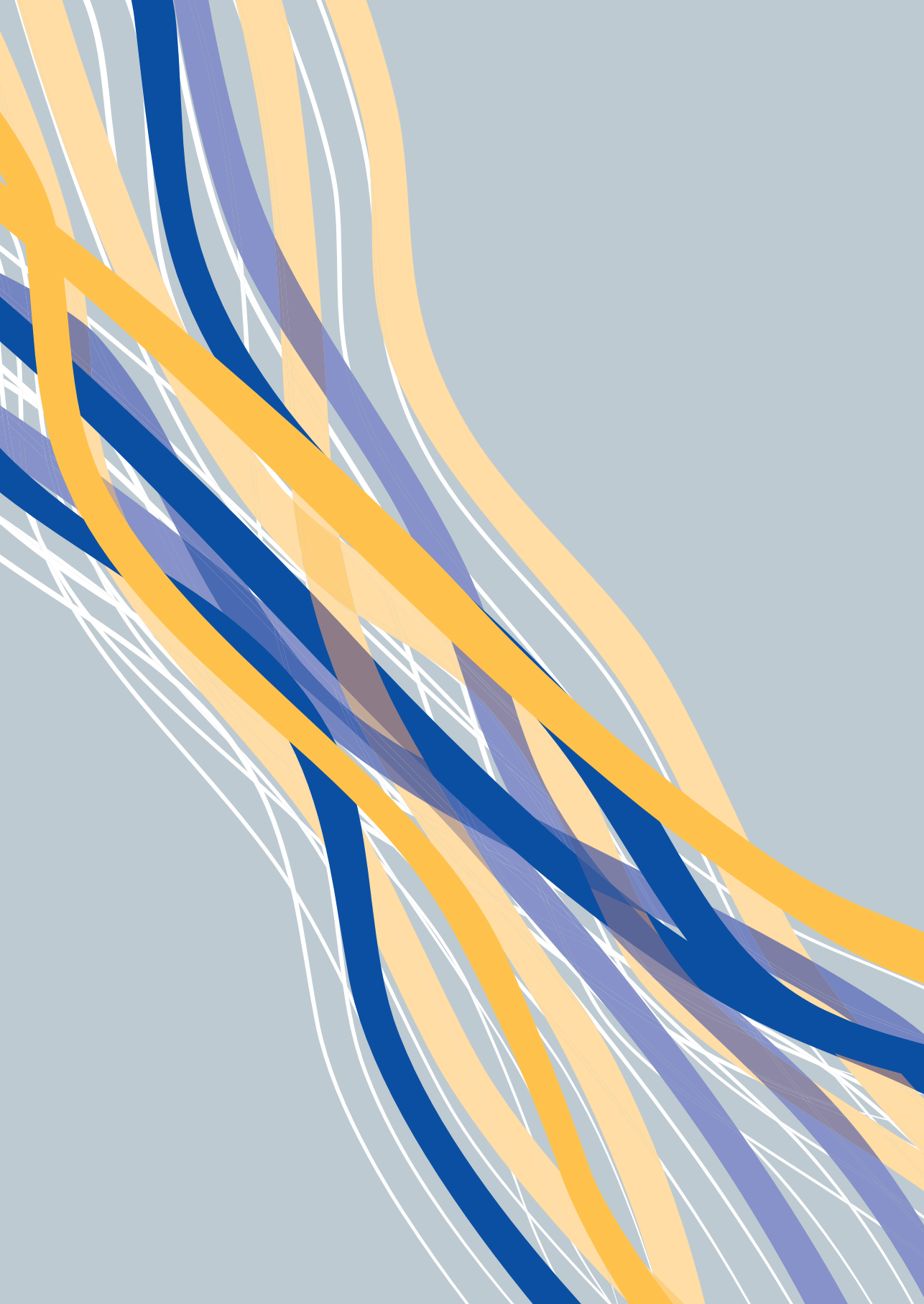

Chapter 4

Optimization of elastin proportion and crosslinking for the large-scale production of collagen-elastin scaffolds as skin substitutes

Roman Krymchenko[1], Gizem Coşar Kutluoğlu[1,2], Dominique Manikowski[2], Claudia Doberenz[2], Bouke K. H. L. Boekema[3,4,5,6], Toin H. van Kuppevelt[1], Willeke F. Daamen[1]

[1] Radboud university medical center, Research Institute for Medical Innovation, Department of Medical BioSciences, Nijmegen, The Netherlands

[2] Innovation, Development and Regulatory Affairs, MedSkin Solutions Dr. Suwelack, Billerbeck, Germany

[3] Alliance of Dutch Burn Care, Burn Research Lab, Beverwijk, The Netherlands

[4] Amsterdam University Medical Center (AUMC), Amsterdam, The Netherlands

[5] Tissue Function and Regeneration, Amsterdam Movement Sciences Research Institute, Amsterdam, The Netherlands

[6] Department of Plastic, Reconstructive and Hand Surgery, AUMC, location VUmc, Amsterdam, The Netherlands

Submitted for publication

Abstract

Despite advancements in clinical practice, the creation of an ideal skin substitute remains a significant challenge. An effective dermal substitute must closely replicate both the structure and function of natural skin while facilitating rapid wound healing. Biomaterials such as collagen and elastin, essential components of the extracellular matrix, are known for their biocompatibility and degradability. Our research aims to investigate the structural, chemical, mechanical, and biological characteristics of composite collagen-elastin scaffolds as dermal templates, with a focus on elastin concentration, lyophilization techniques, crosslinking strategies, and the production of large-sized scaffolds for potential industrial-scale applications. Twelve different scaffold compositions were developed using three ratios of insoluble collagen fibrils and solubilized elastin (95:5, 90:10, and 80:20, w/w), two lyophilization approaches (at room temperature and with dehydrothermal (DHT) treatment) and with and without additional chemical crosslinking. Our findings indicate that increasing elastin content led to larger pore sizes in line with compromised tensile strength, bursting strength, and water absorption. Chemical crosslinking significantly improved mechanical properties and enzymatic resistance, while DHT treatment accelerated drying without seriously affecting physicochemical properties. Among the tested formulations, scaffolds that contained the lowest applied amount of elastin, and underwent DHT treatment followed by consecutive crosslinking, emerged as the most durable and resilient skin substitutes. The selected scaffold demonstrated favorable mechanical stability and structural integrity and reduced enzymatic susceptibility. Further studies are necessary to assess their effectiveness in regenerative medicine and potential in clinical applications.

1. Introduction

Extensive skin wounds remain a challenging yet crucial issue to address [1]. Skin grafting is the traditional and most straightforward method for treating patients with severe dermal wounds caused by burns, trauma, injuries or non-healing wounds [2]. However, patients who undergo skin grafting can experience movement limitations, slow healing processes, hematomas, fragile skin regions during the initial weeks of transplantation, infections by microorganisms, loss of sensation, visible scars or unesthetic appearance [3, 4]. Besides the abovementioned complications, the source material itself can pose additional problems, such as recurrent failure of graft take or limited availability of donor skin tissue. This is why there is a continuous search for advanced grafting approaches (e.g. micrografting [5], fractional grafting [6], bioprinting [7], spraying of autologous cells [8]) and the utilization of various types of biological or synthetic skin substitutes, which are expected to deliver more effective solutions for both patients and surgeons [9].

Collagen, for instance, is the most abundant protein in the human body and represents one example of most commonly used natural biomaterials [10]. Collagen and elastin compose the vast majority of extracellular matrix (ECM) proteins that provide tensile strength and elasticity to skin, comprising up to 90% and 8% of ECM, respectively [11, 12]. Animal-derived collagen is a widely used biomaterial for numerous applications, including wound healing [13]. Advantages of type I collagen in biomaterials are linked but not limited to its low cost, high abundance, good biocompatibility, quick biodegradability and low immunogenicity [14]. Its dermal applications are characterized by stimulating fibroblast proliferation and migration, constraining matrix metalloproteinases, assisting angiogenesis and re-epithelization, maintaining a supportive microenvironment and providing structural assistance for wound healing [15-17]. Depending on the required properties, collagen biomaterials can be created in versatile forms, such as porous sponges, hydrogels, and thin films/membranes [16].

Elastin protein serves as the key component of elastic fibers, enabling the skin's reversible extensibility and supporting its resistance to repetitive mechanical stress [18]. Biological effects of elastin include its ability to be sensed by skin and immune cells [19], reduce amount of myofibroblasts [20], and to effectively promote the creation of new elastic fibers [21] and blood vessels [22]. The main difficulty is that elastic fiber network, in contrast to collagen fibers, cannot be timely and functionally restored upon damage [23]. In biomaterials formulation, elastin-derived peptides [22], synthetic elastin polymers [24], and tropoelastin

protein [25] have found practical applications, whereas other forms (insoluble fibers [22], tropoelastin mRNA [26]) have encountered various issues and complications, e.g. calcification [22] and limited stability [27]. There are four major approaches for creating collagen-elastin biomaterials: casting, electrospinning, bioprinting and decellularization of animal tissue [28]. Casting is an extensively used technique to obtain such biomaterials and involves preparation of protein suspension, pouring it into a mold of the needed form and subsequent solvent removal through the means of freeze-drying, heating, crosslinking or neutralization. MatriDerm is a commercial authorized collagen and elastin based skin substitute that is created with a casting approach [29]. When needed, crosslinking with particular agents (e.g., glutaraldehyde [30], EDC/NHS [22], genipin [31]) can be used as a second step in biomaterial production in order to change their chemical, biological and mechanical characteristics.

This study explores the potential for further improvement of composite collagen-elastin scaffolds as skin substitutes. The research emphasizes the mechanical and physicochemical properties of cast composite collagen-elastin scaffolds, including the fabrication of large scaffolds for potential bulk production. Key aspects include evaluating the impact of elastin supplementation, comparing two lyophilization methods, and analyzing subsequent crosslinking techniques. Furthermore, the cytotoxicity and viability of human skin cells were assessed to determine the scaffolds' suitability for further preclinical and clinical translation.

2. Materials and methods

Unless specified otherwise, all chemicals were purchased from Merck Chemicals/ Sigma-Aldrich.

2.1. Production of collagen-elastin scaffolds

Bovine collagen and soluble elastin were kindly provided by MedSkin Solutions Dr. Suwelack AG. Twelve different scaffold conditions were tested, varying in composition, lyophilization method, and crosslinking strategy. The scaffolds were prepared with three different collagen-elastin ratios: 95:5, 90:10, and 80:20 (w/w), corresponding to 5%, 10%, and 20% elastin (ELN), respectively. Two lyophilization approaches were used: at room temperature (non-crosslinked, **NC**) and with dehydrothermal (**DHT**) treatment at 100 °C. Additionally, scaffolds were tested with and without further chemical crosslinking, resulting in four final crosslinking conditions: non-crosslinked (NC), DHT-treated (DHT), chemically crosslinked (**CC**),

and DHT-treated with chemical crosslinking (**DHT+CC**). Prior usage, soluble elastin was acidified using HCl acid to pH 3.5. The scaffolds were prepared and crosslinked with 33 mM 1-ethyl-3-(3-dimethyl aminopropyl)carbodiimide (EDC) and 6 mM N-hydroxysuccinimide (NHS) in 50 mM 2-morpholinoethane sulfonic acid (pH 5.0) containing 40% ethanol according to an existing protocol [22]. The scaffolds were produced in a single large-scale batch, generating multiple layers with a total surface area of 0.25–0.75 m^2 for each condition. Experimental testing was conducted with a sample size of $n \geq 3$ from the single batch production. Of note, the chemical crosslinking of NC-10% ELN was inadvertently performed using a different method than the other scaffolds. While the other scaffolds were crosslinked individually by dipping each sample separately, all layers of NC-10% ELN were simultaneously submerged in the crosslinking solution. This procedural variation may account for the distinct final thickness observed in CC-10% ELN.

2.2. Analysis of collagen-elastin scaffolds

2.2.1. Structural and Morphological Characteristics

Scanning electron microscopy and pore size calculation

The scaffolds were securely mounted on carbon conductive tape attached to metallic stubs and coated with an ultrathin layer of gold using a sputter coating system (Edwards, Crawley, UK) and examined using a Zeiss Sigma 300 field emission scanning electron microscope (SEM; Carl Zeiss Microscopy Ltd., Cambridge, UK) at an operating voltage of 3 kV.

Longitudinal sections of 150 times magnified images were used to estimate pore size upon processing through ImageJ (version 1.54d; USA) and Adobe Illustrator (version 28.1). The steps included manual adjustment of brightness and contrast, image tracing (the only step performed in Illustrator), threshold determination, binary image processing (opening and watershed) and automatic pore detection and calculation (see Figure S1). Per condition, at least 650 pores were counted and plotted.

Immunostaining for elastin

Scaffolds were embedded in Tissue-Tek O.C.T. compound (Sakure Finetek Europe B.V., Alphen aan den Rijn, The Netherlands), immediately frozen on dry ice and stored at -80°C until sectioning. 7 µm sections were cut using a Microm HM 550 VP (Thermo Scientific, Germany) at -20°C and air dried overnight at room temperature. Samples were blocked for 30 min with 0.5% bovine serum albumin (BSA) in phosphate-buffered saline (PBS, pH 7.4). Staining of elastin peptides was performed

with mouse monoclonal anti-bovine elastin antibody for 1 h (1:200; E4013). Samples were washed with PBS and incubated with biotinylated goat anti-mouse IgG (1:200; Vector Laboratories, BA-9200-1.5) for 1 h at room temperature in 0.5% BSA-PBS and washed with PBS. The VECTASTAIN Elite ABC Kit (Vector Laboratories, USA) was used according to manufacturer's instructions. Elastin was visualized in red with ImmPACT AEC (3-amino-9-ethylcarbazole) HRP substrate kit (Vector Laboratories, USA) and mounted with VectaMount AQ aqueous mounting medium (Vector Laboratories, USA). Sections were imaged with a whole-slide scanner (3DHISTECH, Budapest, Hungary) and accompanying CaseViewer 2.4 software.

2.2.2. Chemical Characteristics

pH

The effect of scaffolds on altering the pH of water was analyzed. 0.1 g of scaffold was incubated in 50 ml of demineralized water and shaken for 30 min. After the incubation, the pH of the solution was tested using a pH meter (WTW, Germany).

Residual moisture content

A gravimetric method (loss on drying) was used to assess the content of residual moisture in lyophilized scaffolds. Approximately 1-2 g of sample were weighed (m_0), placed in a glass dish and dried at 90 ± 2 °C in a vacuum drying cabinet (Memmert GmbH, Germany) for at least 16 h. When the drying process was completed by showing constant weight, the resulting weight (m_1) was recorded again. The residual moisture was calculated using the following formula:

$$Residual\ moisture\ (\%) = \frac{m_0 - m_1}{m_0} \times 100\%$$

Inorganic impurities

Assessment of the amount of non-volatilized residues after flameless combustion of the scaffolds was utilized to estimate inorganic impurities. 1-2 g of each scaffold were weighed (m_0), placed in a porcelain ignition dish and burned with a Bunsen burner. To finalize the burning process, the samples were placed in a high temperature oven (Nabertherm GmbH, Germany) for at least 4 h at 600 ± 50 °C. When the samples were completely combusted, the weight of ash (m_1) was measured. Inorganic impurities were determined subtracting residual moisture according to the equation:

$$Inorganic\ impurities\ (\%) = \frac{m_1}{m_0 \times (100 - Residual\ moisture)/100} \times 100\%$$

Degree of crosslinking

To estimate the degree of crosslinking, 2,4,6-trinitrobenzene sulfonic acid (TNBS) was used as a reagent for the determination of free amine groups present in scaffolds. Briefly, 1.0 mg of non-crosslinked/DHT treated and 2.5 mg of chemically crosslinked or DHT treated and chemically crosslinked samples were soaked in 4% $NaHCO_3$ solution for 30 min. Glycine solutions in 4% $NaHCO_3$ (0-80 µg/ml) were used to construct a calibration curve. 0.08% (w/v) TNBS was added, followed by incubation at 40°C for 2 h. Then, 6 M HCl was added and the samples were incubated at 60°C until all the biomaterials became dissolved. Aliquots of 100 µl were taken and absorbance was measured at 420 nm at SpectraMax iD3 plate reader (Molecular Devices GmbH, Austria). The degree of crosslinking was calculated using the following formula, where N_0 – amount of free amine groups in non-crosslinked scaffold and N1 - amount of free amine groups in a corresponding crosslinked scaffold:

$$Degree\ of\ crosslinking\ (\%) = \frac{N_0 - N_1}{N_0} \times 100\%$$

Fourier-transform infrared spectroscopy

To obtain information about chemical bonds and functional groups within the material, Fourier-transform infrared (FTIR) spectra were recorded using a spectrometer (Perkin Elmer, USA) in the mid-infrared range (4000-650 cm^{-1}) at 21°C. Spectra were plotted using Spectragryph (version 1.2.16.1, 2022) following baseline correction and peak normalization.

2.2.3. Mechanical Characteristics

Wetting dynamics and mechanical manipulation

Scaffolds of approximately 80 × 80 mm were placed in isotonic saline (0.9%) and the visual wetting time was measured using a stopwatch. When a scaffold was wetted, some basic manipulations (flipping, stretching, flattening) were performed to imitate the handling of skin substitutes by a surgeon and evaluate the handleability of such a material as a dermal substitute.

Ultimate tensile strength and Young's modulus

Uniaxial tensile strength tests were performed to determine the maximum mechanical tensile force that a material can withstand. For each run, a bone-shaped specimen (110 × 25 mm) was fixed in Shimadzu EZ-LX testing machine (Shimadzu, Japan), wetted by spraying demineralized water and extended at 50 mm/min in the opposite direction until breakage. The tensile strength was calculated as the

maximum tensile force (F) divided by specimen cross-sectional area (S) in N/mm^2. Young's modulus (modulus of elasticity) was measured at the initial part of the stress/strain curve in N/mm^2.

Bursting strength

The ball burst test was performed to assess the stability of the materials. The sample was clamped in the center between two plates with circular apertures of the device (Zwick/Roell, Germany), wetted by spraying demineralized water and a ball pistol with a diameter of 25.4 mm penetrated the center of the sample. The minimum size of the material was 50 × 50 mm. The burst strength represents the maximum force that can be applied to the material without breaking it in N/mm.

Water absorption

Approximately 1-2 g of the scaffolds were used to determine absorbency of the materials. After measuring the initial weight (m_0), the sample was placed in a metallic wire basket and soaked in isotonic (0.9%) saline for 5 min. Afterwards, the basket was taken out, the excessive liquid was drained for 30 s and the wetted sample was weighed (m_1). The water-holding capacity was calculated as following:

$$Absorbency\ (g/g) = \frac{m_1 - m_0}{m_0}$$

2.2.4. Biological Characteristics

Biodegradation

Round scaffolds of 12 mm diameter were weighed and soaked in 1 ml of 0.25 U/ml collagenase A from *Clostridium histolyticum* (Roche) at 37°C. At various time points, collagenase solution was removed, 0.25 M EDTA (pH 8.0) was added to neutralize the enzyme, followed by washing with demineralized water, freezing and lyophilization. Scaffolds that were not treated with chemical crosslinking reagent were analyzed after 30, 60 and 90 min of incubation. Chemically crosslinked scaffolds were assessed at day 2, 7 and 14.

Cytotoxicity

The cytotoxicity test was performed to examine the *in vitro* cytotoxic effect of collagen-elastin scaffolds on human keratinocyte (HaCaT; Cell Line Service, 300493) and fibroblast (HFF-1; ATCC, SCRC-1041) cell lines. The performed steps were based on ISO 10993. A biomaterial sample (12 mm in diameter and around 1 mm thickness) was submerged in 1 ml Dulbecco's Modified Eagle Medium (DMEM) (Thermo Scientific, USA) supplemented with 10% fetal bovine serum

(FBS; PAN Biotech GmbH, Germany) and 1% penicillin-streptomycin (100 u/ml and 100 µg/ml respectively; VWR International LLC, USA) for 72 h. Low and high density polyethylene sheets samples (2×3 cm) in 2 ml medium were used as negative controls, while natural rubber latex (2×3 cm) in 2 ml medium served as a positive control. Cells were seeded in 48-well plates (HaCaT - 2×10^5 cells/cm^2; HFF-1 - 1×10^4 cells/cm^2) and extraction media (obtained after 72 h of scaffold incubation) were added undiluted to the cells for 24 h. The effect was examined using the microscope (general morphology, vacuolization, detachment, cell lysis and membrane integrity) and quantified using alamarBlue™ Cell Viability Reagent (Invitrogen, USA). Fluorescence intensity was measured at the 540 nm excitation and 590 nm emission wavelengths at a SpectraMax iD3 plate reader (Molecular Devices GmbH, Austria).

Cell viability

Primary fibroblasts were isolated from human tissues. Healthy skin samples obtained from adult patients who underwent elective surgery at the Departments of Plastic and Reconstructive Surgery of the Red Cross Hospital. Consent for the use of anonymized residual tissue was received through the informed opt-out protocol in accordance with the national guidelines (https://www.coreon.org/ accessed on 23 November 2020) and approved by the institutional privacy officers. Viability of the cells was tested when seeded on top of collagen-elastin scaffolds. 3×10^5 primary dermal fibroblasts from 3 donors were seeded separately on pre-wetted scaffolds in cell culture medium. As a control, 3×10^5 cells were also seeded in an empty well of 6-well plate. To ensure cell attachment to the scaffolds and prevent migration to the plastic surface, the concentrated cell suspension (80-100 µl) was placed on top of the scaffold for 2–3 h. Afterward, the wells were filled with sufficient cell culture medium to fully submerge the biomaterials. After 24 h, 72 h and 168 h of incubation at 37°C and 5% CO_2, the viability was assessed with alamarBlue™ Cell Viability Reagent as described above.

Statistical Analysis

All data visualization and statistical analysis were performed in GraphPad Prism version 10.4.1 (GraphPad Software, Boston, Massachusetts USA, www.graphpad.com). Error bars represent standard deviation. NC-5% ELN was used as a control. A p-value of <0.05 (95% confidence interval) was considered statistically significant. Pore size distribution was visualized using violin plots, which display the distribution of values, density, median (dashed line), and quartiles (dotted lines). Statistical analysis for pore size was performed using the Kruskal-Wallis test, followed by Dunn's multiple comparison test to assess differences between groups.

For elasticity, tensile and bursting strength, unpaired t-test with Welch's correction was used to detect significance. In all other measurements, Brown-Forsythe and Welch ANOVA with Dunnett's T3 multiple comparisons test was utilized. For biodegradation, statistical analysis was performed for the values at 1.5 h for NC and DHT scaffolds with NC-5% ELN as a control, and at 14 days for CC and DHT+CC scaffolds with CC-5% ELN as a control. For viability assay, two-way ANOVA with Tukey's multiple comparisons test was applied and statistical significance of the values on day 7 was shown with NC-5% ELN as a control.

3. Results

3.1. Structural and Morphological Characteristics

All collagen-elastin scaffolds were obtained in the form of soft, porous sheets with white or slightly yellow appearance and approximately 1-2 mm thickness (Figure 1A and Table 1). The higher the percentage of added soluble elastin, the stronger the intensity of yellow shades in NC and DHT biomaterials. Chemical crosslinking resulted in shrinkage of the sheets by 18.3 ± 3.5% in x-y directions (Figure 1B) and disappearance of yellowness.

Table 1. Thickness of the investigated scaffolds (n=3, mean ± SD).

Scaffolds	5% ELN	10% ELN	20% ELN
NC	1.6 ± 0.4 mm	1.6 ± 0.4 mm	1.8 ± 0.2 mm
DHT	1.3 ± 0.2 mm	1.9 ± 0.3 mm	1.3 ± 0.3 mm
CC	1.2 ± 0.2 mm	0.6 ± 0.1 mm	1.3 ± 0.2 mm
DHT+CC	1.3 ± 0.5 mm	1.2 ± 0.2 mm	1.1 ± 0.3 mm

Microstructures of the scaffolds (Figures 1C-D and Figures S2-S3) showed more compact and dense structures of crosslinked biomaterials compared to their untreated analogues. Longitudinal sections revealed spherical porosity, whereas cross-sections indicated the signs of directional alignment of the pores, possibly due to freezing and crystallization processes. Pore size was estimated with Feret's diameter (the longest distance between any two points of a pore) using the longitudinal sections of the scaffolds (Figure 1E). Compared to NC-5% ELN control scaffold, pore size was significantly lower in crosslinked analogues with the same elastin concentration. Pore size was also substantially altered with different elastin concentration. The increase of pore size showed the same trend in all conditions: 10% ELN < 5% ELN < 20% ELN.

Elastin immunostaining was used to visualize elastin present in the scaffolds using AEC instead of fluorescent visualization to eliminate overlapping signals from autofluorescence and signal of interest (Figure 1F-G and Figure S4). The higher percentage of elastin in NC and DHT scaffolds resulted in higher intensity of the staining. The intensity of staining in CC and DHT+CC scaffolds, where elastin was covalently bound to collagen, remained approximately the same regardless of elastin concentration and was similar to that in 20% ELN scaffolds without crosslinking. This likely indicates that elastin was already bound to all available sites on the collagen protein, with any excess elastin removed during the washing steps.

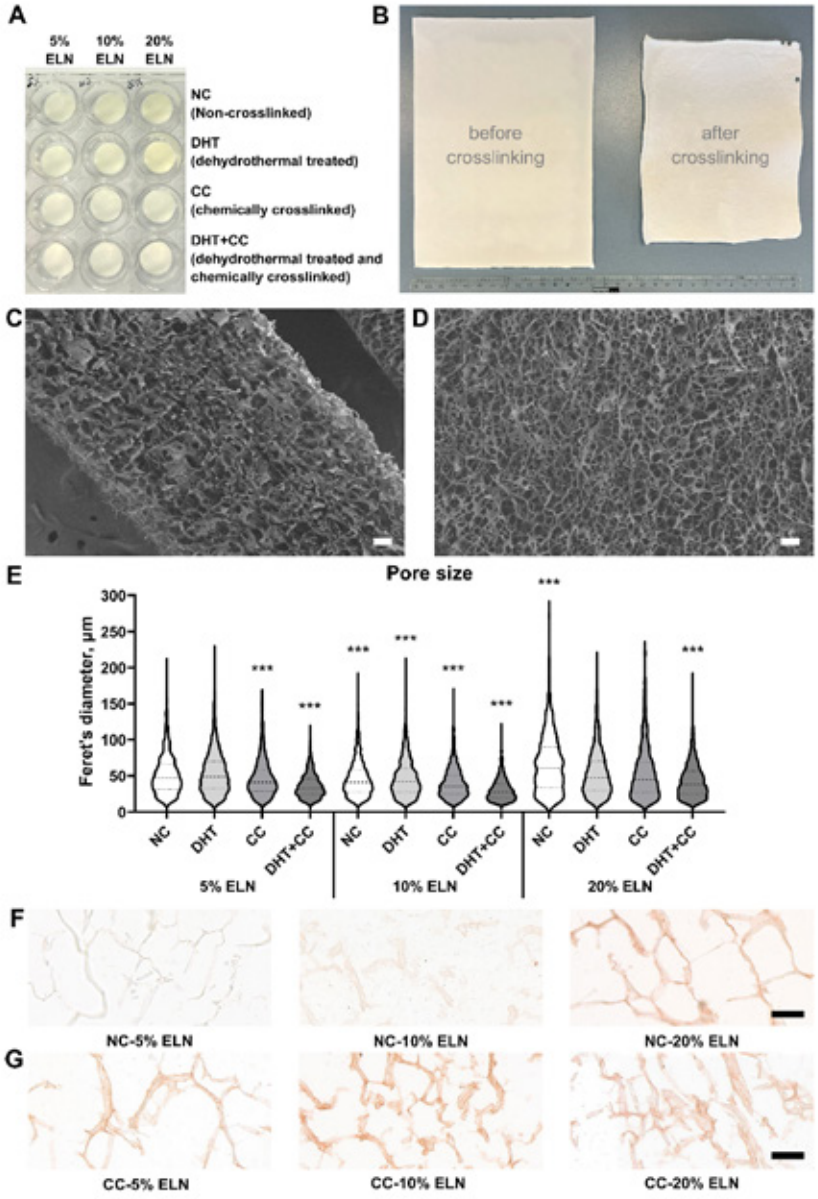

Figure 1. Structural and morphological characteristics of collagen-elastin scaffolds. A) Visual appearance of all twelve different round scaffolds, 12 mm in diameter. B) Comparison of size changes before (left) and after (right) chemical crosslinking of the biomaterials. C,D) Representative SEM images of cross-sections (C) and longitudinal sections (D) of DHT+CC-5% ELN scaffold. Scale bar = 100 µm. E) Pore sizes calculated with Feret's diameter via ImageJ software and shown in violin plot. Comparisons to NC-5% ELN were performed. * $p<0.05$, ** $p<0.01$, *** $p<0.001$. F,G) Representative elastin-stained sections of collagen-elastin scaffolds (F – NC scaffolds, G – CC scaffolds), highlighting elastin in brown. Scale bar = 50 µm.

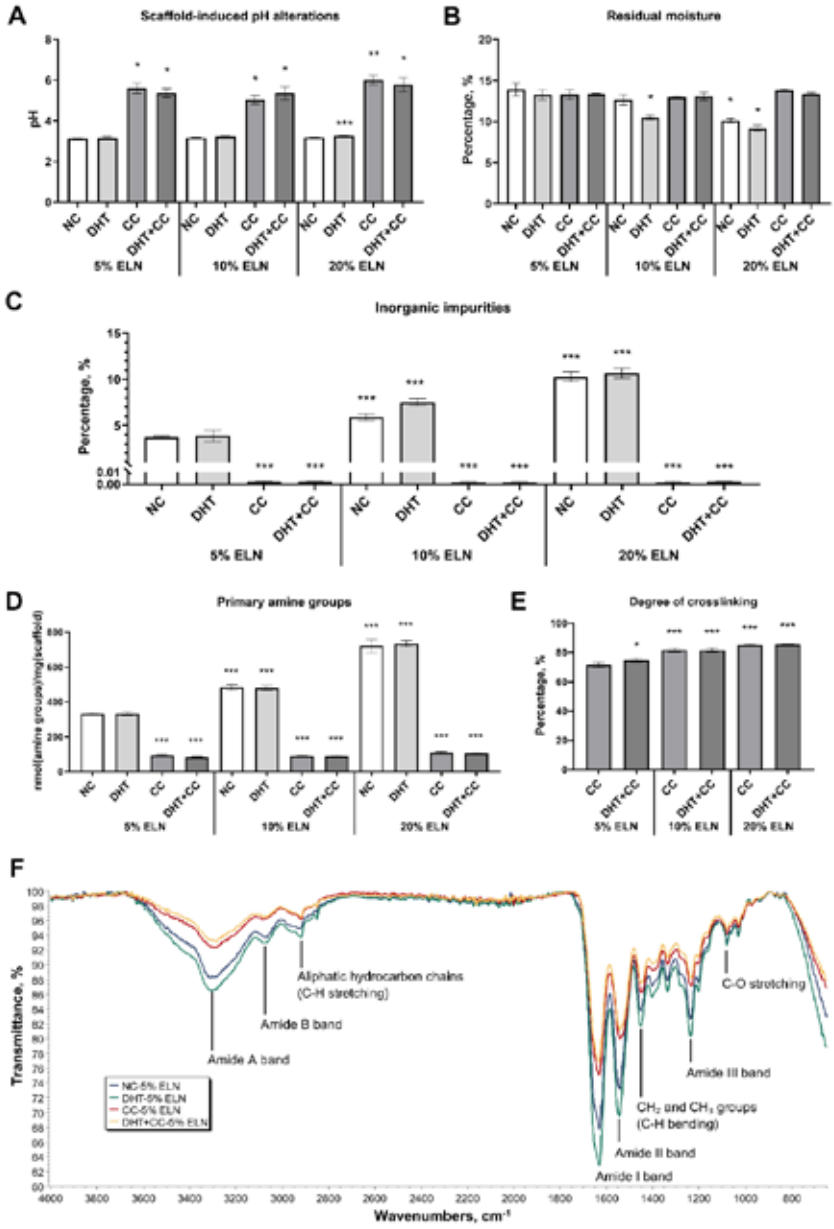

Figure 2. Chemical characteristics of collagen-elastin scaffolds (n=3). A) pH of demineralized water after 30 min of incubation with scaffolds. B) Residual moisture content of collagen-elastin scaffolds. C) Non-volatilized residues after flameless combustion of the scaffolds. D) Free amine groups in collagen-elastin scaffolds assessed through TNBS assay. E) Degree of crosslinking via EDC/NHS treatment calculated through the difference in free primary amine groups. F) FTIR spectra of 5% ELN scaffolds. Comparisons to NC-5% ELN were performed for A-D and to CC-5% ELN for E. Error bars represent standard deviation. * $p<0.05$, ** $p<0.01$, *** $p<0.001$.

3.2. Chemical Characteristics

Scaffolds were incubated in demineralized water after which pH of the solution was measured. The results showed that non-crosslinked scaffolds acidified the solution (pH 3.1), likely due to residual acetic acid remaining after lyophilization (Figure 2A). In contrast, crosslinked scaffolds maintained a neutral pH, as expected after extensive washing steps during the crosslinking process. Controlling residual moisture is needed to check complete lyophilization and is essential for maintaining scaffold integrity and stability, as excess moisture can lead to structural collapse, degradation, or undesired physicochemical changes that compromise mechanical properties and long-term usability. The obtained content revealed that the percentage of soluble elastin added showed the reverse correlation with the residual moisture in the samples (Figure 2B), indicating hydrophobic properties of elastin and that water was mainly bound to collagen. Higher temperatures at lyophilization process also facilitated water removal from the scaffold. Meanwhile, crosslinked samples showed similar results regardless of elastin content.

Inorganic impurities that were assessed with flameless combustion of the scaffolds demonstrated the direct connection between elastin content and remaining residues (Figure 2C). This may be explained by the method to acidify soluble elastin for scaffold creation. Excessive treatments with aqueous solutions during crosslinking of CC and DHT+CC scaffolds eliminated inorganic impurities.

TNBS assay revealed a direct connection between percentage of elastin added to non-crosslinked scaffolds and the amount of primary amine groups, with higher elastin content leading to a decrease in primary amine groups (Figure 2D). DHT treatment did not alter these results. Higher amounts of available amine groups also resulted in higher degrees of crosslinking, possibly involving collagen-elastin, collagen-collagen, and elastin-elastin interactions (Figure 2E). After undergoing crosslinking treatments, the value of primary amine groups was reduced to 95 ± 11 nmol/mg.

FTIR spectra of all tested scaffolds showed similar vibrations that are characteristic for collagen and elastin proteins (Figure 2F, Figures S5-S6 and Table S1). Broad signal from amide A band at approximately 3310-3280 cm^{-1} shows N-H stretching vibration and O-H stretching of hydroxyl groups. Weak amide B band at 3090-3065 cm^{-1} indicates C-N stretching of peptide bonds. EDC/NHS crosslinking reduced the intensity of FTIR signals, with a minor red shift (16–26 cm^{-1}) in Amide A, and a blue shift (6–19 cm^{-1}) in Amide B. Stretching of CH_2 groups, that are for example typically present in the aliphatic side chains of amino acid residues of proline and

hydroxyproline, is detected at 2930-2840 cm^{-1}. Vibrations at 1630 cm^{-1} represent C=O stretching of the carboxyl groups (amide I band). Amide II band which corresponds to N-H bending and C-N stretching is detected at 1550-1540 cm^{-1}. C-H bending vibrations of aliphatic CH_2 and CH_3 groups are found at 1455-1445 cm^{-1}. C-N stretching and N-H bending from amide III band peaked at 1240-1230 cm^{-1}. C-O stretching occurred approximately at 1080 cm^{-1}. The stable positions of the peaks indicate that the secondary structures of collagen and elastin remained intact, confirming effective crosslinking without major disruption to protein secondary structure.

3.3. Mechanical Characteristics

For all tested samples, visual wetting time before basic manipulation test was less than 5 s (Figure 3A). While ten tested of the tested scaffolds passed manipulation tests (flipping, stretching and flattening) without any problem, both NC-20% ELN and DHT-20% ELN scaffolds were difficult to handle due to insufficient rigidity and rapid rupture, which raises significant concerns for clinical application (Figure 3B and Table S2).

Ultimate tensile strength showed a clear difference between non- and crosslinked scaffolds, demonstrating the higher stiffness of crosslinked material and ability to withstand more force before breaking (Figure 3C). The highest tensile strength was detected for CC-10% ELN and the lowest for DHT-20% ELN. Non-crosslinked groups revealed that only 20% of added elastin substantially diminished tensile strength, supporting the results of the manipulation tests. Although CC-20% ELN was the weakest scaffold of the crosslinked samples, it was still stronger than NC-5% ELN.

The Young's modulus demonstrated a clear trend of decreasing elasticity with a higher amount of elastin protein in scaffolds without chemical crosslinking (Figure 3D). In contrast, no clear trend was observed for crosslinked scaffolds. Of note, mature insoluble elastic fibers exhibit elasticity and resilience, whereas solubilized elastin lacks these properties and does not contribute to structural elasticity.

Ball burst tests, another method of testing mechanical stability, were in close conformity with tensile strength tests (Figure 3E), where a higher percentage of elastin in scaffolds without chemical crosslinking appeared to result in lower strength. DHT treated samples showed slightly better performance compared to biomaterials lyophilized at room temperature. CC scaffolds were slightly stronger than their DHT+CC analogues. CC-10% ELN scaffold was the most durable among all tested biomaterials.

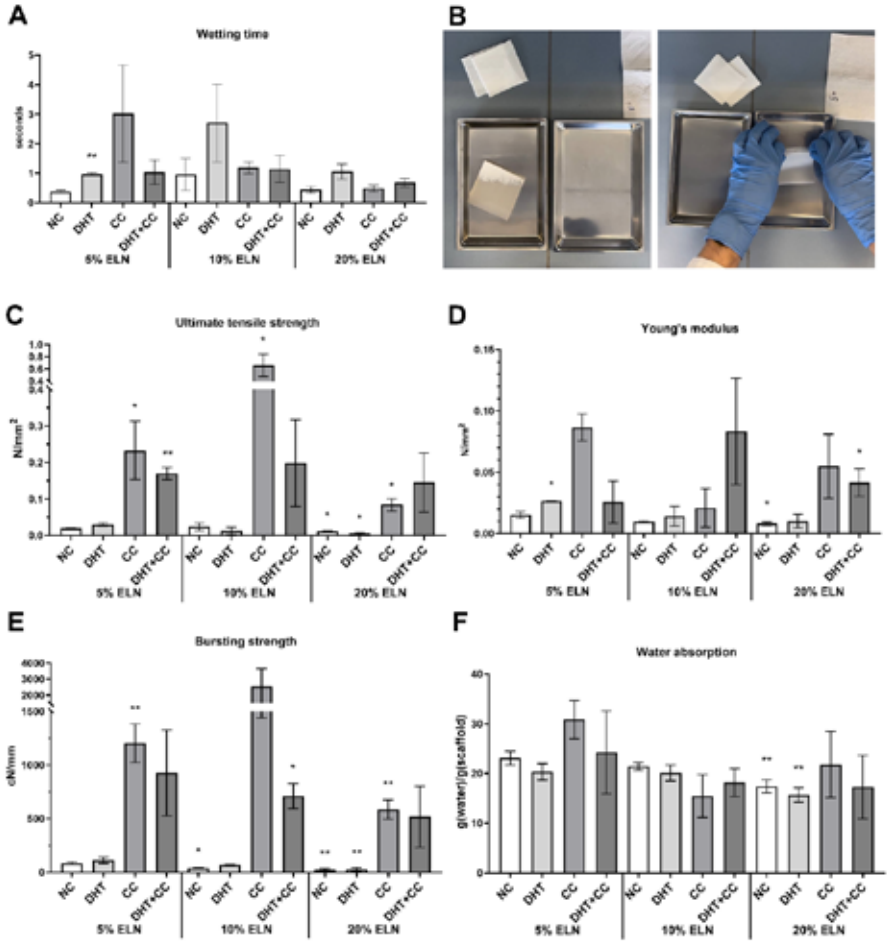

Figure 3. Mechanical characteristics of collagen-elastin scaffolds (n=3). A) Wetting time of collagen-elastin scaffolds 80 × 80 mm in PBS. B) Digital photos showing the wetting of the scaffolds and basic mechanical manipulations. C) Ultimate tensile strength of collagen-elastin scaffolds. D) Young's modulus of collagen-elastin scaffolds. E) Bursting ball tests of collagen-elastin scaffolds. F) Water absorption per g of collagen-elastin scaffold. Comparisons to NC-5% ELN were performed for A, C-F. Error bars represent standard deviation. * $p<0.05$, ** $p<0.01$, *** $p<0.001$.

For all the tested biomaterials, there was a distinct trend seen that a higher percentage of elastin resulted in lower water absorption, except for CC-10% ELN (Figure 3F). All samples showed an absorption higher than 15 g water/g scaffold.

3.4. Biological Characteristics

Without chemical crosslinking, DHT treatment and higher elastin content resulted in slower enzymatic degradation in biomaterials, observed visually (Figure 4A) and by measuring the weight of any remaining material (Figure 4B,C). After 3 h, all scaffolds without chemical crosslinking were completely degraded, except for DHT-20% ELN, which was degraded after 24 h of incubation. Chemical crosslinking with EDC/NHS drastically improved resistance of the scaffolds to biological degradation by collagenase. Biodegradation of such scaffolds was not noticeable after 14 days when checked visually and with basic mechanical manipulations. These biomaterials were firm and stable. A higher percentage of elastin in crosslinked biomaterials resulted in more degradation, opposite to the trend observed in non-crosslinked counterparts.

Cytotoxicity tests were performed using conditioned media after 72 h extraction on two cells lines that represent the majority of skin cells – fibroblasts (HFF-1, Figure 4D) and keratinocytes (HaCaT, Figure 4E). All tested samples showed either the same or higher viability compared to blank and negative controls (Latex). Latex showed a higher negative impact on HFF-1 cells than on HaCaT cells, most likely related to the lower cell density at confluency of the stretched spindle-shaped fibroblasts compared to cobblestone shaped keratinocytes. Results indicated good cytocompatibility of the scaffolds based on conditioned media. However, release of cytotoxic substances may be limited due to crosslinking. Therefore, cell viability assays were performed to demonstrate cytocompatibility. Primary human dermal fibroblasts were used to more closely represent the *in vivo* state of cells, providing more accurate and physiologically relevant data. After seeding primary cells on top of the scaffolds, non-crosslinked biomaterials shrank to 55.0 ± 5.8% in the first 24 h. Crosslinked biomaterials kept their initial size throughout the whole experiment, indicating that they were neither remodeled by cells nor altered by immersion in cell culture media (Figure 4F). Non-crosslinked biomaterials incubated in cell culture medium without cells reduced less in size – only by 25.7 ± 5.7%. Despite varying degrees of size reduction in cell culture media, both with and without cells, biomaterials without chemical crosslinking exhibited improved integrity and mechanical stability, as observed during mechanical manipulations. Cell viability in the scaffolds was preserved or increased compared to day 1 (Figure 4G). While all scaffolds showed no cytotoxic effect, the highest cellular activity was detected in CC-10% ELN scaffold. This could be attributed to the significantly reduced thickness of this scaffold compared to all other biomaterials, which resulted in higher cell number per scaffold volume and potentially enhanced cell-to-cell interactions in thinner biomaterials and subsequently more alamarBlue signal.

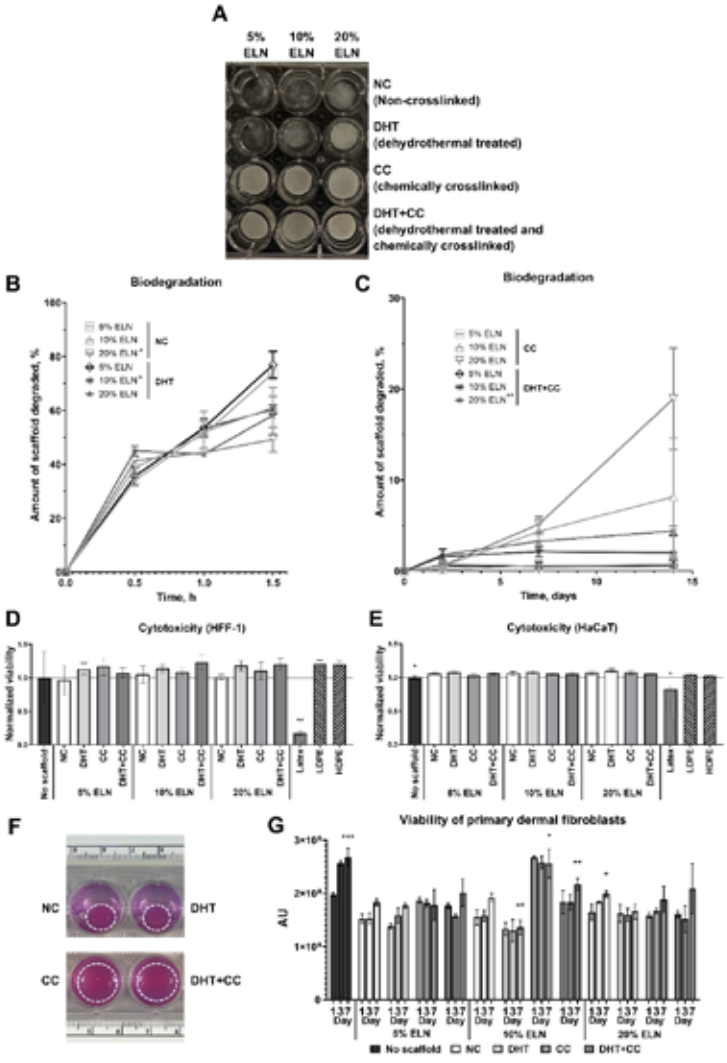

Figure 4. Biological characteristics of collagen-elastin scaffolds (n=3). A) Example of biodegradation of collagen-elastin scaffolds after 1 h of incubation with collagenase at 37°C. B,C) Percentage of scaffold biodegradation through time. Non-crosslinked scaffolds were assessed at 30, 60 and 90 min (B), while crosslinked materials were analyzed at day 2, 7 and 14 (C). D,E) Results of a cytotoxicity test using conditioned media on HFF-1 (D) and HaCaT (E) cells. Scaffolds were incubated for 3 days in media, and cells were incubated in this conditioned media for 24 h (n=3). All values were normalized to the control (medium without scaffold). Latex was used as cytotoxic control, and LDPE (low-density polyethylene) and HDPE (high-density polyethylene) as viable cells control. F) Representative image of four different collagen-elastin scaffolds (NC, DHT, CC and DHT+CC) 24 h after seeding of primary dermal fibroblasts and assessed for viability with alamarBlue reagent. G) Quantitative viability of primary fibroblasts seeded on collagen-elastin scaffolds after 24 h, 72 h and 7 days (3 donors). Comparisons to NC-5% ELN were performed for B, D, E, G and to CC-5% ELN for C. Error bars represent standard deviation. * $p<0.05$, ** $p<0.01$, *** $p<0.001$.

4. Discussion

Research on the development of an ideal skin substitute is still ongoing despite numerous commercially available dermal substitutes that have been implemented in clinical practice [32-34]. The primary objective of any skin substitute is to replicate both the structural and functional properties of native skin while facilitating rapid and effective healing. Nevertheless, various challenges remain in creating materials that can fully mimic the complex biological and mechanical properties of human skin. Native biomaterials such as collagen and elastin have shown particular promise due to their biocompatibility, biodegradability, and ability to closely resemble the native extracellular matrix [28, 35]. Previous subcutaneous implantation studies conducted on Sprague-Dawley rats, have demonstrated the ability of porous collagen scaffolds supplemented with soluble elastin to promote angiogenesis and support tissue formation, highlighting their use in wound healing and regenerative medicine [22]. Moreover, in a porcine model, another collagen-elastin scaffold significantly minimized myofibroblast presence, promoting optimal dermal regeneration while effectively reducing wound contraction [20, 36].

Our current strategy emphasizes the expansion of knowledge and exploration of the potential of collagen-elastin scaffolds to develop a more durable and stable biomaterial. The composition, concentration, and the ratio of collagen/elastin play a crucial role in shaping the properties of biomaterials, making it essential to carefully consider these factors for optimal performance [37]. The supplementation with soluble elastin leads to a more uniform distribution of elastin peptides throughout the skin substitute compared to pulverized insoluble elastic fibers. This is accompanied by a proportional increase in pore size within porous collagen scaffolds [31]. Our results with soluble elastin are consistent with previous studies showing that insoluble elastin reduces the tensile strength of scaffolds in a concentration-dependent manner while having little effect on their microarchitecture, as both porosity and pore size undergo changes but remain within optimal ranges for tissue engineering applications [38]. While various concentrations of soluble elastin were used in biomaterials, 20% may be an upper threshold for its use before structural integrity is compromised. It is noteworthy that 20% ELN scaffolds without chemical crosslinking failed to withstand basic manipulations, although these scaffolds demonstrated sufficient rigidity after being subjected to cell culture media, and especially with cells, which made it possible to handle them without rupture. This observation aligns with prior literature on scaffold shrinkage [39-41] and indicates that such matrices may require some pre-incubation, with medium or patient cells, before being applied to a wound bed.

To reach long-term stability and durability of these materials, we employed EDC/NHS crosslinking. Chemical crosslinking of biomaterials using EDC/NHS forms zero-length intra- and intermolecular covalent bonds between collagen and elastin molecules, as well as collagen-collagen and elastin-elastin bonds. This method activates carboxylic acid groups in proteins with subsequent formation of new amide bonds, enhancing physicochemical and mechanical properties of biomaterials, and resistance to enzymatic degradation of biomaterials [42, 43]. Moreover, this process provides the covalent bonding of soluble elastin to insoluble collagen, forming a stable composite scaffold, resulting in elastin retention. By increasing the chemical interaction between collagen and elastin, we aim to produce a scaffold that retains its mechanical integrity and bioactivity over extended periods, expanding its application in wound healing and skin regeneration, e.g., treatment of traumatic injuries in thick skin regions. Various dermal substitutes have been effectively utilized in treating burns, though their application in thick skin (like palms or soles) has been scarcely documented [44, 45]. Thick skin is distinct from dorsal skin by its greater thickness, dense nerve supply, and lower extensibility. One report of palmar trauma treatment has shown that combining split-thickness skin grafts with collagen dermal substitutes yielded favorable functional and aesthetic outcomes [46]. Our methods involving DHT treatment and chemical crosslinking could further improve dermal substitutes by increasing their stability and durability. This may address the nuances noted by surgeons regarding the preference for a material that simplifies clinical use, requires minimal effort, enhances wound bed preparation, and ensures stability [46, 47].

DHT treatment is a widely used method for stabilizing collagen-based composite materials, which involves exposing collagen to elevated temperatures (above 90°C) under vacuum conditions [48]. DHT treatment is a physical crosslinking technique that facilitates the formation of new covalent and hydrogen bonds [49]. Previous studies reported a 4% reduction in primary amine groups following DHT treatment, while chemical crosslinking significantly decreased amine groups in collagen scaffolds [50]. Although we observed similar changes with EDC/NHS treatment, our collagen-elastin scaffolds showed no statistically significant difference between non-crosslinked and DHT-treated samples with the same elastin content. This could be attributed to the presence of soluble elastin peptides, which may have mitigated the effects of physical crosslinking, or to the need for further optimization of lyophilization temperature and duration to achieve significant changes. It is essential to consider that both temperature and DHT treatment time are critical factors during lyophilization – exceeding 145 °C, for instance, can lead to collagen scaffold denaturation [49]. While previous mechanical tests showed a 3.7-fold improvement

in the performance of DHT treated and EDC/NHS crosslinked collagen scaffolds [50], our DHT+CC scaffolds exhibited a 5- to 30-fold increase in tensile and bursting strength compared to their DHT analogues. Those studies reported that chemical crosslinking does not affect the absorbency of DHT treated collagen scaffolds [50]. In contrast, in our study, the absorbency of DHT+CC-5% ELN was significantly higher than that of DHT-5% ELN, but it did not substantially differ from 10% and 20% ELN. Regarding enhanced resistance to collagenase degradation, effects similar to those reported were observed with both DHT treatment and chemical crosslinking, suggesting that intermolecular crosslinks are more effective than intramolecular ones in improving enzymatic resistance [50]. Similar to the chemical crosslinking of collagen-elastin scaffolds with glutaraldehyde, which has been shown to enhance scaffold strength, reduce biodegradation, and minimize shrinkage, we observed similar effects when using EDC/NHS as a crosslinking agent [51]. Interestingly, in our experiments elastin acted as a protective component against degradation in non-crosslinked biomaterials, similar to the effect of added elastin in genipin-crosslinked scaffolds [31].

To promote a moist environment, an ideal biomaterial for skin wound healing needs to have excellent water absorption capacity. Moreover, maintaining a moist wound environment promotes autolytic debridement, alleviates pain, minimizes scarring, stimulates collagenesis and keratinocyte migration across the wound surface [52]. Moist environment is also known to accelerate healing by providing a sufficient supply of growth factors and other key molecules to the regenerating tissues. Absorbency of the scaffolds may have been affected by the potential washout of soluble elastin, however our findings were in line with previous published experiments – around 18-22 g of water per gram of scaffold for NC-5% ELN scaffolds [31].

While our experiments on collagen-elastin matrices provide valuable insights, there are some limitations that must be considered. Although we aimed to replicate large-scale production of dermal substitutes in terms of quantity, further evaluation is needed for the reproducibility of these procedures and the persistence of their characteristics. For instance, CC-10% ELN scaffolds exhibited superior mechanical properties and cell viability, however these positive effects may be linked to the notably reduced thickness of these scaffolds. Although the reduced thickness of CC-10% ELN was an unintended consequence of soaking multiple sheets together in the crosslinking solution, it may also be applied as a design parameter to obtain improved mechanical properties. Ensuring consistency in upscaling the production process will be critical for broader medical implementation and clinical translation.

Furthermore, given that elastin was not covalently bound in non-crosslinked scaffolds, assessing its levels after biological assays would provide a deeper understanding of its retention and function. Similarly, the final elastin content in crosslinked samples after the chemical treatments can be determined, as some elastin may be lost during processing. In addition, since gamma irradiation, a commonly used sterilization method, is known to partly degrade collagen scaffolds and influence the shrinkage [40], exploring alternative sterilization techniques (e.g., supercritical CO_2, gas plasma, etc. [53]) is essential to preserve scaffold integrity.

Additional research into the cellular interactions and signaling pathways triggered by elastin within the scaffolds would provide a deeper understanding of its role in wound healing. The next steps in accessing the potential use of these dermal templates may include additional *in vitro* testing (assessing protein and gene expression profiles) and the long-term *in vivo* performance (e.g., degradation rates, immune responses, and overall integration with native tissues).

5. Conclusion

In this study, we successfully developed twelve different collagen-elastin scaffolds using widely available and cost-effective biological materials. Our findings revealed that increasing the proportion of soluble elastin led to a larger pore size and enhanced chemical crosslinking efficiency. However, higher elastin content also resulted in lower tensile and bursting strengths, residual moisture, and diminished water absorption. Chemical crosslinking significantly improved mechanical properties and stability against enzymatic digestion, while DHT treatment accelerated the drying process without altering the physicochemical properties. Importantly, all scaffolds demonstrated good biocompatibility, highlighting their potential for biomedical applications. Collagen scaffolds supplemented with 5% soluble elastin that underwent DHT and EDC/NHS treatment was selected as the most promising candidate for further investigation in wound healing because of their favorable mechanical properties and stability. Nevertheless, additional *in vitro* and *in vivo* experiments are crucial to fully explore their potential applications and optimize their effectiveness in preclinical studies and ultimately in clinical practice.

References

1. Lee, S.K., Y.S. An, and W.S. Choy, *Management of Hardware-Exposed Soft Tissue Defects Using Dermal Substitutes and Negative Pressure Wound Therapy.* Annals of Plastic Surgery, 2023. **90**(3): p. 242-247.
2. Ozhathil, D.K., et al., *A Narrative Review of the History of Skin Grafting in Burn Care.* Medicina, 2021. **57**(4): p. 380.
3. Fulchignoni, C., et al., *Matriderm dermal substitute in the treatment of post traumatic hand's fingertip tissue loss.* Journal of Cosmetic Dermatology, 2022. **21**(2): p. 750-757.
4. Khan, A.A., et al., *Skin Graft Techniques.* Clinics in Podiatric Medicine and Surgery, 2020. **37**(4): p. 821-835.
5. Hackl, F., et al., *Epidermal Regeneration by Micrograft Transplantation with Immediate 100-Fold Expansion.* Plastic and Reconstructive Surgery, 2012. **129**(3): p. 443e-452e.
6. Franco, W., et al., *Fractional Skin Harvesting: Device Operational Principles and Deployment Evaluation.* Journal of Medical Devices, 2014. **8**(4).
7. Quílez, C., et al., *Bioprinting for Skin*, in *3D Bioprinting: Principles and Protocols*, J.M. Crook, Editor. 2020, Springer US: New York, NY. p. 217-228.
8. Peirce, S.C. and G. Carolan-Rees, *ReCell® Spray-On Skin System for Treating Skin Loss, Scarring and Depigmentation after Burn Injury: A NICE Medical Technology Guidance.* Applied Health Economics and Health Policy, 2019. **17**(2): p. 131-141.
9. Katiyar, S., et al., *Novel strategies for designing regenerative skin products for accelerated wound healing.* 3 Biotech, 2022. **12**(11): p. 316.
10. Amirrah, I.N., et al., *A Comprehensive Review on Collagen Type I Development of Biomaterials for Tissue Engineering: From Biosynthesis to Bioscaffold.* Biomedicines, 2022. **10**(9): p. 2307.
11. Montagna, W. and P.F. Parakkal, *4 - The Dermis**Written largely by Jeffrey Pinto, University of Oregon Medical School, Portland*, in *The Structure & Function of Skin (Third Edition)*, W. Montagna and P.F. Parakkal, Editors. 1974, Academic Press. p. 96-141.
12. Diller, R.B. and A.J. Tabor, *The Role of the Extracellular Matrix (ECM) in Wound Healing: A Review.* Biomimetics, 2022. **7**(3): p. 87.
13. Avila Rodríguez, M.I., L.G. Rodríguez Barroso, and M.L. Sánchez, *Collagen: A review on its sources and potential cosmetic applications.* Journal of Cosmetic Dermatology, 2018. **17**(1): p. 20-26.
14. Rezvani Ghomi, E., et al., *Collagen-based biomaterials for biomedical applications.* Journal of Biomedical Materials Research Part B: Applied Biomaterials, 2021. **109**(12): p. 1986-1999.
15. Sharma, S., et al., *Collagen-based formulations for wound healing: A literature review.* Life Sciences, 2022. **290**: p. 120096.
16. Chattopadhyay, S. and R.T. Raines, *Collagen-based biomaterials for wound healing.* Biopolymers, 2014. **101**(8): p. 821-833.
17. Sklenářová, R., et al., *Collagen as a Biomaterial for Skin and Corneal Wound Healing.* Journal of Functional Biomaterials, 2022. **13**(4): p. 249.
18. Trębacz, H. and A. Barzycka, *Mechanical Properties and Functions of Elastin: An Overview.* Biomolecules, 2023. **13**(3): p. 574.
19. Senior, R.M., et al., *Val-Gly-Val-Ala-Pro-Gly, a repeating peptide in elastin, is chemotactic for fibroblasts and monocytes.* J Cell Biol, 1984. **99**(3): p. 870-4.

20. de Vries, H.J.C., et al., *Dermal regeneration in native non-cross-linked collagen sponges with different extracellular matrix molecules.* Wound Repair and Regeneration, 1994. **2**(1): p. 37-47.
21. Hinek, A., et al., *Proteolytic digest derived from bovine Ligamentum Nuchae stimulates deposition of new elastin-enriched matrix in cultures and transplants of human dermal fibroblasts.* Journal of Dermatological Science, 2005. **39**(3): p. 155-166.
22. Daamen, W.F., et al., *A biomaterial composed of collagen and solubilized elastin enhances angiogenesis and elastic fiber formation without calcification.* Tissue Engineering Part A, 2008. **14**(3): p. 349-60.
23. Halsey, G., et al., *Role of elastic fiber degradation in disease pathogenesis.* Biochimica et Biophysica Acta (BBA) - Molecular Basis of Disease, 2023. **1869**(5): p. 166706.
24. Stojic, M., et al., *Elastin-Plasma Hybrid Hydrogels for Skin Tissue Engineering.* Polymers, 2021. **13**(13): p. 2114.
25. Mitzmacher, M.G., et al., *Novel Recombinant Tropoelastin Implants Restore Skin Extracellular Matrix.* Journal of drugs in dermatology : JDD, 2020. **19**(12): p. 1166-1172.
26. Lescan, M., et al., *De Novo Synthesis of Elastin by Exogenous Delivery of Synthetic Modified mRNA into Skin and Elastin-Deficient Cells.* Molecular Therapy - Nucleic Acids, 2018. **11**: p. 475-484.
27. Davidson, J.M., et al., *Ascorbate Differentially Regulates Elastin and Collagen Biosynthesis in Vascular Smooth Muscle Cells and Skin Fibroblasts by Pretranslational Mechanisms*.* Journal of Biological Chemistry, 1997. **272**(1): p. 345-352.
28. Miranda-Nieves, D. and E.L. Chaikof, *Collagen and Elastin Biomaterials for the Fabrication of Engineered Living Tissues.* ACS Biomaterials Science & Engineering, 2017. **3**(5): p. 694-711.
29. Haslik, W., et al., *First experiences with the collagen-elastin matrix Matriderm® as a dermal substitute in severe burn injuries of the hand.* Burns, 2007. **33**(3): p. 364-368.
30. Wang, Y., et al., *Tropoelastin Incorporation into a Dermal Regeneration Template Promotes Wound Angiogenesis.* Advanced Healthcare Materials, 2015. **4**(4): p. 577-584.
31. Kamaruzaman, N., et al., *Functionalised Hybrid Collagen-Elastin for Acellular Cutaneous Substitute Applications.* Polymers, 2023. **15**(8): p. 1929.
32. Zhang, M., et al., *Advanced function, design and application of skin substitutes for skin regeneration.* Materials Today Bio, 2024. **24**: p. 100918.
33. Fuenmayor, P., et al., *Skin Substitutes: Filling the Gap in the Reconstructive Algorithm.* Trauma Care, 2024. **4**(2): p. 148-166.
34. Vecin, N.M. and R.S. Kirsner, *Skin substitutes as treatment for chronic wounds: current and future directions.* Frontiers in Medicine, 2023. **10**.
35. Daamen, W.F., et al., *Elastin as a biomaterial for tissue engineering.* Biomaterials, 2007. **28**(30): p. 4378-98.
36. Lamme, E.N., et al., *Extracellular matrix characterization during healing of full-thickness wounds treated with a collagen/elastin dermal substitute shows improved skin regeneration in pigs.* Journal of Histochemistry and Cytochemistry, 1996. **44**(11): p. 1311-22.
37. Serban, M.A., et al., *Modular Elastic Patches: Mechanical and Biological Effects.* Biomacromolecules, 2010. **11**(9): p. 2230-2237.
38. Ryan, A.J. and F.J. O'Brien, *Insoluble elastin reduces collagen scaffold stiffness, improves viscoelastic properties, and induces a contractile phenotype in smooth muscle cells.* Biomaterials, 2015. **73**: p. 296-307.
39. Tamaddon, M., et al., *Monomeric, porous type II collagen scaffolds promote chondrogenic differentiation of human bone marrow mesenchymal stem cells in vitro.* Scientific Reports, 2017. **7**(1): p. 43519.

40. Noah, E.M., et al., *Impact of sterilization on the porous design and cell behavior in collagen sponges prepared for tissue engineering.* Biomaterials, 2002. **23**(14): p. 2855-2861.
41. Meyer, N., et al., *Adjusting the physico-chemical properties of collagen scaffolds to accommodate primary osteoblasts and endothelial cells.* Regenerative Biomaterials, 2023. **10**.
42. Hafemann, B., et al., *Cross-linking by 1-ethyl-3- (3-dimethylaminopropyl)-carbodiimide (EDC) of a collagen/elastin membrane meant to be used as a dermal substitute: effects on physical, biochemical and biological features in vitro.* Journal of Materials Science: Materials in Medicine, 2001. **12**(5): p. 437-446.
43. Jiang, Y.H., et al., *Cross-linking methods of type I collagen-based scaffolds for cartilage tissue engineering.* Am J Transl Res, 2022. **14**(2): p. 1146-1159.
44. Elbadawy, A.M.S.E., et al., *Usage of Dermal Substitutes for Hand Coverage and Reconstruction.* QJM: An International Journal of Medicine, 2021. **114**(Supplement_1).
45. Capo, J.T., et al., *The Use of Skin Substitutes in the Treatment of the Hand and Upper Extremity.* HAND, 2014. **9**(2): p. 156-165.
46. Lucas, D., et al., *Application of Dermal Skin Substitutes for Hand and Finger Palmar Soft Tissue Loss.* Plastic and Reconstructive Surgery – Global Open, 2019. **7**(11): p. e2551.
47. Lou, R.B. and W.L. Hickerson, *The Use of Skin Substitutes in Hand Burns.* Hand Clinics, 2009. **25**(4): p. 497-509.
48. Haugh, M.G., M.J. Jaasma, and F.J. O'Brien, *The effect of dehydrothermal treatment on the mechanical and structural properties of collagen-GAG scaffolds.* Journal of Biomedical Materials Research Part A, 2009. **89A**(2): p. 363-369.
49. Chen, X., et al., *Effect of the Application of a Dehydrothermal Treatment on the Structure and the Mechanical Properties of Collagen Film.* Materials, 2020. **13**(2): p. 377.
50. Salvatore, L., et al., *Exploring the effects of the crosslink density on the physicochemical properties of collagen-based scaffolds.* Polymer Testing, 2021. **93**: p. 106966.
51. Maitz, J., et al., *The effects of cross-linking a collagen-elastin dermal template on scaffold bio-stability and degradation.* J Tissue Eng Regen Med, 2020. **14**(9): p. 1189-1200.
52. Nuutila, K. and E. Eriksson, *Moist Wound Healing with Commonly Available Dressings.* Advances in Wound Care, 2020. **10**(12): p. 685-698.
53. Dai, Z., et al., *Sterilization techniques for biodegradable scaffolds in tissue engineering applications.* Journal of Tissue Engineering, 2016. **7**: p. 2041731416648810.

Supporting Information

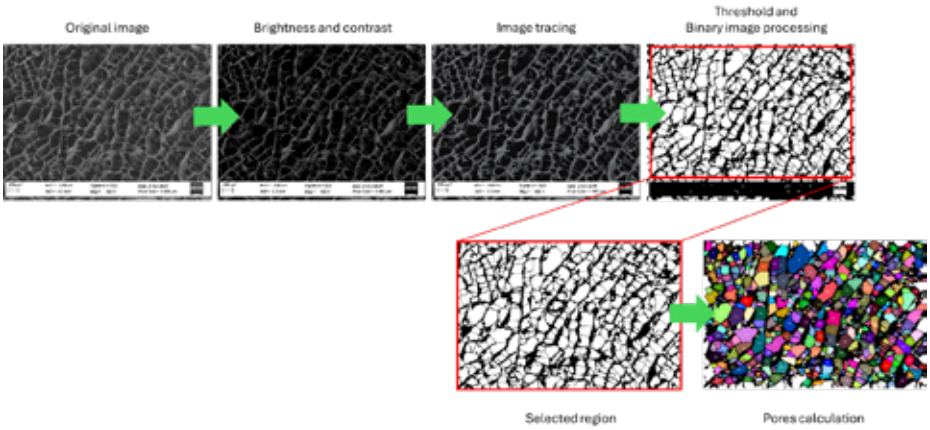

Figure S1. Pore size calculation with ImageJ and Adobe Illustrator. Only the image tracing step was performed in Illustrator.

Cross-sections	5% ELN	10% ELN	20% ELN
NC	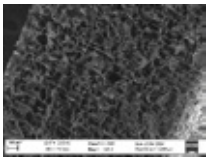	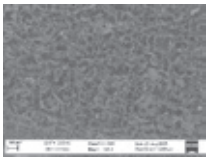	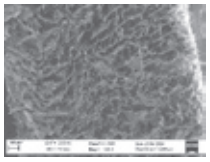
DHT	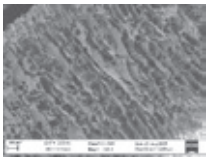	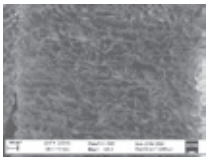	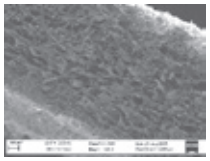
CC	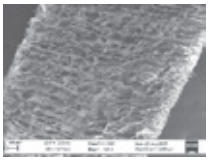	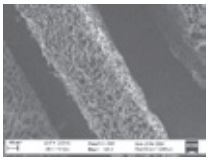	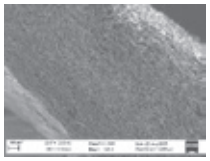
DHT+CC	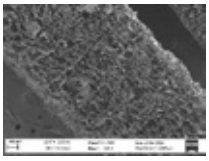	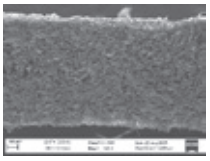	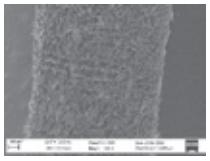

Figure S2. SEM images of cross-sections of collagen-elastin scaffolds showed more compact and dense structures of crosslinked biomaterials compared to their untreated analogues. Scale bars are 100 µm.

Longitudinal sections	5% ELN	10% ELN	20% ELN
NC	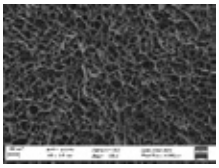	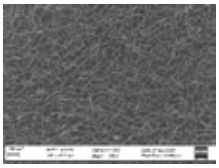	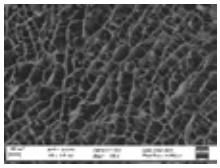
DHT	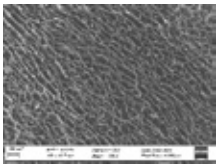	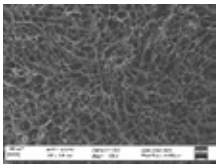	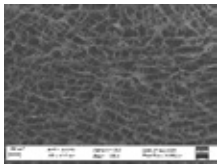
CC	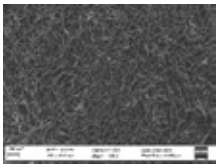	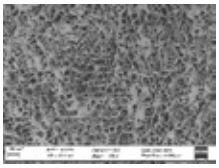	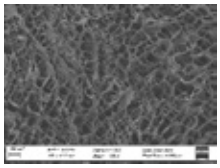
DHT+CC	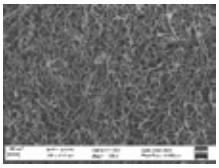	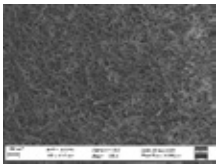	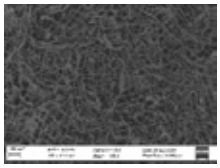

Figure S3. SEM images of longitudinal sections of collagen-elastin scaffolds. Scale bars are 100 μm.

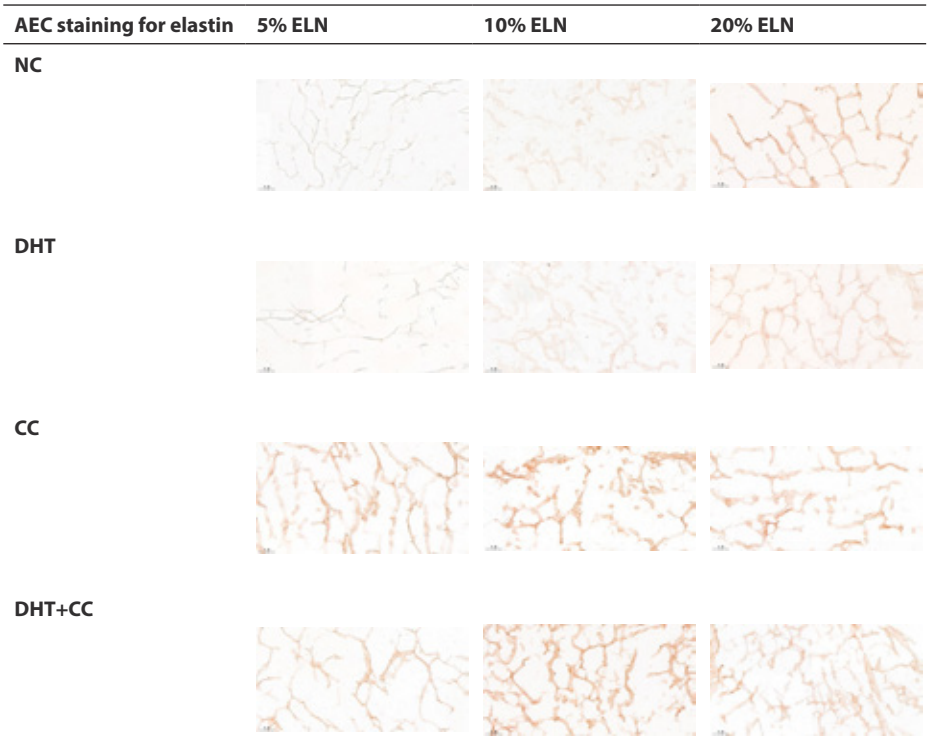

Figure S4. Elastin-stained sections of collagen-elastin scaffolds revealed that the higher percentage of elastin in NC and DHT scaffolds resulted in a greater intensity of staining, while the intensity of staining in the CC and DHT+CC scaffolds was approximately the same, regardless of the elastin concentration. Scale bar is 50 μm.

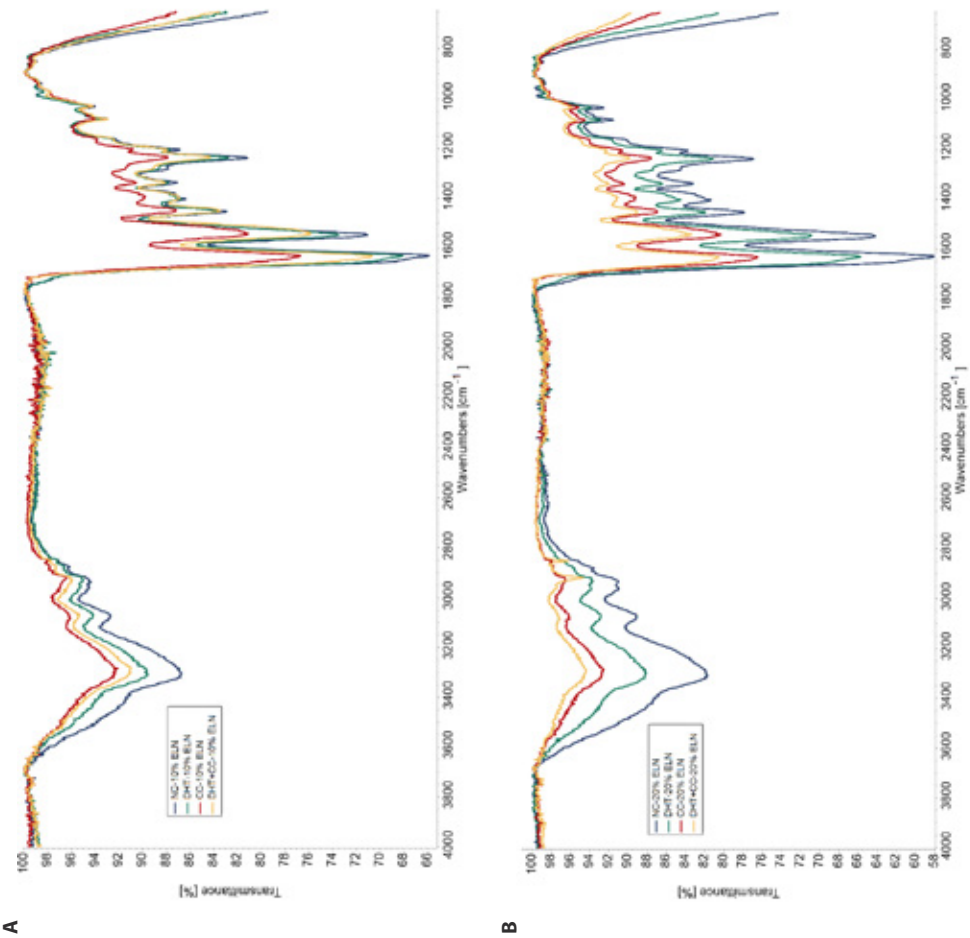

Figure S5. FTIR spectra of 10% ELN (A) and 20% ELN (B) scaffolds displayed comparable vibrations, which are indicative of the presence of collagen and elastin proteins.

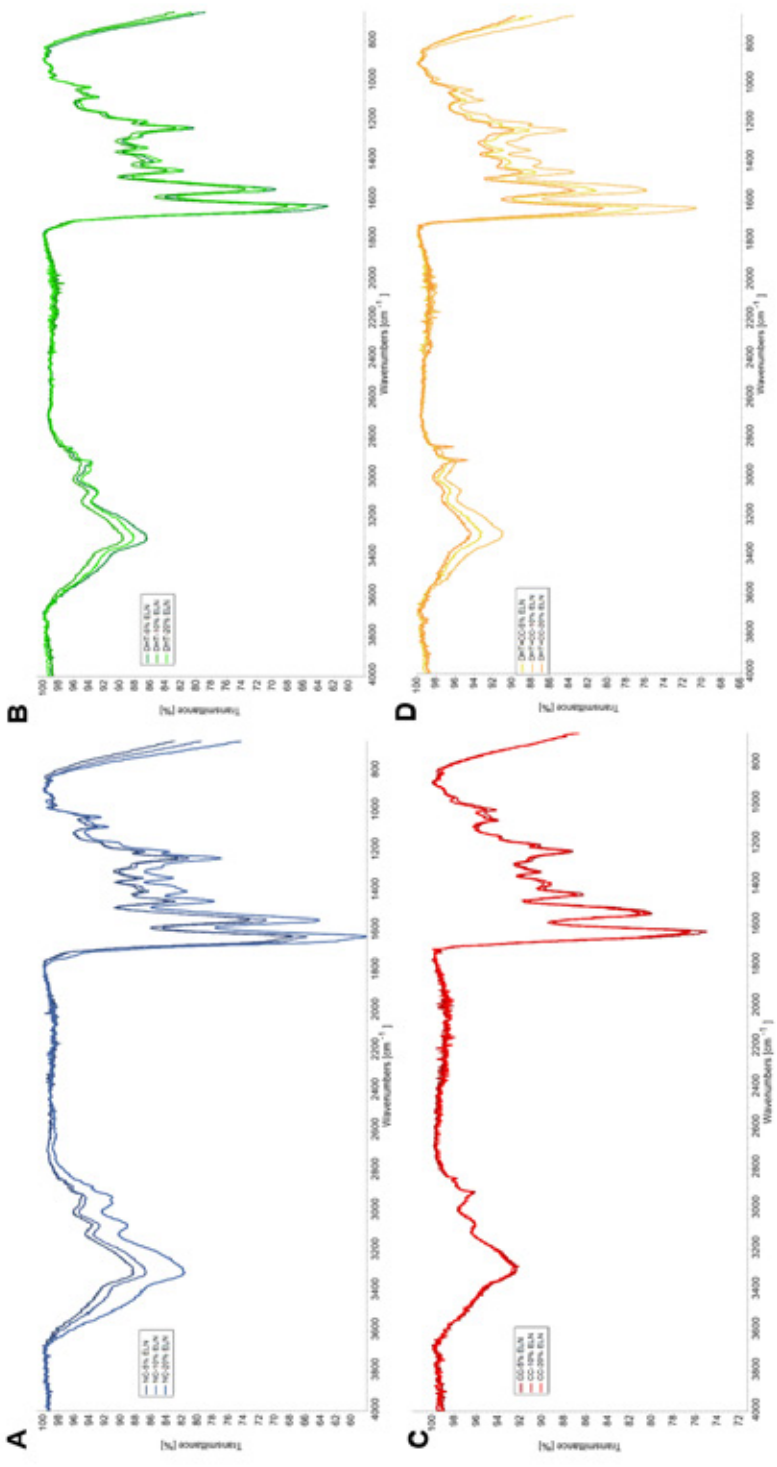

Figure S6. FTIR spectra of NC (A), DHT (B), CC (C) and DHT+CC (D) scaffolds displayed comparable vibrations, which are indicative of the presence of collagen and elastin proteins.

Table S1. FTIR spectral band positions (cm^{-1}) of collagen-elastin scaffolds.

Scaffold	Amide A	Amide B	Amide I	Amide II	Amide III
NC-5% ELN	3310	3067	1630	1544	1237
DHT-5% ELN	3304	3067	1631	1545	1237
CC-5% ELN	3294	3086	1631	1542	1234
DHT+CC-5% ELN	3285	3085	1632	1542	1235
NC-10% ELN	3305	3074	1630	1546	1237
DHT-10% ELN	3310	3068	1631	1546	1237
CC-10% ELN	3285	3080	1631	1543	1235
DHT+CC-10% ELN	3285	3068	1631	1543	1235
NC-20% ELN	3310	3068	1629	1547	1238
DHT-20% ELN	3304	3074	1630	1545	1237
CC-20% ELN	3284	3081	1632	1542	1235
DHT+CC-20% ELN	3287	3082	1632	1542	1235
	ν_{NH}, ν_{OH}	ν_{NH}	$\nu_{C=O}$, ν_{CN}	ν_{CN}, δ_{NH}	ν_{CN}, δ_{NH}

Table S2. Results of the handling assay of wet biomaterials.

Scaffold	Comments on handling	Test Passed
NC-5% ELN	Material was quite fragile. Easy to break but possible to manipulate.	**Yes**
NC-10% ELN	Difficult to manipulate. Material got a bit raptured at two attempts out of three.	**Yes**
NC-20% ELN	Very difficult to manipulate. Material got destroyed in all three attempts.	**No**
DHT-5% ELN	In the series of DHT scaffolds, this one was the easiest to manipulate.	**Yes**
DHT-10% ELN	Easy to manipulate.	**Yes**
DHT-20% ELN	Difficult to manipulate. It was easy to rapture the scaffold with some additional pressure.	**Partially**
CC-5% ELN	Very stiff material. Easy to manipulate.	**Yes**
CC-10% ELN	Less stiff compared to CC-5% ELN analogue but more elastic. Easy to handle.	**Yes**
CC-20% ELN	The least stiff but the most elastic in these series. Easy to handle. No breakage detected.	**Yes**
DHT+CC-5% ELN	Very stiff material. Easy to manipulate.	**Yes**
DHT+CC-10% ELN	Less stiff compared to HY-5% ELN analogue but more elastic. Easy to handle.	**Yes**
DHT+CC-20% ELN	The least stiff but the most elastic in these series. Easy to handle. No breakage detected.	**Yes**

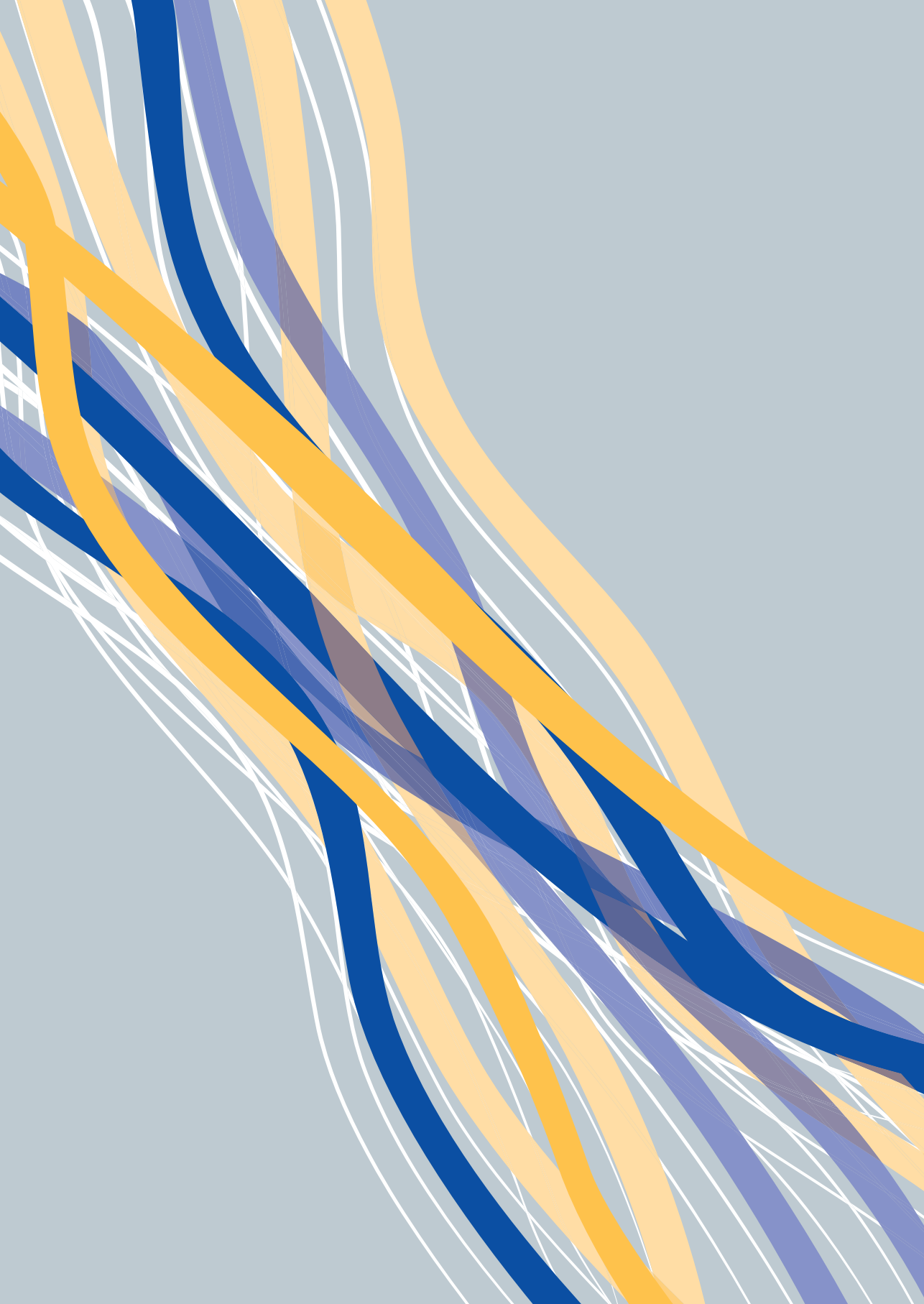

Chapter 5

Comparative in vitro evaluation of elastogenic compounds for pharmacological modulation of extracellular matrix production in human dermal fibroblasts

Roman Krymchenko[1], Nancy Avila-Martinez[1], Bouke K. H. L. Boekema[2,3,4,5], Toin H. van Kuppevelt[1], Willeke F. Daamen[1]

[1] Radboud university medical center, Research Institute for Medical Innovation, Department of Medical BioSciences, Nijmegen, The Netherlands

[2] Alliance of Dutch Burn Care, Burn Research Lab, Beverwijk, The Netherlands

[3] Amsterdam University Medical Center (AUMC), Amsterdam, The Netherlands

[4] Tissue Function and Regeneration, Amsterdam Movement Sciences Research Institute, Amsterdam, The Netherlands

[5] Department of Plastic, Reconstructive and Hand Surgery, AUMC, location VUmc, Amsterdam, The Netherlands

Submitted for publication

Abstract

The balance of collagen and elastic fibers is crucial for skin structure, appearance and function. As interest in skin regeneration and anti-aging grows, the identification of compounds that stimulate elastogenesis remains a key challenge. Many current treatments offer limited effectiveness, highlighting the need for advanced approaches in wound healing and regenerative medicine. Modulating extracellular matrix (ECM) production in dermal fibroblasts is a promising strategy for developing pharmacological therapies targeting skin regeneration, wound healing, and anti-aging. In this study, a panel of pharmacologically active compounds was assessed for their effects on primary human dermal fibroblasts. The tested compounds – retinoic acid (RA), dexamethasone (DXM), minoxidil sulfate (MNX), transforming growth factor beta 1 (TGF-β1), insulin-like growth factor 1 (IGF-1), copper sulfate ($CuSO_4$), dill extract (DE), magnesium ascorbyl phosphate (MAP, a stable vitamin C derivative), heparin (HEP), and γ-aminobutyric acid (GABA) – represent diverse biochemical classes and mechanisms of action. Pharmacological profiling enabled a comparative evaluation and ranking of compounds based on their ECM-modulating efficacy, *viz.* DXM, DE, IGF-1, HEP, RA, and TGF-β1 emerging as the most promising candidates. Moreover, scarring potential, safety, and cytotoxicity were evaluated *in vitro*. Notably, HEP, IGF-1, RA, and DXM also induced initial temporarily morphological changes in fibroblasts, which disappeared at later timepoints. While these effects may reflect adaptive responses, potential long-term consequences cannot be excluded and need further investigation. These findings support further preclinical development of selected compounds as candidates for dermal therapeutics and skin regeneration strategies.

Graphical abstract

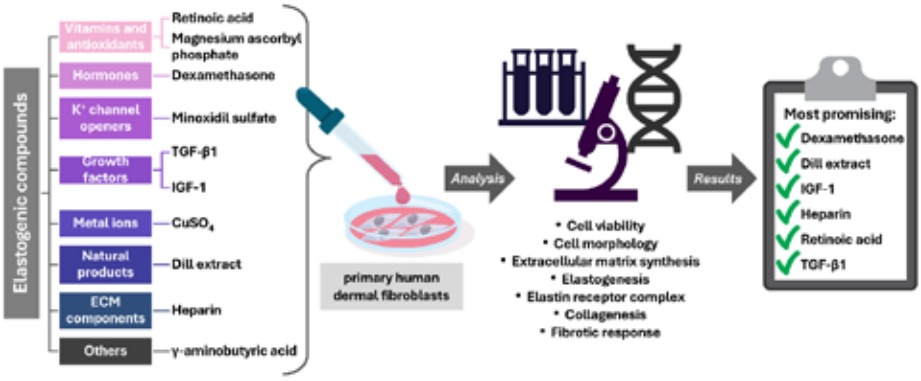

1. Introduction

The skin is a vital organ for the human body. It protects the body from external threats and pathogens, holds internal organs in place, enables sensation and temperature regulation, and provides some important functions, such as sebum secretion, sweat excretion, and the absorption of permeable compounds. The epidermis, a multi-layered epithelium, mainly consists of keratinocytes [1]. Beneath it, the dermis contains fibroblasts, blood and lymphatic vessels, nerve fibers, and the extracellular matrix (ECM) [2]. The dermis also houses immune cells, skin appendages (e.g., hair follicles, glands and nails), and sensory organs. The ECM is a dynamic and flexible framework that undergoes continuous remodeling. It provides structural support to cells, facilitates their interaction with the changing environment, and enables cell-to-cell signaling for adaptation to specific conditions [3].

The skin's mechanical properties and appearance have long been of interest to dermatologists, cosmetologists, and bioengineers, particularly regarding differences in biomechanical parameters across body sites and how these change with aging, injuries, or disease [4]. A complex network of collagen and elastic fibers in our skin is responsible for essential mechanical functionality and healthy appearance [5]. Collagen fibrils and fibers provide tensile strength [6], while elastic fibers allow the tissue to stretch and return to its original shape [7]. Elastic fibers are built up of elastin protein and microfibrillar components, encompassing, though not confined to, fibrillins, fibronectin, fibulins, microfibril-associated glycoproteins (MAGPs), latent transforming growth factor (TGF)-β-binding proteins (LTBPs), elastin microfibril interface-located proteins (EMILINs), lysyl oxidase (LOX) and its family, LOX-like proteins (LOXL) [8].

Elastic fiber production declines significantly with aging and after severe trauma, highlighting the need for therapeutic interventions to boost elastogenesis [8]. Various compounds have been tested for their ability to restore elastic fiber synthesis [9]. Dermal fibroblasts play a central role in this process because they produce and interact with the ECM, including elastic fibers [10]. However, the mechanisms of action for elastogenic compounds vary among different substances. Some act through the elastin receptor complex (ERC) [11], while others influence elastic fiber synthesis via the insulin-like growth factor-1 (IGF-1) receptor [12], mineralocorticoid receptor-independent pathways [13], microRNA modulation [14] or unspecified mechanisms [15].

Discovering new elastogenic compounds for skin regeneration and anti-aging applications is increasingly important due to the limited efficacy of existing

treatments, the difficulties of regenerating elastin fibers and the implications for skin elasticity and mobility, unmet aesthetic needs, potential benefits for wound healing and advancements in regenerative medicine. Previously [9], we categorized elastogenic compounds into several groups, including elastin-based components, ECM components, hormones, potassium channel openers, natural products, metals, antioxidants, and vitamins. A key point is that the underlying mechanisms of action, as well as the efficacy of various compounds in promoting elastin synthesis and fiber assembly, differ significantly depending on the cell type, tissue origin, and experimental model used.

Growth factors are potent signaling molecules crucial for processes like tissue remodeling and matrix synthesis [16, 17]. Among known elastogenic growth factors, IGF-1 and TGF-β1 have demonstrated the most promising effects on elastin synthesis [18]. IGF-1 enhanced elastogenesis in rat aortic smooth muscle cells [19-21] and human dermal fibroblasts [12], but had no effect on rat pulmonary fibroblasts [20]. TGF-β1 promoted elastin production by elevating both tropoelastin mRNA and protein levels across multiple cell types [22-28]. However, it is also widely recognized for its role in driving fibrotic healing through the stimulation of excessive extracellular matrix accumulation and tissue remodeling [29, 30]. Hormones, such as estradiol and aldosterone, influence skin homeostasis and elastogenesis through both systemic and locally produced steroids via sex- and receptor-specific pathways [13, 31-36]. Other hormones, e.g., dexamethasone, have shown variable elastogenic effects [35-40]. Potassium channel openers, particularly minoxidil and diazoxide, demonstrated potential to stimulate elastin synthesis in smooth muscle cells [41, 42] and preserving vascular elastic fibers in mice and rats [41, 43-45], though their dermal application remains underexplored. Copper ions play a vital role in skin repair and elastin synthesis by acting as cofactors for LOX [46, 47], and their administration has been shown to enhance elastin and collagen production [48, 49]. Additionally, several bioactive compounds are especially notable for skin treatments aimed at boosting elastin synthesis, such as derivatives of vitamins A and C [50-57], dill extract (DE) [58-60], polyphenols [61-64], γ-aminobutyric acid (GABA) [65], low molecular weight hyaluronic acid [66-70], heparin (HEP) [71, 72], and versican (VCAN) [73, 74].

In this study, we evaluated different classes of elastogenic compounds using primary human dermal fibroblasts. We selected promising representatives from various categories: retinoic acid (RA), dexamethasone (DXM), minoxidil sulfate (MNX), TGF-β1, IGF-1, copper sulfate ($CuSO_4$), DE, a stable vitamin C derivative (magnesium ascorbyl phosphate, MAP), HEP and GABA. Our comparative analysis examined

their biological activity under identical conditions, identifying the potentially most effective compounds for skin applications, with a focus on elastogenesis, also assessing collagenesis, fibrotic responses, safety, and cytotoxicity profiles *in vitro*.

2. Materials and methods

Unless otherwise specified, chemicals, enzymes, and cell culture supplements were purchased from Sigma-Aldrich (St. Louis, MO, USA), while cell culture media and antibiotics were obtained from Gibco (Grand Island, NY, USA).

2.1. Cell culture experiments with primary human skin fibroblasts

Fibroblasts were obtained from healthy skin samples collected from four adult patients (18-65 years old) undergoing elective surgeries at the Plastic and Reconstructive Surgery Departments of the Red Cross Hospital. The use of anonymized leftover tissue followed an informed opt-out protocol, adhering to national guidelines (https://www.coreon.org/ accessed on 23 November 2020), and was approved by the institutional privacy officers. Before starting the experiments, normal primary human dermal fibroblasts were propagated in 10% fetal bovine serum (FBS) in Dulbecco's Modified Eagle Medium (DMEM) supplemented with penicillin/streptomycin (5 U/ml and 5 µg/ml, respectively) at 37°C in 5% CO_2.

To test the effects of various elastogenic compounds, we tested the concentrations listed in Table 1, selected based on the most potent concentrations reported in the literature [9]. Dill extract was prepared from milled dill seeds (Pit&Pit, Hoogstraten, Belgium) according to a published procedure [75]. Briefly, 5 g of dill seed powder was mixed with 100 ml of demineralized water. The suspension was stirred overnight at 4 °C, centrifuged, and filtered. A control condition without an elastogenic compound was included, along with a 0.04% DMSO control (similar to the highest concentration of DMSO in the final RA, DXM, and MNX). All media were filtered using a 0.2 µm filter before use. The media and compounds were refreshed every 48 h. At the end of the cell culture period, the wells were washed twice with PBS (phosphate-buffered saline) before proceeding to further analysis.

Table 1. List of tested compounds in the experiments with primary human dermal fibroblasts.

Abbreviation	Compound	Solvent	Concentration tested	Manufacturer (catalogue number)
DMSO	Dimethyl sulfoxide	-	0.04%	Sigma-Aldrich (D8418)
RA	Retinoic acid	DMSO	1×10^{-6} M	Sigma-Aldrich (R2625)
DXM	Dexamethasone	DMSO	1×10^{-5} M	Sigma-Aldrich (D4902)
MNX	Minoxidil sulfate	DMSO	1×10^{-4} M	Sigma-Aldrich (M7920)
TGF-β1	Transforming growth factor-β1	H_2O	5 ng/ml	Peprotech (100-21-100UG; Cranbury, NJ, USA)
IGF-1	Insulin-like growth factor-1	H_2O	80 ng/ml	R&D Systems (291-G1; Minneapolis, MN, USA)
$CuSO_4$	Copper(II) sulfate	H_2O	1×10^{-6} M	Sigma-Aldrich (C8027)
DE	Dill extract	H_2O	10%	Pit&Pit (Hoogstraten, Belgium)
MAP	Magnesium ascorbyl phosphate	H_2O	5×10^{-5} M	Sigma-Aldrich (A8960)
HEP	Heparin sodium salt	H_2O	14 U/ml	Sigma-Aldrich (H3393)
GABA	γ-Aminobutyric acid	H_2O	10 µg/ml	Sigma-Aldrich (A2129)

NOTE: Stock solutions of RA (1.7×10-2 M), DXM (7.5×10-2 M), and MNX (2.7×10-1 M) were prepared in DMSO. These stock solutions were subsequently diluted in cell culture media to achieve the desired working concentrations, leading to a concentration of 0.006%, 0.013%, and 0.037% of DMSO in culture medium for the three compounds. Similarly, stock solutions of TGF-β1 (1.0 µg/ml), IGF-1 (1.0 mg/ml), CuSO4 (1.0×10-3 M), MAP (7.4×10-2 M), HEP (2.1×103 U/ml), and GABA (5.0 mg/ml) were prepared in aqueous solution and subsequently diluted in cell culture media for the experiments.

2.2. Cell viability experiment & analysis

To evaluate the impact of elastogenic compounds on the viability of primary human dermal fibroblasts (n = 4 donors), cells were seeded at a low density (9,000 cells per well) in 48-well plates. After 5-6 hours, once attached, the medium was replaced with serum-deprived (0.5% FBS) medium for 24 h, followed by culture in 1% FBS medium (Figure 1). Cell viability was assessed in separate plates on day 0 (before adding compounds) and on days 1 and 3. 10% solution of alamarBlue Cell Viability Reagent (Invitrogen, Carlsbad, CA, USA) was added to the culture medium, and the cells were incubated for 4 h at 37°C with 5% CO_2. Fluorescence intensity was measured using a SpectraMax iD3 plate reader (Molecular Devices, CA, USA) with an excitation wavelength of 540 nm and emission at 590 nm.

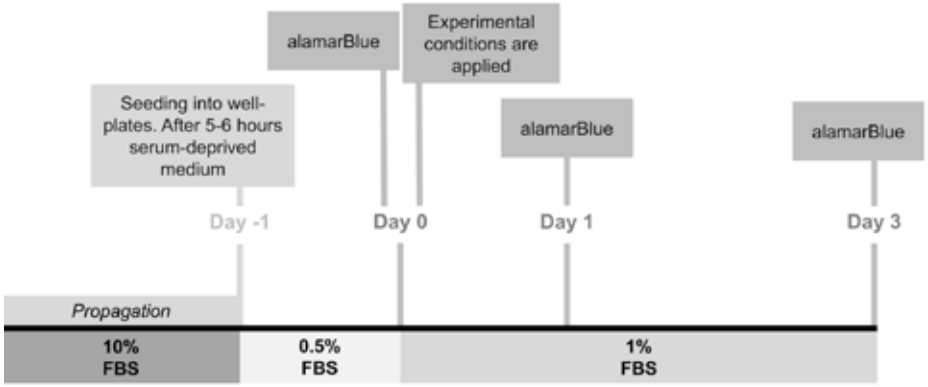

Figure 1. Experimental setup for alamarBlue Cell Viability Assay.

2.3. ECM production experiments & analyses

Figure 2 depicts the timeline of the experiments for the elastogenesis experiment, where fibroblasts were seeded in 12-well plates (for RT-qPCR and Fastin Elastin) and 24-well plates (for all other methods; 60,000 and 30,000 cells per well, respectively). After 5-6 h of attachment, cells were starved (0.5% FBS) for 24 h, then cultured in 2% FBS medium until day 12 and 5% FBS medium until day 24. By examining different time points, we can build a comprehensive picture of cellular responses, from initial gene activation (RT-qPCR) to newly synthesized proteins (immunostaining and Western Blot) and long-term protein expression changes (Picrosirius Red and Fastin Elastin).

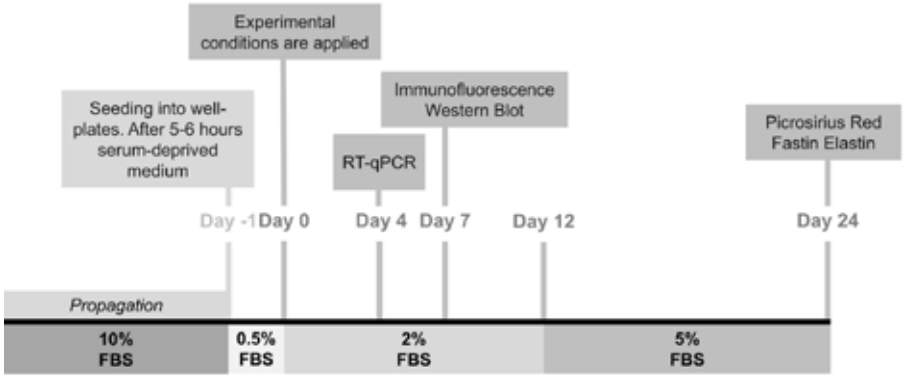

Figure 2. Experimental setup for testing the effects of elastogenic compounds on primary human dermal fibroblasts.

2.3.1. RNA isolation, cDNA synthesis, and gene expression analysis by real-time qPCR

Cellular RNA was extracted from samples collected on day 4 using Trizol reagent. It was followed by chloroform treatment, centrifugation (12,000 × g, 4°C, 15 min), and two-fold dilution with 70% ethanol. Further RNA purification was performed using the RNeasy mini kit (Qiagen, Hilden, Germany) according to the manufacturer's instructions. The RNA quality and concentration were assessed with a NanoDrop ND-1000 spectrophotometer (NanoDrop Technologies, Wilmington, DE, USA) by measuring absorbance ratios at 230, 260, and 280 nm. The isolated RNA was then reverse-transcribed into first-strand cDNA using the iScript cDNA synthesis kit (Bio-Rad Laboratories Inc., Hercules, CA, USA), following the manufacturer's instructions.

Expression levels of 10 genes involved in ECM production were analyzed: *ACTA2, COL1A1, ELN, FN1, FBN1, FBN2, FBLN4, FBLN5, LOX,* and *HMCN1* (Table S1). *YWHAZ* and *GAPDH* were used as reference genes. RT-qPCR primers were designed based on human gene sequences.

PCR amplifications were carried out in duplicate using SYBR Green I master mix (Bio-Rad Laboratories) under the following conditions: 3 min at 95°C, followed by 40 cycles of 15 s at 95°C and 30 s at 60°C (with plate readings). The final steps included 1 min at 95°C and 1.5 min at 65°C. The reactions were run on a CFX Connect Real-Time PCR Detection System (Bio-Rad Laboratories). Data were analyzed using CFX Maestro™ Software (Bio-Rad Laboratories) and visualized with GraphPad Prism (v. 10.4.1, GraphPad Software, Boston, Massachusetts USA, www.graphpad.com). Relative gene expression levels were calculated using the ΔΔCT method.

2.3.2. SDS-PAGE and Western blot analysis

On day 7, cells were dissolved by adding 200 µl of reducing sample buffer to the well plate. The samples were heated at 95°C for 5 min, and 10 µl was separated on a 10% polyacrylamide gel via SDS-PAGE. A molecular weight marker, PageRuler™ Plus Prestained Protein Ladder, was included. Electrophoresis was run at 130 V for 60 min.

Following SDS-PAGE, proteins were transferred to nitrocellulose membranes for Western blotting and immunostaining at room temperature. Membranes were blocked overnight at 4°C with 2% bovine serum albumin in PBST (PBS with 0.1% Tween-20) to prevent non-specific binding. Primary antibodies, monoclonal mouse anti-alpha smooth muscle actin (dilution 1:1,000, Table S2) and monoclonal rabbit anti-GAPDH antibody (1:1,000 dilution, Cell Signaling, USA, 2118), were diluted in blocking buffer and incubated with the membranes for 1 h. After washing with

PBST, membranes were incubated with secondary antibodies, goat polyclonal anti-mouse IgG (H+L) conjugated to IRDye 800CW (LI-COR Biotechnology, Lincoln, NE, USA, 926-32210) and goat anti-rabbit IgG (H+L) conjugated to IRDye 680CW (LI-COR Biotechnology, 926-68071), at a 1:20,000 dilution for 1 h. GAPDH was used as an internal loading control. Signals were detected using the LI-COR® Odyssey® CLx Infrared Imaging System and analyzed with Image Studio™ Software 5.0. Values of signals of interest were normalized by dividing the target protein signal by the internal loading control to exclude discrepancies due to variations in sample loading or protein transfer. Values were subsequently normalized to the experimental control.

2.3.3. Immunofluorescence staining

On day 7, heparan sulfate (HS), versican (VCAN), neuraminidase-1 (NEU-1), and protective protein cathepsin A (PPCA) were visualized at room temperature by immunofluorescence staining on cells fixed with 4% paraformaldehyde in PBS for 10 min. For intracellular detection of α-smooth muscle actin (α-SMA), cells were permeabilized with 0.5% Triton X-100 in PBS for 10 min. The cells were blocked in PBS containing 2% bovine serum albumin for 1 h before incubation with primary antibody (see Table S2, Supporting Information) for 1 h. After washing, cells were incubated with a corresponding secondary antibody for 1 h (Table S2). Nuclei were stained with DAPI (1 µg/ml), and all washes were performed with PBST. Finally, cells were mounted using Mowiol and imaged with a Zeiss Axio Imager A2 microscope (Zeiss Group, Oberkochen, Germany) using Zen 2 (Blue Edition) software.

2.3.4. Picrosirius Red staining

On day 24, collagen protein deposition was assessed using Picrosirius Red staining. Due to an insufficient amount of MNX, it was excluded from this analysis. Cells were first fixed with 3.7% formaldehyde and 2% glacial acetic acid in 28% aqueous ethanol for 10 min. After a single PBS wash, the samples were stained with a solution of Direct Red 80 dissolved in saturated aqueous picric acid (12.5 mg/ml) for 3 h. Excess stain was removed with repeated washes until the rinse water became clear. Brightfield imaging was performed using a Zeiss Axio Imager A2 microscope with Zen 2 software. For quantification, the dye was eluted by incubating the samples with a destaining solution (0.1 M NaOH in 50% aqueous methanol) for 10 min with continuous shaking. The eluted dye was collected in duplicate, and optical density was measured at 540 nm using a SpectraMax iD3 plate reader.

2.3.5. Fastin Elastin assay

The Fastin Elastin Kit (Biocolor, Carrickfergus, UK) was used to measure elastin content in cell culture experiments by day 24, following the manufacturer's protocol. Due to

insufficient quantities of MNX, it was excluded from this analysis. α-elastin standards from the kit (12.5, 25, and 50 µg) were prepared to quantify elastin levels in the samples. Elastin samples were collected by adding 500 µl 0.25 M oxalic acid to the cells, followed by manual scraping of the wells. To solubilize elastin, the samples were treated with oxalic acid at 95°C for 3 h, and the obtained solutions were centrifuged at 13,000 × g for 10 min at room temperature. Aliquots of the supernatant (200 µl) were used to quantify elastin content according to the manufacturer's instructions.

2.4. Statistical analysis

In the graphical figures, individual donors are represented by distinct symbols, which remain consistent across all analyses. For example, if a donor is represented by a circle in one graph, the same symbol is used for that donor in all other graphs. Statistical testing was performed in GraphPad Prism. Relative measurements, normalized to the control condition without DMSO, were compared using a one-sample t-test. A p-value of <0.05 (95% confidence interval) was considered statistically significant. To assess potential solvent-related effects, RA, DXM, and MNX (all dissolved in DMSO) were compared to the DMSO control using one-way ANOVA, followed by Tukey's multiple comparisons test. For the cell viability assay, group comparisons were conducted using two-way ANOVA, followed by Tukey's multiple comparisons test.

3. Results

To assess cell viability following treatment with elastogenic compounds and to exclude cytotoxic effects, an alamarBlue assay was performed at day 0, 1, and 3 (Figure 3A). Despite minor fluctuations in cellular activity, compounds did not show cytotoxicity compared to the control at the same timepoint. Cells exhibited clear signs of proliferation and metabolic activity by day 3, which was significantly increased from day 1 ($p<0.001$). The 0.04% DMSO control did not affect cell proliferation either. The viability of the cells stimulated with IGF-1 was notably higher than with MNX.

Microscopic examination of cell growth and morphology revealed that certain compounds influenced the shape of human primary dermal fibroblasts by day 11 (Figure 3B). Specifically, treatments with IGF-1 and HEP caused the cells to obtain a rounded morphology, although they remained viable. RA had the most pronounced impact, making cells extremely thin, followed by DXM to a lesser extent. This morphological effect was particularly noticeable under serum-deprived conditions. However, by the end of the 24-day experiment, no morphological differences could be observed anymore.

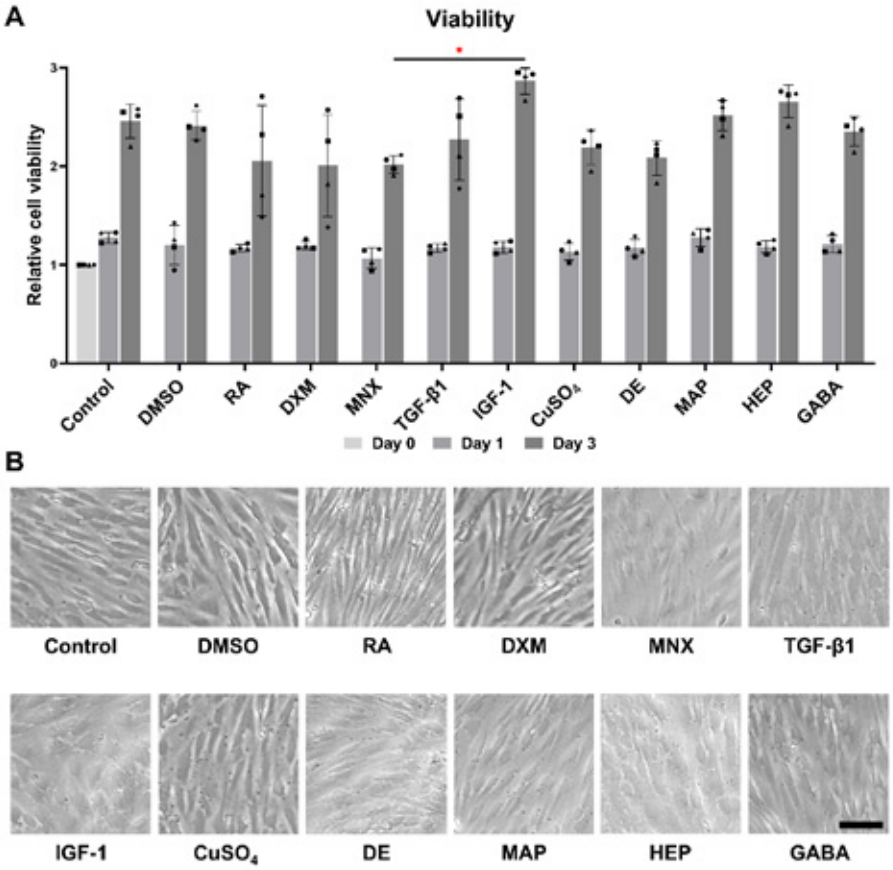

Figure 3. Cellular viability and appearance in the presence of elastogenic compounds (n = 4 donors). A) Relative cell viability measured with alamarBlue assay at day 0, 1, and 3. Cell viability on day 3 was significantly higher than at day 1 for all tested conditions ($p<0.001$). Values are normalized to control (medium without compound) at day 0. Individual donors are represented by different symbols. Error bars represent standard deviation. * $p<0.05$. B) Light microscopical pictures of representative images of fibroblasts from the elastogenesis experiment on day 11. Scale bar is 100 µm. DMSO = dimethyl sulfoxide, RA = retinoic acid, DXM = dexamethasone, MNX = minoxidil sulfate, TGF-β1 = transforming growth factor-β1, IGF-1 = insulin-like growth factor-1, DE = dill extract, MAP = magnesium ascorbyl phosphate, HEP = heparin, GABA = γ-aminobutyric acid.

One of the key objectives of our study was to compare the effects of different elastogenic compounds on dermal fibroblasts under identical conditions. Gene expression analysis of key markers involved in elastic fiber synthesis, including genes associated with tropoelastin and microfibrillar components, showed statistically significant changes on day 4 for some conditions (Figure 4A). TGF-β1 demonstrated the highest potency in *ELN* gene upregulation, as well as enhanced expression of *FBN1*, *FN1*, and *HMCN1*. The second strongest positive impact on *ELN* gene expression was seen with IGF-1 stimulation, although significant downregulation was noted in *FBLN4* and *FBLN5* genes. DXM showed *ELN* gene upregulation compared to DMSO control, accompanied by a significant expression increase in *FBLN5*, *FBN2*, and *FN1*, but also induced a significant decrease in *HMCN1*. RA showed enhanced expression of *HMCN1* and a tendency in the upregulation of *FBN2* (p=0.08). In contrast, HEP demonstrated notable downregulation of *ELN* and *FN1*. DE had a negative effect on *FBLN5*, *FBN1*, and *HMCN1*, however it was accompanied by notable upregulation of *FBN2*. While lysyl oxidase is involved in the synthesis of both elastic and collagen fibers, there were no indications of LOX gene upregulation in this experiment. In contrast, MNX significantly decreased LOX expression, while IGF-1 and DE induced a trend towards LOX expression reduction. Protein analysis of elastin revealed that enhanced elastin production was found in DXM, DE, IGF-1, TGF-β1, RA, HEP, and CuSO4. Thus, DXM, TGF-β1, and IGF-1 demonstrated successful translation of elevated gene expression into protein deposition (Figure 4B). Interestingly, RA and DE led to significant elastin protein overexpression, despite the absence of corresponding changes at the gene-expression level, while HEP, even more surprisingly, decreased *ELN* mRNA levels yet still resulted in elevated elastin protein expression.

Immunostaining for PPCA and NEU-1, two lysosomal components that are also part of the elastin receptor complex (ERC) and implicated in elastic fiber synthesis, did not reveal notable differences between compounds (Figure 5). Control samples appeared to have less signal for NEU-1. Both proteins exhibited both individual and co-localized staining patterns, suggesting that the ERC may be located in regions where these signals overlap. PPCA formed a filamentous, cytoplasmic network, while NEU-1 appeared in small punctate structures, suggesting a lysosomal or vesicular localization. Both PPCA and NEU-1 showed the highest intensities near the perinuclear region, further supporting a mostly intracellular localization. However, due to the limitations of conventional fluorescence microscopy, an extracellular or more dispersed intracellular distribution cannot be fully excluded.

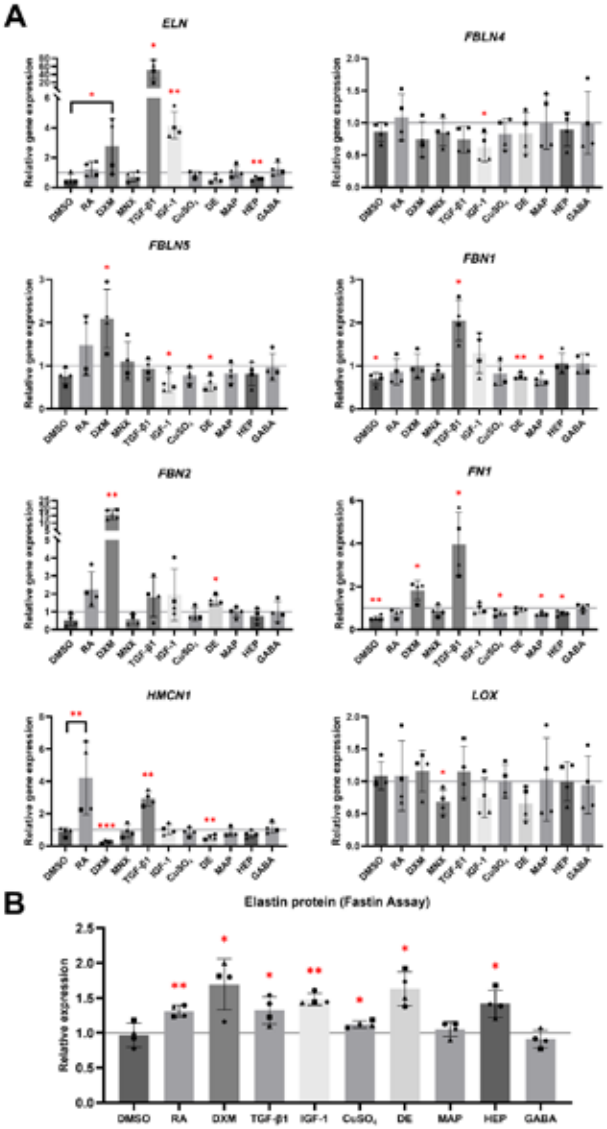

Figure 4. Assessment of elastogenesis by primary human dermal fibroblasts (n = 4 donors). A) Relative expression of genes related to elastic fiber synthesis at day 4 normalized to the control without DMSO. Statistical significance between DMSO and DXM was determined by one-way ANOVA with Tukey's post hoc test. B) Relative elastin protein expression at day 24 measured with Fastin Elastin assay. Individual donors are represented by different symbols. Error bars represent standard deviation. Statistical significance was determined using a one-sample t-test comparing each treatment group to the control without DMSO. * $p<0.05$, ** $p<0.01$, *** $p<0.001$. DMSO = dimethyl sulfoxide, RA = retinoic acid, DXM = dexamethasone, MNX = minoxidil sulfate, TGF-β1 = transforming growth factor-β1, IGF-1 = insulin-like growth factor-1, DE = dill extract, MAP = magnesium ascorbyl phosphate, HEP = heparin, GABA = γ-aminobutyric acid.

We further investigated the impact of tested compounds on collagen synthesis, another essential process in ECM deposition and remodeling after skin injury. Gene expression analysis of type I collagen, the predominant ECM protein in adult skin, revealed two statistically significant differences in gene upregulation (Figure 6A). TGF-β1 and IGF-1 exhibited the strongest stimulatory effects at the mRNA level of type I collagen compared to the control. RA stimulated *COL1A1* gene expression compared to DMSO (vehicle) control (p=0.05). Picrosirius Red staining on day 24 supported the RT-qPCR results on day 4, demonstrating significantly increased collagen deposition with TGF-β1, IGF-1, and RA (Figure 6B). Additionally, DXM, DE, and HEP promoted collagen synthesis in fibroblasts. While IGF-1 and DE demonstrated statistical tendency of LOX gene downregulation (Figure 4A), it did not result in suppressed collagenesis and, on the contrary, significantly increased collagen proteins expression (Figure 6B). Notably, collagen deposition patterns varied among compounds (Figure 6C). DE resulted in the largest collagen clusters visually seen, while TGF-β1 and HEP led to a more uniform collagen distribution (Figure 6C).

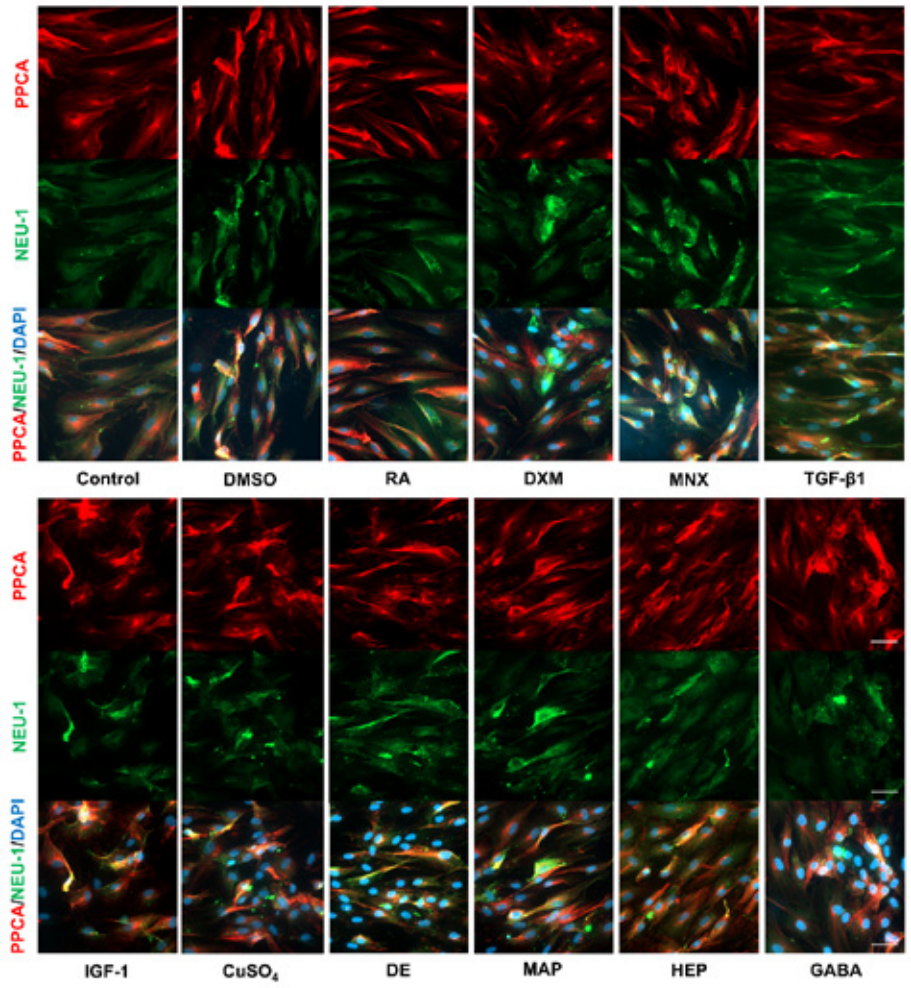

Figure 5. Immunofluorescent analysis of PPCA (red) and NEU-1 (green) of primary human dermal fibroblasts cultured with potentially elastogenic compounds at day 7 (n = 4 donors). Cell nuclei were stained with DAPI (blue). Scale bar is 50 µm. DMSO = dimethyl sulfoxide, RA = retinoic acid, DXM = dexamethasone, MNX = minoxidil sulfate, TGF-β1 = transforming growth factor-β1, IGF-1 = insulin-like growth factor-1, DE = dill extract, MAP = magnesium ascorbyl phosphate, HEP = heparin, GABA = γ-aminobutyric acid.

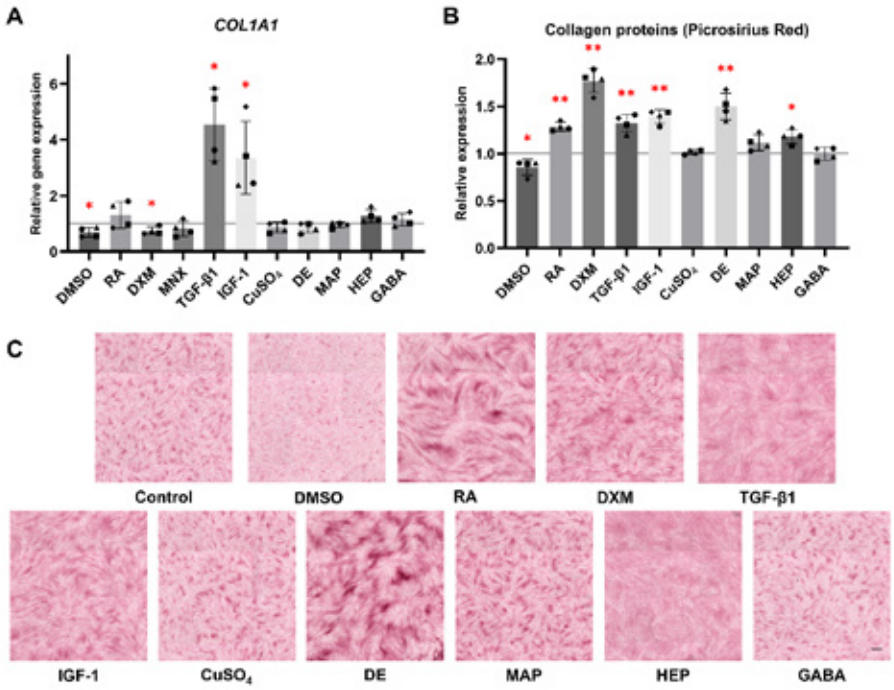

Figure 6. Evaluation of collagenesis by primary human dermal fibroblasts (n = 4 donors). A) Relative expression of COL1A1 gene at day 4. Individual donors are represented by different symbols. B) Relative collagen protein expression at day 24 measured with Picrosirius Red staining. Error bars represent standard deviation. Statistical significance was determined using a one-sample t-test comparing each treatment group to the control without DMSO. * $p<0.05$, ** $p<0.01$. C) Light microscopical images of Picrosirius Red staining. Scale bar is 500 µm. DMSO = dimethyl sulfoxide, RA = retinoic acid, DXM = dexamethasone, MNX = minoxidil sulfate, TGF-β1 = transforming growth factor-β1, IGF-1 = insulin-like growth factor-1, DE = dill extract, MAP = magnesium ascorbyl phosphate, HEP = heparin, GABA = γ-aminobutyric acid.

Another aspect of our study was assessing the potential of elastogenic compounds to influence fibrosis. Although fibrosis is a multifaceted process involving inflammation, various cell types, and extracellular matrix components such as collagens, laminin, and fibronectin [76], we focused on *ACTA2* gene expression and its protein product α-SMA as representative markers. α-SMA is a well-established indicator of myofibroblast activation while driving matrix deposition and tissue remodeling during fibrotic progression, making it a relevant and practical marker for assessing fibrogenic activity [77, 78]. Consistent with its well-documented role, TGF-β1 upregulated *ACTA2* gene expression ranging from 3- to 14-fold across donors (p=0.16, Figure 7A). In contrast, DE exhibited *ACTA2* downregulation, while gene expression was similar between DMSO and MNX. Western blot analysis

confirmed a significant reduction in α-SMA protein expression under DE condition (Figure 7B-C and Figure S1). IGF-1 also demonstrated less α-SMA protein expression compared to the control. While DXM and MNX showed statistically significant decreases compared to the untreated control, their effects were similar to DMSO control. TGF-β1 induced a trend towards upregulation of α-SMA protein expression at least 2-fold, although high donor-to-donor variability compromised statistical significance in both protein and gene expression analyses ($p=0.19$ and $p=0.16$, respectively). Immunostaining for actin filaments and α-SMA further confirmed the notable stimulatory effect of TGF-β1 (Figure 7D). Additionally, HEP, RA, and MAP showed some sporadic α-SMA-positive staining compared to controls (Figure 7D).

Furthermore, we used immunostaining to analyze the deposition of glycosaminoglycan heparan sulfate (HS) and the chondroitin sulfate proteoglycan versican (VCAN). Among the tested conditions, TGF-β1 exhibited the most pronounced HS staining, which was spread widely throughout the extracellular space, forming an interconnected fibrillar pattern (Figure 8A). Moreover, DXM, $CuSO_4$, MAP, and GABA displayed less pronounced fibrillar expression of HS that were similar to each other. In contrast, DE, HEP, and IGF-1 showed minimal HS staining, which was mainly found on the cell surface of fibroblasts and was comparable to the control. With regards to versican staining, TGF-β1 induced the highest expression in fibrillar structures in the extracellular matrix, followed by DXM, DE, and HEP (Figure 8B). All other conditions remained comparable to controls.

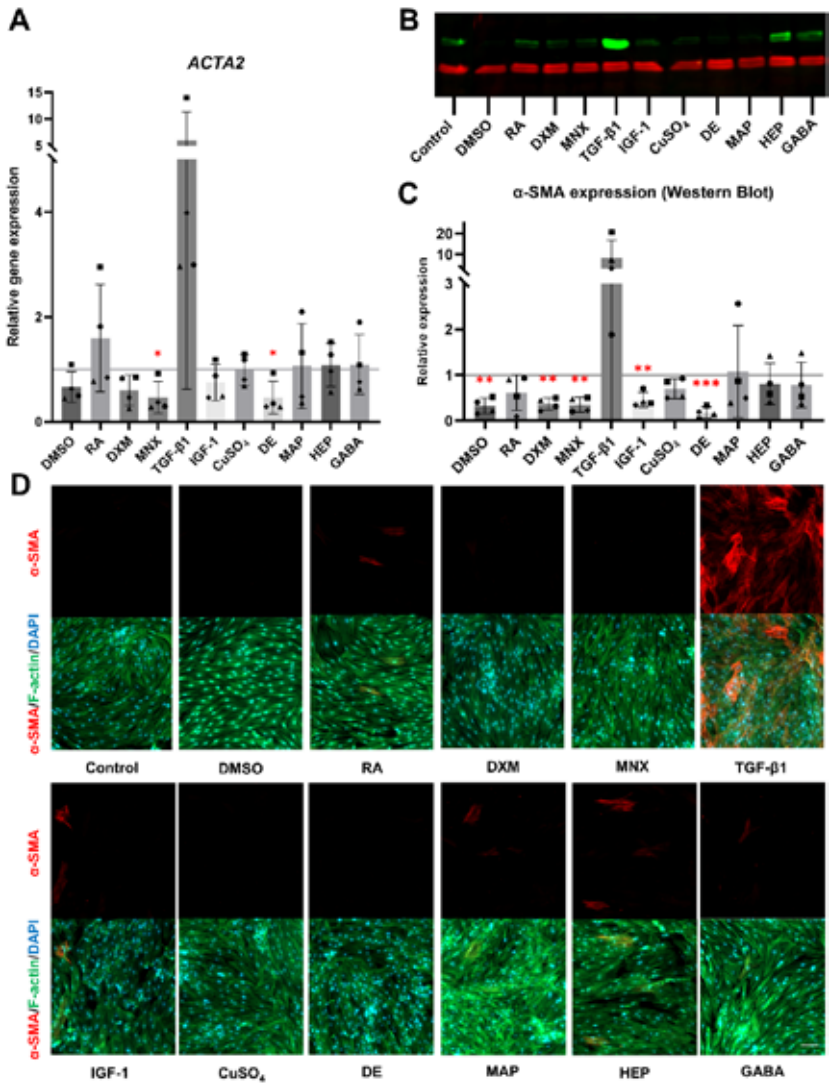

Figure 7. Investigation of fibrotic responses assessed with α-SMA expression of different elastogenic compounds in primary human dermal fibroblasts (n = 4 donors). A) Relative expression of ACTA2 gene at day 4. Individual donors are represented by different symbols. B) Representative Western blot staining for α-SMA (green) from one donor at day 7. GAPDH was used as an internal control (red). C) Quantitative analysis of normalized Western blot results from 4 donors. Error bars represent standard deviation. Statistical significance was determined using a one-sample t-test comparing each treatment group to the control without DMSO. * $p<0.05$, ** $p<0.01$, *** $p<0.001$. D) Immunofluorescent staining of α-SMA (red) and filamentous actin (green) from one donor at day 7. Cell nuclei were stained with DAPI (blue). Scale bar is 100 µm. α-SMA = α-smooth muscle actin, DMSO = dimethyl sulfoxide, RA = retinoic acid, DXM = dexamethasone, MNX = minoxidil sulfate, TGF-β1 = transforming growth factor-β1, IGF-1 = insulin-like growth factor-1, DE = dill extract, MAP = magnesium ascorbyl phosphate, HEP = heparin, GABA = γ-aminobutyric acid.

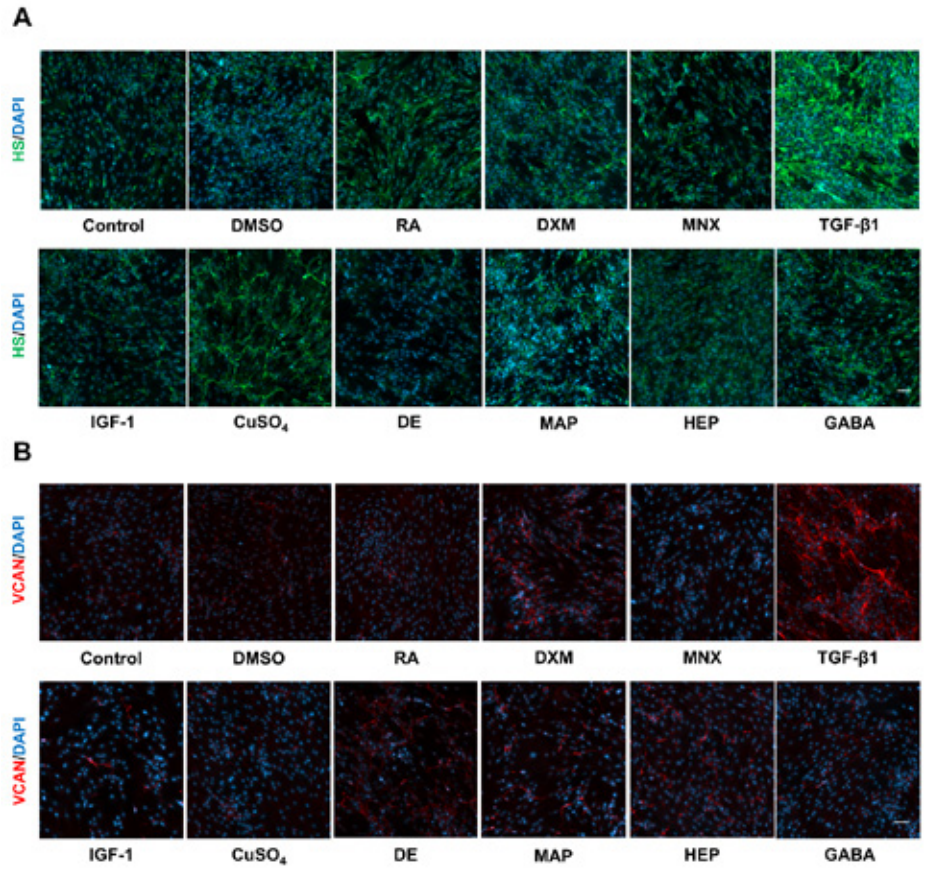

Figure 8. Analysis of heparan sulfate (HS) and versican (VCAN) expression in primary human dermal fibroblasts at day 7 (n = 4 donors). A) Immunofluorescent analysis of HS (green). B) Immunofluorescent analysis of VCAN (red). Cell nuclei were stained with DAPI (blue). Scale bars are 100 µm. Images are representative depictions of one donor. DMSO = dimethyl sulfoxide, RA = retinoic acid, DXM = dexamethasone, MNX = minoxidil sulfate, TGF-β1 = transforming growth factor-β1, IGF-1 = insulin-like growth factor-1, DE = dill extract, MAP = magnesium ascorbyl phosphate, HEP = heparin, GABA = γ-aminobutyric acid.

4. Discussion

Selecting the most potent elastogenic compound is a challenging task, particularly for specific applications such as dermal regeneration. As we reported [9], various classes of compounds exhibit elastogenic properties. These effects have been studied across different organisms, cell types, and experimental conditions. Our current research focuses on comparing these compounds under the same conditions, specifically limiting the investigation to primary human normal adult skin fibroblasts. DXM, DE, IGF-1, HEP, RA, and TGF-β1 showed the most promising elastogenic and collagenic effects under the selected culture conditions. In contrast, the impacts of MNX, $CuSO_4$, MAP, and GABA on dermal fibroblasts were negligible.

Dexamethasone, a powerful synthetic glucocorticoid, has widespread clinical applications, making it an invaluable tool in medical treatment. It is known to suppress collagen and hyaluronic acid production in human skin fibroblast cell lines [79, 80], but its impact on elastin synthesis remains unclear. One study found that injecting dexamethasone into rabbit vocal fold injuries did not change elastin levels [35], whereas *in vitro* experiments using fibroblasts from bovine *ligamentum nuchae* showed a threefold increase in elastin production [37], particularly in older bovine fibroblasts [38]. Conversely, this glucocorticoid has been reported to reduce elastin mRNA expression in normal human fibroblasts [39, 40]. In our experiments, DXM demonstrated one of the strongest effects by stimulating both collagen and elastin production without inducing α-SMA. However, as a corticosteroid, its broad systemic effects may pose limitations [81]. Nevertheless, low-dose topical formulations (0.1% cream) have shown minimal potency compared to other corticosteroids [82]. Hence, DXM holds potential in biomaterial application with local application to a wound site.

Natural extracts represent another class of elastogenic compounds, often composed of complex bioactive mixtures with unique properties distinct from their individual components. Dill extract, for instance, protects the skin's elastic network by inhibiting degradation by elastase in injured mice [58]. The extract enhances LOXL-1 gene expression together with stimulating elastin production when applied to human skin fibroblasts [59]. Moreover, combining dill and blackberry extracts further enhanced elastogenesis in dermal fibroblasts and demonstrated positive effects in clinical trials [60]. Our results show that DE promoted both elastin and collagen production by dermal fibroblasts, but most importantly, it showed the highest potency in reducing α-SMA expression. It is noteworthy that the composition of the extract can be substantially altered by a variety of crucial

factors, such as climate, cultivar selection, seeding dates, harvest timing, and management practices [83]. Key constituents include α-phellandrene, limonene, p-cymene, dill ether, myristicin, and dillapiole, though their relative proportions vary significantly. Further analysis of these compounds may provide deeper insight into the mechanisms underlying elastogenic effects of DE.

IGF-1 is a potent growth factor with elastogenic properties, primarily studied in smooth muscle cells [19, 21]. Interestingly, when tested on pulmonary fibroblasts, no elastogenic response was seen [20]. In dermal fibroblasts, elastogenesis appeared to be driven by robust signaling pathways initiated through the activation of the IGF-1 receptor [12]. Our results confirm a significant elastogenic effect of IGF-1 on dermal fibroblasts. Although IGF-1 offers promising benefits, its clinical translation poses concerns due to serious side effects, including an increased risk of cancer development [84].

Heparan sulfate is known to facilitate microfibril assembly through interactions with fibrillin-1 [85]. Heparin, a structurally similar glycosaminoglycan, mediates tropoelastin coacervation and inhibits elastase activity [86, 87]. This compound enhanced elastin mRNA expression and elastic fiber production across various cell culture experiments with and without biomaterials [71, 88]. Our findings are consistent with these observations. Notably, cells from one donor had higher α-SMA protein expression under HEP condition than the control, indicating possible donor-specific sensitivity to the HEP condition. The safety concerns with heparin are possible thrombocytopenia or excessive bleeding, which is a direct consequence of its powerful anticoagulant properties [89].

All-trans retinoic acid, a derivative of vitamin A, was reported to be advantageous for elastin production by chicken embryonic dermal fibroblasts [52], neonatal rat lung fibroblasts [53], and a human foreskin fibroblast cell line [90]. Regarding human dermal fibroblasts, encapsulation of retinoic acid in nanoparticles significantly reduced cytotoxicity in these cells [90]. Moreover, it effectively minimized skin damage (erythema, swelling, and flaking) in a nude mouse model following the topical application of these nanoparticles, in contrast to free retinoic acid [90]. In our experiments, we noticed an effect on fibroblast morphology. Despite the apparent recovery, the possibility of subtle or delayed long-term effects cannot be excluded and may require further investigation. Similar morphological alterations were observed with other fibroblast types that were exposed to retinoic acid [91, 92] and were associated with reduced proliferation and increased cellular adhesion. Topical application of retinoids is known to be able to cause retinoid dermatitis in

patients. Nevertheless, RA showed elastogenic potency with slight indications of α-SMA expression induction, however, the pro-fibrotic effects of the compound remain ambiguous [93]. Notably, topical application of retinoids is known to cause retinoid dermatitis in patients [94], highlighting a clinical consideration for the use of RA.

TGF-β1 is a well-established regulator of wound healing, with strong preclinical evidence supporting its efficacy. Local application enhanced tissue repair in different animal models [95, 96], and systemic administration accelerated healing in middle-aged rats with incisional wounds [97]. We have observed strong positive HS and VCAN staining with TGF-β1. HS was reported to regulate the signaling of different fibroblast growth factors and other heparin-binding growth factors involved in fibrosis, such as vascular endothelial growth factor, epidermal growth factor, hepatocyte growth factor, TGF-α, and connective tissue growth factor [98]. VCAN is known to play a crucial role in ECM production and fibroblast regulation [99]. It binds to CD44, integrin β1, epidermal growth factor receptor, and P-selectin glycoprotein ligand-1, subsequently affecting cell differentiation and ECM remodeling [100]. Extensive research also highlighted the important role of TGF-β isoforms in scar formation during wound healing [101]. While some preclinical evidence revealed that excessive TGF-β1 levels can worsen scarring, TGF-β3 promoted scar-free healing [102], although topical application of TGF-β3 can still induce TGF-β1 expression, leading to scar formation [103]. Our findings confirm the potent ECM-stimulating properties of TGF-β1, though its pro-fibrotic potential limits its translational application.

Despite MNX, $CuSO_4$, MAP, and GABA demonstrated negligible effects in our experimental conditions on primary dermal fibroblasts, their bioactivity may be used in other therapeutic areas, or they may require specific conditions. For instance, minoxidil, a potassium channel opener, showed promise in the stimulation of cardiovascular elastic fiber formation [41, 104, 105]. Copper is vital for skin homeostasis as a key cofactor for lysyl oxidase enzymes [46, 47], although it exerted a synergistic elastogenic effect on dermal fibroblasts when combined with amino acid mixtures (e.g., glycine, proline, alanine, valine, leucine, lysine) [49]. Vitamin C (L-ascorbic acid) is mainly recognized for its positive effect on collagen synthesis *in vitro* and was thought to have a mainly inhibitory effect on elastin synthesis due to hydroxylation of proline residues, reduced elastin mRNA stability, and inhibited elastin gene transcription [106]. Despite some studies suggesting vitamin C and its derivatives can enhance elastogenesis in certain models [54-57, 107], our findings with a stable derivative (MAP) did not indicate significant collagenic effects or elastogenic capabilities. γ-aminobutyric acid, known as an inhibitory

neurotransmitter, was reported to upregulate elastogenic genes and promote elastic fiber formation in human dermal fibroblasts [65], but our findings did not confirm this.

Various biodegradable and biocompatible biomaterials have been utilized as dermal substitutes, including natural polymers (collagen, gelatin, elastin, hyaluronan, chitosan, silk, fibrin, pullulan), synthetic polymers (polylactic acid, poly(lactic-co-glycolic) acid, polycaprolactone, polyethylene glycol, polyurethane), and composite scaffolds [108-110]. Modifications in composition, surface properties, degradation rates, and delivery methods enhance efficacy at the target site [111]. Additionally, these biomaterials can be engineered as drug depots, enabling covalent binding or localized release of active compounds [112]. Such adjustments help mitigate potential risks of systemic adverse effects, including immunogenicity and carcinogenicity, associated with certain elastogenic compounds while ensuring controlled and localized therapeutic action.

Our study has several limitations. Our investigation of the absolute effects of RA, DXM, and MNX is complicated by their limited solubility in water, necessitating the use of DMSO as a solvent. Although our experiments employed non-toxic concentrations (≤0.04%), DMSO is known to have various therapeutic actions [113], and it is able to influence ECM regulation at the gene level [114, 115]. A more relevant evaluation could be achieved by testing these compounds within biomaterial systems where DMSO is absent. Compound concentrations were selected based on literature data, and further assessments across a concentration range could help identify dose-dependent effects. Using primary fibroblasts from four different donors in this study reflected natural biological variability and enhanced the physiological relevance of our findings. However, donor-to-donor variation also showed differences in activity and, thus, higher standard deviations. Additionally, cell culture conditions could be optimized to enhance ECM production (e.g., 3D cell culture, higher FBS concentration, vitamin C supplementation, and addition of macromolecular crowders) rather than strictly evaluating the direct effects of individual compounds. Additional microscopical visualization of elastin and type I collagen could provide valuable insights into the architecture of synthesized fibers, potentially indicating not just protein deposition but also the formation of a functional ECM network. Moving forward, we aim to expand our compound list to include recombinant human tropoelastin [15, 69, 116, 117], low-molecular-weight hyaluronic acid [66, 69, 70], and recombinant LTBP-4 [118, 119], as they may also serve as potent elastogenic stimulators.

5. Conclusions

To our knowledge, this is the first study to systematically evaluate a large panel of compounds for their elastogenic effects on primary human dermal fibroblasts, identifying DXM, DE, IGF-1, HEP, RA, and TGF-β1 as the most potent. These compounds also demonstrated significant collagenic activity, making them promising candidates for advancing skin regeneration therapies and anti-aging treatments. However, the potential risks of systemic side effects, fibrosis, carcinogenicity, and morphological alterations associated with some of these compounds necessitate a cautious approach and additional examination.

References

1. Whitear, M., *Epidermis*, in *Biology of the Integument: 2 Vertebrates*, J. Bereiter-Hahn, A.G. Matoltsy, and K.S. Richards, Editors. 1986, Springer Berlin Heidelberg: Berlin, Heidelberg. p. 8-38.
2. Whitear, M., *Dermis*, in *Biology of the Integument: 2 Vertebrates*, J. Bereiter-Hahn, A.G. Matoltsy, and K.S. Richards, Editors. 1986, Springer Berlin Heidelberg: Berlin, Heidelberg. p. 39-64.
3. Uitto, J., D.R. Olsen, and M.J. Fazio, *Extracellular Matrix of the Skin: 50 Years of Progress.* Journal of Investigative Dermatology, 1989. **92**(4, Supplement): p. S61-S77.
4. Elsner, P., *Bioengineering of the skin : skin biomechanics*. Dermatology. 2002, Boca Raton: CRC Press. 296 p.
5. Imayama, S. and I.M. Braverman, *A hypothetical explanation for the aging of skin. Chronologic alteration of the three-dimensional arrangement of collagen and elastic fibers in connective tissue.* Am J Pathol, 1989. **134**(5): p. 1019-25.
6. Fratzl, P., *Collagen: Structure and Mechanics, an Introduction*, in *Collagen: Structure and Mechanics*, P. Fratzl, Editor. 2008, Springer US: Boston, MA. p. 1-13.
7. Mecham, R.P. and J.E. Heuser, *The Elastic Fiber*, in *Cell Biology of Extracellular Matrix: Second Edition*, E.D. Hay, Editor. 1991, Springer US: Boston, MA. p. 79-109.
8. Heinz, A., *Elastic fibers during aging and disease.* Ageing Research Reviews, 2021. **66**: p. 101255.
9. Krymchenko, R., et al., *Elastogenesis in Focus: Navigating Elastic Fibers Synthesis for Advanced Dermal Biomaterial Formulation.* Advanced Healthcare Materials, 2024. **13**(27): p. 2400484.
10. Tracy, L.E., R.A. Minasian, and E.J. Caterson, *Extracellular Matrix and Dermal Fibroblast Function in the Healing Wound.* Advances in Wound Care, 2016. **5**(3): p. 119-136.
11. Duca, L., et al., *The Elastin Receptor Complex Transduces Signals through the Catalytic Activity of Its Neu-1 Subunit *.* Journal of Biological Chemistry, 2007. **282**(17): p. 12484-12491.
12. Qa'aty, N., et al., *Synthetic ligands of the elastin receptor induce elastogenesis in human dermal fibroblasts via activation of their IGF-1 receptors.* Journal of Dermatological Science, 2015. **80**(3): p. 175-185.
13. Bunda, S., et al., *Aldosterone stimulates elastogenesis in cardiac fibroblasts via mineralocorticoid receptor-independent action involving the consecutive activation of Galpha13, c-Src, the insulin-like growth factor-I receptor, and phosphatidylinositol 3-kinase/Akt.* J Biol Chem, 2009. **284**(24): p. 16633-16647.
14. Kowara, M., et al., *MicroRNA regulation of extracellular matrix components in the process of atherosclerotic plaque destabilization.* Clinical and Experimental Pharmacology and Physiology, 2017. **44**(7): p. 711-718.
15. Almeida-González, F.R., et al., *A step closer to elastogenesis on demand; Inducing mature elastic fibre deposition in a natural biomaterial scaffold.* Materials Science and Engineering: C, 2021. **120**: p. 111788.
16. Taipale, J. and J. Keski-Oja, *Growth factors in the extracellular matrix.* The FASEB Journal, 1997. **11**(1): p. 51-59.
17. Yun, Y.-R., et al., *Fibroblast Growth Factors: Biology, Function, and Application for Tissue Regeneration.* Journal of Tissue Engineering, 2010. **1**(1): p. 218142.
18. Sproul, E.P. and W.S. Argraves, *A cytokine axis regulates elastin formation and degradation.* Matrix Biol, 2013. **32**(2): p. 86-94.

19. Foster, J.A., et al., *Effect of age and IGF-I administration on elastin gene expression in rat aorta.* J Gerontol, 1990. **45**(4): p. B113-8.
20. Rich, C.B., et al., *IGF-I regulation of elastogenesis: comparison of aortic and lung cells.* American Journal of Physiology-Lung Cellular and Molecular Physiology, 1992. **263**(2): p. L276-L282.
21. Wolfe, B.L., et al., *Insulin-like growth factor-I regulates transcription of the elastin gene.* Journal of Biological Chemistry, 1993. **268**(17): p. 12418-12426.
22. Liu, J.-m. and J.M. Davidson, *The elastogenic effect of recombinant transforming growth factor-beta on porcine aortic smooth muscle cells.* Biochemical and Biophysical Research Communications, 1988. **154**(3): p. 895-901.
23. Kähäri, V.M., et al., *Transforming growth factor-beta up-regulates elastin gene expression in human skin fibroblasts. Evidence for post-transcriptional modulation.* Lab Invest, 1992. **66**(5): p. 580-8.
24. Katsuta, Y., et al., *Fibulin-5 accelerates elastic fibre assembly in human skin fibroblasts.* Exp Dermatol, 2008. **17**(10): p. 837-42.
25. Zhang, M.C., et al., *Transforming growth factor-beta reverses a posttranscriptional defect in elastin synthesis in a cutis laxa skin fibroblast strain.* J Clin Invest, 1995. **95**(3): p. 986-94.
26. Yao, Z., et al., *A Marfan syndrome gene expression phenotype in cultured skin fibroblasts.* BMC Genomics, 2007. **8**: p. 319.
27. Davidson, J.M., O. Zoia, and J.-M. Liu, *Modulation of transforming growth factor-beta 1 stimulated elastin and collagen production and proliferation in porcine vascular smooth muscle cells and skin fibroblasts by basic fibroblast growth factor, transforming growth factor-a, and insulin-like growth factor-I.* Journal of Cellular Physiology, 1993. **155**(1): p. 149-156.
28. McGowan, S.E. and R. McNamer, *Transforming growth factor-beta increases elastin production by neonatal rat lung fibroblasts.* Am J Respir Cell Mol Biol, 1990. **3**(4): p. 369-76.
29. Kanzaki, T., et al., *In Vivo Effect of TGF-β1.* Arteriosclerosis, Thrombosis, and Vascular Biology, 1995. **15**(11): p. 1951-1957.
30. Budi, E.H., et al., *TGF-β as a driver of fibrosis: physiological roles and therapeutic opportunities.* The Journal of Pathology, 2021. **254**(4): p. 358-373.
31. Son, E.D., et al., *Topical application of 17beta-estradiol increases extracellular matrix protein synthesis by stimulating tgf-Beta signaling in aged human skin in vivo.* J Invest Dermatol, 2005. **124**(6): p. 1149-61.
32. Zong, W., et al., *Estradiol plays a role in regulating the expression of lysyl oxidase family genes in mouse urogenital tissues and human Ishikawa cells.* J Zhejiang Univ Sci B, 2015. **16**(10): p. 857-64.
33. Punnonen, R., P. Vaajalahti, and K. Teisala, *Local oestriol treatment improves the structure of elastic fibers in the skin of postmenopausal women.* Ann Chir Gynaecol Suppl, 1987. **202**: p. 39-41.
34. Moset Zupan, A., C. Nietupski, and S.C. Schutte, *Cyclic Adenosine Monophosphate Eliminates Sex Differences in Estradiol-Induced Elastin Production from Engineered Dermal Substitutes.* International Journal of Molecular Sciences, 2021. **22**(12): p. 6358.
35. Yildiz, M., et al., *Effects of Intracordal Estradiol and Dexamethasone Injection on Wound Healing in Vocal Fold Injuries.* J Voice, 2019. **33**(5): p. 759-766.
36. Mitts, T.F., et al., *Aldosterone and Mineralocorticoid Receptor Antagonists Modulate Elastin and Collagen Deposition in Human Skin.* Journal of Investigative Dermatology, 2010. **130**(10): p. 2396-2406.

37. Mecham, R.P., et al., *Elastin synthesis by ligamentum nuchae fibroblasts: effects of culture conditions and extracellular matrix on elastin production.* Journal of Cell Biology, 1981. **90**(2): p. 332-338.
38. Mecham, R.P., et al., *Glucocorticoids stimulate elastin production in differentiated bovine ligament fibroblasts but do not induce elastin synthesis in undifferentiated cells.* Journal of Biological Chemistry, 1984. **259**(20): p. 12414-12418.
39. Kähäri, V.M., *Dexamethasone suppresses elastin gene expression in human skin fibroblasts in culture.* Biochem Biophys Res Commun, 1994. **201**(3): p. 1189-96.
40. Russell, S.B., et al., *Glucocorticoid regulation of elastin synthesis in human fibroblasts: down-regulation in fibroblasts from normal dermis but not from keloids.* J Invest Dermatol, 1995. **104**(2): p. 241-5.
41. Slove, S., et al., *Potassium Channel Openers Increase Aortic Elastic Fiber Formation and Reverse the Genetically Determined Elastin Deficit in the BN Rat.* Hypertension, 2013. **62**(4): p. 794-801.
42. Hayashi, A., et al., *Minoxidil stimulates elastin expression in aortic smooth muscle cells.* Arch Biochem Biophys, 1994. **315**(1): p. 137-41.
43. Coquand-Gandit, M., et al., *Chronic Treatment with Minoxidil Induces Elastic Fiber Neosynthesis and Functional Improvement in the Aorta of Aged Mice.* Rejuvenation Research, 2017. **20**(3): p. 218-230.
44. Fhayli, W., et al., *Chronic administration of minoxidil protects elastic fibers and stimulates their neosynthesis with improvement of the aorta mechanics in mice.* Cellular Signalling, 2019. **62**: p. 109333.
45. Tsoporis, J., et al., *Arterial Vasodilation and Vascular Connective Tissue Changes in Spontaneously Hypertensive Rats.* Journal of Cardiovascular Pharmacology, 1998. **31**(6).
46. Borkow, G., *Using Copper to Improve the Well-Being of the Skin.* Current chemical biology, 2014. **8**(2): p. 89-102.
47. Harris, E.D., et al., *Copper and the Synthesis of Elastin and Collagen*, in *Ciba Foundation Symposium 79 - Biological Roles of Copper*. 1980. p. 163-182.
48. Kothapalli, C.R. and A. Ramamurthi, *Biomimetic regeneration of elastin matrices using hyaluronan and copper ion cues.* Tissue engineering. Part A, 2009. **15**(1): p. 103-113.
49. Chung, K.W., S.H. Song, and M.-s. Kim, *Synergistic effect of copper and amino acid mixtures on the production of extracellular matrix proteins in skin fibroblasts.* Molecular Biology Reports, 2021. **48**(4): p. 3277-3284.
50. Rossetti, D., et al., *A novel anti-ageing mechanism for retinol: induction of dermal elastin synthesis and elastin fibre formation.* International Journal of Cosmetic Science, 2011. **33**(1): p. 62-69.
51. Shao, Y., et al., *Molecular basis of retinol anti-ageing properties in naturally aged human skin in vivo.* International Journal of Cosmetic Science, 2017. **39**(1): p. 56-65.
52. Tajima, S., A. Hayashi, and T. Suzuki, *Elastin expression is up-regulated by retinoic acid but not by retinol in chick embryonic skin fibroblasts.* Journal of Dermatological Science, 1997. **15**(3): p. 166-172.
53. Liu, B., C.S. Harvey, and S.E. McGowan, *Retinoic acid increases elastin in neonatal rat lung fibroblast cultures.* American Journal of Physiology-Lung Cellular and Molecular Physiology, 1993. **265**(5): p. L430-L437.
54. Derricks, K.E., et al., *Ascorbate enhances elastin synthesis in 3D tissue-engineered pulmonary fibroblasts constructs.* Tissue and Cell, 2013. **45**(4): p. 253-260.
55. S. Tajima, H.W., A. Hayashi, *Accumulation of Tropoelastin by a Short-term Ascorbic Acid Treatment in the Culture Medium of Aortic Smooth Muscle Cells in vitro.* The Keio Journal of Medicine, 1995. **44**(4): p. 140-145.

56. Hinek, A., et al., *Sodium l-ascorbate enhances elastic fibers deposition by fibroblasts from normal and pathologic human skin.* Journal of Dermatological Science, 2014. **75**(3): p. 173-182.
57. Widgerow, A.D., et al., *Antioxidants with proven efficacy and elastin-conserving vitamin C-A new approach to free radical defense.* J Cosmet Dermatol, 2023.
58. Aimond, G., et al., *Dill extract preserves dermal elastic fibers network and functionality. Implication of elafin.* Skin Pharmacol Physiol, 2023.
59. Cenizo, V., et al., *LOXL as a target to increase the elastin content in adult skin: a dill extract induces the LOXL gene expression.* Experimental Dermatology, 2006. **15**(8): p. 574-581.
60. Meza, D., et al., *A blackberry–dill extract combination synergistically increases skin elasticity.* International Journal of Cosmetic Science, 2020. **42**(5): p. 444-451.
61. Sinha, A., N. Nosoudi, and N. Vyavahare, *Elasto-regenerative properties of polyphenols.* Biochemical and Biophysical Research Communications, 2014. **444**(2): p. 205-211.
62. Crandall, C.L., et al., *Pentagalloyl Glucose (PGG) Prevents and Restores Mechanical Changes Caused by Elastic Fiber Fragmentation in the Mouse Ascending Aorta.* Ann Biomed Eng, 2023. **51**(4): p. 806-819.
63. Chowdhury, A., et al., *Polyphenol treatments increase elastin and collagen deposition by human dermal fibroblasts; Implications to improve skin health.* Journal of Dermatological Science, 2021. **102**(2): p. 94-100.
64. Duckworth, C., et al., *Effect of ellagic acid and retinoic acid on collagen and elastin production by human dermal fibroblasts.* Biomed Mater Eng, 2023. **34**(5): p. 473-480.
65. Uehara, E., et al., *GABA promotes elastin synthesis and elastin fiber formation in normal human dermal fibroblasts (HDFs).* Bioscience, Biotechnology, and Biochemistry, 2017. **81**(6): p. 1198-1205.
66. Sylvester, A., et al., *Nanoparticles for localized delivery of hyaluronan oligomers towards regenerative repair of elastic matrix.* Acta Biomater, 2013. **9**(12): p. 9292-302.
67. D'Agostino, A., et al., *In Vitro Evaluation of Novel Hybrid Cooperative Complexes in a Wound Healing Model: A Step Toward Improved Bioreparation.* Int J Mol Sci, 2019. **20**(19).
68. D'Agostino, A., et al., *Potential of Biofermentative Unsulfated Chondroitin and Hyaluronic Acid in Dermal Repair.* Int J Mol Sci, 2022. **23**(3).
69. Mitzmacher, M.G., et al., *Novel Recombinant Tropoelastin Implants Restore Skin Extracellular Matrix.* Journal of drugs in dermatology : JDD, 2020. **19**(12): p. 1166-1172.
70. Kim, M.-S., et al., *Evaluation of the Efficacy of an Elastin-Inducing Composition Containing Amino Acids, Copper, and Hyaluronic Acid: Results of an Open Single-Center Clinical Trial Study.* Cosmetics, 2022. **9**(3): p. 51.
71. Saitow, C., D.L. Kaplan, and J.J. Castellot, *Heparin stimulates elastogenesis: Application to silk-based vascular grafts.* Matrix Biology, 2011. **30**(5): p. 346-355.
72. McGowan, S.E., R. Liu, and C.S. Harvey, *Effects of heparin and other glycosaminoglycans on elastin production by cultured neonatal rat lung fibroblasts.* Arch Biochem Biophys, 1993. **302**(2): p. 322-31.
73. Hinek, A., et al., *Retrovirally mediated overexpression of versican v3 reverses impaired elastogenesis and heightened proliferation exhibited by fibroblasts from Costello syndrome and Hurler disease patients.* Am J Pathol, 2004. **164**(1): p. 119-31.
74. Merrilees, M.J., et al., *Use of versican variant V3 and versican antisense expression to engineer cultured human skin containing increased content of insoluble elastin.* Journal of Tissue Engineering and Regenerative Medicine, 2017. **11**(1): p. 295-305.
75. Fhayli, W., et al., *Dill Extract Induces Elastic Fiber Neosynthesis and Functional Improvement in the Ascending Aorta of Aged Mice with Reversal of Age-Dependent Cardiac Hypertrophy and Involvement of Lysyl Oxidase-Like-1.* Biomolecules, 2020. **10**(2): p. 173.

76. Antar, S.A., et al., *Fibrosis: Types, Effects, Markers, Mechanisms for Disease Progression, and Its Relation with Oxidative Stress, Immunity, and Inflammation.* International Journal of Molecular Sciences, 2023. **24**(4): p. 4004.
77. Rockey, D.C., N. Weymouth, and Z. Shi, *Smooth Muscle α Actin (Acta2) and Myofibroblast Function during Hepatic Wound Healing.* PLOS ONE, 2013. **8**(10): p. e77166.
78. Kendall, R.T. and C.A. Feghali-Bostwick, *Fibroblasts in fibrosis: novel roles and mediators.* Frontiers in Pharmacology, 2014. **Volume 5 - 2014**.
79. Choi, D., et al. *β-Ionone Attenuates Dexamethasone-Induced Suppression of Collagen and Hyaluronic Acid Synthesis in Human Dermal Fibroblasts*. Biomolecules, 2021. **11**, DOI: https://doi.org/10.3390/biom11050619.
80. Oikarinen, A., E. Vuorio, and T. Vuorio, *Comparison of the effects of dexamethasone and 13-cis-retinoic acid on connective tissue biosynthesis in human skin fibroblasts.* Archives of Dermatological Research, 1989. **281**(4): p. 273-278.
81. Buchman, A.L., *Side Effects of Corticosteroid Therapy.* Journal of Clinical Gastroenterology, 2001. **33**(4): p. 289-294.
82. Hengge, U.R., et al., *Adverse effects of topical glucocorticosteroids.* Journal of the American Academy of Dermatology, 2006. **54**(1): p. 1-15.
83. Hah, S.-a.A. and O. Ea, *IMPACT OF CULTIVAR AND HARVEST TIME ON GROWTH, PRODUCTION AND ESSENTIAL OIL OF ANETHUM GRAVEOLENS CULTIVATED IN EGYPT.* International Journal of Pharmacy and Pharmaceutical Sciences, 2016. **8**(4): p. 54-60.
84. Bowers, L.W., et al., *The Role of the Insulin/IGF System in Cancer: Lessons Learned from Clinical Trials and the Energy Balance-Cancer Link.* Frontiers in Endocrinology, 2015. **6**.
85. Tiedemann, K., et al., *Interactions of Fibrillin-1 with Heparin/Heparan Sulfate, Implications for Microfibrillar Assembly*.* Journal of Biological Chemistry, 2001. **276**(38): p. 36035-36042.
86. Howard, V., M.M. Suzanne, and S.W. Anthony, *Elastin architecture.* Matrix Biology, 2019. **84**: p. 4-16.
87. Walsh, R.L., et al., *Heparin and heparan sulphate are inhibitors of human leucocyte elastase.* Clin Sci (Lond), 1991. **81**(3): p. 341-6.
88. Wachi, H., Y. Seyama, and S. Tajima, *Modulation of Elastin Expression by Heparin Is Dependent on the Growth Condition of Vascular Smooth Muscle Cells: Up-Regulation of Elastin Expression by Heparin in the Proliferating Cells Is Mediated by the Inhibition of Protein Kinase C Activity.* The Journal of Biochemistry, 1995. **118**(3): p. 582-586.
89. Alban, S., *Adverse Effects of Heparin*, in *Heparin - A Century of Progress*, R. Lever, B. Mulloy, and C.P. Page, Editors. 2012, Springer Berlin Heidelberg: Berlin, Heidelberg. p. 211-263.
90. Lee, W.-R., et al., *Laser-assisted nanoparticle delivery to promote skin absorption and penetration depth of retinoic acid with the aim for treating photoaging.* International Journal of Pharmaceutics, 2022. **627**: p. 122162.
91. Jetten, A.M., et al., *Characterization of the action of retinoids on mouse fibroblast cell lines.* Experimental Cell Research, 1979. **119**(2): p. 289-299.
92. Kirschner, S.E., A. Ciaccia, and J.L. Ubels, *The Effect of Retinoic Acid on Thymidine Incorporation and Morphology of Corneal Stromal Fibroblasts.* Current Eye Research, 1990. **9**(11): p. 1121-1125.
93. Zhou, T.-B., G.P.C. Drummen, and Y.-H. Qin, *The Controversial Role of Retinoic Acid in Fibrotic Diseases: Analysis of Involved Signaling Pathways.* International Journal of Molecular Sciences, 2013. **14**(1): p. 226-243.
94. MacGregor, J.L. and H.I. Maibach, *The Specificity of Retinoid-Induced Irritation and Its Role in Clinical Efficacy.* Exogenous Dermatology, 2002. **1**(2): p. 68-73.

95. Mustoe, T.A., et al., *Accelerated Healing of Incisional Wounds in Rats Induced by Transforming Growth Factor-β.* Science, 1987. **237**(4820): p. 1333-1336.
96. Kane, C.J.M., et al., *Direct evidence for spatial and temporal regulation of transforming growth factor β1 expression during cutaneous wound healing.* Journal of Cellular Physiology, 1991. **148**(1): p. 157-173.
97. Beck, L.S., et al., *One systemic administration of transforming growth factor-beta 1 reverses age- or glucocorticoid-impaired wound healing.* The Journal of Clinical Investigation, 1993. **92**(6): p. 2841-2849.
98. Lord, M.S., et al., *The multifaceted roles of perlecan in fibrosis.* Matrix Biology, 2018. **68-69**: p. 150-166.
99. Jahan, N., et al., *Role of versican in extracellular matrix formation: analysis in 3D culture.* American Journal of Physiology-Cell Physiology, 2025. **328**(1): p. C245-C257.
100. Wu, Y.J., et al., *The interaction of versican with its binding partners.* Cell Research, 2005. **15**(7): p. 483-494.
101. Lichtman, M.K., M. Otero-Vinas, and V. Falanga, *Transforming growth factor beta (TGF-β) isoforms in wound healing and fibrosis.* Wound Repair and Regeneration, 2016. **24**(2): p. 215-222.
102. Le, M., et al., *Transforming Growth Factor Beta 3 Is Required for Excisional Wound Repair In Vivo.* PLOS ONE, 2012. **7**(10): p. e48040.
103. Wu, L., et al., *Transforming Growth Factor β3 (TGFβ3) Accelerates Wound Healing Without Alteration of Scar Prominence: Histologic and Competitive Reverse-Transcription–Polymerase Chain Reaction Studies.* Archives of Surgery, 1997. **132**(7): p. 753-760.
104. Mai, K., et al., *Maintaining and Restoring Gradients of Ions in the Epidermis: The Role of Ion and Water Channels in Acute Cutaneous Wound Healing.* Advances in Wound Care, 2023.
105. Zhang, W., et al., *Potassium channels as potential drug targets for limb wound repair and regeneration.* Precision Clinical Medicine, 2020. **3**(1): p. 22-33.
106. Davidson, J.M., et al., *Ascorbate Differentially Regulates Elastin and Collagen Biosynthesis in Vascular Smooth Muscle Cells and Skin Fibroblasts by Pretranslational Mechanisms*.* Journal of Biological Chemistry, 1997. **272**(1): p. 345-352.
107. Tanaka, A., et al., *Controlled release of ascorbic acid from gelatin hydrogel attenuates abdominal aortic aneurysm formation in rat experimental abdominal aortic aneurysm model.* Journal of Vascular Surgery, 2014. **60**(3): p. 749-758.
108. Rezvani Ghomi, E., et al., *Collagen-based biomaterials for biomedical applications.* Journal of Biomedical Materials Research Part B: Applied Biomaterials, 2021. **109**(12): p. 1986-1999.
109. Kondej, K., et al., *Bioengineering Skin Substitutes for Wound Management—Perspectives and Challenges.* International Journal of Molecular Sciences, 2024. **25**(7): p. 3702.
110. Sheikholeslam, M., et al., *Biomaterials for Skin Substitutes.* Advanced Healthcare Materials, 2018. **7**(5): p. 1700897.
111. Kim, A., et al., *Investigating Immunomodulatory Biomaterials for Preventing the Foreign Body Response.* Bioengineering, 2023. **10**(12): p. 1411.
112. Josyula, A., et al., *Engineering biomaterials to prevent post-operative infection and fibrosis.* Drug Delivery and Translational Research, 2021. **11**(4): p. 1675-1688.
113. Hoang, C., et al., *Application of Dimethyl Sulfoxide as a Therapeutic Agent and Drug Vehicle for Eye Diseases.* Journal of Ocular Pharmacology and Therapeutics, 2021. **37**(8): p. 441-451.
114. Moskot, M., et al., *The Role of Dimethyl Sulfoxide (DMSO) in Gene Expression Modulation and Glycosaminoglycan Metabolism in Lysosomal Storage Disorders on an Example of Mucopolysaccharidosis.* International Journal of Molecular Sciences, 2019. **20**(2): p. 304.

115. Zeng, X., et al., *Dimethyl Sulfoxide Decrease Type-I and -III Collagen Synthesis in Human Hepatic Stellate Cells and Human Foreskin Fibroblasts.* Advanced Science Letters, 2010. **3**(4): p. 496-499.

116. Xie, H., et al., *Treatment of Burn and Surgical Wounds With Recombinant Human Tropoelastin Produces New Elastin Fibers in Scars.* J Burn Care Res, 2017. **38**(5): p. e859-e867.

117. Diller, R.B. and R.S. Kellar, *An acellular tissue engineered biomimetic wound healing device created using collagen and tropoelastin accelerates wound healing.* Journal of Tissue Viability, 2022. **31**(3): p. 485-490.

118. Noda, K., et al., *Latent TGF-β binding protein 4 promotes elastic fiber assembly by interacting with fibulin-5*. Proceedings of the National Academy of Sciences, 2013. **110**(8): p. 2852-2857.

119. Aya, R., et al., *Regeneration of elastic fibers by three-dimensional culture on a collagen scaffold and the addition of latent TGF-β binding protein 4 to improve elastic matrix deposition.* Biomaterials, 2015. **72**: p. 29-37.

Supporting Information

Table S1. RT-qPCR primer sequences.

Gene	Description	Forward sequence 5'3'	Reverse sequence 5'3'
ACTA2	smooth muscle actin alpha 2	CCGACCGAATGCAGAAGGA	ACAGAGTATTTGCGCTCCGAA
COL1A1	alpha-1 type I collagen	GAGAGCATGACCGATGGATT	CGCTGTTCTTGCAGTGGTAG
ELN	elastin	GGTTGTGTCACCAGAAGCAGCT	CCGTAAGTAGGAATGCCTCCAAC
FN1	fibronectin-1	GAAGCCGAGGTTTTAACTGC	ACCCACTCGGTAAGTGTTCC
FBN1	fibrillin-1	ATGGAAGGAGCTGCAAAGATC	GCCGCCAATGGTGGTAACA
FBN2	fibrillin-2	TGGGCGGCCATTTTACAAAG	AACGGCATTTGAAGCTTCCG
FBLN4	fibulin-4	ATTTGGACTTGGCTGGCTTG	AGGCAGAGTTAGGAATGGAACC
FBLN5	fibulin-5	TATTGATGAATGCCGAACCA	ACCTGAGTAGGGGGTCGAGT
LOX	lysyl oxidase	TGCCAGTGGATTGATATTAC	TACGGTGAAATTGTGCAGCC
HMCN1	hemicentin 1	CTTGTGTAGCCACGAATGAGGC	CGCTTCACATTCCAAGGTCAGAG
YWHAZ	zeta polypeptide tyrosine 3-monooxygenase/tryptophan 5-monooxygenase activation protein	CATCTTGGAGGGTCGTCTCA	ACTTTGCTCTCTGCTTGTGAA
GAPDH	glyceraldehyde 3-phosphate dehydrogenase	TGGGTGTGAACCATGAGAAG	TGGGTGTGAACCATGAGAAG

Table S2. Antibodies used for Immunofluorescence.

	Antibody	Isotype	Clone	Cat. No.	Dilution
Primary	Mouse anti-heparan sulfate	IgM, κ-chain	F58-10E4	370255-1 [A]	1:500
	Mouse anti-α-smooth muscle actin	IgG2a	1A4	A-2547 [B]	1:2000
	Mouse anti-versican	IgG1	12C5	12C5 [C]	1:500
	Mouse anti-neuraminidase-1	IgG2b	688215	MAB6860 [D]	1:500
	Rabbit anti-protective protein cathepsin A	IgG	EPR10435	ab184553 [E]	1:500
Secondary	Alexa 488 labelled goat anti-mouse	IgG (H+L)	Polyclonal	A-11001 [F]	1:500
	Alexa 488 labelled phalloidin	-	-	A-12379 [F]	1:300
	Alexa 594 labelled goat anti-mouse	IgG (H+L)	Polyclonal	A-11032 [F]	1:500
	Alexa 594 labelled goat anti-rabbit	IgG (H+L)	Polyclonal	A-11012 [F]	1:500

NOTE: The anti-IgG (H+L) secondary antibody cross-reacted with the IgM primary antibody due to the shared kappa light chains, as confirmed by the absence of signal in the negative control lacking the primary antibody. Phalloidin is not an antibody but a bicyclic heptapeptide toxin which binds selectively to filamentous actin.A: Amsbio, Abingdon, UK; B: Sigma-Aldrich, Saint Louis, MO, USA; C: Developmental Studies Hybridoma Bank, Iowa City, IA, USA; D: R&D Systems, Minneapolis, MN, USA; E: Abcam, Cambridge, MA, USA; F: Invitrogen, Waltham, MA, USA.

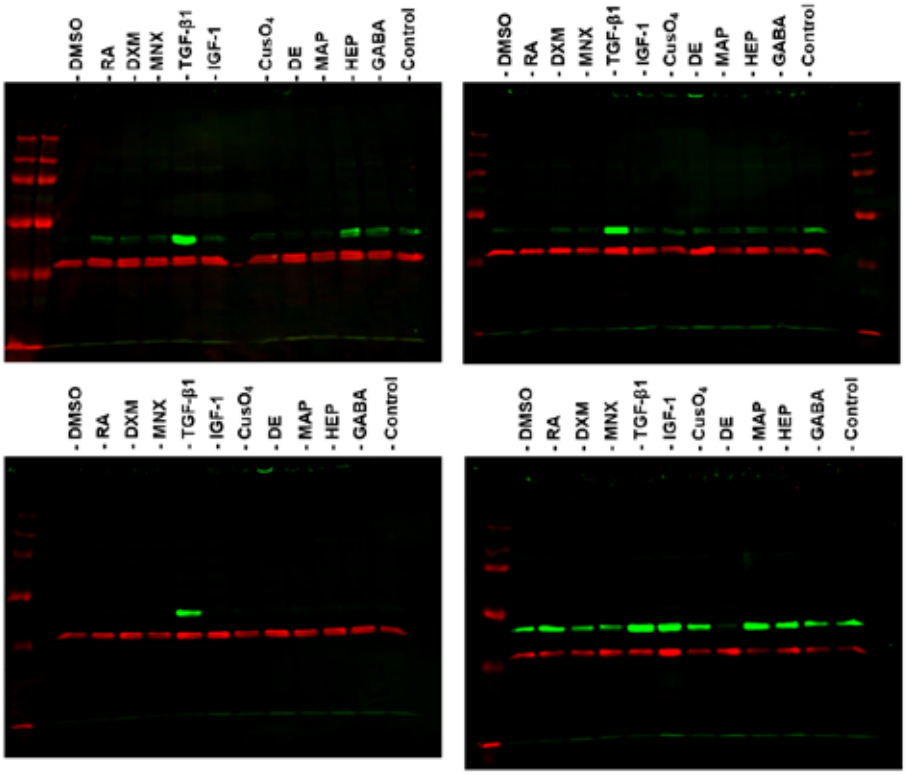

Figure S1. Uncropped western blots stained for α-SMA (green) from four different donors at day 7. GAPDH expression was used as internal control (red).

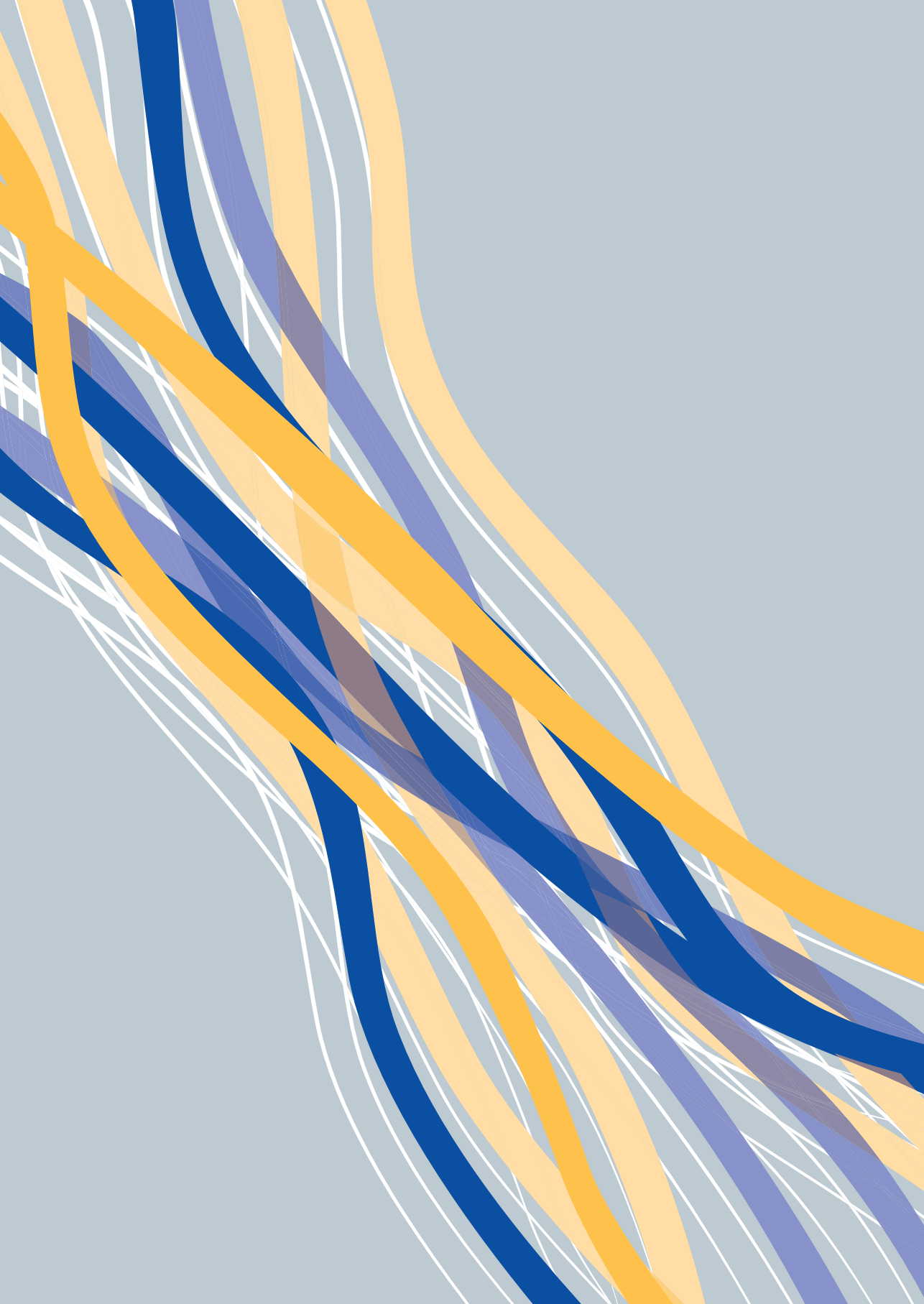

Chapter 6

General Discussion and Future Perspectives

Reactivation of elastogenesis

Elastin, a crucial component of the extracellular matrix, has received relatively little attention in research. The formation of elastic fibers is notably slow after an injury, and these fibers are largely absent in scar tissue [1]. Despite their essential role in maintaining skin elasticity, comprehensive investigations into their function in wound healing and regeneration remain limited [2]. Recent studies have shed light on elastic fiber formation, particularly in terms of molecular pathways, computational simulations, and biomimetic approaches [3-7]. Additionally, progress has been made in identifying the key regulatory proteins and mechanisms involved in elastogenesis [8, 9].

Elastic fibers are composed of an insoluble elastin deposited on the microfibril core [10]. Their assembly follows a controlled, sequential process beginning with the formation of a microfibrillar scaffold – primarily composed of fibrillin-1 – onto which tropoelastin monomers are deposited and subsequently crosslinked into a stable composite [11, 12]. Several key proteins, including fibulin-4 (FBLN4), fibulin-5 (FBLN5), and latent TGFβ-binding protein-4 (LTBP4), are essential for guiding the aggregation, crosslinking, and integration of tropoelastin into the microfibrillar framework [13-15]. The significance of short fibulins (-3, -4, and -5) in elastic fiber development has been further demonstrated in knockout mouse models [16].

Computational studies have greatly expanded our understanding of structural properties of tropoelastin, its flexibility, and self-assembly dynamics. Various modeling techniques – including elastic network models, full-atomistic simulations, and coarse-grained representations – have provided insights into the link between molecular mechanisms and functions [17-19]. These studies highlighted the ability of tropoelastin to retain a dynamic but stable conformation, with specific regions facilitating flexibility and self-organization. Key contributors include the glycine- and proline-rich hydrophobic domains that promote conformational changes [20], the crosslinking lysine-alanine domains (KA domains) capable of transitioning from disordered to ordered states [21], and structural features such as the hinge (domains 20–24), bridge (25–26), and foot (27–36) regions that play critical roles in spatial organization and assembly [18, 22]. Simulations of single amino acid substitutions illustrated how minor alterations can disrupt fiber assembly, contributing to pathological conditions such as cutis laxa [17, 23, 24]. Furthermore, modeling approaches have demonstrated how mechanical properties, conformational shifts, and crosslinking influence elastogenesis and binding to the receptors, offering valuable perspectives for biomaterial development and regenerative medicine applications [18, 21, 25].

Tropoelastin plays a key role in cellular processes by supporting adhesion and migration in fibroblasts, endothelial cells, and mesenchymal stem cells through interactions with specific surface receptors [26-29]. These interactions are important in wound healing, elastic fiber formation, and stem cell regulation. The elastin-binding protein (EBP), a non-enzymatic splice variant of β-galactosidase, functions as a chaperone intracellularly and as part of the elastin receptor complex (ERC) at the cell surface [5]. The ERC binds elastin-derived peptides (EDPs) that are known to regulate cell adhesion, migration, and extracellular matrix remodeling [30]. Notably, full-length tropoelastin does not activate these pathways in the same manner, suggesting that EDPs play a more prominent role in tissue repair mechanisms [5, 31].

Protective protein cathepsin A (PPCA) and neuraminidase-1 (NEU-1) are two lysosomal components that are also connected to ERC and involved in elastic fiber synthesis [32]. In **Chapter 5**, we made first attempts in the colocalization of PPCA and NEU-1 using immunostaining techniques. Both proteins exhibited distinct but also overlapping staining patterns, suggesting that the ERC may be located at sites of colocalization. PPCA displayed a filamentous cytoplasmic distribution, whereas NEU-1 was observed in vesicular or lysosomal structures. Their strongest signal intensities were detected near the perinuclear region, pointing to their intracellular nature as well. Additional insights could be gained by investigating EBP localization. Nevertheless, our preliminary attempts using an anti-β-galactosidase-1 antibody were unsuccessful. To date, no published studies have simultaneously visualized these three ERC components.

Glycosaminoglycans (GAGs), such as heparan sulfate, interact with tropoelastin through positively charged lysine residues and may play a role in guiding elastin assembly [33]. Tropoelastin also binds integrins αvβ3 and αvβ5, influencing fibroblast adhesion and mesenchymal stem cell proliferation and extracellular matrix remodeling through protein kinase B (PKB/AKT) and focal adhesion kinase (FAK) signaling pathways [29, 34]. Unlike fibronectin, which interacts with multiple integrins [35], tropoelastin exhibits a more selective binding profile, potentially allowing for more precise regulation of cell adhesion and tissue repair.

Elastin-derived compounds, particularly solubilized elastin preparations, have demonstrated promising bioactivity in wound healing applications [36-39]. We hypothesize that soluble elastin may be sensed by cells in two ways: 1) as a signal of matrix degradation, thereby initiating an elastogenic response aimed at repairing and restoring the elastic fiber network, and 2) as a direct structural component for new fiber formation. In **Chapter 2**, we analyzed different preparation methods and their influence on the resulting elastin products. The biochemical characteristics

of elastin, including molecular weight, functional groups, and solubility, can be adjusted depending on the method used. Enzymatic digestion with human elastases represents a highly specific and biologically relevant approach that closely mimics natural degradation processes. However, these enzymes are expensive, and such digested elastin preparations are technically challenging to obtain because of the need for precise control over digestion conditions with the generation of consistent fragments to prevent batch-to-batch variations. At the same time, the removal of an enzyme from reaction mixtures poses an additional difficulty. An alternative approach involves using a microcolumn with immobilized elastase, which eliminates the need for enzyme removal while enhancing digestion efficiency by improving substrate interactions and increasing the surface-to-volume ratio [40-42]. Our enzymatically prepared elastin formulations with elastase from porcine pancreas exhibited distinct effects on both fibroblasts and macrophages, although the presence of endotoxin contamination complicated definitive conclusions. So far, our findings support the first hypothesis that soluble elastin can trigger elastogenic responses, while its role as a direct structural component for new fiber formation requires further investigation.

A key area that remains not completely understood is how elastin-derived peptides activate diverse signaling pathways in skin cells [4]. These peptides were reported to activate protein kinase C (PKC), phosphoinositide 3-kinase (PI3K), and phospholipase Cγ (PLCγ) pathways and to influence processes such as cell proliferation, invasion, survival, angiogenesis, and matrix metalloproteinase expression [31, 43]. However, it was unclear which amino acid sequences caused the effects. Comparative studies across different cell sources provide valuable insights into the additional distinctions, e.g., between dermal and cardiovascular elastogenesis. For instance, minoxidil enhanced elastin mRNA expression through a Ca^{2+}-ERK-dependent pathway in smooth muscle cells [44], yet our experiments with minoxidil on dermal fibroblasts in **Chapter 5** did not show noticeable effects, highlighting potential tissue-specific differences in elastogenesis regulation by this compound.

Engineering of novel biomaterial scaffolds

Once the most effective compounds and their optimal concentrations have been identified, the next step is to develop a suitable biomaterial formulation. The concentration used in initial compound testing may not necessarily match the concentration required within the final biomaterial composition [45]. Effective scaffold design for skin regeneration involves replicating the mechanical strength,

elasticity, and microarchitecture of native tissue [46, 47]. Optimizing pore size can tune the function of the scaffold. For example, 1-2 μm pores promote attachment of keratinocytes, 2-12 μm pores aid dermal repair, and 40-100 μm pores support vascularization [48]. Scaffolds must facilitate cell adhesion, growth and differentiation while remaining immunocompatible. Equally important is a degradation rate that is fast enough to avoid encapsulation or rejection, but gradual to maintain structural integrity. Mimicking the native extracellular matrix is crucial to guide cellular behavior and support functional tissue development [49].

There are three main strategies for fabricating collagen-elastin biomaterials: casting, fiber spinning, and bioprinting [50]. Casting is one of the most widely used techniques and was utilized in **Chapters 3 and 4** to develop our biomaterials. This approach involves preparing a protein suspension, pouring it into a mold of the desired shape, and subsequently removing the solvent through freeze-drying/ lyophilization. For instance, a commercially available skin substitute, MatriDerm, is manufactured using this method [51].

An alternative fabrication method is electrospinning, a technique in which ultrafine fibers are produced by applying an electrical charge. While electrospinning enables the formation of highly structured fibers, such fibers require additional crosslinking to maintain stability in aqueous environments [52]. Another advanced technique is bioprinting, which allows the precise construction of multilayered matrices incorporating collagen and elastin [53]. As an alternative approach, collagen-elastin biomaterials can be derived from decellularized animal skin, as seen in commercially available products such as AlloDerm, Permacol, and Enduragen [54-56].

To further modify biomaterial properties, crosslinking can be introduced as a secondary step to adjust chemical, mechanical, and biological characteristics. Collagen-based materials can be crosslinked using physical, chemical, or biological methods to enhance structural integrity, improve resistance to (enzymatic) degradation, and enable the covalent attachment of bioactive molecules. Among the commonly used physical techniques, UV irradiation and dehydrothermal (DHT) treatment are known to be safe and effective [57]. **Chapter 4** highlighted the advantages of DHT treatment in large-scale production, particularly its ability to accelerate the drying process while preserving the physicochemical properties of the biomaterial.

Chemical crosslinking is typically performed using agents such as glutaraldehyde [58], 1-ethyl-3-(3-dimethylaminopropyl)carbodiimide/N-hydroxysuccinimide (EDC/NHS) [39], transglutaminase [59], or genipin [60]. Glutaraldehyde forms highly

stable crosslinks but possesses high risks of cytotoxicity and calcification [61]. Transglutaminase is an acyltransferase enzyme that catalyzes the formation of covalent bonds between the γ-carboxamide group of glutamine residues and the ε-amino group of lysine residues in proteins [62]. Application of transglutaminase is limited by Ca^{2+} dependency when derived from animal tissues, as well as by less pronounced mechanical characteristics compared to genipin and EDC/NHS [63]. Genipin, a naturally derived crosslinker, reacts at a slower rate compared to synthetic alternatives [64]. For the *in vitro* and *in vivo* studies described in **Chapter 3**, we employed EDC/NHS crosslinking, a non-toxic zero-length crosslinker that selectively targets carboxyl and amine groups, ensuring stable crosslink formation while retaining soluble elastin within the biomaterial. This method also exhibited notable differences in mechanical strength and degradation rates, as was investigated in **Chapter 4**. Exploring alternative milder crosslinking strategies could help achieve a balance between mechanical stability, bioactivity, and controlled degradation within skin tissue in humans. For example, riboflavin (vitamin B2) could be considered as a potential biological crosslinker for our scaffolds [65, 66]. Activated by UV or visible light, this crosslinker is already employed in corneal treatments with minimal toxicity [67].

With the rapid advancements in artificial intelligence (AI), its application in biomaterial development is becoming increasingly relevant. AI-driven approaches have the potential to predict structure-bioactivity relationships, optimize scaffold design, and anticipate clinical outcomes, further advancing the field of regenerative medicine [68-72].

Methods for testing of biomaterials

Evaluating the biological effects of novel biomaterials presents challenges when selecting an initial *in vitro* model due to the diverse cellular composition of human skin. However, human dermal fibroblasts play a pivotal role in extracellular matrix (ECM) remodeling during wound healing [73], making them a great option for initial biological assessments. Our studies in **Chapters 2–5** included cell culture experiments using primary human dermal fibroblasts. These primary cells, derived from human skin tissues without modification, better reflect physiological conditions than immortalized cell lines [74]. This makes them highly suitable for investigating cellular responses to biomaterials or individual compounds. Notably, our research highlighted that fibroblast origin and donor-to-donor variations significantly influence ECM remodeling capabilities. While fibroblasts from healthy

adult skin exhibited minimal activity, those derived from eschar tissue and fetal sources were considerably more active. Reticular fibroblasts are responsible for initial wound healing by forming a robust matrix, while papillary fibroblasts are essential for the final remodeling and regeneration of the skin [75, 76]. In addition to fibroblasts, we initiated comparative studies on macrophages to assess immune responses to soluble elastins. Future investigations of elastogenic compounds should include other skin cell types (e.g., keratinocytes, endothelial cells, melanocytes, Langerhans cells) and investigate co-culture models with fibroblasts to better replicate the complex cellular interactions in the skin [77, 78].

To enhance the physiological relevance of our cell culture conditions, we used macromolecular crowders (MMCs) to simulate the crowded molecular environment seen *in vivo* [79, 80]. The excluded volume effect induced by MMCs restricts the free diffusion of test molecules, thereby accelerating ECM deposition, shortening culture periods, and significantly influencing protein folding, molecular interactions, and enzymatic activity [81, 82]. While traditional two-dimensional (2D) cell cultures remain widely used, three-dimensional (3D) skin equivalents are emerging as more sophisticated alternatives [83-85]. These models incorporate epidermal, dermal, and, in some cases, hypodermal layers, offering more relevant systems for wound healing research, both structurally and functionally [86-88]. Additional investigation of skin regeneration processes can be achieved through the use of organotypic systems, including full-thickness skin constructs developed from engineered dermal scaffolds [89]. Skin-on-a-chip systems offer a promising laboratory model to study how different compounds interact with skin tissue and to assess the skin's response, e.g., elastin production and elastic fiber synthesis by fibroblasts and high throughput screening [90]. Furthermore, microfluidic wound healing platforms, or wound-on-chip models, can also replicate tissue injury and repair processes [91-93]. By integrating microchannels for dynamic flow, these systems better mimic physiological blood supply and nutrient delivery [93]. Additionally, real-time imaging enables the tracking of cell migration, proliferation, and cytokine secretion, making these models valuable tools for high-throughput screening of wound-healing compounds [94-96].

Ex vivo tissue models serve as an intermediate step between conventional *in vitro* assays and complex *in vivo* studies [97, 98]. By providing native tissue architecture while allowing precise experimental manipulation, these models provide translationally relevant insights into biomaterial performance [99]. Despite their limitations, such as restricted viability and the absence of systemic responses [100], they offer ethical advantages, cost-effectiveness, and high clinical relevance [101].

Animal models still remain essential in wound healing research, each with distinct advantages and disadvantages [102]. The choice of an appropriate animal model depends on the study objectives, balancing practicality with clinical relevance [103]. In **Chapter 4**, we used a rat model for *in vivo* testing due to rats' relatively low price, ease of handling, and reproducible experimental outcomes. Their rapid wound healing enables efficient study cycles, although, unlike humans who rely on re-epithelialization and granulation tissue formation, rats primarily heal through wound contraction facilitated by the panniculus carnosus muscle and myofibroblasts [104, 105]. Additionally, rat skin is more elastic and loosely attached to underlying structures, limiting its direct applicability to human wound healing [106]. Nevertheless, rat models can still highlight key biological differences, as observed in our studies with collagen-elastin scaffolds. While mice offer an even more cost-efficient and rapid-healing alternative, their thin skin differs significantly from rat and human skin, restricting their relevance for complex wound studies [107]. Rabbits, with their larger skin surfaces, are useful for ischemic ulcer models but pose handling challenges [108]. Pigs provide the most physiologically similar model to human skin in terms of structure and healing mechanisms, making them the gold standard for translational research [109, 110]. Furthermore, porcine models allow for the testing of dermal templates followed by autologous skin grafting, mirroring clinical approaches for treating large wounds [111]. However, the high costs of pig models and ethical considerations associated with animal testing limit their routine use. To enhance the utility and translational value of these preclinical models, emerging real-time, non-invasive imaging techniques, such as multiphoton microscopy, combined with AI-assisted image analysis, are increasingly being used to assess tissue regeneration, minimizing animal sacrifice [112, 113].

Translating biomaterials from the lab into clinical applications requires extensive preclinical validation, clinical trials, and regulatory approvals. Scaling up production adds another layer of complexity, involving process optimization, cost management, and quality control [114]. Laboratory-scale protocols must often be re-engineered to be translated into industrial production [115, 116]. Factors such as mixing dynamics, temperature regulation, and (bio)reactor design must be optimized to maintain product consistency. Additionally, impurities present in raw materials may accumulate during large-scale production, further emphasizing the need for quality control measures [116]. Establishing reliable supply chains is crucial for ensuring batch-to-batch reproducibility and compliance with Good Manufacturing Practices (GMP) [117]. Clinical investigations of dermal biomaterials in the Netherlands must adhere to the European Union's Medical Device Regulation (MDR), which outlines three types of clinical investigations: those for conformity assessment to obtain or extend CE marking (Articles 62 and 74.2), post-market clinical follow-up

studies involving additional invasive or burdensome procedures (Article 74.1), and other clinical investigations outside the previous ones, which fall under national regulations (Article 82). Finally, the cost of a dermal biomaterial must remain reasonable to ensure feasibility in both production and clinical application [118]. Even if a biomaterial offers superior regenerative or scarless healing potential, its widespread use will depend on its affordability or reimbursement from insurance companies for both patients and healthcare providers.

Future Perspectives

In addition to the *in vitro* and *in vivo* advancements discussed earlier, several future research directions emerge from the findings presented in **Chapters 2–5**. For studies involving solubilized elastins, obtaining endotoxin-free enzymatic preparations is critical to fully explore the biological potential of such compounds. Further evaluation of fibroblast responses under pro-fibrotic conditions, such as under TGF-β1 stimulation, may offer clearer insights into the anti-scarring potential of these elastins. The role of the elastin receptor complex in elastogenesis also needs deeper investigation, particularly through the colocalization of its three components and the analysis of downstream intracellular signaling in human dermal fibroblasts. Additionally, fluorescent tagging of solubilized elastins could help validate the hypothesis that these molecules contribute directly to the formation of new elastic fibers. The exploration of other classes of elastogenic compounds may be expanded to include agents such as low-molecular-weight hyaluronan, estradiol, and recombinant human tropoelastin. Following the identification of the most promising candidates, their synergistic effects could be assessed to further enhance regenerative outcomes. These insights will be essential for optimizing dermal scaffold development with elastic fiber regeneration.

For scaffold engineering, future studies could investigate alternative crosslinkers and broader concentration ranges. Testing these scaffolds in different animal models could improve the evaluation of their *in vivo* performance and translational potential. A consistent emphasis should be placed on the formation of mature, functional elastic fibers rather than isolated elastin protein deposition. Bridging the gap between research and clinical application will also require addressing key challenges related to regulation, scalability, and cost barriers. In the end, the successful development of a dermal biomaterial will depend on achieving a balance between biological efficacy, affordability, and clinical feasibility to enable widespread utilization in wound management and regenerative medicine.

References

1. Roten, S.V., S. Bhat, and J. Bhawan, *Elastic fibers in scar tissue.* Journal of Cutaneous Pathology, 1996. **23**(1): p. 37-42.
2. Krymchenko, R., et al., *Elastogenesis in Focus: Navigating Elastic Fibers Synthesis for Advanced Dermal Biomaterial Formulation.* Advanced Healthcare Materials, 2024. **13**(27): p. 2400484.
3. Shin, S.J. and H. Yanagisawa, *Recent updates on the molecular network of elastic fiber formation.* Essays Biochem, 2019. **63**(3): p. 365-376.
4. Daamen, W.F. and D. Quaglino, *Signaling pathways in elastic tissues.* Cellular Signalling, 2019. **63**: p. 109364.
5. Ozsvar, J., et al., *Tropoelastin and Elastin Assembly.* Frontiers in Bioengineering and Biotechnology, 2021. **9**.
6. Loffet, E.A., et al., *Elastic fibers define embryonic tissue stiffness to enable buckling morphogenesis of the small intestine.* bioRxiv, 2023: p. 2023.07.18.549562.
7. Sivaraman, B., C.A. Bashur, and A. Ramamurthi, *Advances in biomimetic regeneration of elastic matrix structures.* Drug Delivery and Translational Research, 2012. **2**(5): p. 323-350.
8. Sun, B., et al., *PAD2-mediated citrullination of Fibulin-5 promotes elastogenesis.* Matrix Biology, 2021. **102**: p. 70-84.
9. Zhang, X., et al., *Elastic Fibre Proteins in Elastogenesis and Wound Healing.* International Journal of Molecular Sciences, 2022. **23**(8): p. 4087.
10. Kozel, B.A. and R.P. Mecham, *Elastic fiber ultrastructure and assembly.* Matrix Biology, 2019. **84**: p. 31-40.
11. Kielty, C.M., et al., *Fibrillin Microfibrils*, in *Advances in Protein Chemistry*. 2005, Academic Press. p. 405-436.
12. Trask, T.M., et al., *Interaction of Tropoelastin with the Amino-terminal Domains of Fibrillin-1 and Fibrillin-2 Suggests a Role for the Fibrillins in Elastic Fiber Assembly*.* Journal of Biological Chemistry, 2000. **275**(32): p. 24400-24406.
13. Dabovic, B., et al., *Function of Latent TGFβ Binding Protein 4 and Fibulin 5 in Elastogenesis and Lung Development.* Journal of Cellular Physiology, 2015. **230**(1): p. 226-236.
14. Kumra, H., et al., *Fibulin-4 exerts a dual role in LTBP-4L–mediated matrix assembly and function.* Proceedings of the National Academy of Sciences, 2019. **116**(41): p. 20428-20437.
15. Nakamura, T., *Roles of short fibulins, a family of matricellular proteins, in lung matrix assembly and disease.* Matrix Biology, 2018. **73**: p. 21-33.
16. Yanagisawa, H. and E.C. Davis, *Unraveling the mechanism of elastic fiber assembly: The roles of short fibulins.* The International Journal of Biochemistry & Cell Biology, 2010. **42**(7): p. 1084-1093.
17. Yeo, G.C., et al., *Subtle balance of tropoelastin molecular shape and flexibility regulates dynamics and hierarchical assembly.* Science Advances, 2016. **2**(2): p. e1501145.
18. Tarakanova, A., et al., *Molecular model of human tropoelastin and implications of associated mutations.* Proceedings of the National Academy of Sciences, 2018. **115**(28): p. 7338-7343.
19. Tarakanova, A., et al., *Coarse-grained model of tropoelastin self-assembly into nascent fibrils.* Materials Today Bio, 2019. **3**: p. 100016.
20. Rauscher, S. and R. Pomès, *The liquid structure of elastin.* eLife, 2017. **6**: p. e26526.
21. Reichheld, S.E., et al., *Conformational Transitions of the Cross-linking Domains of Elastin during Self-assembly*.* Journal of Biological Chemistry, 2014. **289**(14): p. 10057-10068.

22. Baldock, C., et al., *Shape of tropoelastin, the highly extensible protein that controls human tissue elasticity.* Proceedings of the National Academy of Sciences, 2011. **108**(11): p. 4322-4327.
23. Yeo, G.C., et al., *Tropoelastin bridge region positions the cell-interactive C terminus and contributes to elastic fiber assembly.* Proceedings of the National Academy of Sciences, 2012. **109**(8): p. 2878-2883.
24. Miao, M., et al., *Single nucleotide polymorphisms and domain/splice variants modulate assembly and elastomeric properties of human elastin. Implications for tissue specificity and durability of elastic tissue.* Biopolymers, 2017. **107**(5): p. e23007.
25. Tarakanova, A., et al., *Tropoelastin is a Flexible Molecule that Retains its Canonical Shape.* Macromolecular Bioscience, 2019. **19**(3): p. 1800250.
26. Yu, Y., et al., *Characterization of Endothelial Progenitor Cell Interactions with Human Tropoelastin.* PLOS ONE, 2015. **10**(6): p. e0131101.
27. Al Halawani, A., et al., *Tropoelastin Promotes the Formation of Dense, Interconnected Endothelial Networks.* Biomolecules, 2021. **11**(9): p. 1318.
28. Lee, P., G.C. Yeo, and A.S. Weiss, *A cell adhesive peptide from tropoelastin promotes sequential cell attachment and spreading via distinct receptors.* The FEBS Journal, 2017. **284**(14): p. 2216-2230.
29. Yeo, G.C. and A.S. Weiss, *Soluble matrix protein is a potent modulator of mesenchymal stem cell performance.* Proceedings of the National Academy of Sciences, 2019. **116**(6): p. 2042-2051.
30. Tembely, D., et al., *The Elastin Receptor Complex: An Emerging Therapeutic Target Against Age-Related Vascular Diseases.* Frontiers in Endocrinology, 2022. **13**.
31. Scandolera, A., et al., *The Elastin Receptor Complex: A Unique Matricellular Receptor with High Anti-tumoral Potential.* Frontiers in Pharmacology, 2016. **7**.
32. Hinek, A., et al., *Lysosomal Sialidase (Neuraminidase-1) Is Targeted to the Cell Surface in a Multiprotein Complex That Facilitates Elastic Fiber Assembly*.* Journal of Biological Chemistry, 2006. **281**(6): p. 3698-3710.
33. Gheduzzi, D., et al., *Heparan sulphate interacts with tropoelastin, with some tropoelastin peptides and is present in human dermis elastic fibers.* Matrix Biology, 2005. **24**(1): p. 15-25.
34. Lee, P., et al., *A Novel Cell Adhesion Region in Tropoelastin Mediates Attachment to Integrin αVβ5* *This work was supported, in whole or in part, by National Institutes of Health Grant EB014283 (to A. S. W.). This work was also supported by the Australian Research Council, the Australian Defense Health Foundation, and the National Health and Medical Research Council (to A. S. W.) and by an Australian Postgraduate Research Award Ph.D. scholarship (to P. L.). A. S. W. is the scientific founder of Elastagen Pty. Ltd.* Journal of Biological Chemistry, 2014. **289**(3): p. 1467-1477.
35. Johansson, S., et al., *Fibronectin-integrin interactions.* FBL, 1997. **2**(4): p. 126-146.
36. Wen, Q., S.M. Mithieux, and A.S. Weiss, *Elastin Biomaterials in Dermal Repair.* Trends in Biotechnology, 2020. **38**(3): p. 280-291.
37. de Vries, H.J.C., et al., *Dermal regeneration in native non-cross-linked collagen sponges with different extracellular matrix molecules.* Wound Repair and Regeneration, 1994. **2**(1): p. 37-47.
38. Lamme, E.N., et al., *Extracellular matrix characterization during healing of full-thickness wounds treated with a collagen/elastin dermal substitute shows improved skin regeneration in pigs.* Journal of Histochemistry and Cytochemistry, 1996. **44**(11): p. 1311-22.

39. Daamen, W.F., et al., *A biomaterial composed of collagen and solubilized elastin enhances angiogenesis and elastic fiber formation without calcification.* Tissue Engineering Part A, 2008. **14**(3): p. 349-60.
40. Slysz, G.W. and D.C. Schriemer, *On-column digestion of proteins in aqueous-organic solvents.* Rapid Communications in Mass Spectrometry, 2003. **17**(10): p. 1044-1050.
41. Yuan, F.-F., et al., *Efficient and rapid digestion of proteins with a dual-enzyme microreactor featuring 3-D pores formed by dopamine/polyethyleneimine/acrylamide-coated KIT-6 molecular sieve.* Scientific Reports, 2024. **14**(1): p. 15667.
42. Nagy, C., R. Szabo, and A. Gaspar, *Microfluidic Immobilized Enzymatic Reactors for Proteomic Analyses—Recent Developments and Trends (2017–2021).* Micromachines, 2022. **13**(2): p. 311.
43. Le Page, A., et al., *The role of elastin-derived peptides in human physiology and diseases.* Matrix Biology, 2019. **84**: p. 81-96.
44. Lannoy, M., et al., *Inhibition of ERK1/2 Phosphorylation: A New Strategy to Stimulate Elastogenesis in the Aorta.* Hypertension, 2014. **64**(2): p. 423-430.
45. Wojciechowski, J.P., et al., *A Facile Method to Quantify Synthetic Peptide Concentrations on Biomaterials.* ACS Applied Materials & Interfaces, 2024. **16**(37): p. 49880-49888.
46. Sindhi, K., et al., *The role of biomaterials-based scaffolds in advancing skin tissue construct.* Journal of Tissue Viability, 2025. **34**(2): p. 100858.
47. Bertsch, C., et al., *Biomimetic Bilayered Scaffolds for Tissue Engineering: From Current Design Strategies to Medical Applications.* Advanced Healthcare Materials, 2023. **12**(17): p. 2203115.
48. Mukasheva, F., et al., *Optimizing scaffold pore size for tissue engineering: insights across various tissue types.* Frontiers in Bioengineering and Biotechnology, 2024. **Volume 12 - 2024**.
49. Aazmi, A., et al., *Biofabrication methods for reconstructing extracellular matrix mimetics.* Bioactive Materials, 2024. **31**: p. 475-496.
50. Miranda-Nieves, D. and E.L. Chaikof, *Collagen and Elastin Biomaterials for the Fabrication of Engineered Living Tissues.* ACS Biomaterials Science & Engineering, 2017. **3**(5): p. 694-711.
51. Haslik, W., et al., *First experiences with the collagen-elastin matrix Matriderm® as a dermal substitute in severe burn injuries of the hand.* Burns, 2007. **33**(3): p. 364-368.
52. Rnjak-Kovacina, J., et al., *Electrospun synthetic human elastin:collagen composite scaffolds for dermal tissue engineering.* Acta Biomaterialia, 2012. **8**(10): p. 3714-3722.
53. Derr, K., et al., *Fully Three-Dimensional Bioprinted Skin Equivalent Constructs with Validated Morphology and Barrier Function.* Tissue Engineering Part C: Methods, 2019. **25**(6): p. 334-343.
54. Wainwright, D.J., *Use of an acellular allograft dermal matrix (AlloDerm) in the management of full-thickness burns.* Burns, 1995. **21**(4): p. 243-248.
55. Saray, A., *Porcine Dermal Collagen (Permacol) for Facial Contour Augmentation: Preliminary Report.* Aesthetic Plastic Surgery, 2003. **27**(5): p. 368-375.
56. McCord, C., et al., *Use of Porcine Acellular Dermal Matrix (Enduragen) Grafts in Eyelids: A Review of 69 Patients and 129 Eyelids.* Plastic and Reconstructive Surgery, 2008. **122**(4): p. 1206-1213.
57. Wang, W., et al., *Physical crosslinkings of edible collagen casing.* International Journal of Biological Macromolecules, 2015. **81**: p. 920-925.
58. Wang, Y., et al., *Tropoelastin Incorporation into a Dermal Regeneration Template Promotes Wound Angiogenesis.* Advanced Healthcare Materials, 2015. **4**(4): p. 577-584.
59. Lockhart-Cairns, M.P., et al., *Transglutaminase-Mediated Cross-Linking of Tropoelastin to Fibrillin Stabilises the Elastin Precursor Prior to Elastic Fibre Assembly.* Journal of Molecular Biology, 2020. **432**(21): p. 5736-5751.

60. Kamaruzaman, N., et al., *Functionalised Hybrid Collagen-Elastin for Acellular Cutaneous Substitute Applications.* Polymers, 2023. **15**(8): p. 1929.
61. Gough, J.E., C.A. Scotchford, and S. Downes, *Cytotoxicity of glutaraldehyde crosslinked collagen/poly(vinyl alcohol) films is by the mechanism of apoptosis.* Journal of Biomedical Materials Research, 2002. **61**(1): p. 121-130.
62. Chen, T., et al., *Enzyme-catalyzed gel formation of gelatin and chitosan: potential for in situ applications.* Biomaterials, 2003. **24**(17): p. 2831-2841.
63. Nair, M., et al., *Tunable bioactivity and mechanics of collagen-based tissue engineering constructs: A comparison of EDC-NHS, genipin and TG2 crosslinkers.* Biomaterials, 2020. **254**: p. 120109.
64. Slusarewicz, P., K. Zhu, and T. Hedman, *Kinetic characterization and comparison of various protein crosslinking reagents for matrix modification.* Journal of Materials Science: Materials in Medicine, 2010. **21**(4): p. 1175-1181.
65. Arrizabalaga, J.H. and M.U. Nollert, *Riboflavin-UVA crosslinking of amniotic membranes and its influence on the culture of adipose-derived stem cells.* Journal of the Mechanical Behavior of Biomedical Materials, 2020. **106**: p. 103729.
66. Lee, Y.B., et al., *Green Chemistry for Crosslinking Biopolymers: Recent Advances in Riboflavin-Mediated Photochemistry.* Materials, 2023. **16**(3): p. 1218.
67. Melcher, S., et al., *Analysis of riboflavin/ultraviolet a corneal cross-linking by molecular spectroscopy.* Heliyon, 2023. **9**(2): p. e13206.
68. Gharibshahian, M., et al., *Recent advances in artificial intelligent strategies for tissue engineering and regenerative medicine.* Skin Research and Technology, 2024. **30**(9): p. e70016.
69. Filippi, M., M. Mekkattu, and R.K. Katzschmann, *Sustainable biofabrication: from bioprinting to AI-driven predictive methods.* Trends in Biotechnology, 2025. **43**(2): p. 290-303.
70. Nosrati, H. and M. Nosrati, *Artificial Intelligence in Regenerative Medicine: Applications and Implications.* Biomimetics, 2023. **8**(5): p. 442.
71. Zhang, Z., et al., *AI-driven 3D bioprinting for regenerative medicine: From bench to bedside.* Bioactive Materials, 2025. **45**: p. 201-230.
72. Asadi Sarabi, P., et al., *AI-Based solutions for current challenges in regenerative medicine.* European Journal of Pharmacology, 2024. **984**: p. 177067.
73. Dong, X., et al., *Dermal fibroblast-derived extracellular matrix (ECM) synergizes with keratinocytes in promoting re-epithelization and scarless healing of skin wounds: Towards optimized skin tissue engineering.* Bioactive Materials, 2025. **47**: p. 1-17.
74. Kaur, G. and J.M. and Dufour, *Cell lines.* Spermatogenesis, 2012. **2**(1): p. 1-5.
75. Mauroux, A., et al., *Papillary and reticular fibroblasts generate distinct microenvironments that differentially impact angiogenesis.* Acta Biomaterialia, 2023. **168**: p. 210-222.
76. Woodley, D.T., *Distinct Fibroblasts in the Papillary and Reticular Dermis: Implications for Wound Healing.* Dermatologic Clinics, 2017. **35**(1): p. 95-100.
77. Iqbal, M.Z., et al., *Breathing new life into tissue engineering: exploring cutting-edge vascularization strategies for skin substitutes.* Angiogenesis, 2024. **27**(4): p. 587-621.
78. Schutte, S.C., F. Kadakia, and S. Davidson, *Skin-Nerve Co-Culture Systems for Disease Modeling and Drug Discovery.* Tissue Engineering Part C: Methods, 2021. **27**(2): p. 89-99.
79. Tsiapalis, D. and D.I. Zeugolis, *It is time to crowd your cell culture media – Physicochemical considerations with biological consequences.* Biomaterials, 2021. **275**: p. 120943.
80. Doubková, M., et al., *Harnessing the Biomimetic Effect of Macromolecular Crowding in the Cell-Derived Model of Clubfoot Fibrosis.* Biomacromolecules, 2024. **25**(10): p. 6485-6502.

81. Kuznetsova, I.M., K.K. Turoverov, and V.N. Uversky, *What Macromolecular Crowding Can Do to a Protein.* International Journal of Molecular Sciences, 2014. **15**(12): p. 23090-23140.
82. Assunção, M., et al., *Cell-Derived Extracellular Matrix for Tissue Engineering and Regenerative Medicine.* Frontiers in Bioengineering and Biotechnology, 2020. **8**.
83. Choudhury, S. and A. Das, *Advances in generation of three-dimensional skin equivalents: pre-clinical studies to clinical therapies.* Cytotherapy, 2021. **23**(1): p. 1-9.
84. Carlson, M.W., et al., *Three-Dimensional Tissue Models of Normal and Diseased Skin.* Current Protocols in Cell Biology, 2008. **41**(1): p. 19.9.1-19.9.17.
85. Amantino, C.F., et al., *Development of 3D skin equivalents for application in photodynamic biostimulation therapy assays using curcumin nanocapsules.* Heliyon, 2024. **10**(12): p. e32808.
86. Tsao, C.-T., et al., *A simple material model to generate epidermal and dermal layers in vitro for skin regeneration.* Journal of Materials Chemistry B, 2014. **2**(32): p. 5256-5264.
87. Zimoch, J., et al., *Bio-engineering a prevascularized human tri-layered skin substitute containing a hypodermis.* Acta Biomaterialia, 2021. **134**: p. 215-227.
88. Workman, V.L., et al., *Development of a tissue-engineered skin model with epidermal, dermal and hypodermal components.* In vitro models, 2023. **2**(6): p. 297-306.
89. Mulder, P.P.G., et al., *Full Skin Equivalent Models for Simulation of Burn Wound Healing, Exploring Skin Regeneration and Cytokine Response.* Journal of Functional Biomaterials, 2023. **14**(1): p. 29.
90. Mohamadali, M., et al., *Design and evaluation of a skin-on-a-chip pumpless microfluidic device.* Scientific Reports, 2023. **13**(1): p. 8861.
91. Gupta, S., et al., *Fibroblast Derived Skin Wound Healing Modeling on Chip under the Influence of Micro-Capillary Shear Stress.* Micromachines, 2022. **13**(2): p. 305.
92. Shabestani Monfared, G., P. Ertl, and M. Rothbauer, *An on-chip wound healing assay fabricated by xurography for evaluation of dermal fibroblast cell migration and wound closure.* Scientific Reports, 2020. **10**(1): p. 16192.
93. Biglari, S., et al., *Simulating Inflammation in a Wound Microenvironment Using a Dermal Wound-on-a-Chip Model.* Advanced Healthcare Materials, 2019. **8**(1): p. 1801307.
94. Yamagishi, M., et al., *Quantitative live-cell imaging of secretion activity reveals dynamic immune responses.* iScience, 2024. **27**(6): p. 109840.
95. Kijanka, G.S., et al., *Real-time monitoring of cell migration, phagocytosis and cell surface receptor dynamics using a novel, live-cell opto-microfluidic technique.* Analytica Chimica Acta, 2015. **872**: p. 95-99.
96. Yamagishi, M., et al., *Quantitative live-cell imaging of secretion activity reveals dynamic immune responses.* bioRxiv, 2022: p. 2022.02.09.479547.
97. Wurbs, A., et al., *A human ex vivo skin model breaking boundaries.* Scientific Reports, 2024. **14**(1): p. 24054.
98. Wang, E.H.C., et al., *The Development of Human Ex Vivo Models of Inflammatory Skin Conditions.* International Journal of Molecular Sciences, 2023. **24**(24): p. 17255.
99. Hughes, D.L., et al., *Dynamic Physiological Culture of Ex Vivo Human Tissue: A Systematic Review.* Cancers, 2021. **13**(12): p. 2870.
100. Gonzalez, C., A.J. Velarde-Salcedo, and G. Navarro-Tovar, *Basis of nanomaterials evaluation in respiratory ex vivo models: Physiological and biochemical biomarkers, perspectives, challenges, and opportunities.* Materials Letters, 2025. **382**: p. 137798.
101. Yoon, D.J., et al., *A tractable, simplified ex vivo human skin model of wound infection.* Wound Repair and Regeneration, 2019. **27**(4): p. 421-425.

102. Parnell, L.K.S. and S.W. Volk, *The Evolution of Animal Models in Wound Healing Research: 1993–2017.* Advances in Wound Care, 2019. **8**(12): p. 692-702.
103. Mukherjee, P., et al., *Role of animal models in biomedical research: a review.* Laboratory Animal Research, 2022. **38**(1): p. 18.
104. Ghanbari, M., Y. Salkovskiy, and M.A. Carlson, *The rat as an animal model in chronic wound research: An update.* Life Sciences, 2024. **351**: p. 122783.
105. Masson-Meyers, D.S., et al., *Experimental models and methods for cutaneous wound healing assessment.* International Journal of Experimental Pathology, 2020. **101**(1-2): p. 21-37.
106. Wei, J.C.J., et al., *Allometric scaling of skin thickness, elasticity, viscoelasticity to mass for micro-medical device translation: from mice, rats, rabbits, pigs to humans.* Scientific Reports, 2017. **7**(1): p. 15885.
107. Grada, A., J. Mervis, and V. Falanga, *Research Techniques Made Simple: Animal Models of Wound Healing.* Journal of Investigative Dermatology, 2018. **138**(10): p. 2095-2105.e1.
108. Schivo, M., et al., *A rabbit model for assessment of volatile metabolite changes observed from skin: a pressure ulcer case study.* Journal of Breath Research, 2017. **11**(1): p. 016007.
109. Sullivan, T.P., et al., *THE PIG AS A MODEL FOR HUMAN WOUND HEALING.* Wound Repair and Regeneration, 2001. **9**(2): p. 66-76.
110. Meyerholz, D.K., et al., *Swine models in translational research and medicine.* Veterinary Pathology, 2024. **61**(4): p. 512-523.
111. Tapking, C., D. Popp, and L.K. Branski, *Pig Model to Test Tissue-Engineered Skin*, in *Skin Tissue Engineering: Methods and Protocols*, S. Böttcher-Haberzeth and T. Biedermann, Editors. 2019, Springer New York: New York, NY. p. 239-249.
112. Wang, S., et al., *Towards next-generation diagnostic pathology: AI-empowered label-free multiphoton microscopy.* Light: Science & Applications, 2024. **13**(1): p. 254.
113. Pinto-Coelho, L., *How Artificial Intelligence Is Shaping Medical Imaging Technology: A Survey of Innovations and Applications.* Bioengineering, 2023. **10**(12): p. 1435.
114. Đorđević, S., et al., *Current hurdles to the translation of nanomedicines from bench to the clinic.* Drug Delivery and Translational Research, 2022. **12**(3): p. 500-525.
115. Thakkar, R., et al., *A Comparison Between Lab-Scale and Hot-Melt-Extruder-Based Anti-inflammatory Ointment Manufacturing.* AAPS PharmSciTech, 2020. **21**(5): p. 200.
116. Yang, Y., et al., *From Lab Scale to Mass Production: A Project-Based Learning on the Preparation of (S)-Epichlorohydrin for Enhancing College Student Engineering Practical Abilities.* Journal of Chemical Education, 2021. **98**(12): p. 3804-3812.
117. Sahoo, R.N., N. Pedamallu, and B.R. Jena, *Chapter 20 - World Health Organization and International Council for Harmonization guidelines for "Good Manufacturing Practices"*, in *Physico-Chemical Aspects of Dosage Forms and Biopharmaceutics*, A.K. Nayak and K.K. Sen, Editors. 2024, Academic Press. p. 367-385.
118. Krishani, M., et al., *Development of Scaffolds from Bio-Based Natural Materials for Tissue Regeneration Applications: A Review.* Gels, 2023. **9**(2): p. 100.

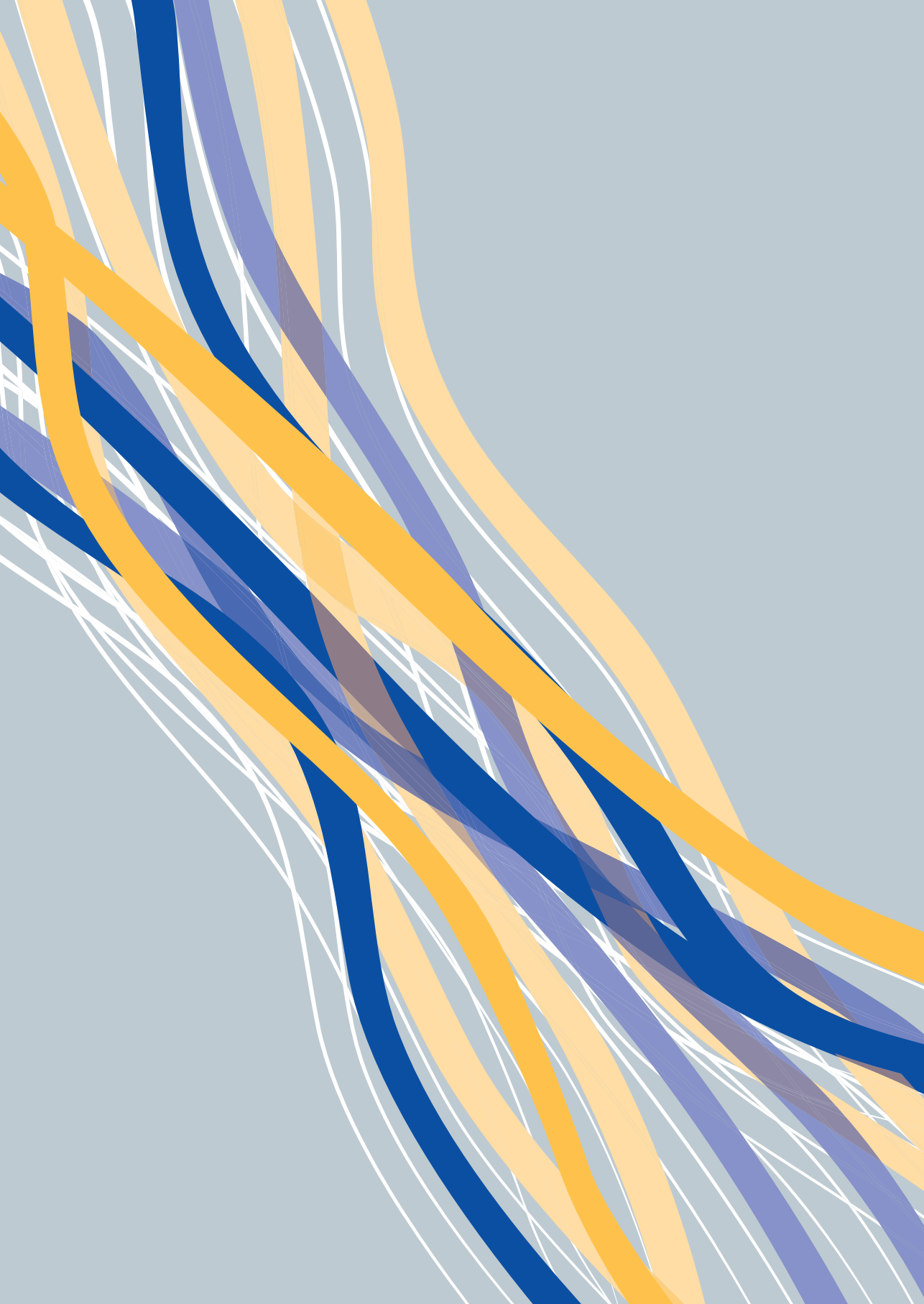

Appendices

Summary

The skin is one of the most important organs in the human body. When severely injured, a set of different ECM components are synthesized during the wound healing process. However, unlike collagen, which accumulates in scars, elastic fibers remain short and disorganized, reducing flexibility and healing outcomes. Current treatments such as split-thickness skin grafts cannot restore lost elastic fibers. To address this, we embarked on engineering novel biomaterials that enhance elastic fiber synthesis and assembly, promoting functional skin regeneration with reduced scarring potential.

Chapter 1 is dedicated to a general overview of the mechanisms of elastogenesis and its relevance to biomaterial development for skin repair. Various bioactive agents with elastogenic potential were analyzed and categorized to various classes, *i.e.,* elastin-based materials, ECM components, hormones, potassium channel openers, vitamins, antioxidants, natural compounds, and metal ions. The shortlisted compounds have demonstrated the ability to enhance elastin production or even elastic fiber assembly.

In **Chapter 2** we investigated the differences between distinct methods of solubilization of elastic fibers and their regenerative potential using primary human dermal fibroblasts and macrophages. Five soluble elastin preparations were obtained through chemical hydrolysis and/or enzymatic digestion techniques. Continuous oxalic acid hydrolysis emerged as an efficient alternative to traditional multi-step methods, preserving bioactivity while streamlining production. All analyzed compounds maintained low expression of a fibrotic marker α-smooth muscle actin in fibroblast cells. Enzymatically processed solubilized elastin led to the highest ECM deposition, particularly elastin, collagen, and fibrillin-2 but triggered a pro-inflammatory M1-like subtype in macrophage studies. The chemically hydrolyzed elastins on the other hand sustained an M0-like phenotype.

Since among all formulations, elastins solubilized with oxalic acid or potassium hydroxide demonstrated the most promise for incorporation into dermal scaffolds, they were chosen to be studied further for production of collagen-elastin biomaterials, as was described in **Chapter 3**. The effects of these biomaterials were studied on different fibroblast subtypes – fetal, eschar-derived, and healthy adult – as well as in a preclinical rat model. Fetal fibroblasts displayed the most robust ECM deposition, followed by eschar-derived cells cultured in these collagen-elastin biomaterials, while adult fibroblasts had the weakest response. Incorporation of

soluble elastins into collagen scaffolds significantly reduced α-SMA expression compared to collagen-only constructs. Notably, scaffolds containing elastin hydrolysates after basic hydrolysis promoted a better wound healing, with reduced contraction, improved ECM organization, and enhanced vascularization, compared to untreated wounds.

Chapter 4 focused on the large-scale production of other collagen-elastin scaffolds, with a focus on optimizing their composition, fabrication techniques, and scalability. Twelve formulations were prepared with varying collagen-to-elastin ratios, lyophilization conditions (room temperature vs. dehydrothermal treatment) and chemical crosslinking. Increasing elastin content enlarged pore sizes but weakened mechanical properties. Dehydrothermal treatment accelerated lyophilization without significantly altering scaffold characteristics. Crosslinking significantly improved structural stability and resistance to enzymatic degradation. A dehydrothermal-processed formulation with 5% elastin and chemical crosslinking demonstrated the best mechanical integrity and degradation profile, making it the most appropriate option for industrial-scale production.

Chapter 5 describes the evaluation of ten bioactive compounds, beyond elastin-based compounds, for their ECM stimulatory effects with particular focus on elastogenic effects using primary human dermal fibroblasts. These are retinoic acid, dexamethasone, minoxidil sulfate, TGF-β1, IGF-1, copper sulfate, dill extract, magnesium ascorbyl phosphate, heparin, and γ-aminobutyric acid. The comparative analysis of ECM production – assessed using RT-qPCR, Western blotting, immunofluorescence, and quantitative colorimetric protein assays – identified dexamethasone, dill extract, IGF-1, heparin, retinoic acid, and TGF-β1 as the most promising candidates, highlighting new directions for biomaterial innovations targeting skin regeneration.

The results of this thesis were discussed in a broader scientific perspective in **Chapter 6**. The general discussion was divided into three topics: 1) reactivation of elastogenesis at the cellular level, 2) engineering of novel collagen-elastin biomaterials, and 3) testing of biomaterials in pre- and clinical models. Advances in molecular biology, biomaterials engineering, and computational modeling were discussed. Collagen-elastin scaffolds can benefit from innovative fabrication techniques, while crosslinking must balance stability and biocompatibility. Advanced cell culture and microfluidic models, additionally stimulated by the need for more ethical alternatives to animal testing, improve *in vitro* and preclinical

research. The final clinical translation requires navigating regulations, process technology, and cost challenges.

Overall, this thesis contributes to the development of regenerative dermal biomaterials that combine efficacy, affordability, and translational potential for widespread use in regenerative medicine, with a particular emphasis on the essential role of elastic fibers in restoring skin functionality and long-term tissue resilience.

Samenvatting

De huid is een van de belangrijkste organen van het menselijk lichaam. Bij ernstige verwondingen worden tijdens het wondgenezingsproces verschillende componenten van de extracellulaire matrix (ECM) gesynthetiseerd. In tegenstelling tot collageen, dat zich ophoopt in littekens, blijven elastische vezels echter kort en ongeorganiseerd, wat leidt tot verminderde flexibiliteit en slechtere resultaten na genezing. Transplantaties van dunne huid (epidermis en een deel van de dermis) kunnen verloren elastische vezels niet herstellen. Om dit probleem aan te pakken, ontwikkelen we nieuwe biomaterialen die de aanmaak en opbouw van elastische vezels stimuleren, met als doel functionele huidregeneratie en vermindering van littekenvorming.

Hoofdstuk 1 biedt een algemeen overzicht van de mechanismen van elastogenese (vorming van elastische vezels) en hun relevantie voor de ontwikkeling van biomaterialen voor huidherstel. Verschillende bioactieve stoffen met elastogene eigenschappen werden geanalyseerd en onderverdeeld in verschillende klassen: elastine-gebaseerde materialen, ECM-componenten, hormonen, kaliumkanaalopeners, vitaminen, antioxidanten, natuurlijke verbindingen en metaalionen. De geselecteerde stoffen toonden het vermogen om de productie van het eiwit elastine of zelfs elastische vezels te verbeteren.

In **Hoofdstuk 2** onderzochten we de verschillen tussen verschillende methoden voor het oplosbaar maken van elastische vezels en hun herstellend vermogen met behulp van primaire humane dermale fibroblasten en macrofagen. Vijf oplosbare elastinepreparaten werden verkregen via chemische hydrolyse en/of enzymatische bewerking. Continue oxaalzuurhydrolyse bleek een efficiënt alternatief voor de traditionele methode in meerdere stappen, met behoud van bioactiviteit terwijl het een gestroomlijnd productieproces mogelijk maakte. Alle geanalyseerde verbindingen vertoonden een lage expressie van α-smooth muscle actine (α-SMA) in fibroblastcellen, een marker voor fibrose. Enzymatisch verkregen oplosbaar elastine leidde tot de hoogste ECM-synthese, met name van elastine, collageen en fibrilline-2. Studies met macrofagen lieten zien dat macrofagen in een meer neutraal M0-fenotype bleven in celkweek met chemisch gehydrolyseerde elastines, terwijl het pro-inflammatoire M1-fenotype geactiveerd werd door enzymatisch gehydrolyseerde elastines.

Aangezien elastines die met oxaalzuur of kaliumhydroxide waren opgelost meer potentie toonden voor opname in dermale scaffolds, werden deze verder onderzocht voor de productie van collageen-elastine biomaterialen, zoals

beschreven in **Hoofdstuk 3**. De effecten van deze biomaterialen werden onderzocht op verschillende subtypes fibroblasten – afkomstig uit foetale huid, escharweefsel, of gezonde volwassen huid – en in een preklinisch ratmodel. Foetale fibroblasten zorgen voor de meeste ECM-synthese, gevolgd door eschar cellen, terwijl volwassen fibroblasten weinig ECM aanmaakten. De toevoeging van oplosbare elastines aan collageenscaffolds verminderde de expressie van α-SMA significant vergeleken met constructen met alleen collageen. Opmerkelijk is dat scaffolds met elastinehydrolysaten uit basische hydrolyse wondgenezing meer bevorderden, met minder contractie, verbeterde ECM-organisatie en verhoogde vascularisatie.

Hoofdstuk 4 richtte zich op de grootschalige ontwikkeling van andere collageen-elastine scaffolds, met nadruk op optimalisatie van hun samenstelling, fabricage-technieken en opschaalbaarheid. Twaalf formuleringen werden bereid met verschillende collageen-elastine verhoudingen, lyofilisatiecondities (kamer-temperatuur versus dehydrothermale behandeling) en chemische crosslinking. Verhoogde elastineconcentraties vergrootten de poriegrootte, maar verzwakten de mechanische eigenschappen. Dehydrothermale behandeling versnelde het vries-droogproces zonder de eigenschappen van de scaffold significant te veranderen. Crosslinking zorgde voor een aanzienlijke verbetering van de structurele stabiliteit en de weerstand tegen enzymatische afbraak. Een formulering die verwerkt werd via dehydrothermale behandeling met 5% elastine en chemische crosslinking toonde de beste mechanische integriteit en minste degradatie, en bleek het meest geschikt voor industriële productie.

Naast de elastine-gebaseerde componenten uit eerdere hoofdstukken, beschrijft **Hoofdstuk 5** de evaluatie van tien bioactieve stoffen op ECM-stimulerende en elastogene effecten met behulp van primaire humane dermale fibroblasten. Deze stoffen zijn retinoïnezuur, dexamethason, minoxidilsulfaat, TGF-β1, IGF-1, kopersulfaat, dille-extract, magnesiumascorbylfosfaat, heparine en γ-aminoboterzuur. De vergelijkende analyse van ECM-productie – beoordeeld met RT-qPCR, Western blot, immunofluorescentie en kwantitatieve colorimetrische eiwittesten – identificeerde dexamethason, dille-extract, IGF-1, heparine, retinoïnezuur en TGF-β1 als de meest veelbelovende kandidaten, waarmee nieuwe richtingen worden gegeven voor innovatie van biomaterialen gericht op huidregeneratie.

De resultaten van dit proefschrift worden breder wetenschappelijk besproken in **Hoofdstuk 6**. De algemene discussie werd onderverdeeld in drie onderwerpen: 1) heractivering van elastogenese op cellulair niveau, 2) ontwikkeling van nieuwe collageen-elastine biomaterialen, en 3) testen van biomaterialen in preklinische en

klinische modellen. Vooruitgang in moleculaire biologie, biomaterialentechnologie en computationele modellering kwamen aan bod. Collageen-elastine scaffolds kunnen profiteren van innovatieve fabricagetechnieken, terwijl crosslinking een evenwicht moet vinden tussen stabiliteit en biocompatibiliteit. Geavanceerde celkweek- en microfluïdica-modellen, mede gedreven door de noodzaak tot ethischere alternatieven voor dierproeven, verbeteren *in vitro* en preklinisch onderzoek. De uiteindelijke klinische vertaling vereist navigatie door regelgeving, opschaalbaarheid en kostenefficiëntie.

Samenvattend draagt dit proefschrift bij aan de ontwikkeling van regeneratieve dermale biomaterialen die effectiviteit, betaalbaarheid en klinische toepasbaarheid combineren voor breed gebruik in de regeneratieve geneeskunde, met bijzondere nadruk op de essentiële rol van elastische vezels in het herstellen van huid-functionaliteit en langdurige weefselresistentie.

Research Data Management

Ethics and funding

Adult fibroblasts were obtained from skin samples of patients undergoing elective surgery at the Department of Plastic and Reconstructive Surgery, Red Cross Hospital (Beverwijk, NL). Eschar samples were collected from burn patients undergoing debridement between post-burn days 13 and 19 at the hospital. Fetal fibroblasts were derived from fetal skin obtained following pregnancy termination between gestational weeks 16 and 22, with written informed consent from the donors at the Center for Contraception, Abortion, and Sexuality (CASA, Leiden and The Hague, NL). Use of anonymized residual tissue was approved via the informed opt-out protocol, following national ethical guidelines (https://www.coreon.org/, accessed on 23 November 2020) and institutional privacy regulations. For buffy coats, informed consents were given in accordance with the Declaration of Helsinki and Dutch national and Sanquin internal ethic boards (Blood bank Sanquin, Nijmegen, NL).

All procedures were executed according to the regulations for animal experimentation in the Dutch Experiments on Animals Act (Wod) and the European Union (directive 2010/63/EU). Authorization for these procedures was granted by the Dutch Central Authority for Scientific Procedures on Animals (CCD). The experiments detailed in Chapter 4 were conducted under project license AVD10300202317189 and followed protocol 2023-0016-003. The work described in this doctoral thesis was funded by the European Union's Horizon 2020 research and innovation programme under the Marie Skłodowska-Curie grant agreement No 955722.

Data collection, analysis and storage

For Chapters 2-5, all raw and processed data were systematically documented in laboratory notebooks, digital platforms such as Labguru and iVentionLES (Central Animal Facility), and a secure department server (H: drive), accessible only to authorized personnel. The data supporting these chapters originated from laboratory-based cell culture experiments (Chapter 2-5) and studies involving animal models (Chapter 4). Information for Chapter 1 was gathered through literature review, with analysis conducted using departmental computing resources. All processed data, along with key documentation – including research protocols, experimental designs, and explanatory readme files – were archived in the Radboud Data Repository's Research Documentation Collection.

Data sharing

All processed datasets and related documentation are securely stored in the Data Sharing Collection within the Radboud Data Repository (RDR) for long-term access (DOIs: 10.34973/p1jd-3d12; 10.34973/qs9v-vj42; 10.34973/cbbe-xr98; 10.34973/sahs-vz71). Metadata for these records follows RDR guidelines. All research findings will be published in open-access journals, with references accessible through PubMed. The datasets supporting each chapter will be available in the RDR and structured for reusability, incorporating detailed descriptions of sample processing, data acquisition, and image analysis. After publications in scientific journals, the data will be published with open access under the CC-BY-NC-4.0 license, ensuring access for a minimum of 10 years. This includes accompanying metadata and necessary documentation for proper interpretation. The data is saved in widely used file formats (e.g. txt, docx, pdf, csv, xlsx, tif, png, etc.). Research data from animal experiments will be published with restricted access under the RUMC-RA-DUA-1.0 license, requiring a signed Data Use Agreement and explicit approval of each access request by the designated Data Access Committee or collection manager.

Curriculum vitae

Roman was born in 1995 in Severodonetsk, Luhansk region, Ukraine. In 2013, he completed his high school education with the highest distinction, earning a gold medal. He obtained his Bachelor's and first Master's degree in Organic Chemistry at Taras Shevchenko National University of Kyiv, Ukraine. His research was conducted in the group of Prof. Vasyl Pivovarenko and focused on the synthesis of molecular tweezers with two and three chromophores – adenosine-5'-triphosphate receptors.

In 2018, he spent one semester at Uppsala University, Sweden, through the Erasmus+ Exchange Mobility Program. He gained his first work experience through a 4-year internship in organic synthesis at Enamine Ltd., Kyiv, Ukraine.

Subsequently, Roman was awarded a scholarship to pursue the European Erasmus Joint Master Degree in Translational Cosmetic and Dermatological Sciences (EMOTION). He successfully completed a second Master's degree with a specialization in clinical research at the University of Eastern Piedmont, Novara, Italy, and at the University of Namur, Belgium. He also carried out a one-semester professional internship in the Biochemistry group of Dr. Toin van Kuppevelt and Dr. ir. Willeke Daamen at Radboud university medical center, Nijmegen, the Netherlands. His project focused on the role of elastin receptor signaling on the regenerative capacity of lung epithelial (stem) cells.

Upon obtaining his Erasmus Mundus Master's degree, Roman continued in the same research group as a PhD candidate, supported by a prestigious Marie Skłodowska-Curie Actions fellowship – Europe's most competitive research and innovation grant. His project, part of the SkinTERM consortium, focused on skin tissue engineering and regenerative medicine. His research specifically addressed elastin and its biological and biomechanical characteristics for developing biomaterials for scarless skin regeneration. During his PhD, he completed secondments at three partner institutions: the Association of Dutch Burn Centers, Beverwijk, the Netherlands; the University of Zürich, Switzerland; MedSkin Solutions Dr. Suwelack AG, Billerbeck, Germany. Throughout his doctoral journey, Roman presented his research findings at both national (31st and 32nd Annual Meeting of the NBTE) and international conferences (7th TERMIS World Congress; 2024 ETRS-WHS-SkinTERM Meeting; 12th European Elastin Meeting).

In parallel with his research at Radboudumc, Roman volunteered as a translator and clinical support coordinator for 22 severely wounded Ukrainian soldiers. He collaborated closely with Dr. Vincent Stirler, Dr. Erik van de Krol, and Kseniya Negrutsa-Godska from the Netherlands for Ukraine Foundation.

As of June 2025, Roman continues to work as a Research Technician at Radboudumc and Sanquin, Amsterdam, the Netherlands. His current project focuses on molecular mechanisms of iron recycling in health and anemia of inflammation in the research group of Dr. Hanke Matlung and Dr. Robin van Bruggen.

List of publications

Related to this thesis:

Krymchenko, R., Coşar Kutluoğlu, G., van Hout, N., Manikowski, D., Doberenz, C., van Kuppevelt, T. H., Daamen, W. F. Elastogenesis in focus: Navigating elastic fibers synthesis for advanced dermal biomaterial formulation. *Adv. Healthcare Mater.* **2024**, 13, 2400484.
https://doi.org/10.1002/adhm.202400484

Krymchenko, R., Pfirrmann, M., van der Leeuw, S., Avila-Martinez, N., Versteeg, E. M. M., Meuwese, R. T. C., Vlig, M., Verdoes, M., Boekema, B. K. H. L., van Kuppevelt, T. H., Daamen, W. F. Preparation, fractionation, and characterization of solubilized elastin and comparison of cellular response on fibroblasts and macrophages. *Int. J. Biol. Macromol.* **2025**, 315(Pt 1):144548.
https://doi.org/10.1016/j.ijbiomac.2025.144548

Krymchenko, R., Avila-Martinez, N., Gansevoort, M., Bakker, G. J., Gomes L. N. P., M., Vlig, M., Versteeg, E. M. M., Boekema, B. K. H. L., van Kuppevelt, T. H., Daamen, W. F. Collagen-elastin dermal scaffolds enhance tissue regeneration and reduce scarring in preclinical models. *Mater. Today Bio* **2025**, 102239.
https://doi.org/10.1016/j.mtbio.2025.102239

Other:

Avila-Martinez, N., Pfirrmann, M., Gomes, M.L.N.P., Krymchenko, R., Versteeg, E. M. M., Vlig, M., Verdoes, M., van Kuppevelt, T. H., Boekema, B. K. H. L.; Daamen, W. F. Effect of Hyaluronan in Collagen Biomaterials on Human Macrophages and Fibroblasts *In Vitro. J. Funct. Biomater.* **2025**, 16, 167.
https://doi.org/10.3390/jfb16050167

PhD portfolio of Roman Krymchenko

Department: **Medical BioSciences**
PhD period: **15/09/2021 – 15/12/2024**
PhD Supervisor(s): **Dr. ir. W.F. Daamen**
PhD Co-supervisor(s): **Dr. A.H.M.S.M. van Kuppevelt, Dr. ir. B.K.H.L. Boekema**

Training activities	Hours
Courses	
• SkinTERM Personal Development Plan (2021)	12.00
• SkinTERM Data Management (FAIR principles) (2021)	10.00
• SkinTERM Workshop A: Biomaterials (2021)	28.00
• Social Dutch I (0-halfway A1) (2021)	54.00
• SkinTERM Intellectual property rights (2021)	9.00
• SkinTERM Writing a scientific paper (2021)	9.00
• SkinTERM Workshop C: Hair regeneration biology (2021)	18.20
• SkinTERM Scientific poster design (2021)	10.00
• SkinTERM Workshop B: Skin tissue engineering (2021)	18.20
• Radboudumc - Introduction day (2021)	6.00
• RIMLS - Introduction course "In the lead of my PhD" (2021)	15.00
• Social Dutch II (halfway A1-A1) (2021)	67.50
• Radboudumc - Scientific integrity (2022)	20.00
• Radboudumc - Laboratory animal science (for Radboudumc researchers working with laboratory animals) (2022)	84.00
• SkinTERM Career perspectives after your PhD (2022)	9.00
• SkinTERM Communication and presentation skills (2022)	9.00
• SkinTERM Advanced microscopy and image analysis (2022)	10.00
• SkinTERM Workshop D: Regeneration in Acomys sp. (2022)	21.00
• Avondcursus NT2 voor beginners II (A1-A2) (2022)	154.00
• Avondcursus Nederlands voor halfgevorderden (A2-B1) (2023)	161.00
• Radboudumc - eBROK course (2023)	42.00
• Avondcursus NT2 voor gevorderden (B1-B2) (2024)	161.00
• Career development workshop "The next step in my career" (2024)	24.00
• Avondcursus NT2 voor vergevorderden (B2-C1) (2024)	161.00
Seminars	
• RIMLS Meet the Expert 'Biomaterials Testing' (2021)	2.00
• RIMLS Meet the Expert 'Communicating your science: Vlogging and blogging for beginners' (2021)	1.50
• RIMLS Meet the Expert 'Adobe Illustrator - Fantastic tools and where to find them' (2021)	2.00
• RIMLS Meet the Expert 'Development and culturing of iPSCs' (2021)	2.00
• Online webinar "From Academia to Industry: Taking iPSC-Derived Muscle Cells to the Clinic" (2022)	1.00
• Research Integrity Round: 'Publication ethics: Promises, problems and perspectives' (2022)	1.50
• PON PhD Day 2022 (2022)	4.50
• Radboud Research Rounds 'Advanced biomaterials for tissue repair' (2022)	1.50
• Electron Microscopy Seminar: When Light is Not Enough (2022)	1.50
• RIMLS Meet the Expert 'LinkedIn can contribute to your career!' (2022)	2.00
• RIMLS Meet the Expert 'Molecular imaging in mouse and rat models' (2022)	1.50
• Research Integrity Round 'Patents at Radboudumc: a blessing or a curse?' (2023)	1.50
• RIMLS Meet the Expert 'Flow cytometry' (2023)	2.00
• Research Integrity Round 'Research ethical issues in the physician/researcher/patient/participant quadrangle' (2023)	1.50
• Oral presentation at the research program 'Tissue Modeling and Regeneration' (2024)	4.00

Conferences	
• RIMLS PhD retreat (2021)	14.00
• New Frontiers Symposium Translational Glycoscience (2021)	12.50
• NBTE 30th Annual Meeting incl. poster presentation (2022)	17.00
• ESOF 2022 Marie Skłodowska-Curie Actions Satellite Event (2022)	8.00
• RIMLS PhD retreat incl. poster presentation (2022)	21.00
• NBTE 31st Annual Meeting incl. oral presentation (2022)	17.00
• NBTE 32nd Annual Meeting incl. oral presentation (2023)	25.00
• The 7th TERMIS World Congress incl. poster presentation (2024)	8.00
• Radboudumc PhD retreat incl. oral presentation (2024)	24.00
• Annual Meeting 2024 of the European Tissue Repair Society (ETRS), Wound Healing Society (WHS) and SkinTERM incl. oral presentation (2024)	80.00
• The 12th European Elastin Meeting incl. oral presentation (EEM2024) (2024)	32.00
Teaching activities	
Supervision of internships / other	
• Literature Thesis Supervision (2021)	15.00
• Supervising a practical for MED-BMS34 Reconstructive and regenerative medicine course (2023)	8.00
• Supervising a practical for MED-MIN13 Medical Biotechnology towards Clinical Practice (2023)	24.00
• Student internship coaching (2023)	70.00
• Supervising a practical for MED-BMS34 Reconstructive and regenerative medicine course (2024)	8.00
Total	**1526.40**

Acknowledgements

This PhD project has been a collaborative journey worth acknowledging all the incredible people I had the opportunity to work with and cooperate with. The journey was certainly not easy, and at times, extremely tough due to the limited time, but it would not have been accomplished without the enormous support, assistance, and guidance I received. Referring to everyone in this section by their first names is a deliberate choice to highlight the familiarity, trust, and connection I felt with each of you. If I have accidentally missed someone, please accept my sincere apologies and know that your help has not gone unnoticed.

First of all, I would like to thank my main supervisors, **Willeke** and **Toin**, who chose me from among all applicants back in January 2021. I am very proud that you both introduced me to an entirely new experimental world – from organic chemistry to biological assays and *in vivo* experiments – and helped me become a better researcher.

Willeke, it is difficult to put into words just how much of an impact you had on my professional and personal development. Thanks to your guidance, I was able to complete my PhD in just three years and three months. In that short time, we managed to deliver five strong scientific publications, none of which would have been possible without your tireless support, sharp scientific insight, and constant encouragement. Besides the academic aspect, you never dismissed what I was going through and always helped me find practical, fair solutions. You were the only person in the entire Radboudumc community who not only truly supported me when the full-scale invasion of my home country began, but who also remained caring and supportive throughout my employment, and even beyond. I knew I could reach out to you anytime, whether it was after working hours or during the weekend, and you would respond thoughtfully and patiently.

Toin, I want to thank you for taking the lead to make the whole SkinTERM project happen. Even after your retirement, you never left me or any of us alone with our questions or concerns. Your thoughtful questions during the scientific meetings always pushed me to think beyond the initial scope of my project and to develop new ideas. I also genuinely appreciate that during my interview, you warned me that not all experiments go as planned and that failure is part of the process. It helped me stay realistic. But above all, I am most grateful for the positivity and belief you showed me throughout my PhD journey.

Bouke, I am very happy that you agreed to become my third supervisor and share your expertise and wisdom with me. I appreciate that I could always count on your support and understanding. I have never regretted that you joined my supervision team. I think that our manuscripts were significantly improved with your remarks and suggestions. I am also grateful to your colleagues – **Marcel**, **Esther**, **Patrick**, **Anouk**, and all the team – for the warm welcome to me and Nancy during our first secondment at ADBC. **Madalena**, it was also a pleasure and fun to work with you in Beverwijk. It was such a great and valuable secondment to start with.

My second secondment opened a new experimental chapter in my career – working with blood cells. I am thankful for the great time spent in the research lab of **Thomas** and **Agnes**. Special thanks go to **Hyrije** for her tireless efforts in teaching us as much as possible, and of course to **Mahrukh** and **Zohaib** for their warm support, both inside and outside the lab. **Zuzana**, thank you also for helping me navigate such an extremely expensive Swiss environment, and for the sincere talks we shared.

My concluding secondment was also quite unique and was excellently organized by **Claudia** and **Dominique**. I am thankful to **Gizem** for the amazing time at MDS and the warm welcome outside the work from both her and **Ömer**. I think we did a really great job in such a short period of time. This exchange also helped me recharge my internal battery for completing the PhD and delivering another manuscript.

Of course, I would like to acknowledge my main research group – Matrix Biochemistry (MxB).

Nancy, ¡muchas gracias por estar conmigo durante nuestro proyecto! Out of all my colleagues, I spent the most time together with you, both at work and outside: in Nijmegen, at various conferences, and during our secondments in Beverwijk and Zurich. We both went through tough times, but with mutual support, we managed to overcome many challenges. We were always in touch and knew that we could count on each other. Your friendliness and wide smile made the atmosphere in our lab much warmer. I wish you continued proactivity and fulfillment in your next job. I am sure you will find something nice that meets your expectations.

Merel, you were an example for me on how to achieve results from anything I do – whether executing SDS-PAGE, qPCR, culturing cells, getting animal experiments up and running, or even submitting a PhD thesis. Your dedication and quality of work truly deserve recognition.

Rob, I am thankful for the great talks and time we have worked together. It was also awesome to play volleyball and improve our skills. And of course, I need to acknowledge your inputs in the solubilization of elastin. Your HElp and help were essential for my project, you know. Your patience, even in very stressful situations, is something I really need to learn from for my future life.

Lieke, I think you are the kindest person in our lab, and I am thankful for your positive and caring vibes. I knew that I could ask you any question I had and you would do your best to answer them, even if you were buried in the amount of work you had. You are a curious and dedicated person, and I believe you will reach every goal you set.

Thierry, thank you very much for your valuable guidance on Western blots, sincere talks, and amazing time at bouldering sessions. Despite working on a different topic, you contributed substantially to my project by teaching lab techniques and asking insightful questions during presentations.

Danique, your contribution to my PhD life goes far beyond elastin and elastin hydrolysates. I am enormously thankful for your management of the whole SkinTERM project. I do think that you performed a great job, and you are an irreplaceable person there. I could feel all the love and energy you dedicated to SkinTERM, and I truly valued it. Thank you for being there in both good and hard times, and for all the assistance and support besides work.

Elly, you were my first supervisor when I joined the lab. I am very thankful that, besides teaching me how to purify elastic fibers and work responsibly in the biochemical lab, you pushed me out of my comfort zone and stimulated me to learn Dutch. I always appreciated being able to approach you with any practical question.

Dear **Paola**, **Ahmed**, **Aarti**, **Bart**, **Lars**, **Tika**, **Theo**, and **Priyanka**, it was such a pleasure working with all of you. I am thankful for the great times and all the best in your future endeavors.

I would aslo like to express my gratitude to the entire SkinTERM consortium – all other ESRs (**Masi**, **Haarsha**, **Prerna**, **George**, **Jiazheng**, **Irene**), PIs and collaborators (**Leen**, **Robert**, **Colin**, **Herbert**, **Gustavo**, **Marta**, **Dongsheng**, **Hans**, **Daniela**, **Vincent**, **Joaquin**, **Laurent**, **Amulya**, **Leon**, **Denis**, **Franck**, **Agnes**, **Bert**, **Michele, Yuval**). I remember each of you and thank you for your support, collaboration, and warm conversations.

Although I did not supervise many students, I was extremely lucky with those I did. **Sjoerd**, you were the first and the last student I was capable of dedicating my time, energy, and assistance to. Thanks to Rob, I got the great opportunity to supervise you during your Master's internship, and I am happy that you contributed to my elastin research. **Noor**, supervising your literature thesis helped me to better focus on my own topic, and you provided a solid background to start building a great review that we published together in a scientific journal. I am also grateful to my colleagues for allowing me to occasionally supervise **Martin** and **Steven**. Guys, I got connected with you pretty much despite not being your formal supervisor. Hope to see you soon at bouldering, in the gym, or at my place!

I would like to thank the entire Team 1, led by **Mayke**, for supporting me and my colleagues in executing animal experiments. Special thanks go to Maikel and Tim. **Maikel**, I felt an immediate connection with you – as you said, it felt like we had met before. Your vivacious energy and enthusiasm charged me with the motivation to finish my PhD. You showed me a new way of working and perceiving the stress: start with what you can do, think actively, act ad hoc in unexpected situations, and accept the outcome. Your humor brightened even the darkest moments of my PhD. I also appreciate how you supported my ambition to learn as much practical work as possible – it helped me land my current job. **Tim**, your cheerful and helpful attitude, combined with excellent organizational skills, made working at CDL both efficient and enjoyable. You always took our experiments seriously, and your inputs, especially on bandaging, helped me feel less alone. I am also very grateful to **Manon**, **Kitty**, **Stef**, **Stephanie**, **Helma**, **Alinde**, **Jeannette**, **Miriam**, and **Anke** for their dedication and support. Your active involvement meant a lot!

My PhD track was also enriched by my volunteer work with severely wounded Ukrainian soldiers at Radboudumc. **Vincent**, you are the person I am enormously proud to know and to have the opportunity to work with. I would never ever expect that such a random request from my Ukrainian colleague to help a doctor with translation would drastically change my life. You are all-in-one – a knowledgeable doctor, caring father and husband, reliable partner, strict commander, cheerful friend, true researcher, and simply a great person. Thank you deeply for all the things you were and are doing for my severely wounded compatriots. When everyone around says 'NO', you are the only one who says 'YES'. I miss every single moment, the good and the hard ones, that we had to go through during the treatment of all the soldiers. I learnt a lot from you, and I am proud of my tiny inputs in the great and important things you are doing together with all your multidisciplinary team. **Erik**, **Thomas**, **Franz**, **Claire**, **Nens**, **Kseniya**, **Indy**, **Bart**, **Lucas**, **Kim**, **Laura**, **Valentyna**, **Tim**, and others, huge thank you to all of you!

A special thank you to the people from my EMOTION Master and my Ukrainian Master. I need to confess that it was the most unforgettable and the warmest memories I cherish throughout my life. Without the active support and recommendation letters from **Armando**, **Tracey**, **Joachim**, **Michela**, **Vasyl**, and **Jean-Pierre**, I would never have been accepted into the SkinTERM project.

Дорогі **мамо** й **тату**, я щиро дякую вам за всі зусилля та любов, що ви в мене вклали. Безумовно, вам є чим пишатися. Можливо, якби ви не налаштовували мене відмінно вчитись та не наполягали на подальшому житті за кордоном, то сьогодні ви б не тримали в руках цю дисертацію, а моє життя склалося зовсім інакше. Я дуже сподіваюся, що ви разом знайдете нову домівку з мирним небом. Хоч клята війна й позбавила вас дому, але з іншого боку вона дала мамі та Тимофію змогу пожити в такій чудовій країні, як Нідерланди, і бути поруч зі мною. **Тімоха**, дякую тобі за підтримку та слова гордості за мене. Тепер твоя черга гарно опанувати якусь галузь, або навіть декілька, та будувати власне життя, якого ти забажаєш. У тебе наразі вже є міцний фундамент та зразок того, яким крутим і небанальним може бути навчання. **Бабуля**, я тебе дуже люблю та радий, що ти також поруч зі мною та завжди за мене переживаєш і підтримуєш. Тепер тобі треба тільки підучити англійську і зможеш читати мою дисертацію замість книжок Мариніної.

Також я вдячний за підтримку та постійні хвилювання з боку **мами Наташі**. Попри болючість запитань про прогрес моєї докторантури, Ви завжди цікавилися цим. Ви одразу бачили, коли щось ішло не так, і намагалися підбадьорити. Звісно, не можу не подякувати **родинам Боярських**, які регулярно запитували, як там «конячі шиї» та регенерація шкіри.

Анюто, моє кохання та моє сонце, ти як ніхто інший знаєш, наскільки важко мені дався цей шлях, наскільки тернистим та непростим він виявився. Я неймовірно вдячний тобі за твою безмежну підтримку та непохитну витримку. Ми пережили надзвичайно складні часи, особливо в перші роки моєї докторантури, але все це вже позаду. Новина, якою ти скрасила мій останній робочий день, надала сил та мотивацію йти до кінця. Далі нас чекає захопливе та світле майбутнє. Так, батьківське життя буде зовсім іншим, як ми жили досі. Проте тепер в нашому домі лунатиме дитячий сміх і крики, буде купа підгузків, розкидані іграшки, дитячі книжки, розмазана їжа, помальовані меблі та стіни. Я готовий розпочати цей етап разом із тобою! **Донечко**, я дякую тобі, що ти прийшла в наше життя та надала мені вагомий поштовх та тверду рішучість вчасно дописати дисертацію та захистити звання доктора. Лише погляд у твої ніжні оченята переконує

мене, що варто було пройти цей важкий шлях, щоб зараз насолоджуватися щасливими моментами з тобою та мамою.

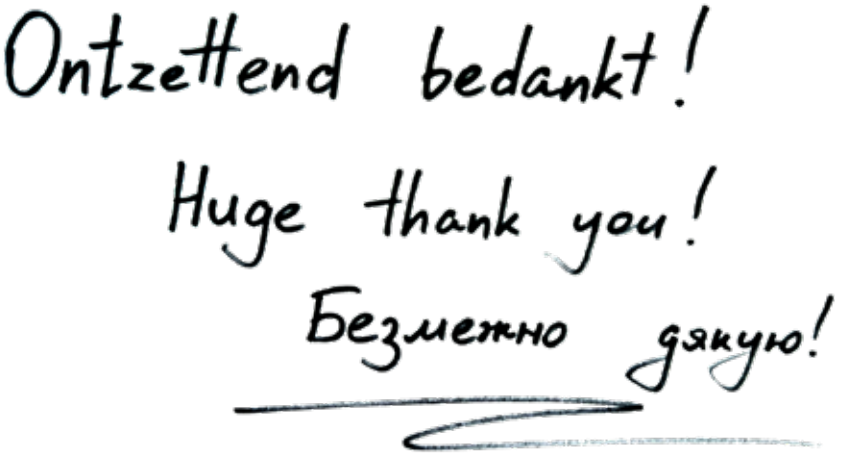

Radboudumc
university medical center

IN DEI NOMINE FELICITER

Radboud University